THERMAL RADIATION EXCHANGE

BETWEEN THE SUN AND SKY,

AND THE EARTH

A thesis submitted as a partial fulfilment for the requirements of the Degree of Master of Engineering, Mechanical Department, University of Canterbury, Christchurch, New Zealand.

By

Thai Van Thanh

B.E. (Hons.) 1973

A C K N O W L E D G E M E N T

For help in carrying out the investigation and in the preparation of this thesis I sincerely thank the following:

- Mr. G. Whittle and Dr. G.J. Parker for their joint supervision of the project.

- Dr. D. Lindley for his initial suggestion of the solar water heating study.

- Dr. D.E. Greenland and Mrs. R. Moran of the Geography Department for help with the long wave radiation study and valuable data of total and diffuse solar radiation.

- The staff of the Mechanical Department workshop for their great work in manufacturing, installing and repairing the solar panel and others in Chemical and Electrical Workshop for servicing of the equipment.

- The staff of Christchurch Weather Office for access to their meteorological records.

- Miss T.T. Nga for constant encouragement during my course of study and for typing the final thesis.

Christchurch, Feb 1974

Thai Van Thanh

C O N T E N T S

S U M M A R Y

Radiation exchange is an important factor in the thermal environment of building and ground surfaces. During daytime these surfaces receive a substantial amount of energy from the Sun in the form of solar radiation. In addition to this, another component of energy input is also received, of smaller amount but continuously day and night, from the sky and near-by objects around these surfaces, in the form of long wave-length radiation. At night-time, this source of input is normally not enough to compensate for the outgoing radiation from building and ground surfaces, resulting a net radiation loss to the sky.

In the first part of this investigation, the aims were to study the long wave radiation from Sky and devise a simple instrument to measure this component of heat exchange with some trial measurements under Christchurch conditions. The study was carried out in two ways:

1. To study the analytical approach which leads to the theoretical estimation of sky radiation by Elsasser's and others'charts.

2. To review the experimental approach which introduces the methods of sky radiation measurement and the empirical formulae proposed by some observers to estimate this radiation input from meteorological soundings.

A simple radiometer was made which enables the sky radiation and hence the heat loss by radiation from any surface of known temperature to be estimated.

A series of trial measurement at night and daytime under Christchurch weather conditions were carried out with this radiometer. The results gave good examples of the variation of sky radiation corresponding to air temperature and sky cloudiness conditions. Quantitatively, the amounts of sky radiation estimated from some measurements were 25%to 30% higher than the values calculated by the empirical formulae at the same conditions due to systematic error. For some other measurements of different method the results are close to Swinbank's empirical formula $R_L = 1.195 \sigma T_a^4 - 17.09$. Analysis showed that this formula may be applied for all cases if the systematic error is eliminated. Modification for the radiometer and precautions necessary to improve the accuracy of measurement are also proposed.

The second part of this investigation is concerned with the solar radiation component. It consists of:

1. A brief investigation of solar radiation data for Christchurch through literature and records of Meteorological Offices.

2. A study on the performance of a common type flat plate solar water heater under Christchurch weather conditions.

Mean radiation data for Christchurch in the last 5 years are presented and compared with the standard year solar radiation values proposed earlier. Sources of information for these data are located and the method to estimate radiation intensity on inclined surfaces is also presented.

Tests were carried out during the last 3 months of 1973 to measure the energy collection and efficiency of operation

for a solar water heater under Christchurch conditions. Results are presented in forms of tables and graphs to show some examples of the variation in energy collection, efficiency of operation and water temperature with weather conditions.

Estimation for whole year contribution potential based on the test results was also given with some recommendations of angles of inclination for more possible collection.

I N T R O D U C T I O N

In thermal environmental engineering, various methods of heating, ventilating and air-conditioning are used to maintain the indoor conditions of temperature, humidity and air movement at some desired levels to provide comfortness for different types of occupants.

One factor in the variation of temperatures of the inside surfaces of any covered space is the temperature of the outer surfaces. These outer surfaces continuously exchange heat with the surroundings, the two most important modes of heat exchange are convection and radiation.

During daytime, any surface on the Earth receives some amount of radiation from the Sun, the Sky and nearby objects around the surface. To maintain equilibrium, these surfaces in turn re-radiate energy due to their temperatures and also exchange heat by convection with the air stream in the atmosphere. An illustration of these modes of heat transfer is shown in Fig. I .

Considering the radiation exchange only, the 5 main factors in order of importance are:

1. Direct short wave radiation from the Sun.
2. Diffuse short wave radiation from Sky.
3. Reflected short wave radiation from ground and surroundings.
4. Long wave radiation from Sky, heated ground and nearby objects.
5. Outgoing long wave radiation from building and ground surfaces to the Sky.

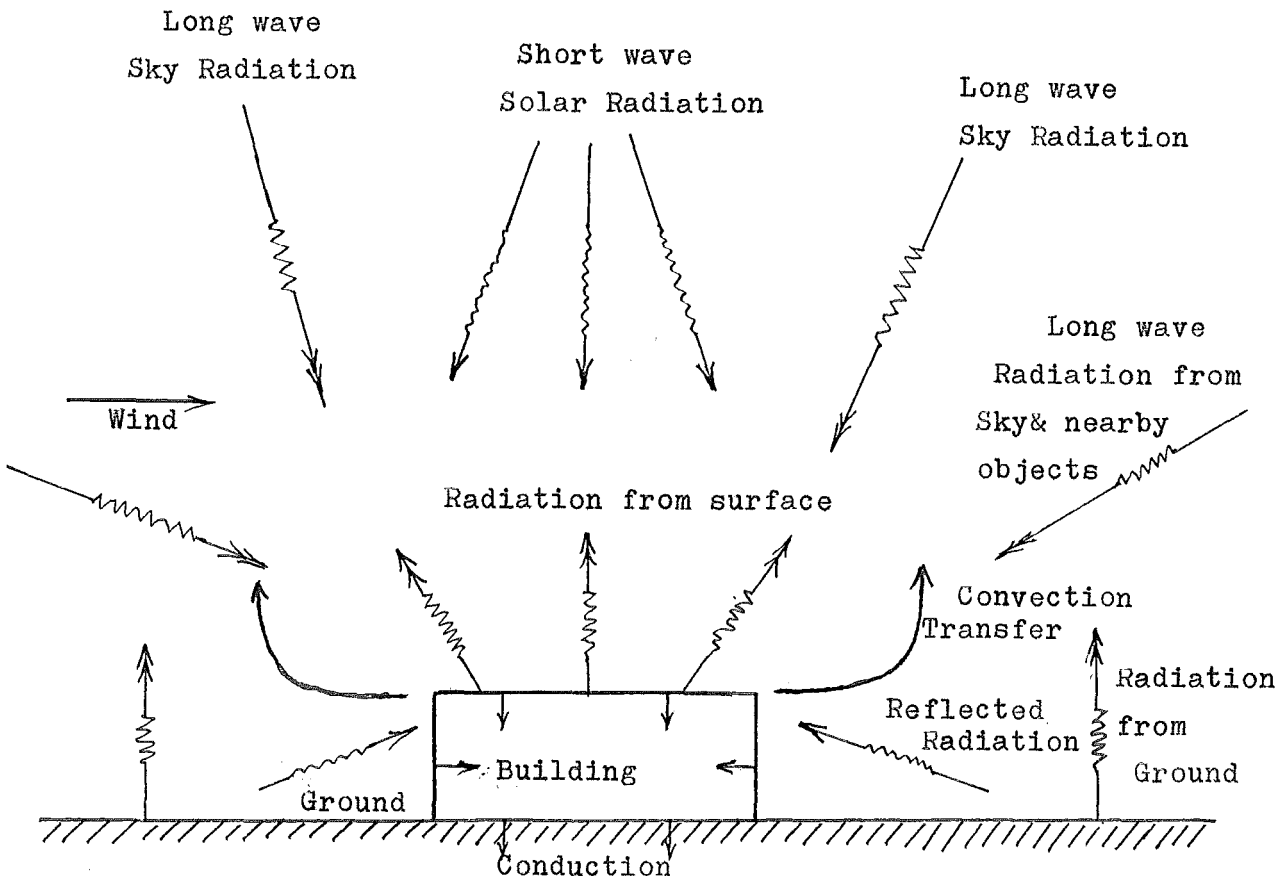

Fig.I Modes of Heat Transfer in thermal environment of Building and Ground

At night-time, with the absence of solar radiation, the incoming long wave radiation from Sky and surroundings are usually not enough to compensate for the re-radiation from ground and building surfaces resulting in a cooling effect. This radiation heat loss is intensive under some weather conditions.

About 96% of the energy from the solar radiation is concentrated in the short wavelengths from 0.4 to 4 μ. Radiation from the Sky or any surface due to their temperatures is in the region $>4\mu$ in wavelengths. Therefore solar radiation is usually referred as shortwave radiation and the other is called long wave radiation.

The atmosphere above the Earth, besides its vital role of supplying oxygen, acts as a necessary moderator for the radiation exchange between the Earth and the outer space. Without it, the Earth will be unbearable hot during daytime due to solar radiation and excessively cold at night due to nocturnal radiation. The term nocturnal radiation refers to the long wave radiation to the cold night sky from surfaces on the Earth.

A surface at the outer edge of the atmosphere receives 2 cal/cm^{2}min if placed at right angle to the solar beam. This value is termed the Solar Constant. Only 0.3 to 0.8 of this amount can be received by the Earth surface due to the presence of the atmosphere. The heat loss at night due to radiative cooling effect depends very much on the sky conditions over the place and amounts up to about 0.4 cal/cm^{2}min for cloudless sky.

Solar radiation is the vital source of energy for the life on the Earth so that much attention have been paid to it while long wave radiation on the other hand has not been well studied because of its apparently less importance and also the difficulty of isolating it from other transfers. Studies of long wave radiation exchange have been done mostly by meteorologists who are interested in the change and prediction of weather conditions, the heat balance of the Earth as well as the prediction of frost cover on ground surfaces. In the engineering and architectural fields, the usefulness of the knowledge of sky radiation and radiative cooling, such as for heating and cooling load calculations, building designs and natural air-conditioning application, has also been mentioned.

Solar radiation has long been considered as an important source of energy in the future as traditional sources such as coal and oil become depleted and more expensive. Up to date, the contributions of solar energy and the other sources such as wind, geothermal fields, nuclear power are still small compared with the traditional sources.

Since the reduction of oil production from late 1973, the energy shortage in the world is now more serious than ever. Research to utilize other alternative sources are being initiated or revised in many places.

In New Zealand, which is experiencing a recurrent winter shortages, there is revived interest in promoting research to study increased utilization of other sources of energy available here, solar radiation is one to be mentioned.

The initial purpose of this research was to deal with

long wave radiation study and to have some trial measurement at Christchurch. However, along with the trend mentioned above, solar radiation and the application of it to water heating was included as a starting point for more intensive research of the utilization of solar energy to be carried out by the Mechanical Engineering Department in the coming years.

Therefore the study of thermal radiation exchange between the Sun and Sky, and the Earth, in this particular case, is comprised of two parts:

Part I: Study of long wave radiation from Sky and trial measurement under Christchurch weather conditions.

Part II: Study of solar radiation and the performance of a flat plate solar water heater under Christchurch weather conditions.

P A R T I

STUDY OF LONG WAVE RADIATION FROM THE SKY AND TRIAL MEASUREMENT UNDER CHRISTCHURCH WEATHER CONDITIONS

N O M E N C L A T U R E

A	area of the sensing plate , cm^2
α_s, α_L	absorptivity of the sensing surface for short wave and long wave radiation
C	convection coefficient , $cal/cm^2{}^oChr$
C	conduction component of heat transfers
e	water vapour pressure , mb (milli-bar)
ϵ	effective emissivity of the atmosphere
ϵ_L	emissivity of the sensing surface
f_b	radiation flux of a black body , cal/cm^2hr
f_{iso}	radiation flux of an isothermal layer in the atmosphere cal/cm^2hr
ϕ	relative humidity of the air
H	convection component of heat transfer
h_c	wind coefficient , cal/cm^2hr^oC
I	transmitted radiation intensity , cal/cm^2
I_o	incident radiation intensity , cal/cm^2
k	absorption coefficient of a gas
l	generalized absorption coefficient for all wavelengths
p	air pressure , mb(millibar)
p_o	standard air pressure = 1000 mb
Q	electrical heat input , mW/cm^2
r	correlation coefficient of curve fitting
R	net radiation loss from a surface , mW/cm^2
R_b	black body radiation at air temperature , mW/cm^2
R_L	long wave radiation incoming from the Sky , mW/cm^2
R_{Lv}	long wave radiation obtained by a vertical surface , mW/cm^2
R_s	short wave solar radiation , mW/cm^2
R'_L	long wave radiation from Sky estimated from obtained data , mW/cm^2
$t_a(T_a)$	air temperature , ^oC (^oK) , also t and T
$t_p(T_p)$	temperature of the sensing plate , ^oC (^oK)
T_s, T_L	transmission coefficient for short and long wave radiation (of the cover system of the radiometer)
$T(u)$	general transmission function of water vapour

T_f transmission coefficient of an air layer

t_w wet bulb temperature of air , ^oC

u optical thickness of water vapour in the atmosphere g/cm

U_b overall heat transfer coefficient of the back insulation in the radiometer , $W/m^{2o}C$ or $mW/cm^{2o}C$

V voltage of the extra heating

η efficiency of electrical heating

Δt temperature difference , ^oC

ω specific humidity of water vapour in the air , g (gramme)

z height of the measuring site above sea level , m

ζ zenith distance (angle from overhead direction) , degree

CONSTANT AND CONVERSION FACTORS

σ = Stefan-Boltzmann constant = $5.67 \times 10^{-9} mW/cm^{2o}K^4$

1 cal/cm^2hr = 11.6 W/m^2 = 1.16 mW/cm^2

CHAPTER I LONG WAVE RADIATION FROM THE SKY: ANALYTICAL APPROACH

In a radiation heat transfer problem, the intensity of the sources involved must be known. For long wave radiation exchange occuring in the atmosphere, the temperatures of the radiating surfaces on the Earth can be measured quite easily and accurately so that the outgoing radiation can be calculated from the Stefan-Boltzmann Law. The problem then lies in the question of how much long wave radiation is coming from the Sky or what is the effective radiant temperature of the Sky.

Ångström (1) 1915, Simpson (2) 1928, Brunt (3) 1929 and several other meteorologists did early studies of this problem, but the most extensive study was that of Elsasser in 1942 (4) . He reviewed those earlier studies and analysed the nature of this long wave sky radiation which lead to methods of calculating this radiation intensity from meteorological measurements.

1.1 COMPONENTS OF SKY RADIATION

The principal constituents of the atmosphere covering the Earth consist of oxygen, nitrogen, water vapour, carbon dioxide, carbon monoxide, ozone and dust particles. Among these substances the most important constituents taking part in the radiation exchange between the Earth and the Sky are water vapour, CO_2 and O_3 .

The molecules of these substances reflect and transmit part of the incoming radiation from other sources, the rest

of these radiation are absorbed in the molecules, raising their temperatures, and radiation is then emitted back to the surroundings.

The distribution of these particles in the atmosphere is random, therefore this long wave radiation from the sky has a diffuse characteristic.

Because of the low temperature of these particles, their self-emission is negligible and the radiation from them is due entirely to the absorption of incident radiation from other sources. Therefore at wavelengths where these substances show strong absorption, the radiation from them is also most intense, so that their emissivity is practically equal to their absorptivity. The absorption coefficients of the 3 main substances in the atmosphere are shown in Fig. 1.1. It can be seen from this diagram that the absorption coefficients are usually high for wavelengths $>4\mu$ except in the region from 8 to 12μ where there is very weak absorption by water vapour and CO_2 . This region is called the "window" of the atmosphere where radiation from the Earth surface is freely lost to the outside sky. The relative importance of each of the 3 main substances in long wave radiation emission can also be seen. The most important one is water vapour.

1.2 ABSORBTIVITY OF WATER VAPOUR

The schemetic view of the absorption spectrum of water vapour and CO_2 is shown in Fig. 1.2 . This spectrum consists of numerous narrow strips of intense absorption called spectral lines. There are several hundred lines in the water vapour spectrum alone.

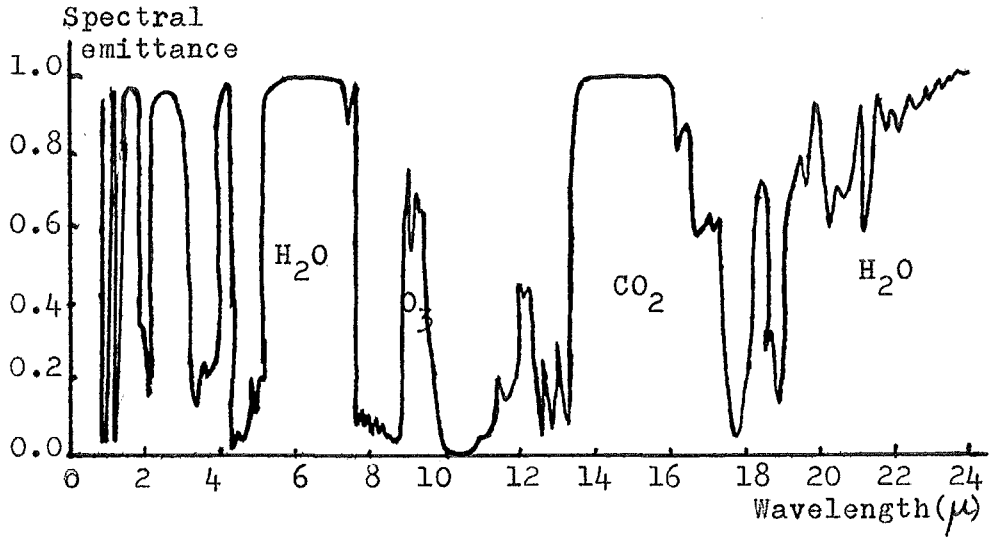

Fig. 1.1 Absorption(emission) coefficients of three main constituents in sky radiation

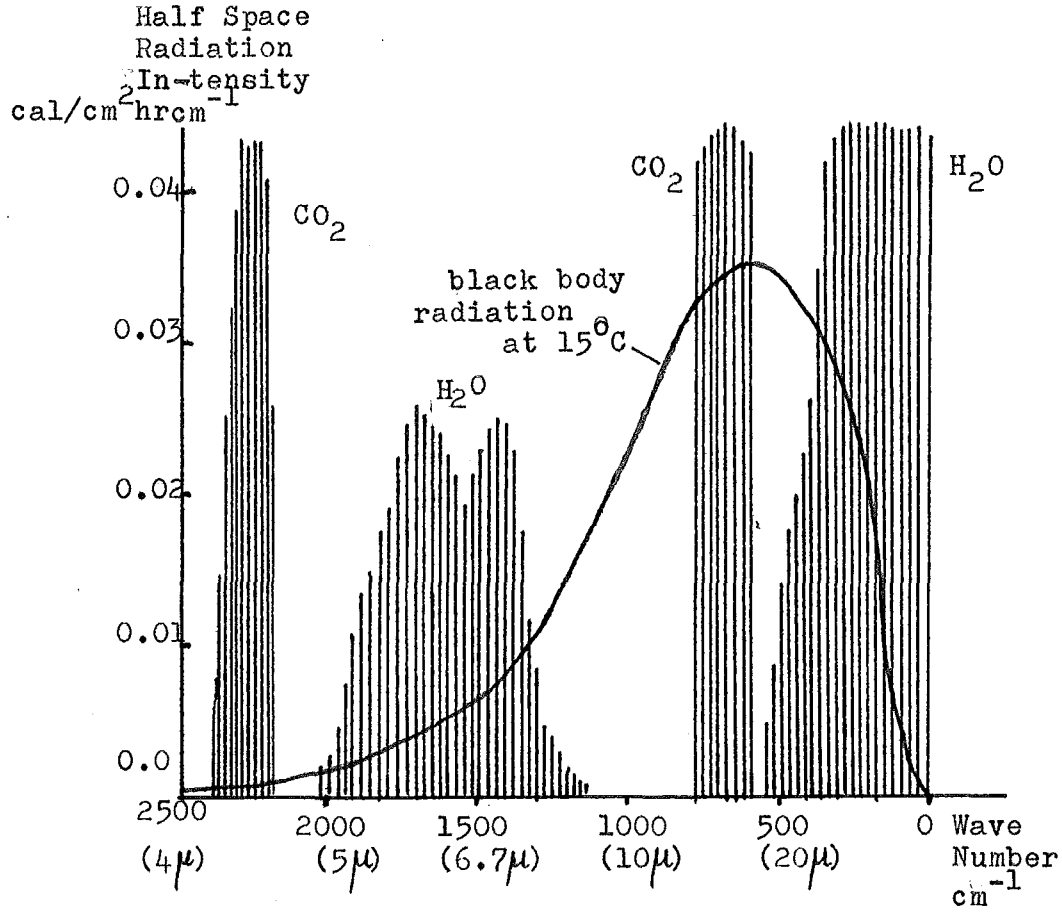

Fig. 1.2 Absorptivity spectrum of H_2O and CO_2

The strongest ablorption of water vapour is concentrated in 2 portions: one near the 6 μ and one at wavelengths $>18\mu$.

According to Elsasser (4), a homogeneous beam of radiation is absorbed in a medium of thickness u according to the law:

$$I = I_0 \exp(-ku)$$

where I = transmitted radiation intensity

I_0 = incident radiation intensity

k = absorption coefficient

This equation holds generally for mono-chromatic radiation (i.e. single wavelength radiation). If the radiation is a mixture of wavelengths, k must be a function of wavelengths and the transmitted intensity is the integral of the above equation over the whole wavelengths.

In this case, a general transmission function T(u) is defined as the ratio I/I_0 with I, I_0 are intensities integrated over the whole wavelengths. For water vapour absorption spectral lines, Elsasser (4) arranged those lines in groups and smoothed the spectrum to give an approximate analytical expression for the mean transmission due to a group of lines as follows:

$$T(u) = 1 - \phi\left(\sqrt{lu/2}\right) \qquad (1.1)$$

where $\phi(x)$ is a statistical function, equals $\frac{2}{\sqrt{\pi}}\int_0^{\infty} e^{-x^2} dx$

The constant l, called the generalized absorption coefficient, has the same effect as the absorption coefficient k and it measures the intensity of absorption due to the group. The numerical values of l for each group can be found from the absorption curve for water vapour at all wavelengths. Fig. 1.3 extracted from Ref. (4) shows values of l for

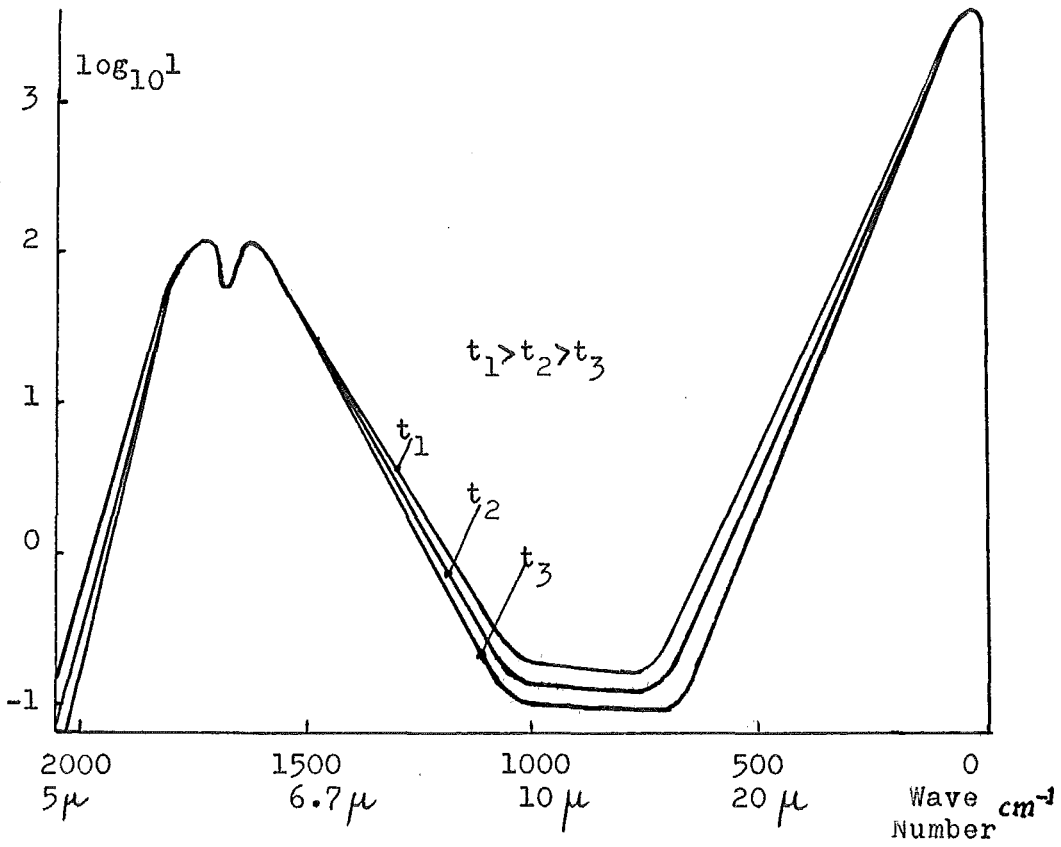

Fig. 1.3 Generalized absorption coefficient l for water vapour

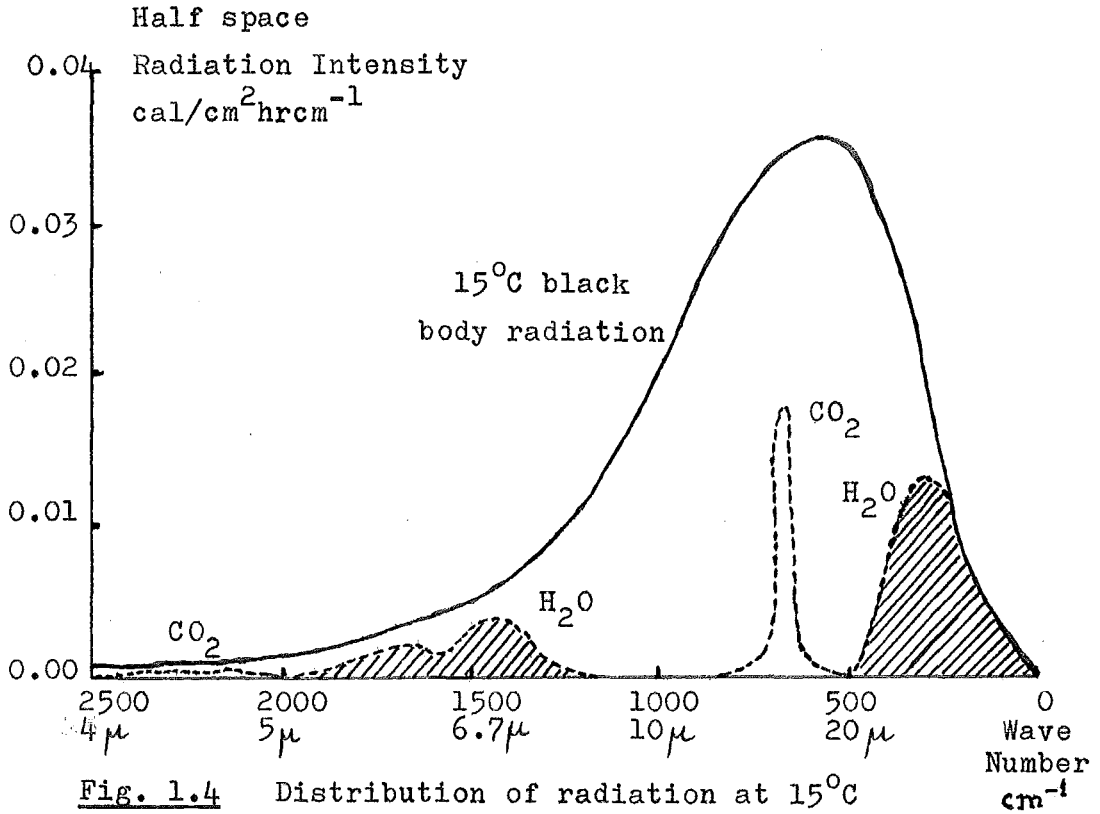

Fig. 1.4 Distribution of radiation at 15°C

different wavelength λ.

The optical thickness u measures the amount of water vapour in the path of a radiation ray. The absorption depends only on the total mass of water vapour encountered by the radiation rays not on the way in which this water is distributed along the path.

It is known that the absorption of a constituent in a mixture depends on its temperature, partial pressure, optical thickness and the total pressure of the mixture (5) . For water vapour in atmosphere, Schnaidt (6) found that its absorptivity is proportional to the square root of air pressure. This result was later confirmed by Strong's experiments (7) .

With such dependence of absorptivity, the optical thickness of water vapour in the atmosphere in vertical direction is given by:

$$u = 1/g \int_{p}^{p_o} \omega \sqrt{p/p_o}\, dp \qquad (1.2)$$

where g = acceleration of gravity

p = air pressure at the point in mb

p_o = standard pressure 1000mb

ω = specific humidity

There is also a small variation of the absorptivity of water vapour with temperature. This variation was calculated by Elsasser and found to be very small so that the absorption of water vapour can be considered independent of temperature. Fig. 1.3 also shows this small variation of l with temperature.

Therefore for any thickness u of the water vapour layer the transmission coefficient can be computed for any group of spectral lines giving the total transmission for the whole spectrum.

1.3 RADIATION FROM WATER VAPOUR COMPONENT

Consider a black body surface and an adjacent isothermal layer of absorbing substance thickness u, transmission coefficient T_f, being in an equilibrium condition under a common temperature T. The radiation flux from the black body surface is f_b. By Kirchhoff's Law the absorbing layer transmits an amount $f_b T_f$ and absorbs $(1-T_f)\, f_b$, it must therefore emit a flux of equal amount $(1-T_f)\, f_b$. If f_{iso} is the radiation flux from the isothermal layer, then

$$f_{iso} = (1 - T_f)\, f_b \qquad (1.3)$$

Now assume that in the atmosphere at some level which has a layer of water vapour optical thickness u below it, there is a thin sheet of moist air having thickness du. Assume also that the temperature of the air layer from the ground to that thin sheet of moist air is the same at T. From equation (1.3) the radiation flux from the thin layer du is:

$$df_{iso} = - f_b \frac{dT_f}{du}\, du \qquad (1.4)$$

where f_b is the radiation flux from the ground transmitted through the water vapour layer u.

df_{iso} is the radiation flux from the thin sheet which actually reaches the ground without being re-absorbed in layer u.

In order to compute the total flux, the atmosphere is assumed to consist of an infinite numbers of thin sheets water vapour and equation (1.4) is integrated over the whole thickness of the atmosphere and over the whole wavelengths of the water vapour absorption spectrum.

Hence total incoming flux from the sky due to water vapour

can be calculated by:

$$F = -\int du \int_0^\infty d\lambda \, f_b \frac{dT_f}{du} \qquad (1.5)$$

Although this equation can give a theoretical estimation of the radiation from water vapour component in the atmosphere the calculations are lengthy and require data of the vertical distribution of air temperature, pressure and humidity.

1.4 RADIATION FROM CARBON DIOXIDE AND OZONE

After water vapour, CO_2 is the next important component in sky radiation. It has 3 absorption bands in the long wavelength region, the most intense band is concentrated at 15 μ region (Fig. 1.2). Although the absorption at 4 μ is also strong, the portion of the black body radiation at normal temperature in the atmosphere is small in this region so that the emission of CO_2 in wavelength near 4 μ is only important for high temperature. The absorption at 10 μ is small, as the case of water vapour, and can be neglected, producing the window region in the atmosphere absorption spectra.

The analysis made for water vapour can also be applied for CO_2. The procedure is somewhat simpler due to the fact that the CO_2 radiation is confined to narrow band so that the black body flux f_b may be represented by the intensity at the band centre. For a 15°C black body radiation coming in, the portion of re-radiation from CO_2 is about 1/8 of that from water vapour. Fig. 1.4 extracted from a paper by Brooks (8) shows this radiation distribution.

For Ozone, Fig. 1.1 shows strong absorption of this substance in the region of 10 μ, where water vapour and CO_2 has weakest absorption. However, because Ozone only appears at high altitude, its effect on the thermal radiation near the ground is not important and usually neglected. For radiation study near the stratosphere, O_3 has much more contribution.

From the above analysis, if the emissivity of each component of sky radiation can be measured, the total sky radiation can be estimated at any temperature from all the flux of each component given by equation (1.5). This total is not simply the addition of the above 3 components but a little smaller because each gas is somewhat opaque to the other so that not all the re-radiation can reach the earth surface.

Measurement of the emissivity of water vapour and CO_2 have been done by Brooks (9), Elsasser (10), Falckenberg (11) and several other workers. Fig. 1.5 and 1.6 are extracted from Elsasser's paper to show the emissivity of these two components.

Based on these results, several analytical methods have been proposed in the form of radiation charts to enable sky radiation to be estimated from meteorological soundings.

1.5 ESTIMATION OF LONG WAVE RADIATION FROM SKY BY CHARTS

Three radiation charts have been devised to help in solving the equation of sky radiations, however the data of vertical distribution of air temperature, humidity and pressure are still required. These data can be estimated from temperature and pressure lapse rate in the atmosphere or by

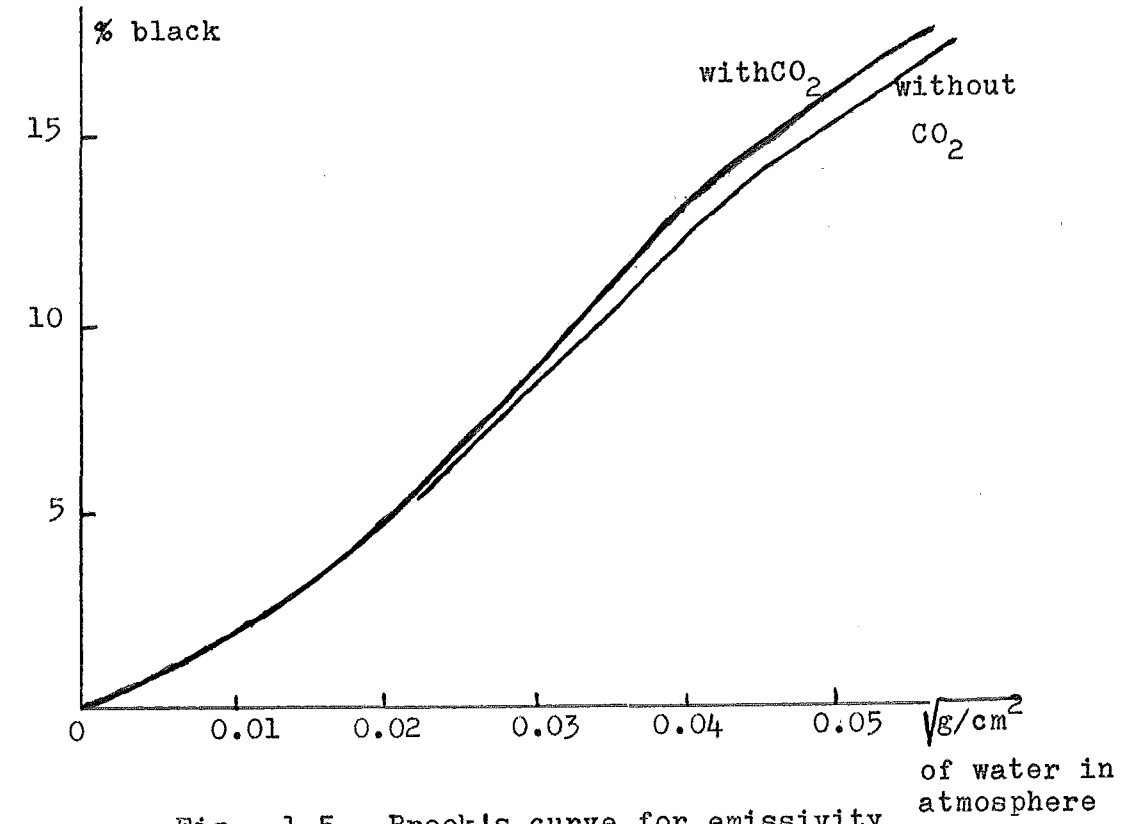

Fig. 1.5 Brook's curve for emissivity of water vapour at 15°C

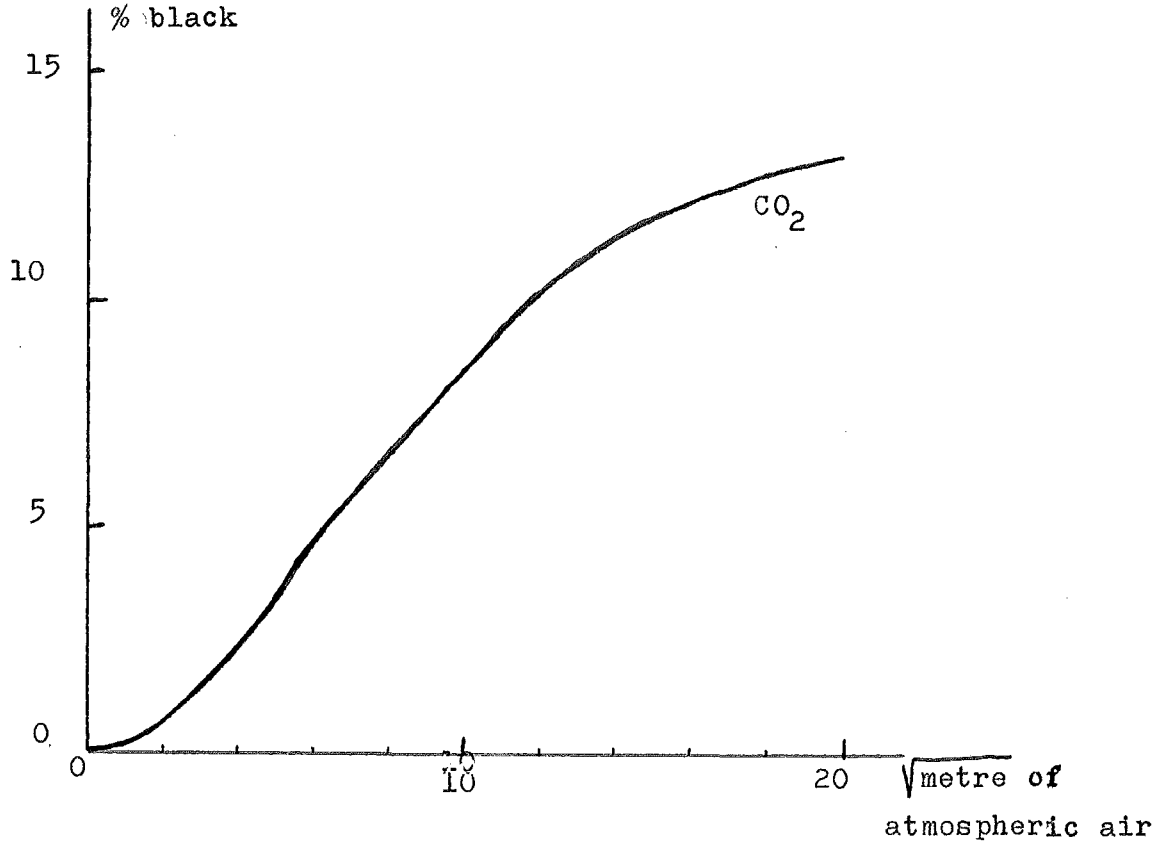

Fig. 1.6 Emissivity of CO_2

direct measurements.

Elsasser chart: Introduced in 1942, uses t as the independent variable (abscissa) and Q (a function of u and T) as ordinate. The radiation intensity is represented by areas enclosed by lines of constant u, t and the curves representing the relationship between t and u in the atmosphere at different levels.

Moller chart: Introduced in 1943, uses u as the abscissa and a variable quantity P (a function of u and T but different from Q) as ordinates. Isotherms and isopleths (lines of constant temperature and lines of constant moisture) are permanently shown on the chart.

Yamamoto chart: Introduced in 1952, uses black body flux as the independent variables. The chart is rectangular, abscissa is proportional to σT^4 and ordinates are proportional to Q/T^3 .

The horizontal axis is normally labeled in terms of both precipitate water and Acos ζ where ζ equals zenith distance, the vertical axis is in terms of both ζ and pressure.

With the Elsasser chart, the initial step is to calculate optical thickness u for given heights in the atmosphere from the values of specific humidity and pressure given in the soundings. These are plotted on the chart and radiation coming in and radiation loss are given by areas enclosed by these curves.

From work at Kew, Robinson (12) found that the Elsasser chart gave results 6 to 14% too high for moderate amounts of radiation, but results corrected to ±3% for high amounts. The

reasons for the inaccuracies are:

1. The proportion of CO_2 in the atmosphere varies although the chart assumes it is concentrated in a limited band centre at 15μ.

2. The chart ignores the effect of emission of radiation by particulate matter.

3. Elsasser's original theory made insufficient allowance for the variation of emissivity of water vapour with temperature and assumed emissivities that are too high for moderate amounts of moisture but more correct for larger amounts.

However, Elsasser and others' charts are useful where the radiation at some heights in the atmosphere is required for meteorological purposes. The requirement of vertical distribution of air temperature and pressure restricts their usage as the estimation of radiation on the Earth surface for engineering and architectural purposes.

CHAPTER II LONG WAVE RADIATION FROM SKY: EXPERIMENTAL APPROACH

Analytical investigations of sky radiation and the radiation charts were not introduced until the late 1940's . Before these, the problems of sky radiation and nocturnal radiation were studied experimentally by Ångström, Brunt and others. They devised instruments to measure this long wave radiation and proposed empirical formulae to fit the results of their observations. After the introduction of the theoretical analysis of sky radiation, more instruments were devised to test the theory and more empirical formulae were proposed to give better agreement with theory and with more observations carried out at different places on the Earth.

2.1 MEASUREMENT OF LONG WAVE RADIATION

If a horizontal plate is exposed to the sky at night it will cool. This is the basis for most of the instruments to measure long wave radiation. There are 3 types of instruments basing on this principle:

(a) Open type instrument with a horizontal black surface receiving radiation from the whole sky.

(b) Box-type instrument in which the receiver is placed at the bottom of a box with a hole at the top.

(c) The telescope type in which the receiver is located in the focal plane of a concave mirror.

Types (b) and (c) can only observe a limit angle of the sky at a time. The radiation of the whole sky then can be measured by pointing the instrument to different zones of the

sky and taking the total with addition of some correction factor depending on the instrument. These types of instrument are not as good as type (a) for total sky measurement but they are useful to obtain the distribution of sky radiation over the zenith angle (zenith angle is the angle from the overhead direction).

For type (a) instruments, the black surface receiver exchanges heat with the sky in the modes as shown in Fig. 2.1 . The components which are interested in the long wave radiation exchange are R_p and R_L . The difficulty arises as how to eliminate the other components. Several methods can be applied to reduce these to negligible amounts compared with R_p and R_L. The solar radiation R_s appears only at daytime so this can be avoided by using the instrument at night-time only. In cases where measurements at daytime are required, a solarimeter is normally set besides the long wave intrument to measure R_s and this is subtracted from the total radiation received by the black surface. The convection component is rather more difficult to eliminate. One method is to compensate the fall of temperature of the black plate by electrical heating. The energy input can be known when the instrument reached the temperature equilibrium with the surrounding air so that no convection transfer occurs between the plate and the air.

Ångström in 1915 (1) used a radiometer consisted of four exactly equal thin strips of manganin, dimensions 2 cm x 0.3 cm. Two are blackened while other two are kept reflecting. Junctions of thermocouples are alternately fastened to the black and reflecting strips. The black strips are electrically heated until all strips are at the same temperature. The

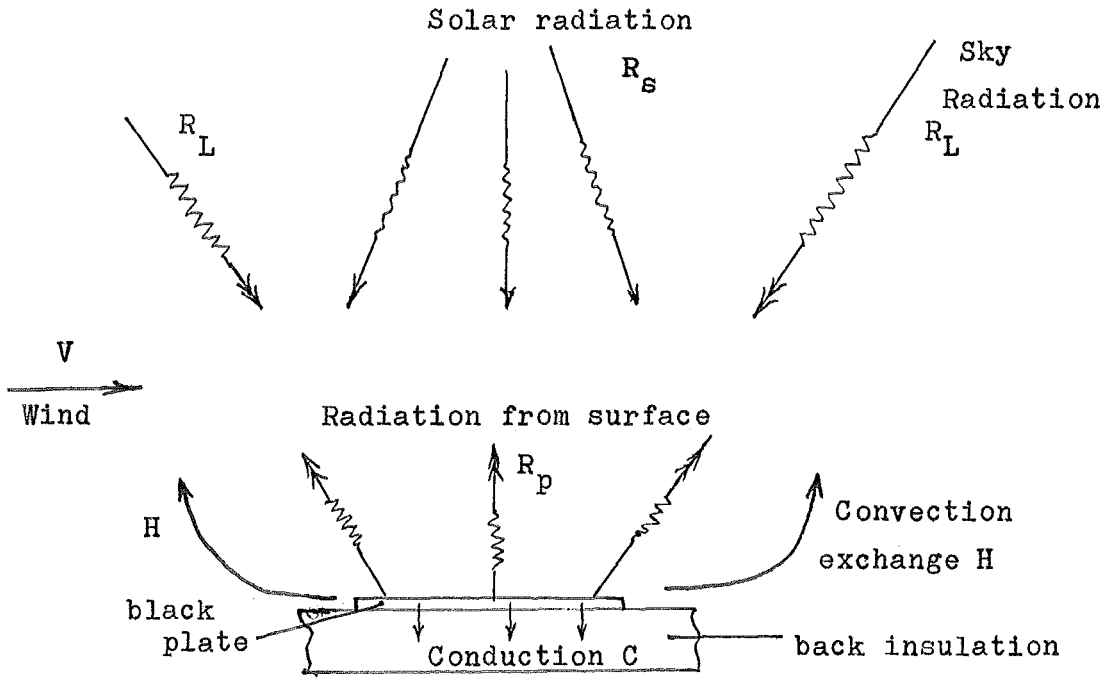

represents long wave radiation

represents short wave radiation

represents conduction

represents convection

Fig. 2.1 Heat exchange at a black surface exposed to the sky

effect of wind on this instrument was found to be considerable in spite of the heating compensation, giving a too low estimation of heat loss to the sky.

Albrecht in 1928 (13) used a plate which is heated sucessively with 2 different currents producing the amount of heat Q_1 and Q_2 . If R is the radiative heat loss:

$$Q_1 - R = C(t_{p1} - t_{a1}) = C\,\Delta t_1$$

$$Q_2 - R = C(t_{p2} - t_{a2}) = C\,\Delta t_2$$

C is a coefficient depending on wind velocity but it is assumed to remain constant during the time of measurement.

Two equations above give the radiation heat loss R as:

$$R = \frac{Q_2\,\Delta t_1 - Q_1\,\Delta t_2}{\Delta t_1 - \Delta t_2}$$

Aldrich in 1922 (14) refined Ångström instrument and developed a new instrument called the Melikeron (honey-comb) shown in Fig. 2.2 . The essential part was a honey-comb like structure made by strips of a special alloy 1.2 cm wide and 0.05 mm thick. These strips were insulated from each other by a shellac cover and connected in series so that the compensating current would heat them homogeneously. A slanting mirror was placed underneath the honey-comb to reflect the escaped radiation back to the strips. A hemisphere cover were used but there was no mention of the material for this cover. A removable glass hemisphere was also provided for solar radiation measurement. The effect of wind is much less for this instrument due to the hemispherical cover.

The American Society of Heating and Ventilating Engineers

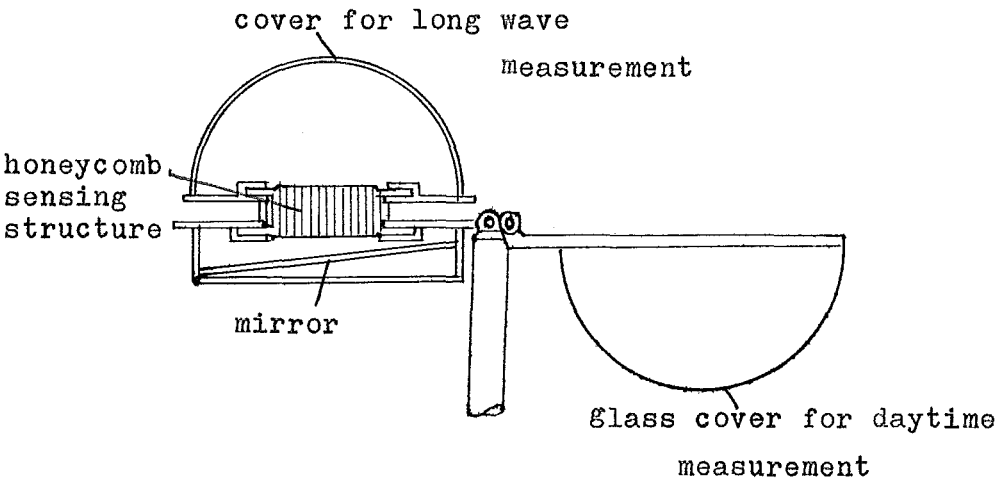

Fig. 2.2 The Melikeron radiometer

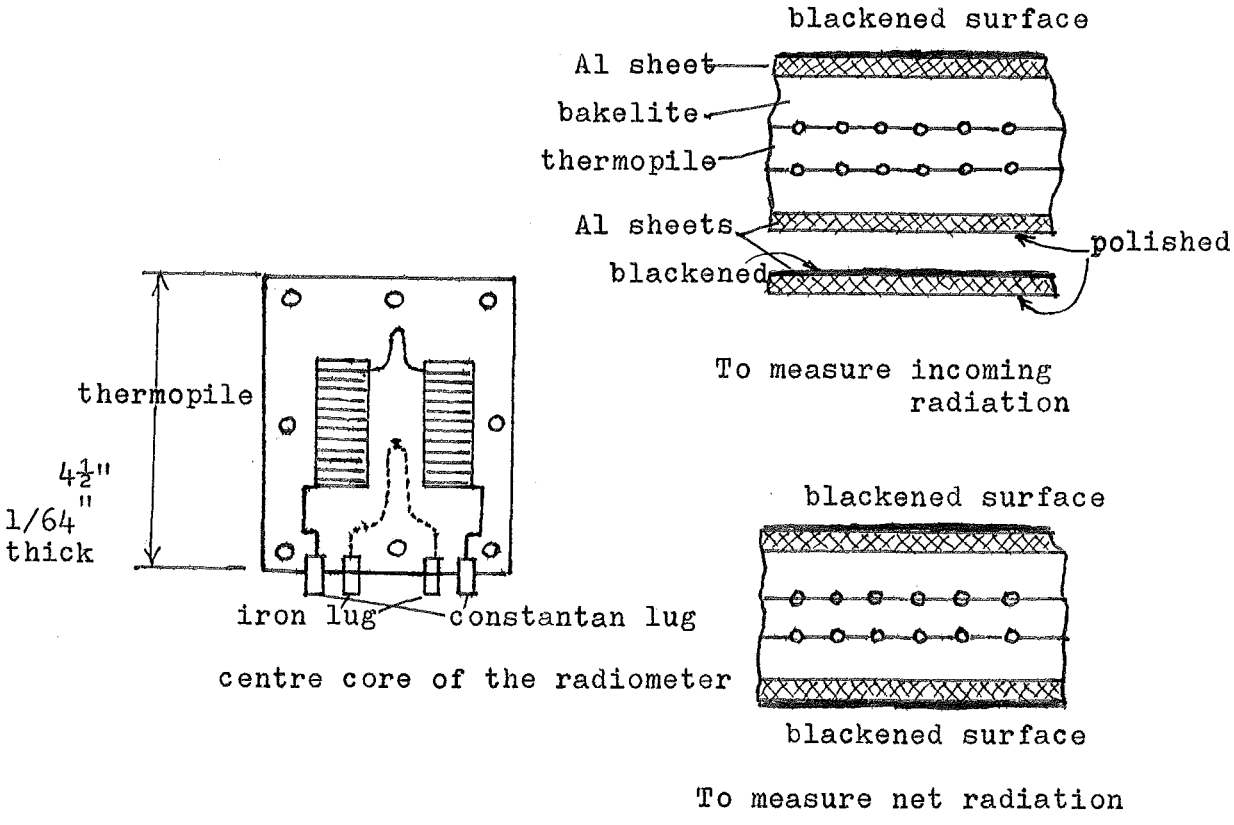

Fig. 2.4 Gier & Dunkle's Radiometer

(ASHVE) in 1951 carried out a research of the significance of long wave radiation exchange on the heat load and heat loss calculations for building purposes (15). This was one of very few studies on long wave radiation with engineering purposes. ASHVE developed a type of radiometer called convection compensated radiometer which based on similar principle used by Albrecht.

A small blower were added to ensure constant convection coefficient C during period of measurements. A heat-flow meter and a second heater were also added to the back of the plate to measure and reduce the back loss. These additions are required because the instrument were designed to measure radiation at daytime as well so that the plate temperature could be high resulting a significant conduction loss through the back. Fig. 2.3 shows the main components of the ASHVE radiometer.

Gier and Dunkle (16) later developed an aspirated black plate radiometer which can measure long wave radiation from the sky as well as net radiation exchange between the Earth surface and the sky. Fig. 2.4 shows the construction of this radiometer.

It consists essentially of a thermopile made of constantan wire wounded on a bakelite sheet and silver plated over half of the width. This centre thermopile is covered on top by a blackened thin aluminum sheet. To measure the incoming radiation from the sky the underside of the thermopile is covered with a thin aluminum sheet, another sheet, blackened on the top surface and polished on the bottom, is placed underneath the first sheet to serve as a shield from radiation from

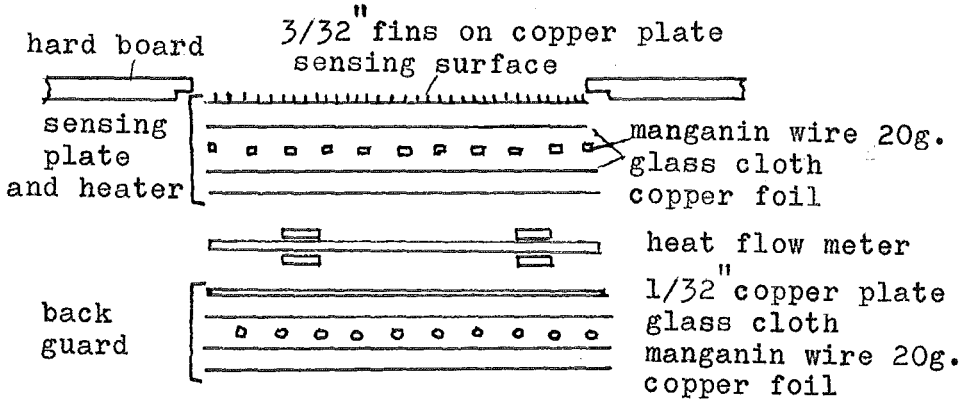

Fig. 2.3 The ASHVE Radiometer (main elements)

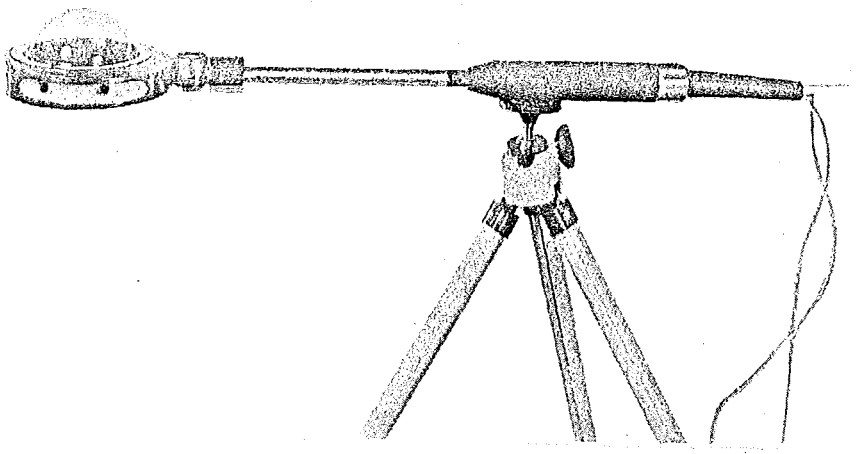

Fig. 2.5 Funk's Radiometer

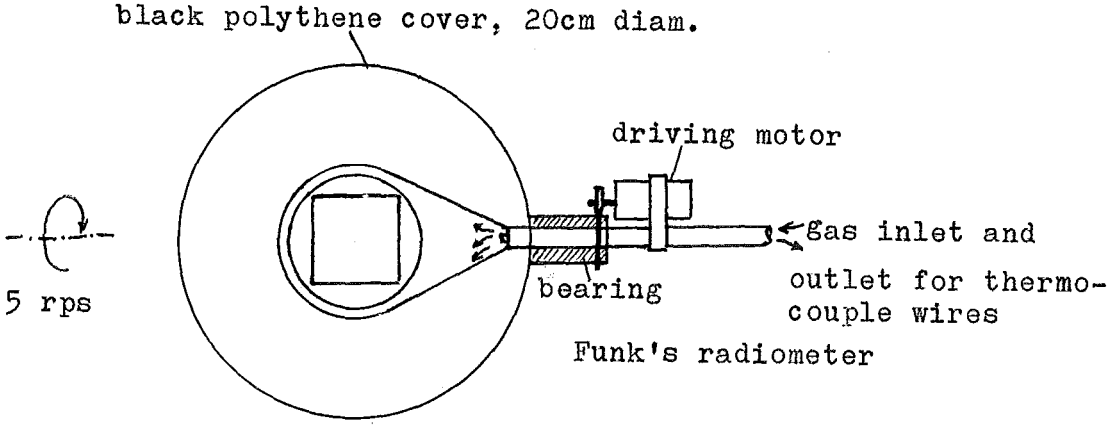

Fig. 2.6 Modified Funk Radiometer

below and prevent back loss as well. To measure the net radiation exchange the underside of the centre thermopile is covered by a thin aluminum sheet similar to the top cover. A blower is also used to give a constant air flow on the top and bottom surfaces of the whole assembly.

Output of the thermopile in mV, and the mean plate temperature T_m are measured to obtain the total incoming long wave radiation by:

$$R_L = kV + \sigma T_m^4$$

where k is a constant found by calibration.

The nett exchange between the sky and ground is given by:

$$R = kV$$

Although the methods using compensating heating and constant air stream can eliminate the convection component in the radiation study of heat exchange, they are prone to large error because the sky radiation intensity is low, increasing the convection loss may offset the radiation effect.

Earlier instruments avoided using a cover on the receiver surface to eliminate convection transfer because no material was known to transmit long wave radiation at that time. Glass transmits a large portion of short wave radiation but it is almost opaque to long wave radiation. With the advance of chemical technology, several types of plastic have been found transparent to long wave radiation.

Therefore Funk in 1959 (17) used similar construction of the sensing elements as Gier & Dunkle to develop a new type of instrument called Polythene Shielded Net Radiometer which are widely in use today. Fig. 2.5 .

In principle, the measuring element consists of a thermopile centre and aluminum sheet covers as for the other instruments but the size is smaller, 2 cm to 5 cm in diameter. Hemisphere made of 0.002" thick polythene film covers the top, and bottom if measuring net radiation, of the receiver surface with retaining ring to keep it air-tight. A constant supply of dry air keeps these covers inflated and prevents the convection exchange between the plate and the air. The output of thermopile element, which consists of 10 to 50 junction thermocouples in series, is measured in mV and from the calibrated sensitivity of the radiometer the incoming radiation or net radiation exchange can be obtained.

Paltridge (18) modified Funk's radiometer by using a black polythene cover instead of transparent polythene. Thick black polythene layer, 0.12 mm, showed about 40% transmittance to long wave radiation (wavelength $>14\,\mu$) but very little transmittance to short wave radiation so that it can be used in the presence of solar radiation . The shell is also spun continuously at about 5 rps (revolution per second) to reduce the effect of short wave heating. Fig. 2.6 shows this modified long wave net radiometer.

At present, none of the above instruments is considered as standard but the most widely used for long wave and net radiation study is the Funk and the modified radiometer.

2.2 EMPIRICAL FORMULAE FOR SKY RADIATION

As seen from the analysis in Chp. I, the incoming sky radiation does not follow any simple law because of the great variation of moisture and temperature distribution found in

the atmosphere. Upper air soundings are not always available for the estimation from analytical calculations or radiation charts, therefore obsevers in the past tried to correlate the incoming radiation with the elements of observations at the ground such as temperature, pressure, moisture content.

These effort have led to a number of empirical formulae, some only valid for a particular site, some claimed to have universal application for any places.

Ångström in his early research in 1915 measured the sky radiation with his own instrument (described in earlier part) and proposed this relationship between clear sky radiation and the radiation of a black body at air temperature:

$$R_L / \sigma T_a^4 = a - b10^{-\gamma e} \qquad (2.1)$$

where a, b, γ are constants and e is vapour pressure of the air in mb. These constants were changed several time to give better fit with a greater number of observations originally suggested by Angstrom as:

$$a = 0.806 \ , \quad b = 0.236 \ , \quad \gamma = 0.052$$

Observations from other observers were also tried to fit into this form by Raman (19) giving a wide variation in the values of these constants. Several examples of other constants are shown below:

Observations from	a	b	γ
Kimball , U.S.A.	0.80	0.325	0.070
Eckel & Kanzelhohe, Austria	0.71	0.24	0.074
Rananathan & Desai, India	0.78	0.27	0.040
Raman , Poona, India	0.79	0.273	0.051

Usually the individual observations also showed wide scattered about these curves.

Brunt in 1932 (20) analysed the observations of Dines & Dines made in England (1927) and proposed the following relation:

$$R_I/R_b = a + b\sqrt{e} \qquad (2.2)$$

where a and b are constants having values:

$$a = 0.53 \ , \quad b = 0.065 \ , \quad R_b = \sigma T_a^4$$

with correlation coefficient $r = 0.97$

Elsasser in his review of these studies (1942) presented a table of different constants a and b with correlation coefficient r for various observations made at several different places. Some of these values are extracted as below:

Observations from	a	b	r
Asklof, Upsala, Sweden	0.43	0.082	0.83
Ångström, Mt. Whitney, USA	0.50	0.032	0.30
Kimball, various places in USA	0.53	0.062	0.88
Raman, Poona, India	0.62	0.029	0.68

These correlation coefficients were not as high as that of Brunt's analysis.

In formulae (2.1) and (2.2) the height of the observer above the ground and the change in temperatures were not taken into account. With equal temperature and vapour pressure at the ground, the total amount of moisture overhead is less at a higher level than at sea level. This amount of moisture is the most important constituent in the long wave sky radiation as seen from Chp. I . To modify this lack of attention for

height and temperature in Ångström and Brunt formulae, Robitzsch (21) suggested another formula:

$$\frac{R_L}{R_b} = \frac{0.135p + 6\ e}{T_a} \qquad (2.3)$$

where p = air pressure in mb

T_a = air temperature at the measuring site

However this new formula was not widely recognised because Raman found that the series of observations leading to this relationship was having systematic error.

In 1963, Swinbank (22) criticised again three inadequacies of Brunt's and Angtrom's formulae:

1. The wide variation with locality of the constants a, b, γ.

2. The lack of dependence on elevation. Later experiments showed that the amount of water vapour above any given level in the atmosphere is proportional to the cube of the atmospheric mass above that level (23).

3. The ratio R/R_b which can be considered as the effective emissivity ϵ of the atmosphere does not depend on temperature according to those formulae. In the case of a limited isothermal atmosphere, ϵ would be less than one and independent of temperature only if the atmosphere were of a constant greyness. This is not the case for water vapour emission. Therefore in principle, ϵ must be temperature dependent in any circumstances.

Using the results of Dines's observations, which Brunt used to arrived at his formula, Swinbank found the regression line between R_L and σT_a^4 as:

$$R_L = -11.29 + 1.029\,\sigma T_a^4 \quad \text{in mW/cm}^2$$

with a remarkable correlation coefficient r= 0.988.

Swinbank also gave reason for the high correlation between $R_L/\sigma T_a^4$ and $\sqrt{e}$ for this same set of observations (i.e. 0.97 by Brunt's formula). The significant was due to high correlation between σT_a^4 and $\sqrt{e}$ (r =0.954) at that locality When the correlation between temperature and humidity at a place is poor, variation in a and b can result when trying to fit the data into the form

$$R_L/\sigma T_a^4 = a + b\sqrt{e} \quad \text{or} \quad R_L/\sigma T_a^4 = a - b10^{-\gamma e}$$

Further measurements were made by Swinbank with Funk radiometer to support his proposal of the sole dependence on temperature of sky radiation. His observations combined with those of others were plotted showing a close fit to the regression line:

$$R_L = -17.09 + 1.195\,\sigma T_a^4 \quad \text{in mW/cm}^2 \qquad (2.4)$$

with correlation coefficient r = 0.988

Fig. 2.7 is the graph extracted from Swinbank's results. Same results were also plotted versus $\sqrt{e}$ giving regression line :

$$R_L/\sigma T_a^4 = 0.64 + 0.037\sqrt{e}$$

showing not as good fit as the above estimation and yet another set of a and b for Brunt formula. Fig. 2.8 is also extracted from the same paper to show this relation.

To give a clearer idea of the dependence of ϵ in temperature, Swinbank went on to analyse the correlationbetween

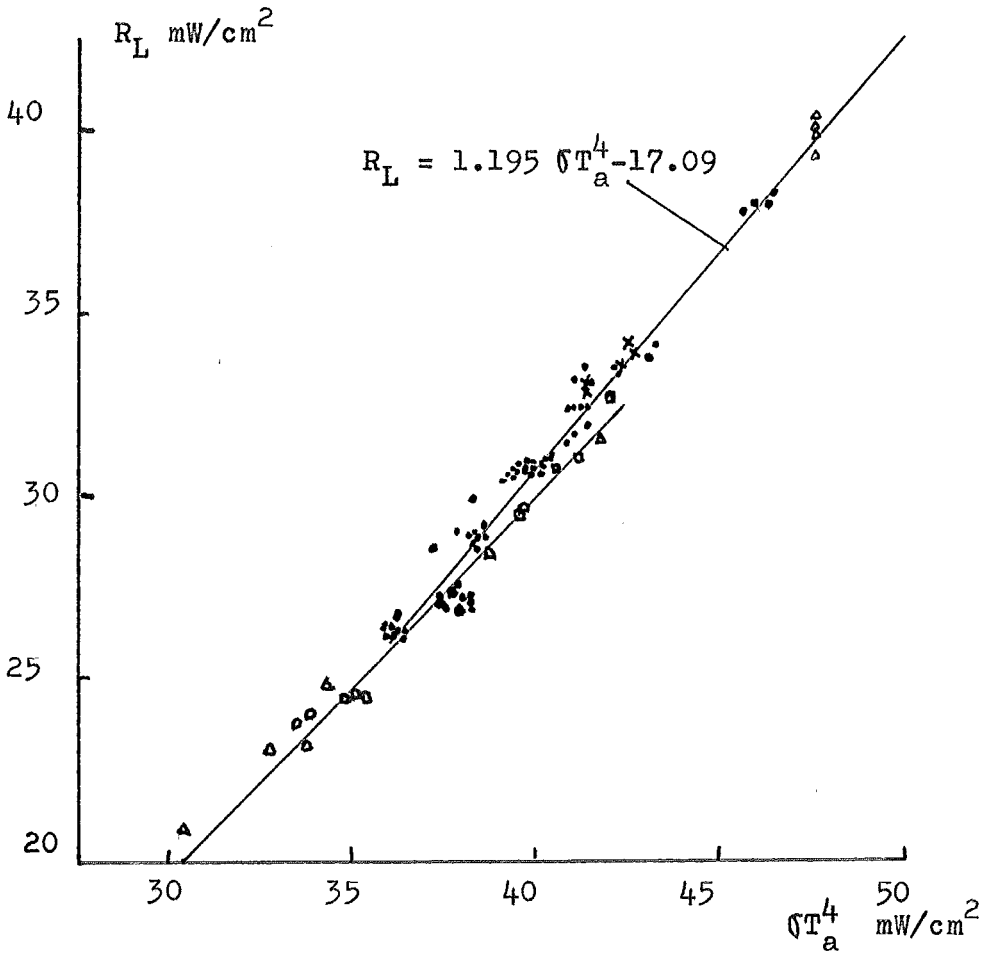

Fig. 2.7 Results of Swinbank's experiments

(extracted from Ref. 22)

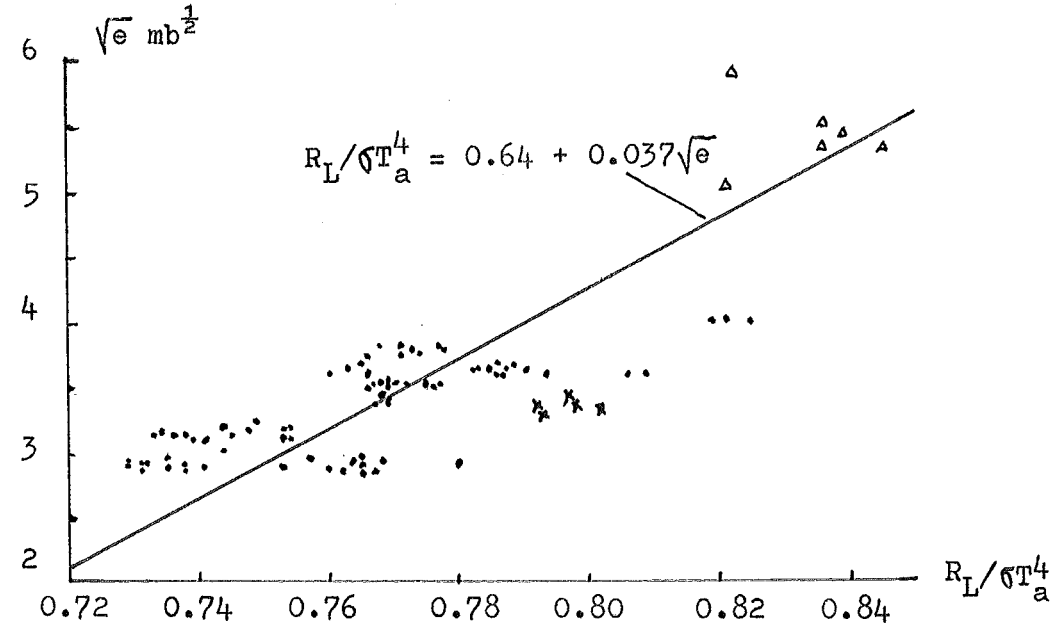

Fig. 2.8 Results of Swinbank's experiments

(extracted from Ref. 22)

$\log_{10} R_L$ and $\log_{10} T_a$ to see if a power other than four is more suitable for the above expression.

The analyses based on his observations and Dines' earlier observations gave another expression for R:

$$R_L = 5.31 \times 10^{-14} T_a^6 \quad \text{(for Swinbank's observation)} \quad (2.5)$$
$$r = 0.985$$

and $R_L = 5.21 \times 10^{-14} T_a^6$ (for Dines' observation) r= 0.989

The close results of these two analyses supported the expression in this form, the former formula was suggested because of larger observations. This suggested that the effective emissivity of sky depends on T^2 which seems rather high compared with the variation of 1 with temperature shown in Fig. 1.3 .

These expressions proposed by Swinbank are no doubt simpler and more significant than Brunt's formula. However because this was arrived at empirically so that neither can be used confidently in a region where it has not been tested by direct measurements.

As shown by Businger in the Discussion Part of Swinbank's paper, large deviation ($> 5\%$) from Swinbank's first expression were experienced.

Deacon (24) proposed a correction term to Swinbank's first formula for the effect of change in elevation:

$$R_L = R_s - 0.035(z/1000)\ \sigma T_a^4 \quad (2.6)$$

where R_s = sky radiation estimated by Swinbank's formula

z = elevation of measuring site in metre above sea level

Idso & Jackson (25) in a recent paper (1969) did a theoretical analysis of the atmospheric thermal radiation by

using a computer to calculate this radiation based on the emission spectrum of the three components H_2O, CO_2, and O_3 in the atmosphere.

This analysis showed that in the region -50°C to 80°C the relationship of R_L with T_a^4 is quite linear. For very low temperature range R_L varies with a power of T_a less than four. Thus there appears to be no theoretical justification for the power of T_a being greater than four for any temperature obtainable on the Earth . The dependence of the effective emissivity of the sky on T^2 as proposed by Swinbank is then much overestimated. Therefore Idso & Jackson postulated that immediately above 273°K atmospheric thermal radiation may be described by an exponential function of temperature :

$$R_L = T^4(1- c \exp(-d(273 - T)^2) \qquad (2.7)$$

assuming that the variation of effective emissivity ϵ of the sky is symmetrical about 273°K.

In equation (2.7) c and d are constants, the term $(273 - T)^2$ keeps R from being greater than black body radiation at too high and too low temperature.

Observation made by Idso & Jackson, in addition to Swinbank's results, had been fitted to this latest proposed formula giving correlation coefficient r = 0.992 with

$$c = 0.261 \qquad d = 7.77 \times 10^{-4}$$

Therefore Idso & Jackson's sky radiation formula was suggested as:

$$R_L = \sigma T_a^4 \left[1 - 0.261\, e^{(-7.77 \times 10^{-4}(273-T_a)^2)}\right] \qquad (2.8)$$

in mW/cm^2

From their analysis and the expanded numbers of data involved, Idso & Jackson concluded that this equation

accurately describes a general relation between clear sky atmospheric radiation and screen level air temperature, and this should be valid at any latitude and for any air temperature reached on the Earth.

To find out if the difference in sky radiation given by formulae (2.4), (2.5) and (2.8) is significant. These functions are plotted and compared with the black body radiation curve as shown in Fig. 2.9 .

It is noticed, from this plot, that differences are large for air temperature below $5^{o}C$ and above $35^{o}C$. In the range from 5 to $35^{o}C$, maximum difference is only 7.6% which is rather small for engineering applications. For the range of temperature normally encountered in thermal environmental engineering problems, only at low air temperature ($<5^{o}C$) that the discrepancy due to those formulae is significant. However, not any of those formulae is widely recognised as standard so that their uses depend on convenience and whether local measurements have been made to justify them.

2.3 FACTORS AFFECT SKY RADIATION AND RADIATIVE HEAT LOSS

Considering all the proposed formulae from (2.1) to (2.8) the dependence of sky radiation on the amount of water vapour in the atmosphere is always recognised either explicitly such as formulae (2.1, 2.2) or implicitly by the relationship between water vapour and temperature as other formulae. This is in agreement with the results of analytical investigation in Chp. I. However these formulae are valid only for clear sky condition. During cloudy periods, they give too low sky radiation because the cloud, however thin, can also act as

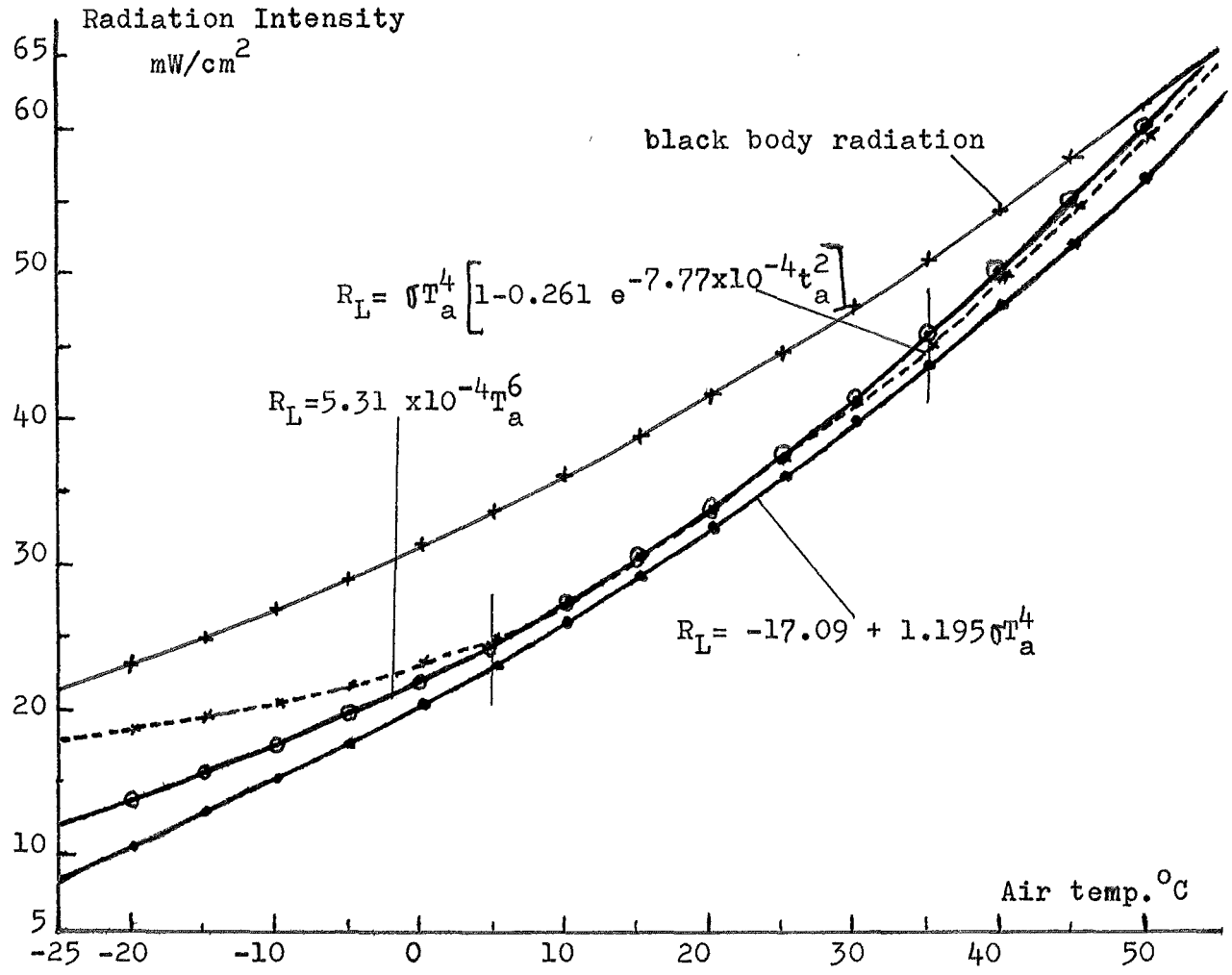

Fig. 2.9 Comparisons of the empirical formulae proposed for long wave sky radiation

a black body and re-radiates all the radiant heat coming in back to the earth. The Elsasser chart provides the estimation of the sky radiation in intermittent condition by taking the optical thickness u into account, but if the sky is completely covered by even a thin cloud he suggested the black body line corresponding to $u = \infty$ to be used. Actual measurements by Dines (26) showed the average radiation in completely overcast conditions is about 96% of black body radiation.

Attempts have been made by Askof and Ångström (27) to modify the empirical formulae for cloudy sky estimation. The net heat loss from ground under fully overcast condition is estimated by:

$$R = \beta(R_b - R_L) \qquad (2.9)$$

where R_b = radiation of black body at air temperature

R_L = sky radiation calculated by Angstrom formula (2.1)

β is always < 1 and depends on the height of the cloud deck as shown below:

cloud height	1.5	3	7	(Km)
β	0.14	0.25	0.8	

This variation of β suggested that the heat loss is more when sky is covered by high cloud than when it is covered by low cloud.

All the above formulae were arrived at from measurement made for horizontal surface. For engineering purposes, the variation of incoming sky radiation with inclination and orientation is also interesting. Because of the diffuse characteristic of sky radiation, large variation with inclination and orientation as for solar radiation is not

expected, however the effect of radiation from other objects around the surface may be important. Parmelee and Aubele in their study with the ASHVE convection compensated radiometer (16) showed that the ratio of long wave radiation received by a vertical surface on clear days over that received by a horizontal surface varies from 1.13 to 1.30. This ratio is smaller for other inclination e.g. 1.1 to 1.2 for 30° from vertical, 1.02 to 1.07 for 60° from vertical. In general, the long wave radiation received by an inclined surface is extremely variable because the ground contribution depends very much on the ground cover and proximity of the surface. Based on the analysis of Brunt (20), the radiation received by a vertical surface from a cloudless sky was proposed as:

$$R_{Lv} = R_b \, (0.30 + 0.028 \sqrt{e}) \qquad (2.10)$$

This equation can be used to estimate the contribution of ground and surroundings to the total radiation on a vertical surface.

With the knowledge of the incoming radiation to any surface from above considerations, the net radiation loss from the surface then depends on its emissivity ϵ_p and temperature t_p and is given by:

$$R = \epsilon_p \sigma T_p^4 - R_L \qquad (2.11)$$

CHAPTER III LONG WAVE RADIATION MEASUREMENT UNDER CHRISTCHURCH WEATHER CONDITIONS

For Christchurch , no data of the long wave sky radiation have been available either from literature or from the Christchurch Weather Office. Under Christchurch weather condition with large portion of clear night sky during winter time, this component of radiation exchange can be significant.

3.1 DEVELOPMENT OF THE RADIOMETER

(A) DESCRIPTION OF THE RADIOMETER

In order to carry out some measurement of this sky radiation, a radiometer capable of measuring long wave radiation is required. Because the required accuracy for this initial study is not as high as that for meteorological study, it was decided to make a simple low cost radiometer instead of buying a more sensitive but expensive one.

A flat plate type instrument which receives total hemispherical sky radiation is preferred to restricted view type radiometer because the former is more easier to use and simpler to make. The design of the radiometer used in this experiment was based on the principles of the ASHVE convection compensated radiometer and the Funk's polyethylene shielded net radiometer. Main elements of the radiometer are described below and shown in Fig. 3.1 .

1. Sensing element:

This is a copper plate, 20 gauge, 8 cm diameter. The thickness and size of this plate was chosen so that it gives a negligible thermal resistance and thermal inertia effect

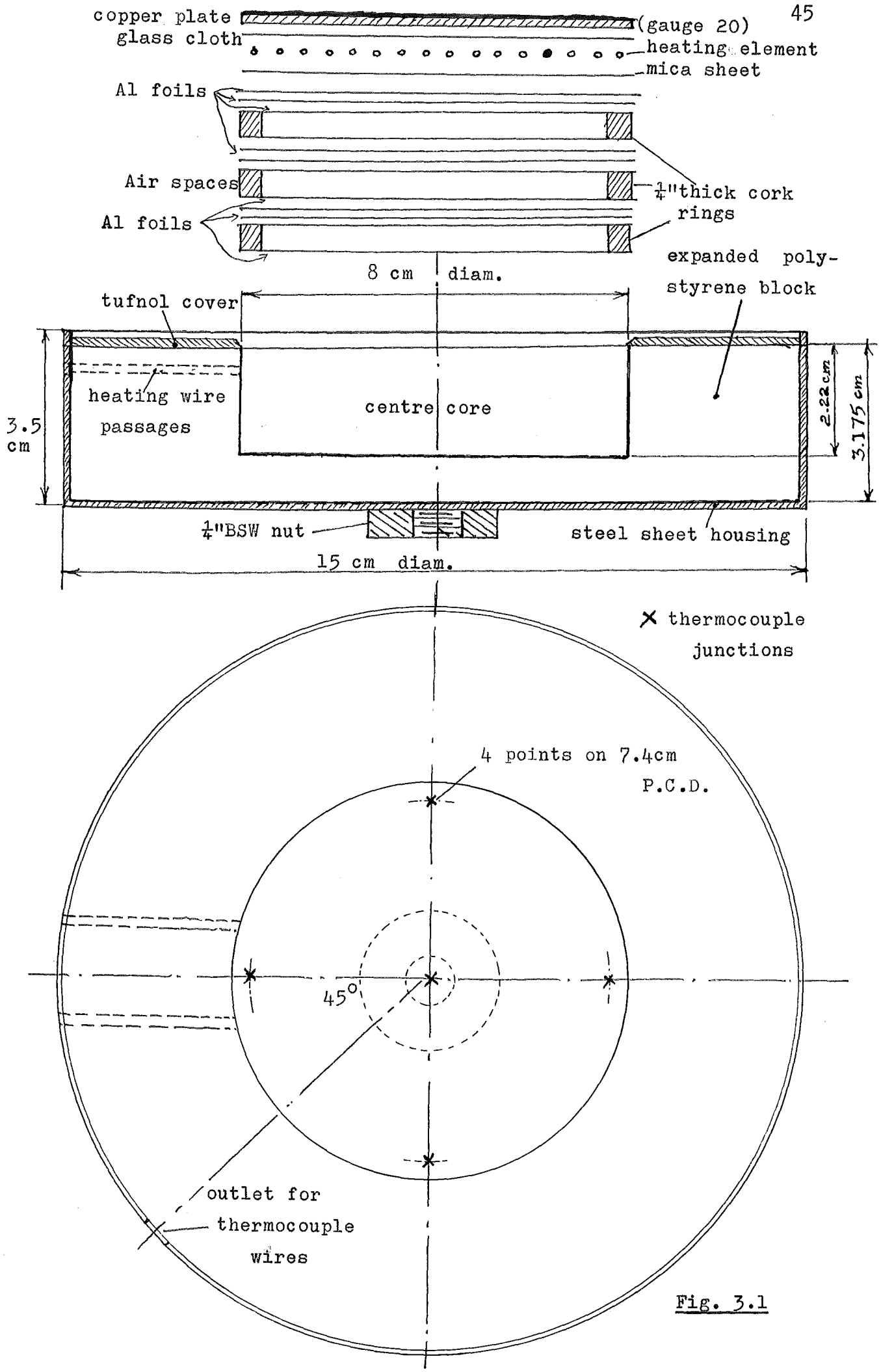
copper plate
glass cloth
(gauge 20)
heating element
mica sheet
Al foils
Air spaces
Al foils
¼"thick cork rings
8 cm diam.
expanded polystyrene block
tufnol cover
heating wire passages
centre core
3.5 cm
2.22 cm
3.175 cm
¼"BSW nut
steel sheet housing
15 cm diam.
× thermocouple junctions
4 points on 7.4cm P.C.D.
45°
outlet for thermocouple wires

Fig. 3.1

while it also ensures a uniform temperature over the surface. The size of this plate is larger compared with Funk's radiometer to enable the heating element to be attached underneath. The surface is painted matt black to give an emissivity and absorptivity of 0.95 .

2. Measuring element:

Five 30 gauge copper-constantan thermocouples are attached to the upper surface of the sensing plate, four around the edge and one at the centre. Care has been taken to make sure the thermocouple junctions are in good contact with the plate. These junctions are soldered and flattened before cemented to the copper plate by araldite adhesive. Outputs from these thermocouples can be measured individually, in parallel or in series as desired.

Individually, these points give the temperature distribution over the plate surface. A uniform plate temperature is assumed when the difference between the five points is less than $1^{o}C$.

If connected in parallel, the output shows the average temperature of the plate. The necessary condition that the five branches must have the same resistance is satisfied because these branches are of same materials and nearly equal length.

The series connection of these thermocouples gives the effect of a thermopile where all five outputs are added up. This has advantage over parallel connection when output is small.

3. Insulation:

To concentrate on the radiation exchange, other forms

of heat transfer such as conduction and convection must be minimized or eliminated. In this case, the conduction loss from the heated plate to the back and around is minimized by an insulation structure consisted of aluminum foils, air spaces and expanded polystyrene block. Aluminum foil with high reflectivity is lined on the inside surface of the housing and used to form air spaces beneath the copper plate. Expanded polystyrene which has high thermal resistance and low density due to numerous air spaces inside its structure is preferred than fibreglass which has same resistance but heavier density.

Fig. 3.1 shows the components of the insulation structure. A cylindrical expanded polystyrene block of 15 cm diameter and 3.175 cm thick is the largest part of the whole structure. At the centre, a 8 cm diameter and 2.22 cm depth core is cut from the block. This core is lined with aluminium foil and it provides space for the sensing plate, heating element and air spaces insulation.

Air space is formed by facing aluminium foils on both side of a cork ring, 8 cm O.D., 7 cm I.D. and $\frac{1}{4}$" thick. Three such air spaces are stacked into the core and bonded to the polystyrene wall by Bostik adhesive before the heating element and sensing plate is assembled.

4. Heating element:

A heating element is added to provide extra heating during severe weather conditions. In order to distribute the heat supply uniformly to the plate, the heating wire is arranged as shown in Fig. 3.2 . This arrangement was chosen after several trials because it gives less than $1^{o}C$ difference

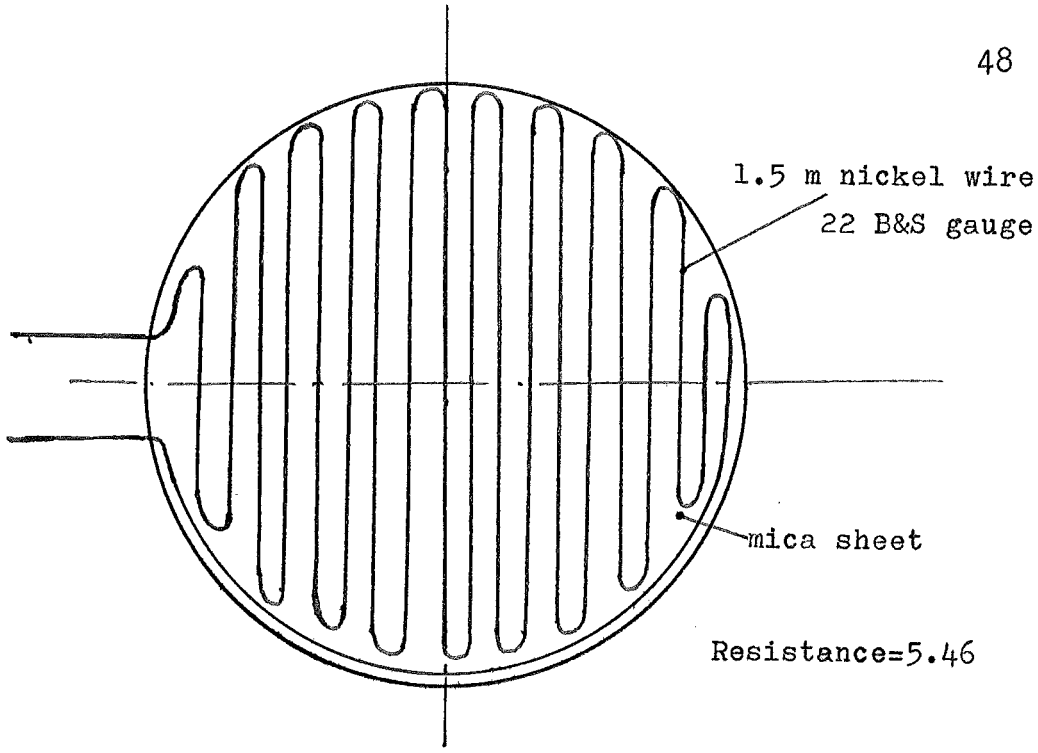

Fig. 3.2 Arrangement of the heating element

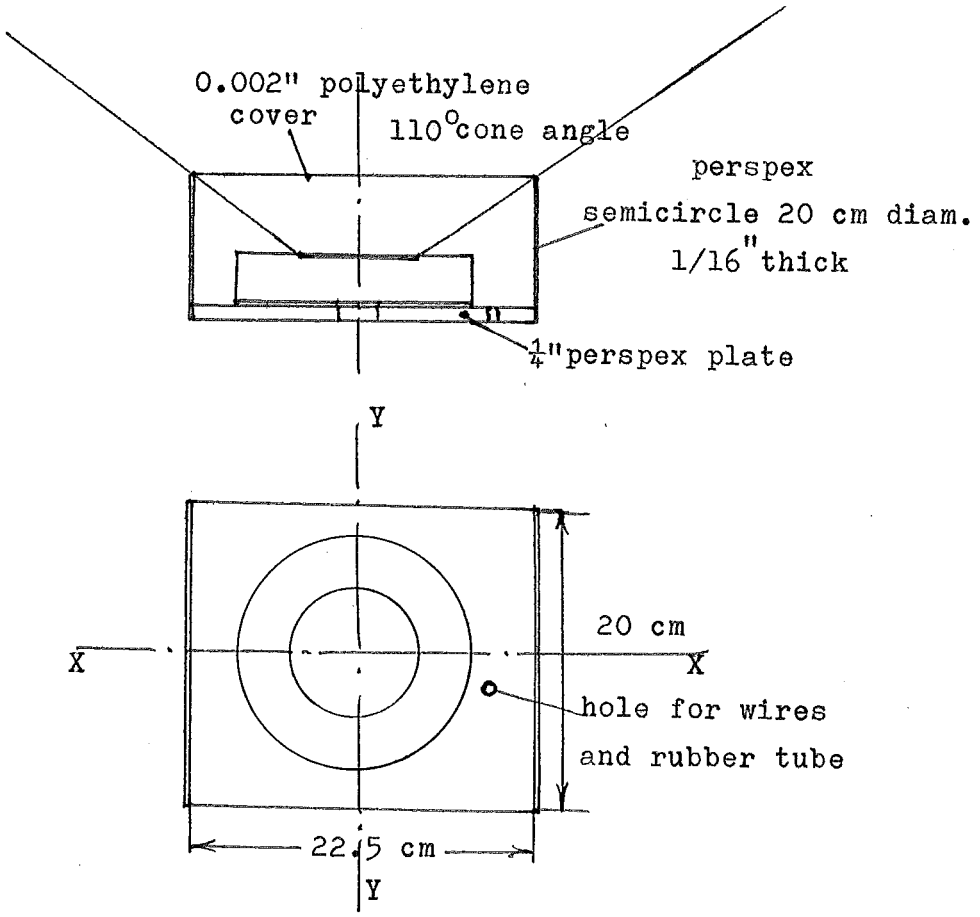

Fig 3.3 The cover of the radiometer

in temperature among five thermocouple points.

The wire is 1.5 metre long, gauge 22 B & S made of nickel. The winding of the wire like that in Fig. 3.2 gives resistance of 5.46 Ω for this element. The element is then cemented to a thin mica sheet for rigidity and electrical insulation, on the top surface a piece of glass cloth separates the sensing plate and the heating wire. This cloth provides electrical insulation but restricts the heat flow upward very little. The whole polystyrene block is placed in a steel housing, covered on the top by a tufnol ring. This ring is sealed around the periphery by araldite leaving only the sensing black plate exposed to the sky.

5. The cover:

This is an important part of the radiometer. A suitable cover must:

- transmit all the radiant energy at the wavelength to be studied.

- minimize the convection heat transfer from air to plate or vice versa.

- protect the sensing element and the insulation structure from the rain.

For radiometer to measure solar radiation, glass cover is commonly used because it is transparent to short wave radiation but almost opaque to radiation $> 4\,\mu$ in wavelengths. The latter property makes glass unsuitable as a cover for long wave radiation instrument. With the advance of chemistry technology, polyethylene has been found to have considerable transmittance for long wave radiation. Funk (17) when used

polyethylene cover for his radiometer estimated that 0.002" polyethylene film absorbs only about 1% of the long wave radiation, and Suomi et al (28) placed an upper limit of 3% on the absorption of such a film. When the radiometer is in equilibrium with its environment, it is assumed that $\frac{1}{2}$ of the absobed radiation is re-emitted in the direction of the transmitted energy i.e. only 1.5% of the radiation is prevented from passing through the film. Reflection by the film has a greater effect in reducing transmission. For a thin polyethylene film, this loss due to reflection is about 4% (29).

Hemispherical polyethylene film 0.001" to 0.002" thick can be produced by a method described in Ref. (18). In this method, vacuum is produced in the cavity of a heated mould and covered by polyethylene sheet. The diameter of the hemisphere produced was about 20cm. Because no tool for this process is available, a design of the cover shown in Fig. 3.3 is substituted.

In this design, a half cylindrical window of 0.002" polyethylene film is made, supported by two perspex side walls, 20 cm diameter semi-circle and 1/16" thick. The polyethylene film and support walls are glued to a perspex base 20 cm x 22.5 cm rectangular.

In the direction YY as shown in Fig. 3.3, there is no restriction in the view of the sensing plate but in XX direction, part of the hemispherical view is restricted by the supporting walls. The cone angles vary because of the semicircle curve, minimum cone angle is 110^{o}. As noticed by some observers, the most important contribution of long wave radiation from sky comes from the region near the zenith so

that the effect of the perspex wall is small. Therefore one can assume that the total transmittance of long wave radiation by this cover is 0.95.

This cover design can also give effective protection for the whole radiometer from weather effect. The polythene cover is kept under light positive pressure by air supplied through a small rubber tube. This tube is inserted through a small hole in the perspex base plate with other electrical wire and thermocouple leads.

The whole assembly can be mounted on a camera tripod and set at any inclination facing any direction in the sky. Fig. 3.4, 3.5 and 3.6 show the radiometer and typical installations. Some remarks for the manufacturing are presented in Appendix 3.

(B) CHARACTERISTICS OF THE RADIOMETER

1. Time constant for the heating and cooling operation:

Due to the heating installation, the radiometer has a rather large time constant (For a system receiving heat input, time constant is the time taken for the system to attain 63.2% of the temperature difference between the initial and final state). The time constant for the heating process from 13°C to 68.2°C is 5 minutes, same as from 68.2°C to 87°C. Time constant for the cooling from 87°C down to 17°C is 6 minutes. Fig. 3.7 illustrated these measurements. This large time constant does not allow it to respond quickly with fast fluctuation. However it has an averaging effect which smooths out the fluctuation . For long wave radiation at night-time, there is very little fluctuation so that this large time constant is not a problem.

Fig. 3.4 Close up view of the radiometer

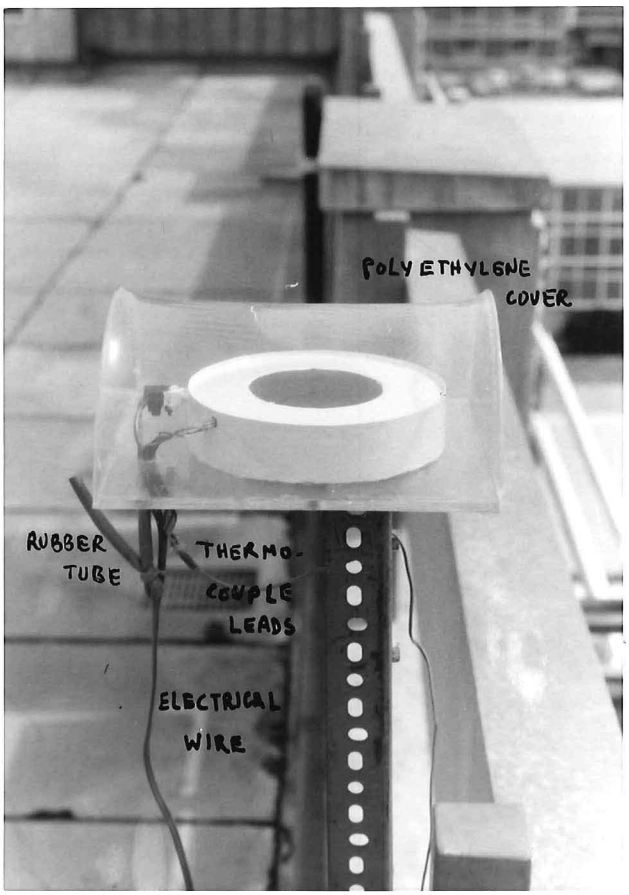

Fig. 3.5 Radiometer in horizontal position
(Measurements in December)

Fig. 3.6 Radiometer in inclined position

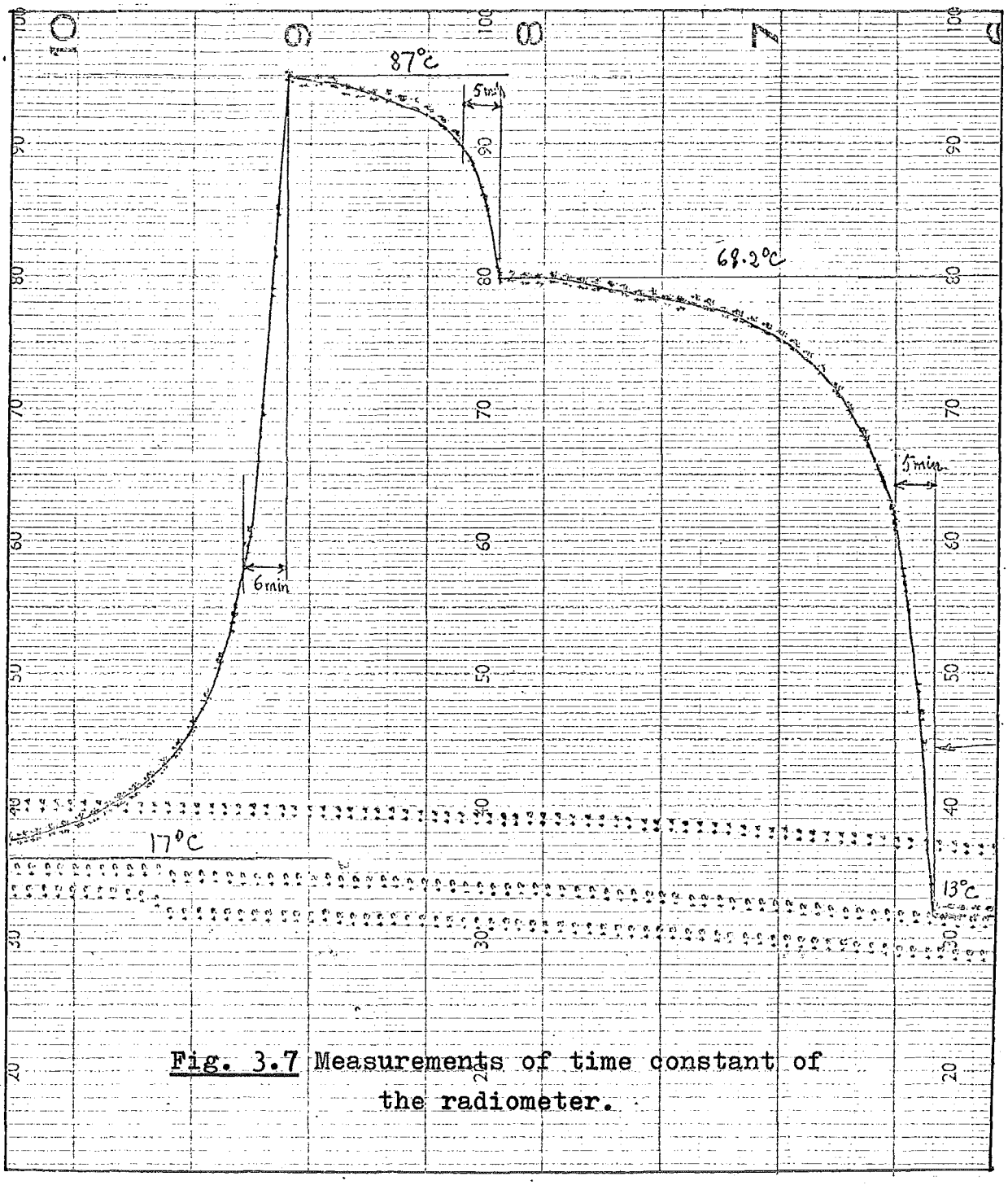

Fig. 3.7 Measurements of time constant of the radiometer.

2. Effect of wind:

Due to the cover the wind effect on the radiometer is small. Tests were carried out in a wind tunnel. When the radiometer is heated by 5 volts D.C. current, the outputs from thermocouples (five connected in parallel) are shown below :

Wind speed	0	20	35	(Km/hr)
Output	1.4	1.37	1.25	(mV)

Maximum difference from 0 to 35 Km/hr wind wpeed is 0.15 mV corresponding to about 3.5°C. The corresponding plate temperature for 5 volts input is about 75°C. The relative change in temperature is 4.7%.

3. Resistance of the back insulation:

According to the Institute of Heating and Ventilating Engineer Guide Book 1970, the thermal resistance of an air space with multiple aluminium foil has a high resistance because radiation is largely prevented. The resistance of the same air space structure is also higher when the heat flows downward than when it flows upward. Table A3.6 from that Guide Book suggested a thermal resistance of 1.76 $m^{2o}C/W$ for low emissivity multiple foil insulation with air space on one side. Therefore the thermal resistance of the whole insulation at the back of the sensing plate can be estemated as:

Air space and multiple foils	Resistance	= 1.76$m^{2o}C/W$
1 cm expanded polystyrene, having conductivity=0.033$\frac{W}{m^oC}$	"	= 0.33$m^{2o}C/W$
Outside surface	"	= 0.053$m^{2o}C/W$
	Total resistance	= 2.143$m^{2o}C/W$

Overall heat transfer coefficient $U_b = 0.466$ W/m^2°C

In daytime when the radiometer receives both long wave radiation from the sky and short wave solar radiation, the plate temperature can be as high as 70°C with an average air temperature of about 20°C. The back loss then is about 23.3 W/m^2 or 2 cal/cm^{2}hr, compared with the heat input of 75 to 80 cal/cm^{2}hr this heat loss is only 2.5 to 3% and can be neglected.

At night, without extra heating the plate temperature is normally below or equal to air temperature, the temperature difference is seldom more than 5°C. Therefore the amount of heat transfer from the air to the plate through the back insulation is negligible. For cases where extra heating is required, the plate temperature may be 5°C higher than air temperature resulting a back loss of about 2.33 W/m^2 or 0.2 cal/cm^{2}hr. Compared with the incoming radiation of about 20 cal/cm^{2}hr, this back loss can also be neglected.

3.2 HEAT BALANCE EQUATIONS FOR THE RADIATION MEASUREMENT WITH THIS RADIOMETER

Fig. 3.8 shows the components of heat exchange for this radiometer.

Under steady state condition, the heat balance equation at daytime operation is:

$$T_s \alpha_s R_s + \alpha_L T_L R_L = \epsilon_L \sigma T_p^4 + h_c(t_p - t_a) + U_b(t_p - t_a) \qquad (3.1)$$

where α_s = short wave absorptivity of the plate

α_L = long wave " " "

T_s = short wave transmittance of the cover

T_L = long wave " " "

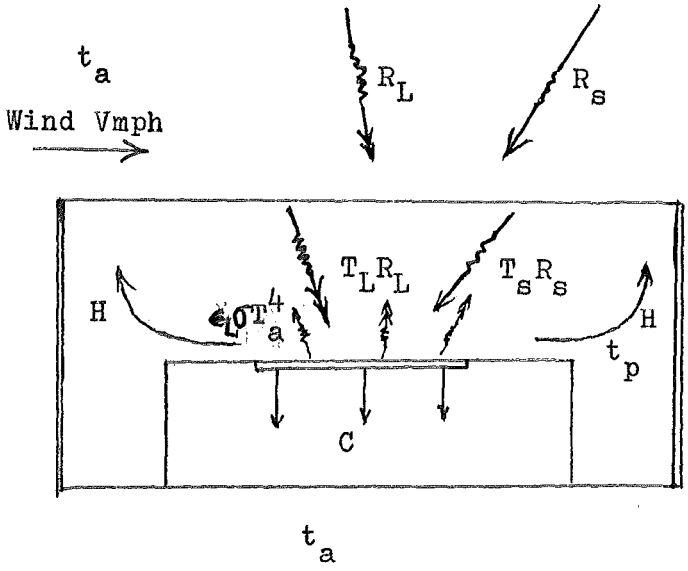

Fig. 3.8 Heat exchange at the radiometer surface

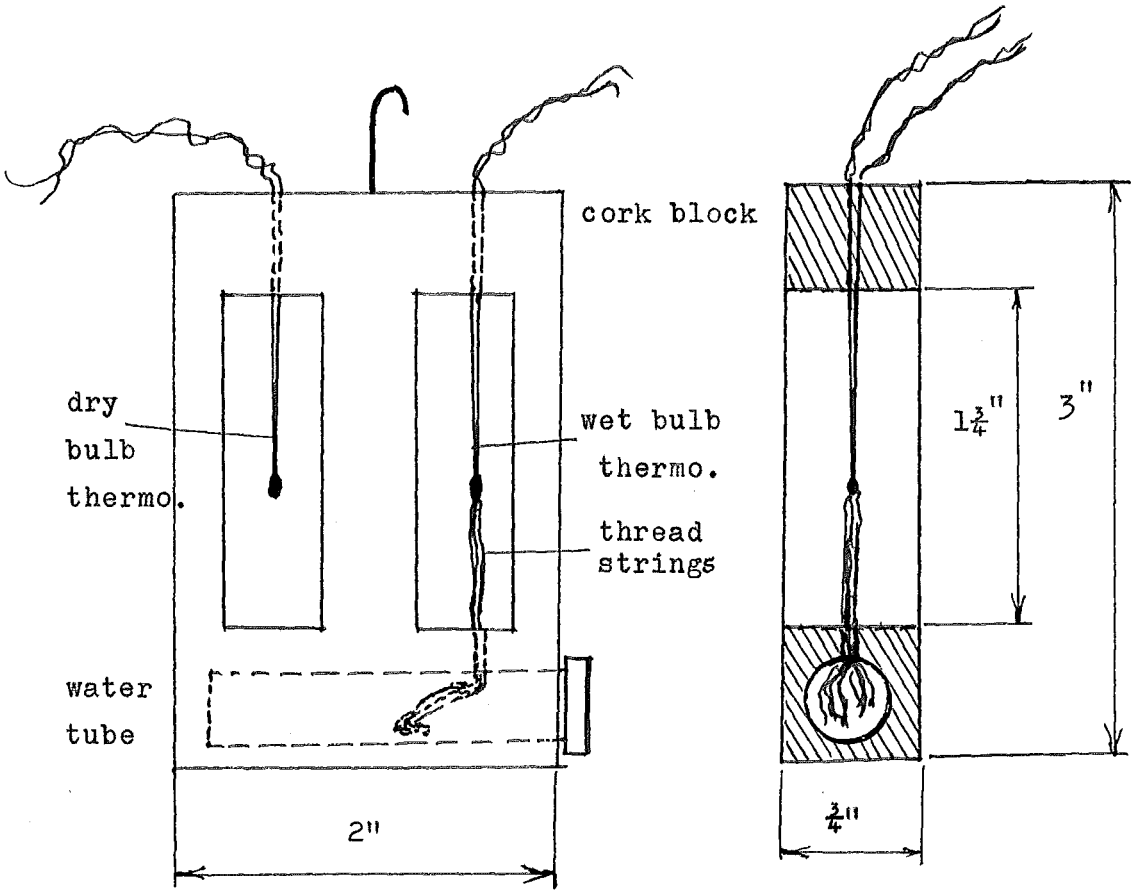

Fig. 3.9 Wet and dry bulb air temp. measurement

h_c = convection coefficient

U_b = overall heat transfer coefficient of back insulation

R_s = short wave solar radiation

R_L = long wave sky radiation

t_p = plate temperature

t_a = air temperature

In this equation, if the last two terms of the RHS can be considered negligible, the intensity of long wave sky radiation can be estimated in terms of the plate temperature and solar radiation intensity:

$$R_L = \frac{\epsilon_L \sigma T_p^4 - T_s \alpha_s R_s}{T_L \alpha_L} \qquad (3.2)$$

If on the other hand, the sky radiation can be estimated by some other method, the solar radiation intensity may be known by this relation:

$$R_s = \frac{\epsilon_L \sigma T_p^4 - T_L \alpha_L R_L}{T_s \alpha_s} \qquad (3.3)$$

Normally R_s is measured by local Meteorological Office so that equation (3.2) can be used to estimate daytime long wave radiation from the sky.

At night-time, there is no solar radiation and the heat balance equation is:

$$\alpha_L T_L R_L = \epsilon_L \sigma T_p^4 + hc(t_p - t_a) + U_b(t_p - t_a)$$

t_p is normally less than t_a during these periods, this means that there is some convection and conduction heat input to the plate from the air. However the temperature difference is usually small so that these two components are negligible.

The night sky radiation is then given by:

$$R_L = \frac{\epsilon_L \sigma T_p^4}{T_L \alpha_L} \qquad (3.4)$$

When extra heating is required, the electrical energy input Q can be known from the voltage supply and the resistance of the heating element. The heat balance equation in these cases is:

$$\alpha_L T_L R_L + Q = \epsilon_L \sigma T_p^4 + hc(t_p - t_a) + U_b(t_p - t_a)$$

t_p is then higher than t_a but the difference is also small so that the last two terms in RHS can be neglected.

The night sky radiation is given by:

$$R_L = \frac{\epsilon_L \sigma T_p^4 - Q}{\alpha_L T_L} \qquad (3.5)$$

3.3 MEASUREMENT WITH THE RADIOMETER

During the period from late August to late September 1973, trial measurements of long wave radiation under Christchurch conditions were made with the above designed radiometer. The measurement were aimed to verify the variation of sky radiation with the degree of cloudiness of the sky as expected from theoretical analysis, to obtain some quantitative values of the long wave radiation from clear sky received at Christchurch and compare these with what is proposed to be from the empirical formulae given in Section 2.2 .

(A) EXPERIMENTAL SET UP

To obtain a clear view of the sky and avoid as much obstacle as possible, the radiometer was mounted on a tripod and placed on the roof of the West Hall, Ilam Halls of

Residence, University of Canterbury.

Wet and dry bulb temperature of air near the site were also measured by gauge 30 copper-constantan thermocouples, the two thermocouples were shielded from direct radiation by a cork block containing water tube as shown in Fig. 3.9 . The output of all five thermocouple points on the sensing plate were connected in parallel to read average temperature of the plate. A 24 channel Brown Electronik chart recorder was used to record variation of the plate temperature, wet and dry bulb air temperature. Extra heating is provided by a regulated D.C. voltage supplier.

At the initial stage of the experiment, direct temperature measurement circuit was used so that all thermocouple outputs are compared with the built in reference junction with temperature compensation circuit and printed on chart under scale from o to 200^{o}F. Fig. 3.10, 3.11 and 3.12 show the charts output under such connection. These showed the typical variation of day and night-time measurement. However check measurement of air temperature with mercury thermometer showed that the recorded temperature were too low. Information obtained from the manufacturer pointed out that the resistor in the reference junction must be changed for different type of thermocouples. The existing resistor in the recorder was for use with iron-constantan thermocouples, therefore the difference in emf (electro-motive force) versus temperature between the two types of thermocouple gave erroneous measurement of temperature.

Because a compensation resistor for copper constantan thermocouple was not available, indirect measuring circuit

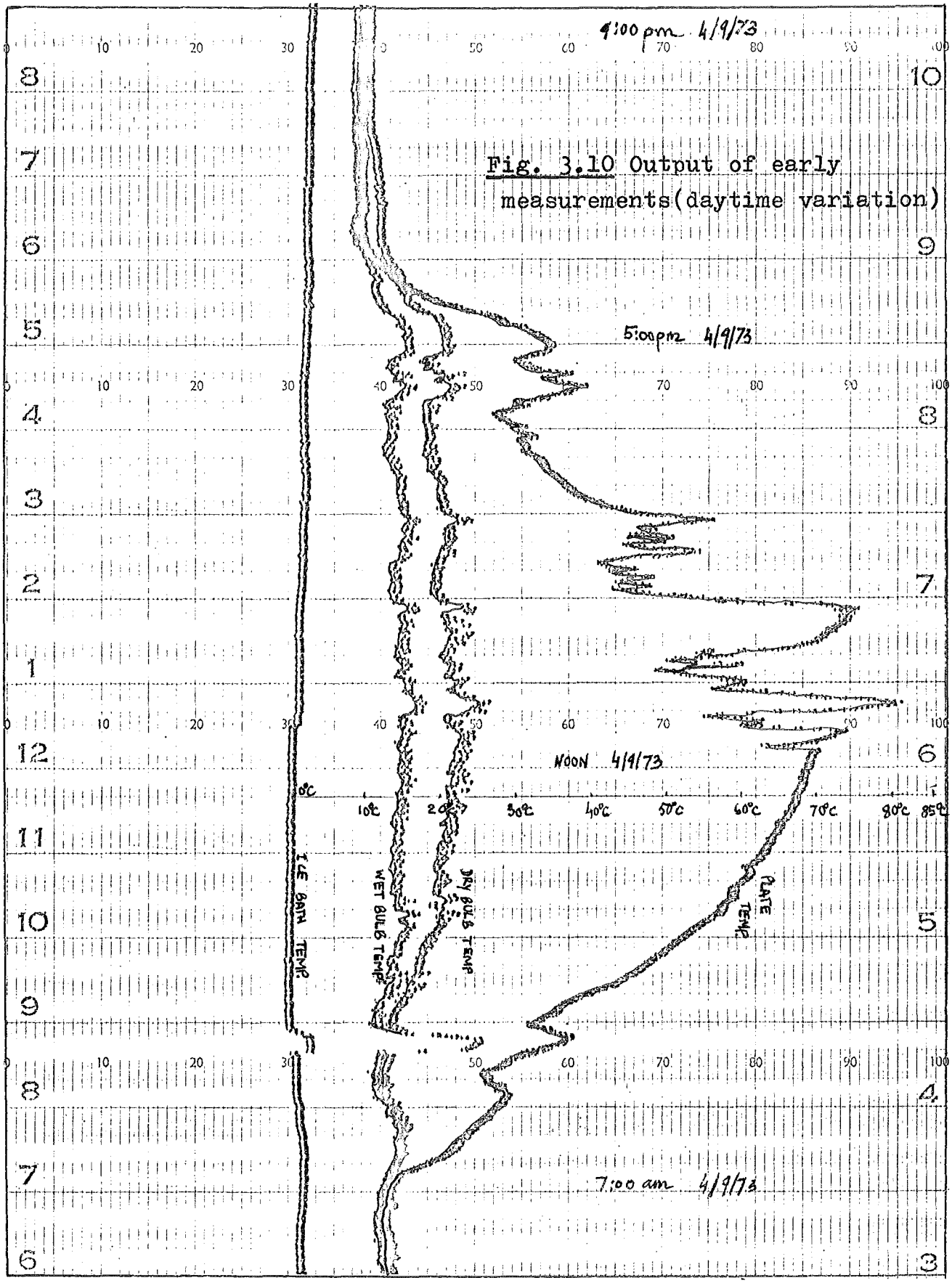

Fig. 3.10 Output of early measurements (daytime variation)

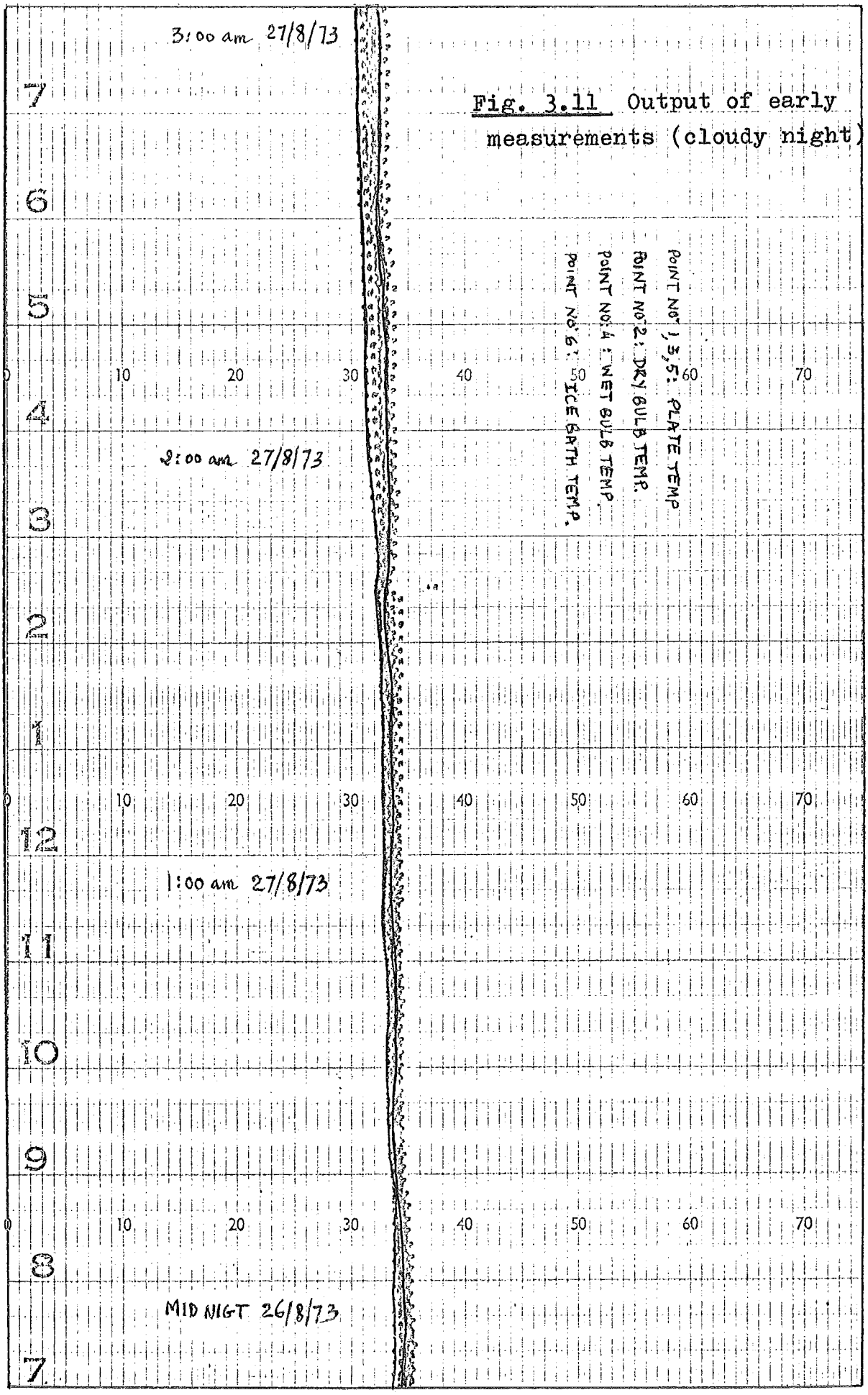

Fig. 3.11 Output of early measurements (cloudy night)

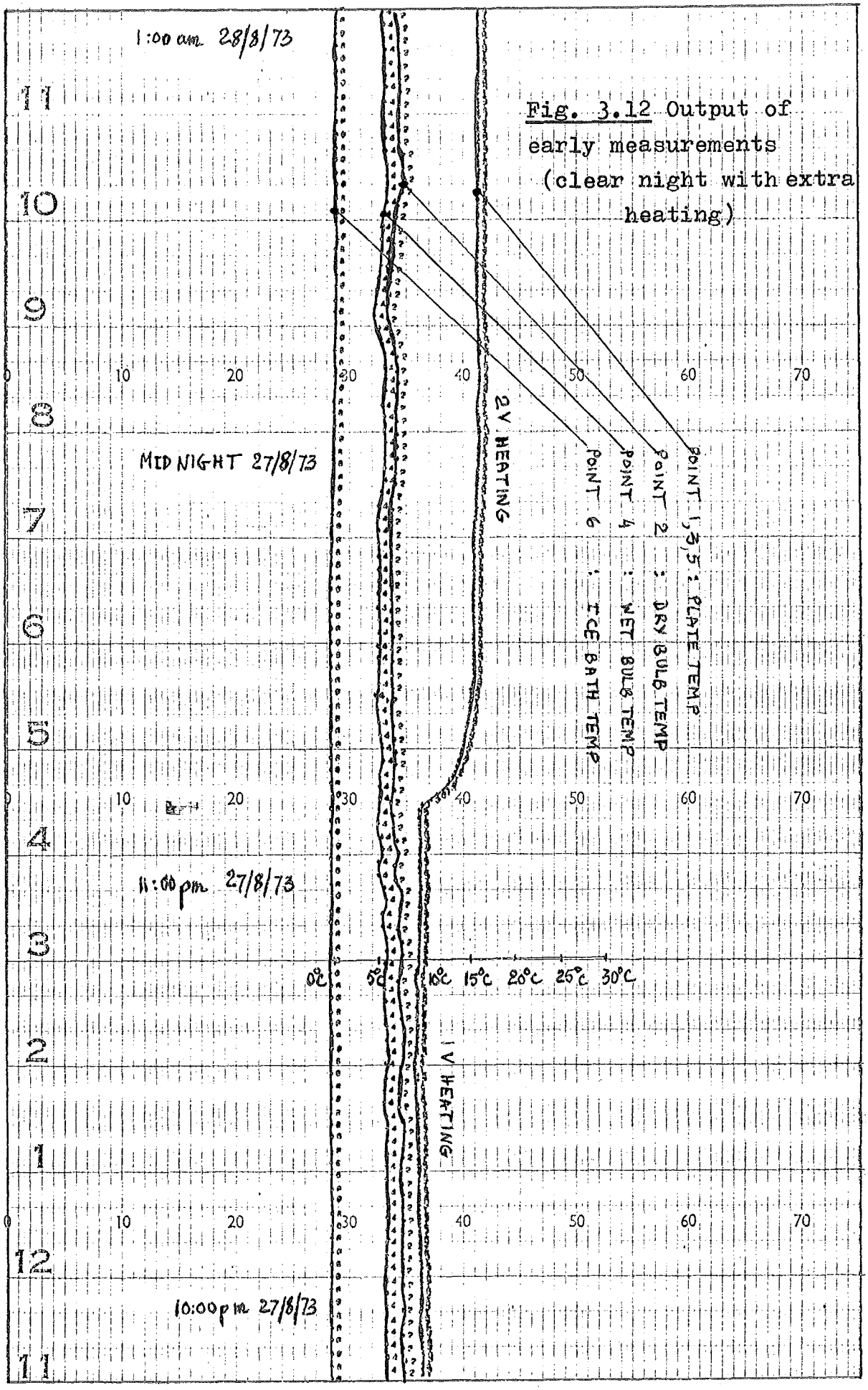

Fig. 3.12 Output of early measurements (clear night with extra heating)

was used instead. The outputs of thermocouples from radiometer and air temperature measurement are compared with that of a reference thermocouple kept at $0^{o}C$ in a thermosflask containing ice cubes. Difference is the emf measured in mV and printed on chart under 0 to 5 mV scale. Fig. 3.13 shows diagram of the two methods of connection.

(B) RESULTS OF THE EXPERIMENT

1. Qualitative verification:

From the 4 September onward, 0 to 5 mV scale was used throughout with chart speed of one inch per hour. Compared with the previous charts, these new charts show the variation of temperatures of plate and air more clearly, especially at night-time.

As shown by equation (3.4), long wave sky radiation is proportional to temperature of the sensing plate raised to 4th power. Therefore variation in this temperature corresponds to the change in magnitude of the sky radiation. These variations are typified by the following figures:

Fig. 3.14: clear night sky starting from late afternoon, extra heating was required to raise the plate temperature up in-side the measuring range: little incoming radiation from the sky, large heat loss by radiation.

Fig. 3.15: thin cloud over the sky and windy condition, the plate temperature was also below air temperature but still inside the scale ($>0^{o}C$): reasonable radiation from sky and rather constant throughout the night, heat loss by radiation is small.

Fig. 3.16: intermittent condition where the sky changed from clear and calm to cloudy and windy periods.

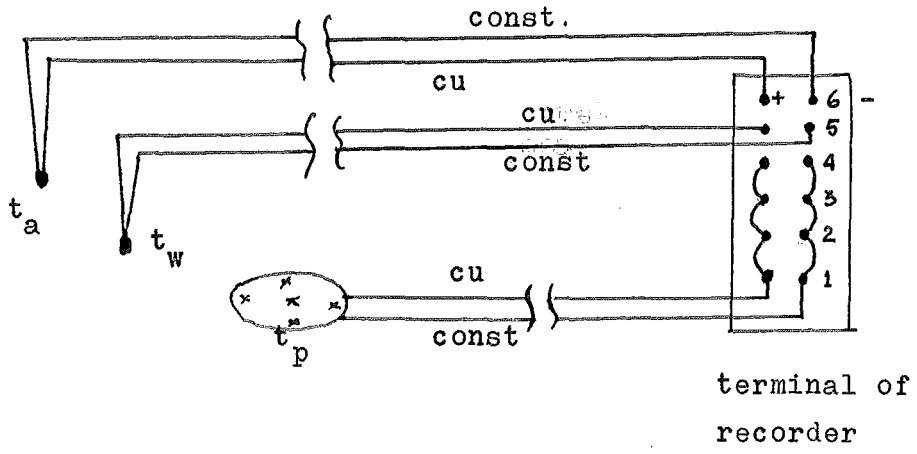

a. Connection for direct temp. recording

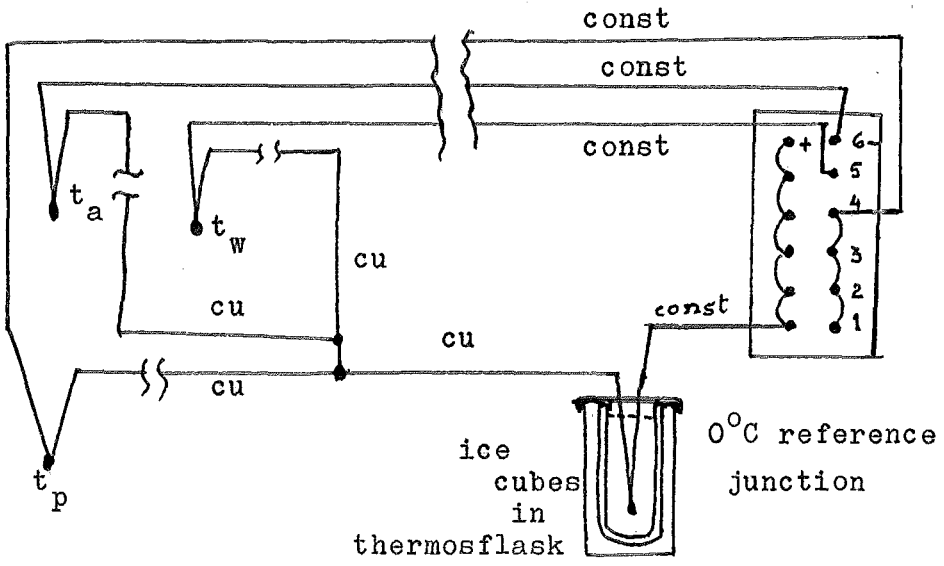

b. Connection for millivolt recording

Fig. 3.13 Methods of connection for temp. measurement by thermocouples

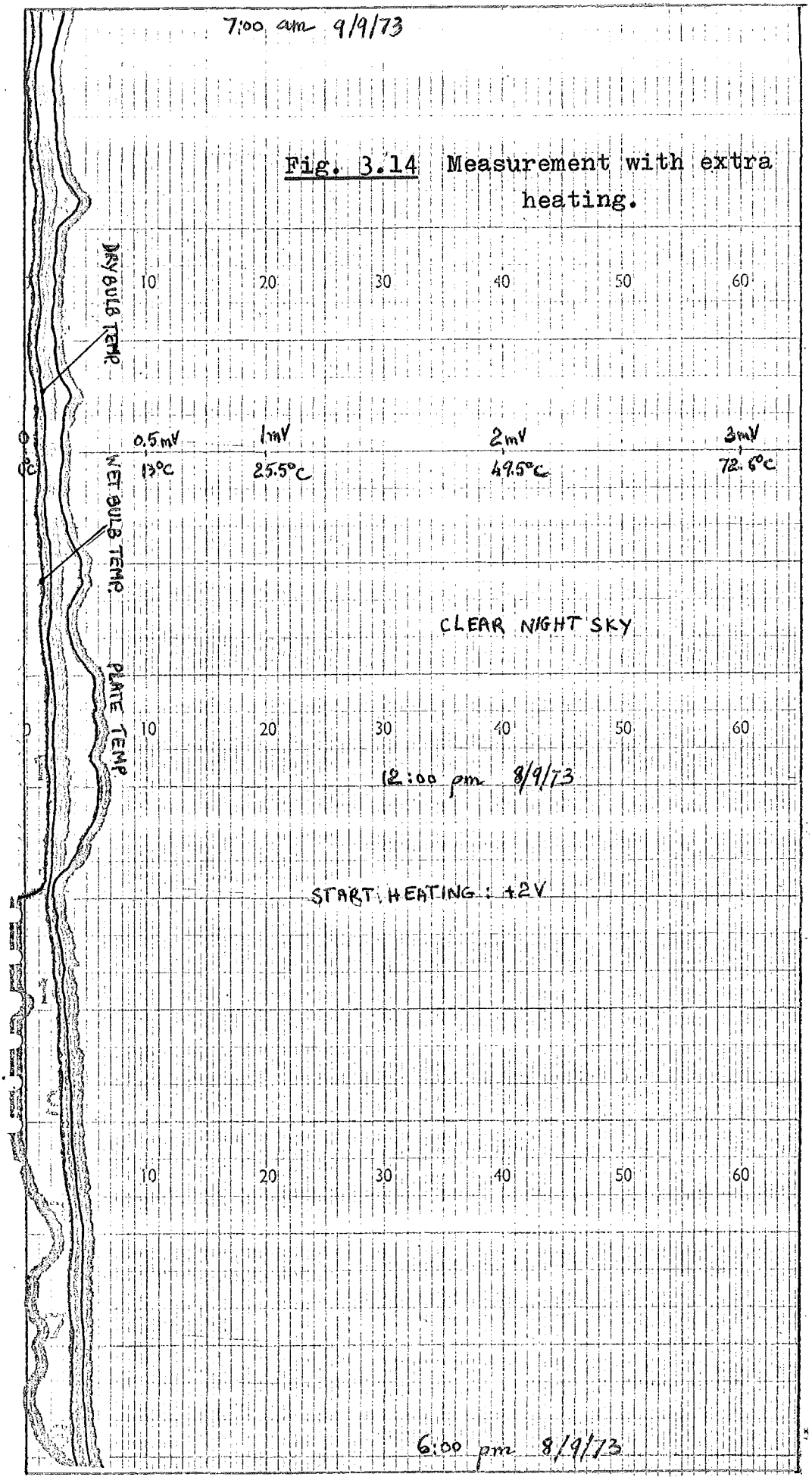

Fig. 3.14 Measurement with extra heating.

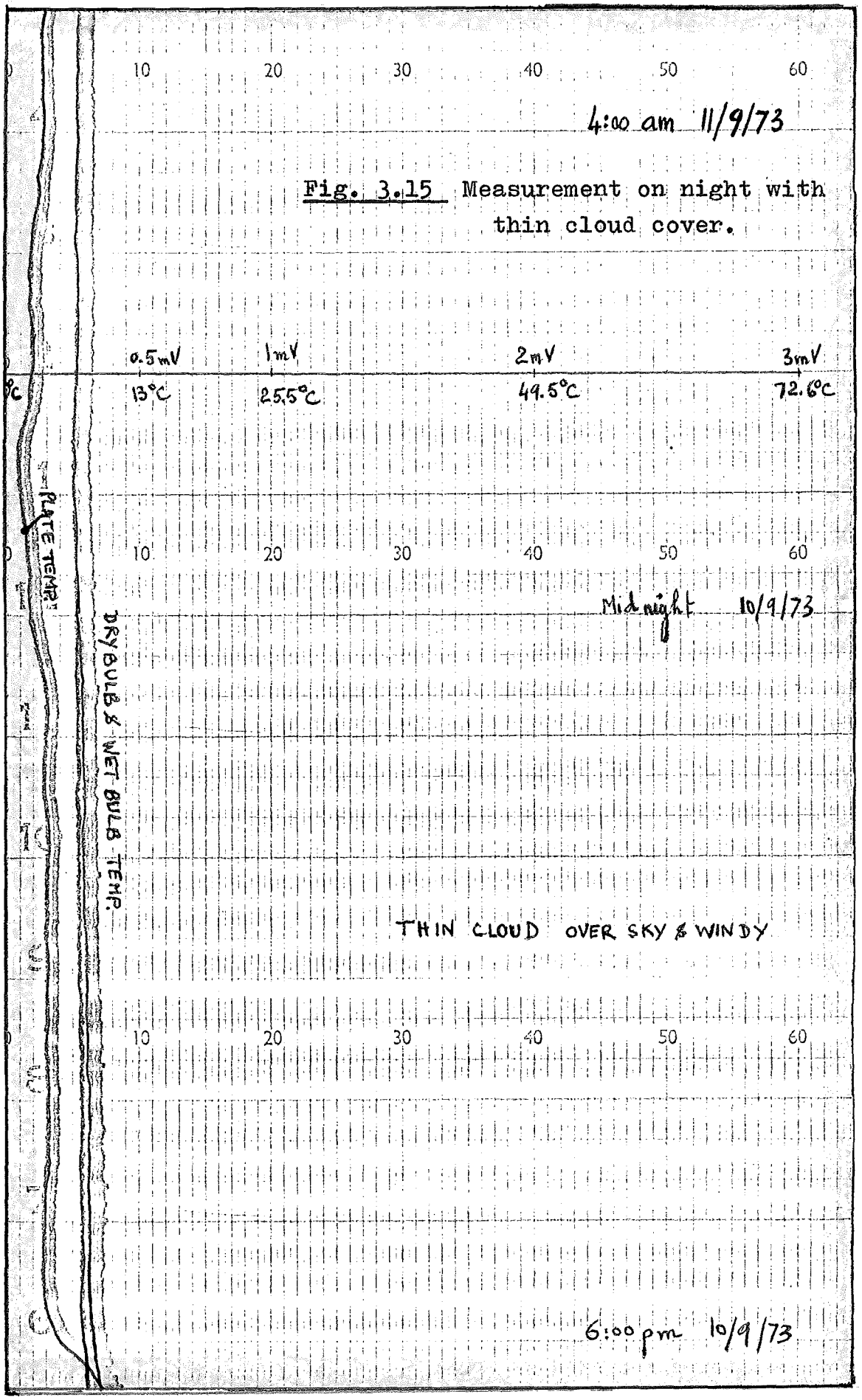

Fig. 3.15 Measurement on night with thin cloud cover.

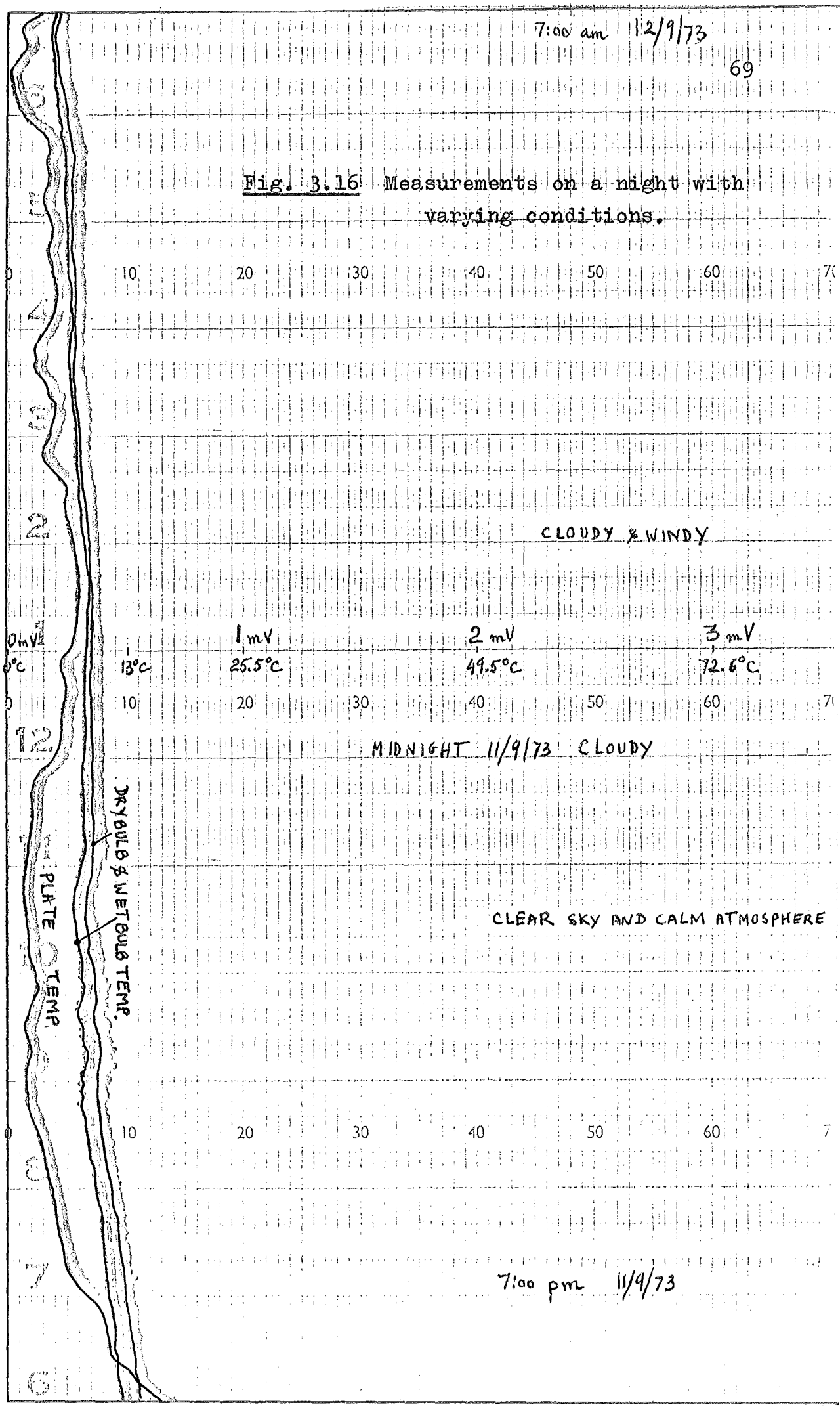

Fig. 3.16 Measurements on a night with varying conditions.

Plate temperature was much lower than air temperature during clear period and became closer to it when cloud began to cover the sky. This corresponds to the increase in sky radiation with the degree of cloudiness.

Fig. 3.17: cloudy night, plate temperature was about the same as air temperature throughout the night: the sky radiates as a black body at air temperature, very little heat loss by radiation.

Some experiment with the radiometer set at 45^{o} inclination from horizontal and facing North have also been tried. The results showed a general increase in plate temperature even in clear night sky periods. This agrees with what expected because an inclined surface receives less radiation from the whole sky but it receives a more amount of long wave radiation from the nearby objects and some amount reflected from them. The overall effect is an increase in incoming radiation and reduction in heat loss. Common experience in winter time also shows that a horizontal surface is more prone to frost cover than a sloping surface at the same site.

Fig. 3.18: illustrates the variation of air and plate temperature at inclined position during cloudy and clear night periods.

Later in the investigation from 20 October, the radiometer was set up near the solar water heater on the roof of the Chemical Engineering Building, University Campus. The same connection to give emf in mV was used, at the same time with other outputs from thermocouples inside the solar panel. The following figures confirm the trend of variation in sky radiation noticed above.

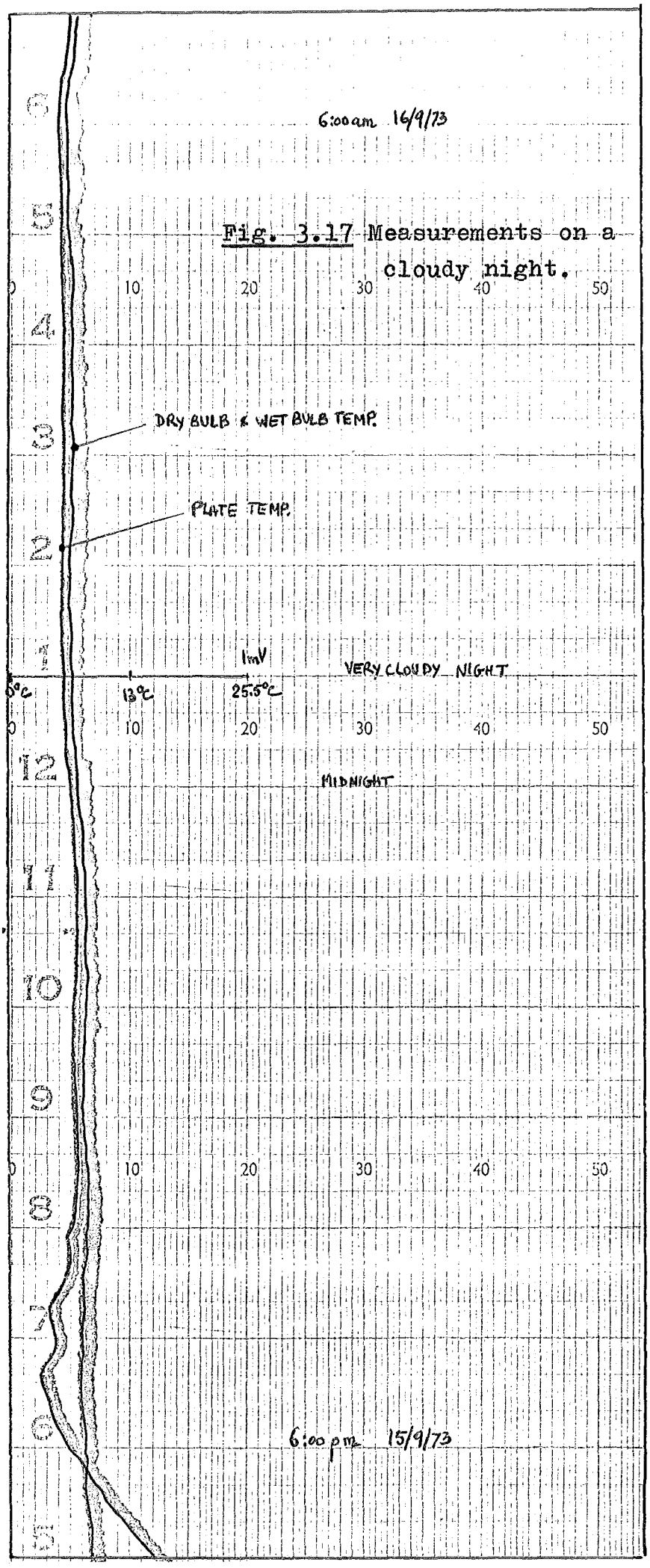

Fig. 3.17 Measurements on a cloudy night.

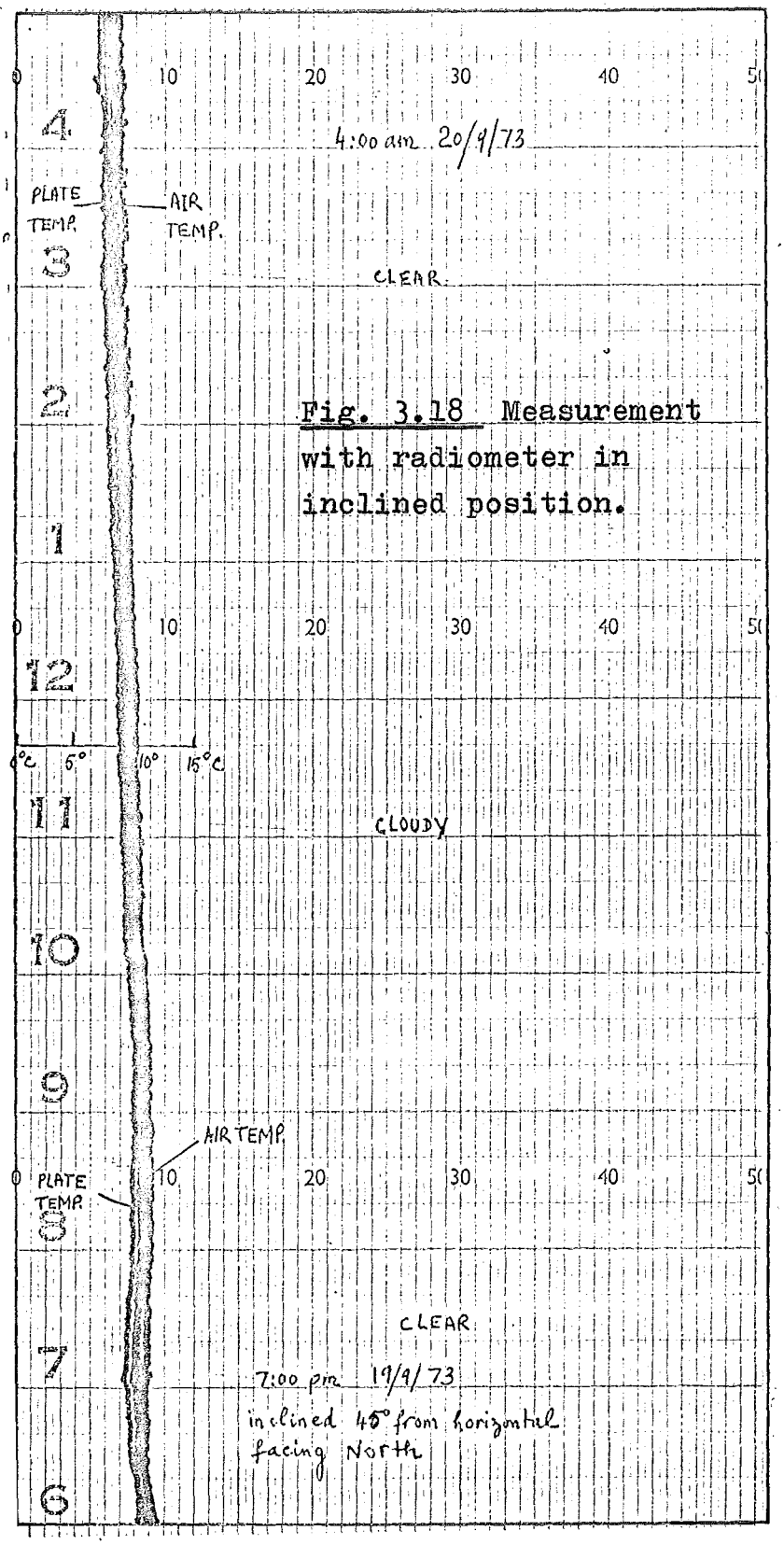

Fig. 3.18 Measurement with radiometer in inclined position.

Fig. 3.19: clear and calm sky resulting low plate temperature. Little variation in all the temperatures recorded showed a constant incoming radiation from the clear sky.

Fig. 3.20: again shows the change in radiation from clear sky to cloudy condition. Little variation in air temperature was recorded although there was a large change in plate temperature.

Fig. 3.21: shows a typical daytime operation when the sky condition changed from intermittent cloudy to clear. Compared this figure with Fig. 3.22 which was reproduced from the chart of the output from an Eppley solarimeter used by the Weather Office, although this radiometer can not respond to the change as quick as the Eppley solarimeter, it effectively shows the average of these fluctuation.

2. Quantitative results:

From the records of temperature variation charts, clear sky periods were selected and hourly mean temperatures of plate, dry bulb and wet bulb are measured. These clear sky periods were chosen according to observation made frequently during the experimental nights.

The long wave radiation from clear sky is calculated from equation (3.4) and (3.5). With $T_L = 0.95$; $\alpha_L = \epsilon_L = 0.95$, equation (3.4) becomes:

$$R_L = \sigma T_p^4 / 0.95 \qquad (3.6)$$

with $\sigma = 5.67 \times 10^{-9}$ mW/cm^2 $^oK^4$

For cases where heating was provided, Q is calculated from the voltage V and the resistance R of the heating element. The heat input per unit area is:

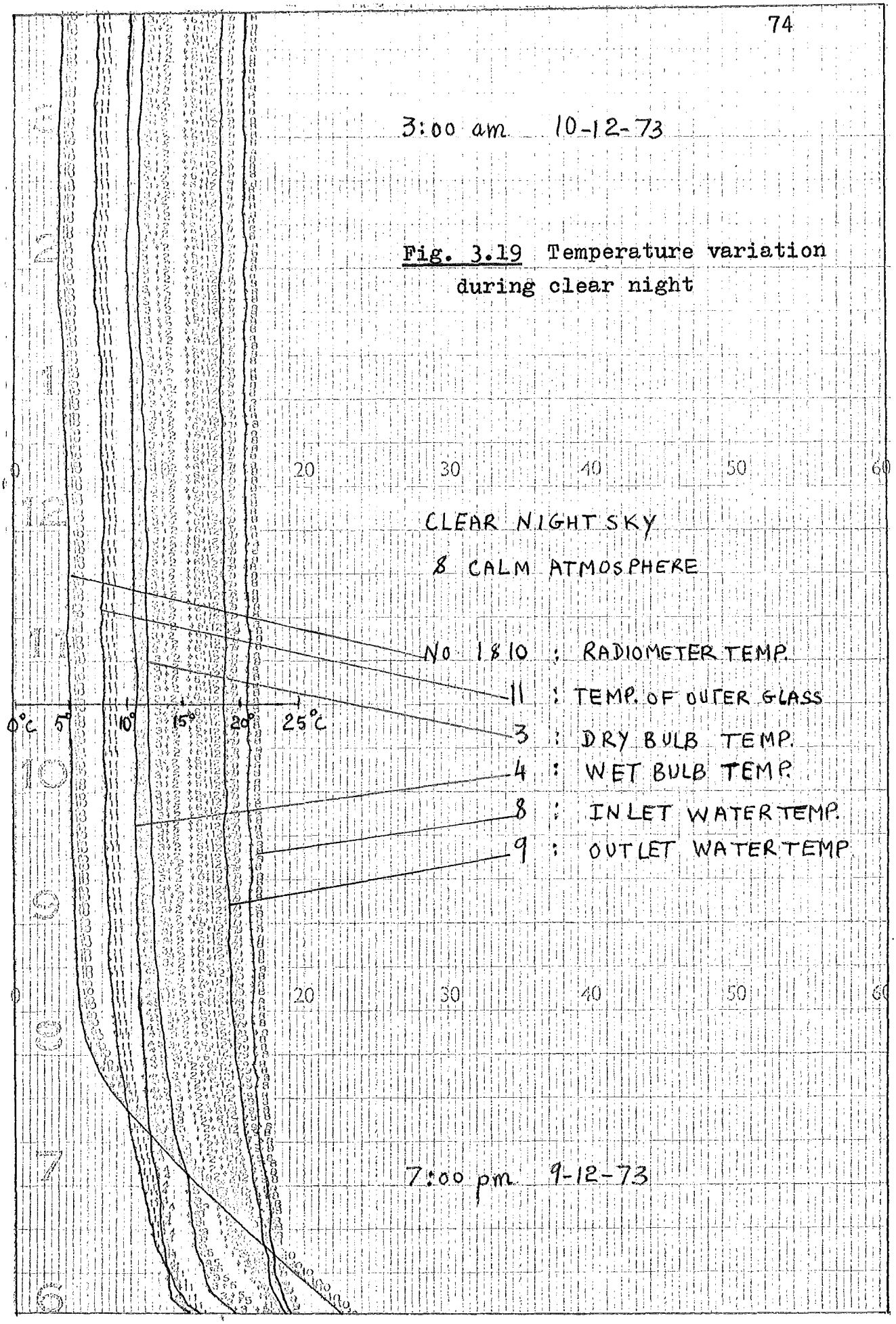

Fig. 3.19 Temperature variation during clear night

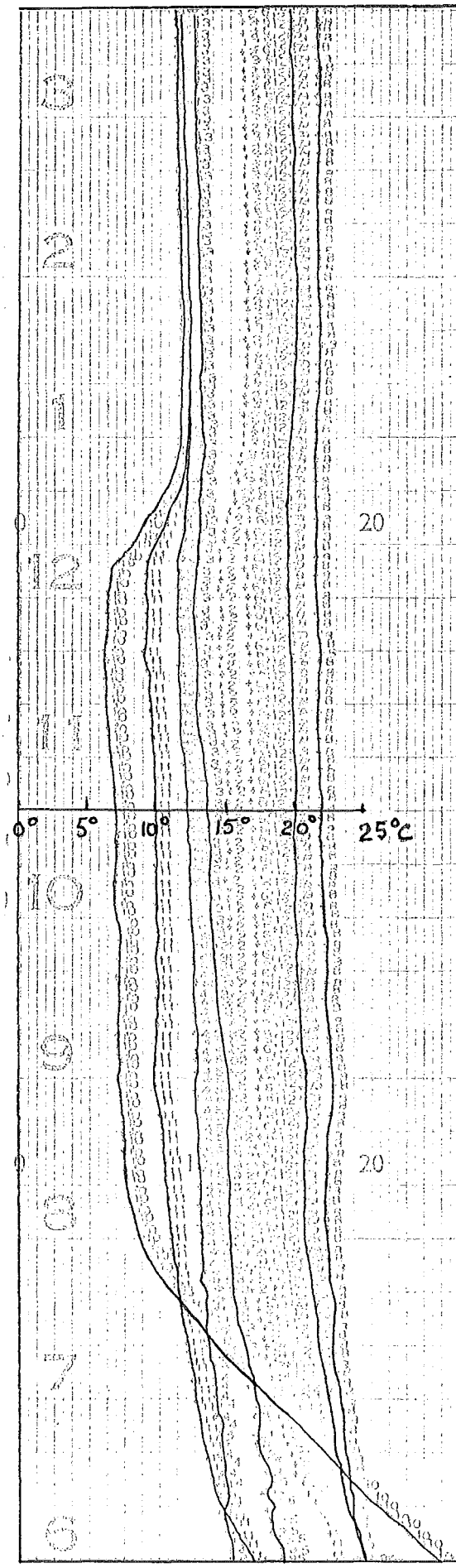

3:00 am 11-12-73

Fig. 3.20 Temperature variation during a night with changing conditions.

CLOUDY SKY

20 30 40 50

NO: 18 10 : RADIOMETER TEMP.
11 : TEMP. OF OUTER GLASS
8 : INLET WATER TEMP.
9 : OUTLET WATER TEMP.
3 : DRY BULB TEMP.
4 : WET BULB TEMP.

CLEAR & CALM SKY

9:00 pm 10-12-73

20 30 40 50

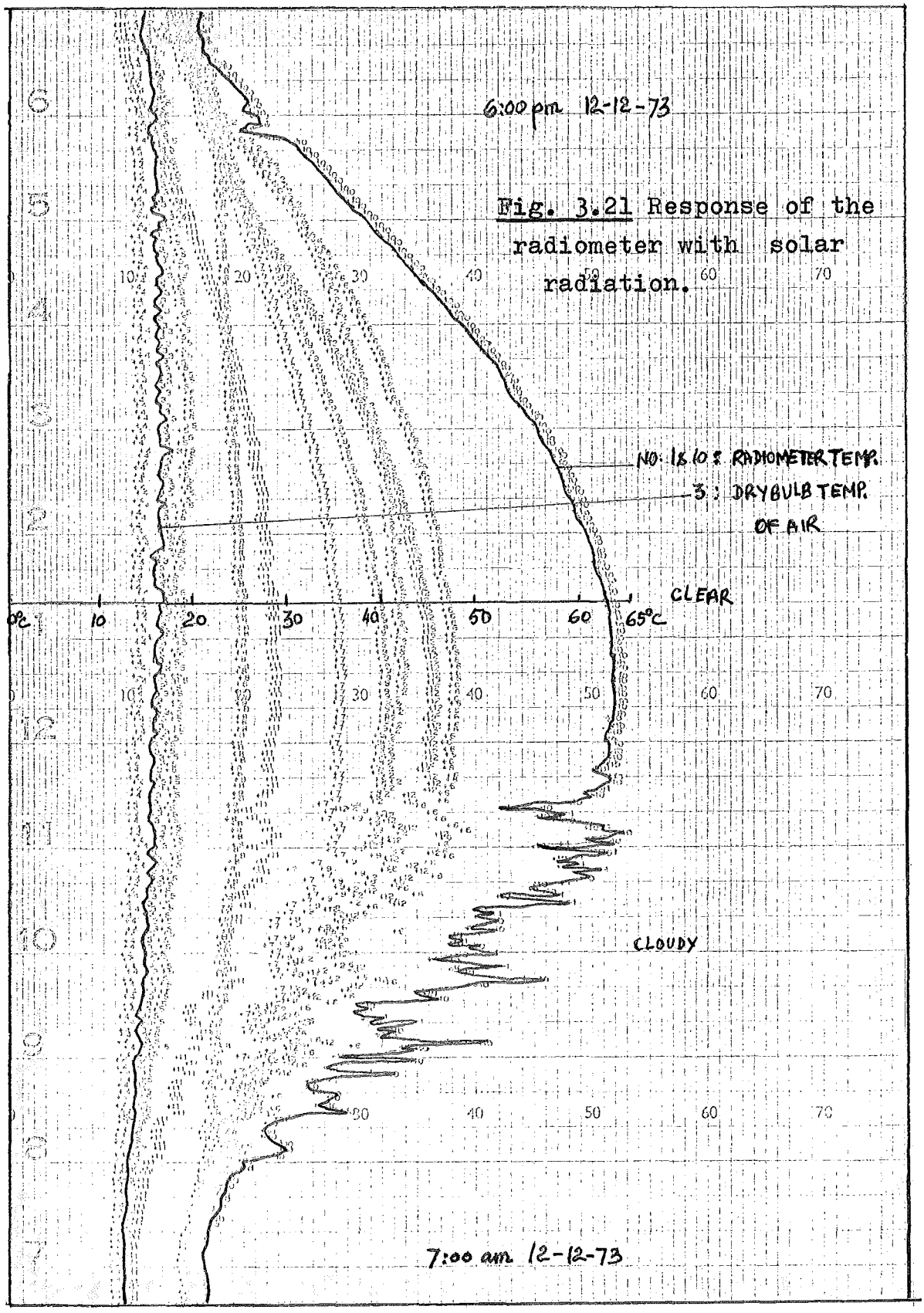

Fig. 3.21 Response of the radiometer with solar radiation.

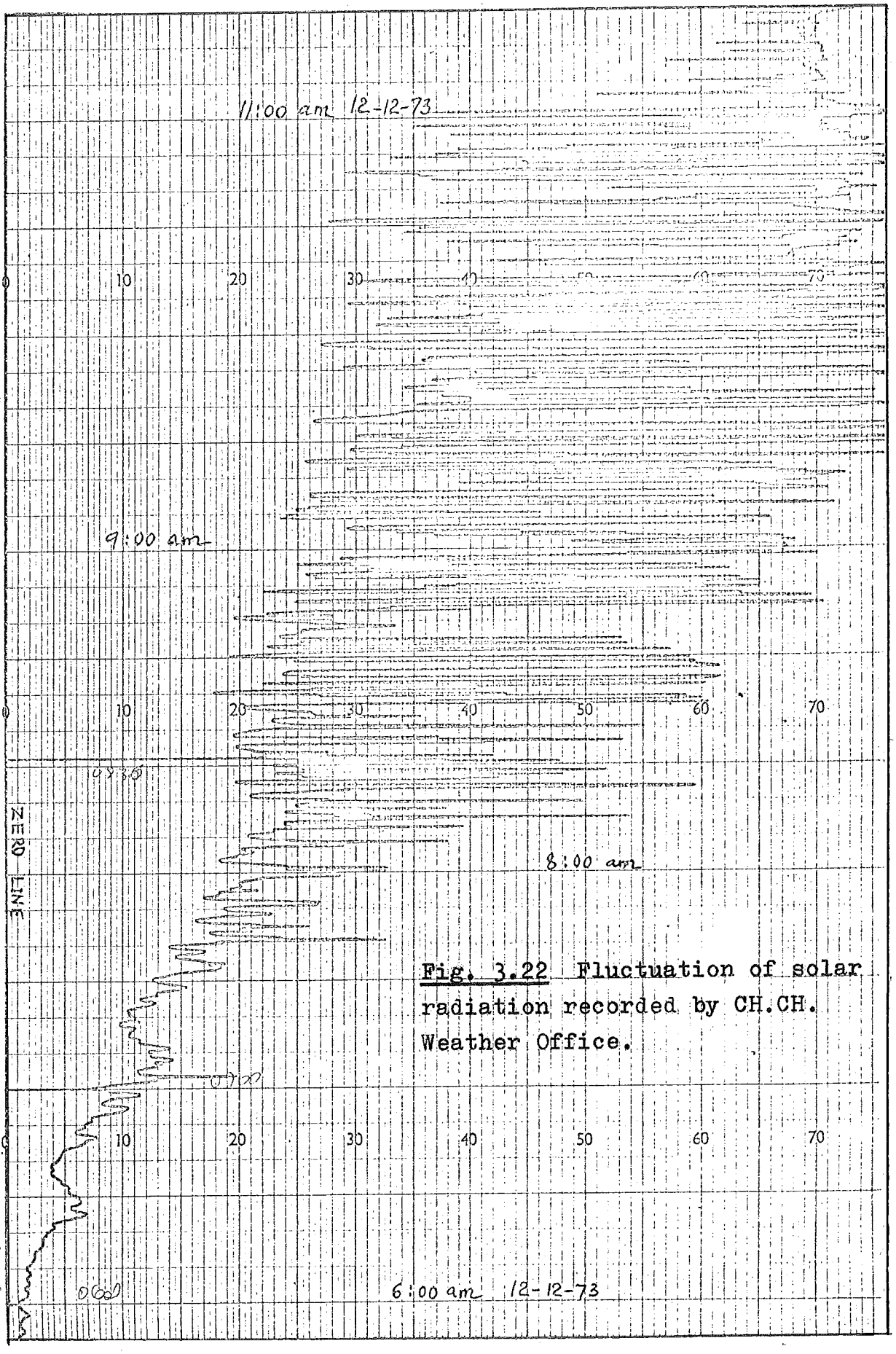

Fig. 3.22 Fluctuation of solar radiation recorded by CH.CH. Weather Office.

$$Q = \eta \frac{V^2}{RA} \quad mW/cm^2$$

A = area of sensing plate = 50.25 cm^2

R = 5.46 ohms

η = efficiency of the heating, assumed to be 85% (i.e. 85% of the heating goes to the plate)

The vapour pressure of atmosphere for these periods is calculated by:

$$e = \phi e_s$$

where e_s = vapour pressure of saturated air at dry bulb temperature. ϕ = relative humidity of air.

Regression lines for e_s values corresponding to temperature in the range from $0^{\circ}$to $30^{\circ}C$ tabulated in Roger & Mayhew's Table of Thermodynamic Properties of air and steam were calculated in order to extrapolate e_s for different air temperatures. A programme to use with H.P. 9100A calculator to facilitate these calculations is presented in Appendix 1.

Typical calculations for a clear sky period are shown in Appendix 2.

The results of experiment during September and November 1973 are presented in Table 3.1, 3.2, 3.3 .

Plots to compare these experimental values with those proposed by formulae (2.2), (2.4), (2.5) and (2.8) are shown in Fig. 3.23 and 3.24.

Incidentally during the time these experiments were carried out, a Ph.D. student of the Geography Department was performing experiments on the radiation balance for Christchurch. Net radiation exchange at night can be obtained from her measurements with the Funk radiometer at the

TABLE 3.1 Measurements of long wave radiation(no extra heating)

Date	Time period	t_p °C	t_a °C	t_w °C	σT_p^4 mW/cm^2	σT_a^4 mW/cm^2	R_L mW/cm^2	R mW/cm^2	R_L' mW/cm^2	$\sqrt{e}$ mb$^{\frac{1}{2}}$
10-9 pm	07-08	4	8.5	7.5	33.45	35.68	35.3	5.15	30.53	3.16
	08-09	4	8.5	7.5	33.45	35.68	35.3	4.80	30.88	3.16
	09-10	4	8	7.2	33.45	35.43	35.3	4.80	30.63	3.16
	10-11	4	8	7	33.45	35.43	35.3	4.70	30.73	3.11
	11-12	3.5	7.8	7.2	33.21	35.33	35.0	5.25	30.08	3.10
	12-1	2	7.5	7	32.5	35.18	34.2	6.68	28.50	3.07
11-9 am	1-2	2	7.5	6.8	32.5	35.18	34.2	6.60	28.58	3.04
	2-3	2	7.2	7	32.5	35.03	34.2	5.5	29.53	3.12
	3-4	3	7.8	7	32.97	35.33	34.7	4.88	30.45	3.09
	4-5	3.5	7.8	7	33.21	35.33	35.0	4.34	30.99	3.09
	5-6	4	7.3	7	33.45	35.08	35.3	3.80	31.28	3.13
11-9 pm	8-9	3.5	10.2	8.8	35.03	36.60	36.9	8.01	28.65	3.22
	9-10	2.2	10	8	32.59	36.45	34.3	6.60	29.85	3.10
	10-11	2	9	7.8	32.5	35.93	34.2	7.40	28.53	3.13
	11-12	2.5	9.2	8	32.74	36.04	34.4	6.68	29.36	3.15
12-9 pm	7-8	0	7	6	31.56	34.93	33.2	8.30	26.63	2.97
	8-9	0	7	6	31.56	34.93	33.2	7.94	26.99	2.97
13-9 pm	7-8	2.8	9.5	8	32.88	36.19	34.6	7.4	28.79	3.11
	8-9	2	9	7	32.5	35.93	34.2	7.14	28.79	2.94
	9-10	0.8	7.2	6	31.94	35.03	33.7	6.76	28.27	2.94
	10-11	0.2	7	6	31.66	34.93	33.4	5.95	28.98	2.97
	11-12	1.2	7	6	32.12	34.93	33.8	5.05	29.88	2.97

TABLE 3.2 Measurements of long wave radiation(no extra heating)

Date	Time period	t_p °C	t_a °C	t_w °C	$\sqrt{e}$ $mb^{\frac{1}{2}}$	σT_p^4 mW/cm^2	σT_a^4 mW/cm^2	R_L mW/cm^2
14-9 pm	8-9	7.5	14.2	13.8	3.93	35.18	38.66	37.0
	9-10	6.2	13	11.8	3.63	34.53	38.02	36.3
	10-11	4.5	12.2	11	3.54	33.7	37.59	35.5
	11-12	5.5	12.5	11	3.49	34.18	37.75	36.0
15-9 am	0-1	7	13.5	12.2	3.63	34.93	38.28	36.8
	1-2	6	11.8	11	3.55	34.43	37.38	36.2
	2-3	6	13	11.8	3.63	34.43	38.02	36.2
	3-4	7.5	14	13.5	3.90	35.18	38.55	37.1
	4-5	8.5	14.2	13.5	3.84	35.68	38.66	37.6
	5-6	8	14	13	3.8	35.43	38.55	37.3
9-12 pm	9-10	5.2	12.4	11	3.46	34.01	37.70	35.8
	10-11	5	12	11	3.5	33.94	37.50	35.7
	11-12	5	11.9	10.6	3.45	33.93	37.42	35.7
10-12 am	0-1	4.8	11.8	10.5	3.44	33.79	37.30	35.6
	1-2	4.5	11.1	10.2	3.4	33.59	37.05	35.4
	2-3	4.2	11	10.1	3.39	33.46	36.98	35.3
10-12 pm	9-10	7.2	14.4	13	3.74	35.05	38.76	36.9
	10-11	7.1	14	12.6	3.69	34.95	38.54	36.8
	11-12	6.5	13.2	12	3.6	34.80	38.09	36.6
19-12 pm	9-10	1.5	9.5	8	3.13	32.26	36.19	33.9
	10-11	1	9	7.8	3.13	32.03	35.93	33.7
	11-12	1	9	7.5	3.05	32.03	35.93	33.7
20-12 am	0-1	0.5	8.5	7.1	3.0	31.8	35.68	33.5
	1-2	0.2	8.5	7	2.98	31.66	35.68	33.4
	2-3	0	8	7	3.02	31.56	35.43	33.2
2-12 am	1-2	4.2	8.8	8	3.14	33.45	35.83	35.2
	2-3	4	8.7	8	3.13	33.36	35.77	35.1

TABLE 3.3 Measurements of long wave radiation (with extra heating)

Date	Time period	t_p °C	t_a °C	t_w °C	$\sqrt{e}$ $mb^{\frac{1}{2}}$	σT_p^4 mW/cm^2	σT_a^4 mW/cm^2	Q mW/cm^2	R_L mW/cm^2
9-9 am	0-1	7.8	3.5	2	2.44	35.33	33.21	12.4	23.4
	1-2	5.5	2.8	1.8	2.44	32.88	34.18	"	20.9
	2-3	4	2	1	2.42	33.45	32.5	"	21.5
	3-4	4	2	1	2.42	33.45	32.5	"	21.5
	4-5	3	1.5	0.5	2.38	32.97	32.26	"	21.1
	5-6	4.5	2	0.8	2.41	33.7	32.5	"	21.6
16-9 pm	10-11	6.5	5.2	4.8	2.82	34.68	34.04	12.4	22.8
	11-12	7.2	5.2	4.8	2.82	35.03	34.04	"	23.2
17-9 am	0-1	7	5	4.5	2.81	34.93	33.94	12.4	23.1
	1-2	7.2	3.5	3.5	2.80	35.03	33.21	"	23.2
	2-3	7.2	2.8	2.8	2.73	35.03	32.88	"	23.2
	3-4	9	3	3	2.75	35.93	32.97	"	24.2
	4-5	10.5	3.5	3.5	2.80	36.70	33.21	"	25.0
	5-6	11	4	4	2.85	36.96	33.45	"	25.2
10-9 am	0-1	4.8	3.1	2.2	2.55	33.84	33.02	12.4	21.9
	1-2	4	2	1.5	2.52	33.45	32.50	"	21.5
	2-3	3	1.1	0.2	2.40	32.97	32.08	"	20.9
	3-4	2.5	0.5	0	"	32.74	31.80	"	20.7
	4-5	"	0.5	0	"	"	"	"	"
	5-6	"	0	0	"	"	31.56	"	"

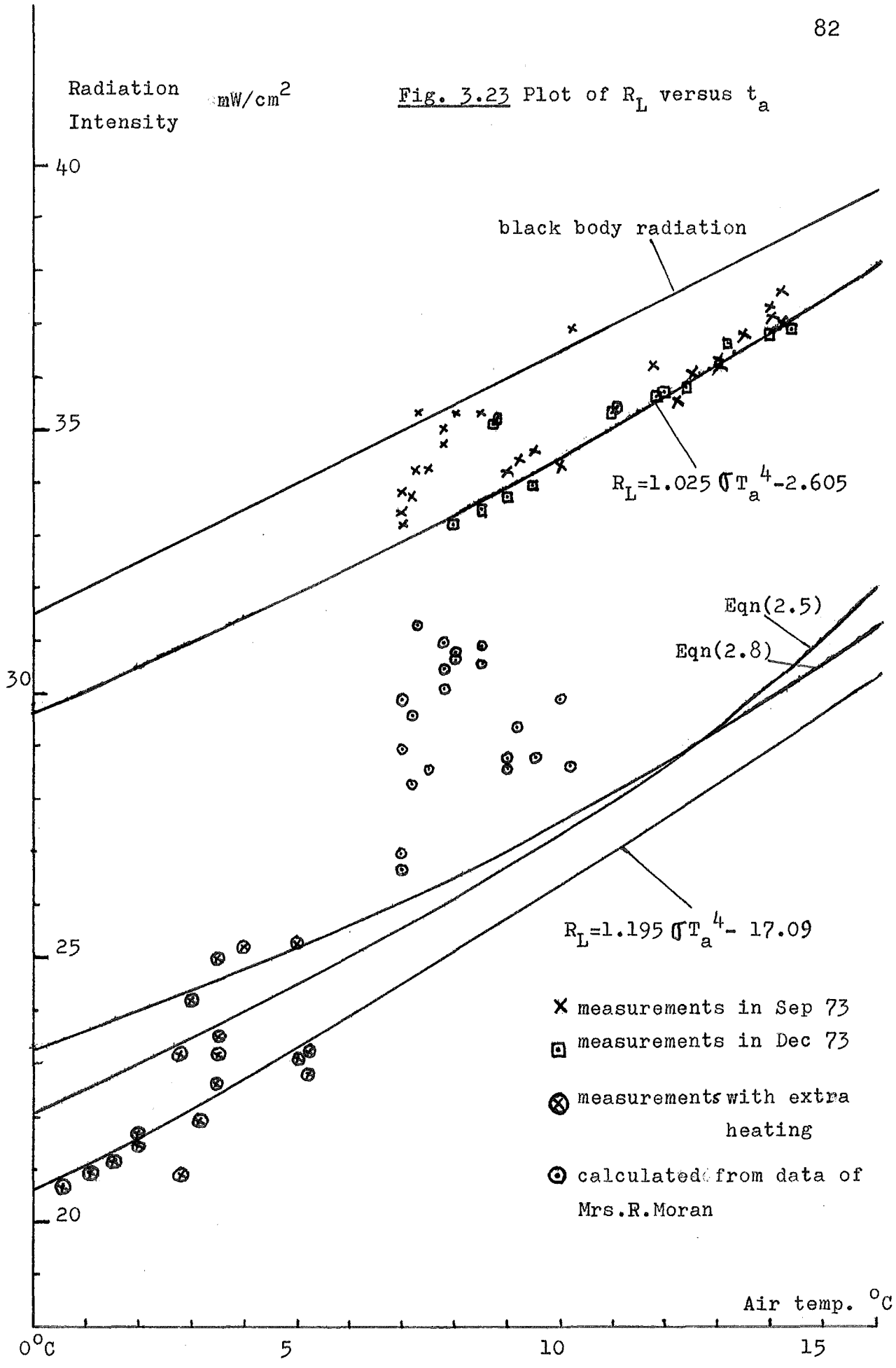

Fig. 3.23 Plot of R_L versus t_a

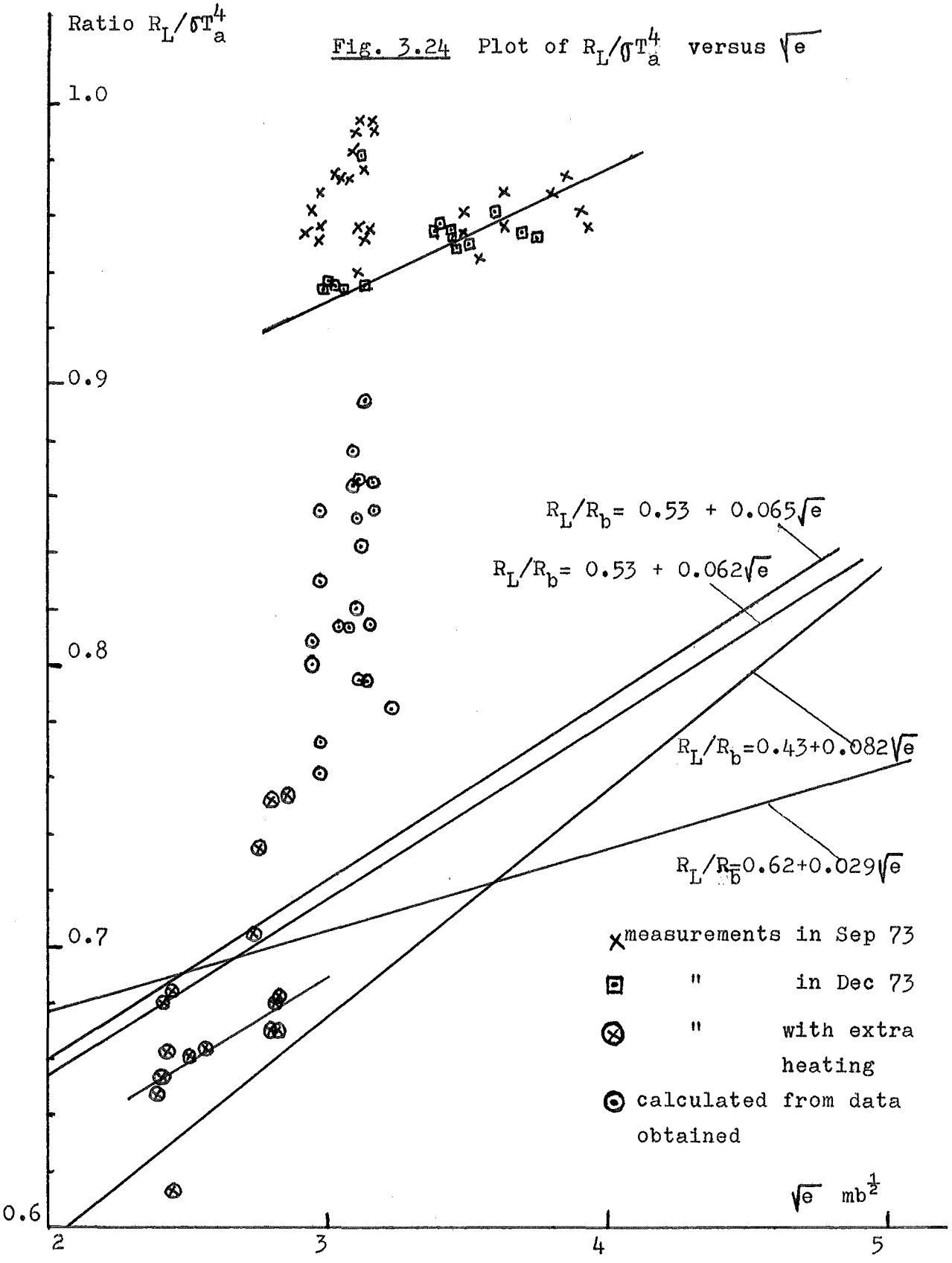

Fig. 3.24 Plot of $R_L/\sigma T_a^4$ versus $\sqrt{e}$

measuring site of the Christchurch Weather Bureau. Outputs from the radiometer were connected to an electronic integrator and recorded by the number of counts during a fixed period. These net radiation represent the heat loss from ground surface to the sky which is $R = R_G - R_L$. The Funk radiometer used were set at 1.5 m from ground so that the outgoing radiation from the ground surface can be assumed as the radiation of a black body at screen level air temperature. The incoming radiation from sky is then calculated by the difference between R_G and R. Normally there is little difference in air temperature between the Airport, where measurements of Weather Office records are made, and the University Campus where our records are measured. Therefore our recorded air temperatures were used to estimate the outgoing radiation from ground and hence obtain the incoming sky radiation which should not be different greatly for the two measuring sites. Some data available for the same periods of measurement were obtained. Results of R_L' estimated from such calculations are also presented in Table 3.1 and shown in Fig. 3.23 for comparisons.

3.4 DISCUSSIONS OF THE RESULTS

(A) Magnitude of R_L

As seen from Fig. 3.23 and 3.24 there are three groups of points which represent different conditions of measurement. The upper group comprises of clear sky measurements at Ilam Halls of Residences in September and some in December when the radiometer was set up near the solar water heater on the Chemical Engineering Building.

This group is very close to the black body line and show a much larger incoming radiation from the sky compared with values proposed by other formulae.

The middle group represents the calculated incoming sky radiation based on the data of net radiation loss obtained from other and the air temperature at the measuring site. This group also has higher values than any of those calculated by the formulae.

The lower group comprises of all the points which represent the result of measurement during some clear cold nights in September where extra heating was required to allow the plate temperature to be measurable. These points scatter around the lines representing the three proposed formulae in a region where the discrepancy between them is largest.

If considering the first two groups only, one may conclude that the incoming radiation from the Christchurch night sky is approximately 20% to 30% greater than any of the accepted formulae predict. However, the good fit of the last group with the proposed formulae raised doubt on that conclusion.

One reason for the large R_L obtained may be due to the existence of thin cloud high above the sky which gives an apparent clear sky condition. As can be seen from the analytical part, the appearance of cloud and hence increase water vapour in the path length of the long wave radiation rays leads to increase in R_L. However, this effect of cloud is only important for some points which represent the measurement of clear sky periods in intermittent clear and cloud nights. (e.g. points representing measurements on 10 Sept and

11 Sept). For other points, clear sky conditions can be assured.

The main reason for this large R_L is more likely due to condensing of water vapour on the sensing plate and on the inside of the polythene cover. One notice which is common for all measurements under this condition is that the plate temperature was always lower than dew point temperature of the air (for e.g. at 4am to 5am on 15 Sept, t_a = 14.2°C, t_w = 13.5°C giving a dew point temperature of 12.5°C, the corresponding plate temperature was 8.5°C). Thin film of water vapour then covered the plate and absorbed long wave radiation, keeping the plate at high temperature than it should be.

Excluded those points very close to the black body line, all the rest of the upper group lie nearly in a straight line. Indeed, the regression line for those point is:

$$R_L = 1.025\ \sigma T_a^4 - 2.605$$

with correlation coefficient $r = 0.955$

(cf Swinbank's $R_L = 1.195\ \sigma T_a^4 - 17.09$)

This line is nearly parallel to Swinbank's line so that one may expect that if the condensing of water vapour does not occur the incoming radiation may be close to Swinbank's line. In this case the difference is nearly constant at 8 to 9 mW/cm^2 for the whole range of temperature normally encountered in the atmosphere.

The calculated values of R_L in the middle group show no trend at all, variation is random within the limited data available. In these calculations the outgoing radiation were assumed as black body radiation at screen air temperature, if the actual temperature of the ground beneath the Funk

radiometer were measured, they must be usually lower than air temperature giving less outgoing radiation and hence less incoming component R_L.

The lower group of points has a majority close to Swinbank's line which support the suggestion made when considering the regression line of the upper group. Air temperature during the measurements giving the points in this group were low so that extra heating were provided. This avoided the problem of dew forming on the sensing plate and on the polythene cover as in upper group measurements.

The trends of the three groups are not shown as clear in the R_I/R_b versus $\sqrt{e}$ graph as in the R_L versus t_a graph.

If straight lines are drawn for the upper and lower groups in Fig. 3.24, they are nearly parallel to the Brunt's line $R_I/R_b = 0.53 + 0.065\sqrt{e}$ except one is at lower and one at higher level than Brunt's line. The fact that the regression lines of the upper and lower groups are parallel in two graphs shows that one group of points was having a systematic error but the trend is the same. This error is, as said before, due to the water vapour condensing in the radiometer and can be avoided by extra heating during night-time measurements.

(B) Performance of the radiometer

1. Response:

Although the time constant of the radiometer is large, it is good enough for the measuring of long wave radiation at night because there is no frequent fluctuation as for solar radiation at daytime. The figures illustrated show that this radiometer was able to respond with the change in cloudiness

conditions and giving the variation in long way sky radiation. For solar radiation, although the minute fluctuation during a short period can not be recorded exactly, the average output shows a close relationship with the fluctuation.

2. Reliability:

In the quantitative analysis where all the points of experimental results are plotted, it is seen that the measurements in December are in consistent with those in September. They form a straight line with good correlation coefficient within a large range of temperature. The radiometer can be considered to be reliable to give such consistency.

(C) Accuracy of the measurement

In the above calculations, there are a few assumptions on the transmittance of the cover, absorptivity and emissivity of the sensing plate and the efficiency of the heating element. Although these assumptions were based on results of tests or measurements presented in the references, the actual values may be different due to difference in construction and weather conditions ... Therefore the effect of these factors in the final estimation of the radiation measured can not be assessed accurately. If calibration of the radiometer can be made, these effect can be eliminated by the effective sensitivity of the radiometer.

Assuming that: the error in estimating $T_L \alpha_L = 0.9$ is 10%

" " " " $\epsilon_L = 0.95$ is 5%

the error in temperature = $\pm 1^{\circ}C$

the error in Q = 5%

Analysis in Appendix 4 shows that the percentage error for case of maximum R_L measured (with extra heating) is 13%

and for minimum R_L is 13.6%. The largest error in the group are the estimation of $T_L \alpha_L$ and ϵ_L. If these two factors can be known more accurately the overall accuracy of R_L can be improved.

-ooOoo-

C O N C L U S I O N S F O R P A R T I

From the study of long wave sky radiation and the development of a simple radiometer for trial measurements under Christchurch weather conditions the following points were concluded:

1. Long wave radiation from the sky is due to the radiation emission of the three components in the atmosphere covering the Earth: water vapour, CO_2 and O_3. The strongest emission coefficients for these radiation component lie from 6 to 8μ and $> 14\mu$ in wavelengths. The region from 8 to 12μ is called the "window of the atmosphere" where radiation from the Earth surface is freely lost to the outer space.

2. Calculations to estimate the sky radiation are possible by using radiation charts which require the measurement of air temperature, pressure and humidity at several vertical levels in the atmosphere. This method is only useful for meteorological purposes, for engineering applications it is not of much use because such measurements are usually not available.

3. Measurements of long wave clear sky radiation in the past have led to several empirical formulae for estimation of this component from air temperature and humidity measurements at the site only. None of those formulae is recognised as standard although the three following are widely used and the difference is small in the range of temperature encountered in engineering applications:

(a) $R_L = -17.09 + 1.195\ \sigma T_a^4$

(b) $R_L = 5.31 \times 10^{-14} T^6$

(c) $R_L = \sigma T_a^4 (1 - 0.261e^{-7.77 \times 10^{-14} (t_a)^2})$

Radiation loss from any surface can be calculated if its temperature, emissivity are known or estimated and use one of the above equations. For cloudy conditions, 0.8 to 0.96 of the black body radiation at air temperature is obtained from the sky.

4. The radiometer developed in this study is able to show the variation of the incoming sky radiation with changing conditions of air temperature and cloudiness of sky. It also enables this radiation to be estimated with 13% accuracy provided extra heating is used to avoid dew forming on the cover and the sensing plate. Use of this radiometer for recording the variation of solar radiation at daytime is also suitable although the quantitative analysis requires further study.

5. Trial measurements of long wave radiation at Christchurch with the above developed radiometer during September and December 1973 gave results of clear sky radiation close to Swinbank's formula although parts of the results

gave 25%to 30% higher than the values proposed by this formula due to systemetic error in the measurement. This finding is based on limited measurements, because there is no past work to compare; further measurements will be required to verify this relationship.

-ooOoo-

RECOMMENDATIONS FOR FURTHER WORK

1. For the radiometer:

The developed radiometer can be used to carry out further measurements to verify the results found from these trial measurements. The method to manufacture hemispherical polythene cover described in Ref. (18) is worth trying to improve the appearance and performance of the radiometer.

The direct measurement of radiation intensity can be obtained if this radiometer can be calibrated by facing it to a known black body radiator and measure its millivolt output (31). This facility is not available in the Department at present.

2. For long wave radiation measurement:

Precautions must be taken to avoid the cases of low temperature or any time where the plate temperature is lower than dew point temperature of air which cause the condensing

of water vapour in the radiometer resulting too high estimations. Heating provided by 1 to 2 volts D.C. current is suggested to avoid the above problem in any case.

3. For solar radiation measurement:

The radiometer showed good response to this type of measurement during the test carried out with the solar water heater. The quantitative analysis to estimate solar radiation intensity from temperature of the sensing plate may be useful for solar radiation study. A glass hemisphere to cover the sensing plate for measuring solar radiation can eliminate the long wave component and makes the quantitative analysis easier.

R E F E R E N C E S

1. Ångström A. : A study of the radiation of the atmosphere, Smithsonian Misc. Coll. 65, 3, 1915.
2. Simpson G.C. : Mem. Roy. Met. Soc. III, No. 21, 1928.
3. Brunt D. : The transfer of heat by radiation and turbulence in the lower atmosphere, Proc. Roy. Soc. A., 124, 1929, p. 201.
4. Elsasser W.M. : Heat transfer by Infra-red radiation in the atmosphere, Havard Met. Stud. No.6, Havard University, Massachusetts, 1942.
5. Mc Adams : Heat Transmission, 3rd Ed., Mc Graw-Hill Book Comp., 1954, p. 82.
6. Schnaidt F. : Gerland's Beitrz., Geophysics,54, 1939, p. 203.
7. Strong J. : Study of atmospheric absorption and emission in the Infra-red spectrum, Jou. of the Franklin Inst.,2,1941,p.232.
8. Brooks F.A. : Observations of atmospheric radiation, Mass. Inst. Tech.,Papers in Physical Oceanography and Meteorology 8,1941,p.2.
9. Brooks F.A. : Atmospheric radiation and its reflection from the ground, J.of Met.,9, 1952, pp.41-52.
10. Elsasser W.M. : A heat telescope and the measurement of the Infra-red radiation emission at the atmosphere, Mem. Wea. Rev.,69,1941,p.1.
11. Falckenberg G. : Experimentelles zur Druckabhangig Keit der Absorption des Wasserdamfes und de Kohlensäure Met. Zeits. 55,1938,p.174.
12. Robinson G.D. : Notes on the measurement and estimation of atmospheric radiation, Part I, Quar. J. of Roy. Met. Soc. 73, pp.127-150; Part II, - ditto-, 76, pp. 37-51.
13. ALbrecht F. : Die Messung und Registrierung der Strahlungs differenz Ausstralung-Einstralung miteinen Effektiv Pyranometer, Met. Zeits., 45, 1928, p.465.

14. Aldrich L.B. : The Melikeron, an approximately black body pyrometer, Smithsonian Misc. Coll. 72, 13, 1922.

15. Parmelee G.V. & Aubele W.W. : Radiant energy emission at Atmosphere and Ground, H.P.A.C., 1951, pp.120-129.

16. Gier J.T. & Dunkle R.V. : Total Hemispherical Radiometer Proc. of the Amer.Inst.of Elect. Eng., 70, 1951, pp.339-343.

17. Funk J.P. : Polythene -Shielded Net Radiometer, J. of Scien.Inst.,36,1959, pp. 267-270.

18. Paltridge G.W. : A net long wave radiometer, Quart. J. of Roy.Met.Soc.,95, 1969, pp.635-638.

19. Raman P.K. : Heat radiation from the clear atmosphere at night, Proc.Ind.Acad.Sci., 1,1935, p.815 and 4, 1936, p.243.

20. Brunt D. : Notes on radiation in the atmosphere, Quart.J.Roy.Met.Soc.,58, 1932,p.389.

21. Robitzsch M. : Strahlungsstudien, Arb.Obs.Lindenberg, 15,1926,p. 194.

22. Swinbank W.C. : Long wave radiation from clear sky, Quart. J.Roy.Met.Soc.,89,1963, pp.339-348.

23. Banon J.K. & SteeleL.P. : Met. Res. Cttee.,M.R.P.No.978.

24. Deacon E.L. : Water vapour over Sahara and Tiros III Obser.,J.Of Atmos. Scien.,20,1963,p.614.

25. Idso S.B. & Jackson R.D.: Thermal radiation from the atmosphere,J.of Geo.Res.,74,23,1969,p.5397.

26. Dines W.H. & Dines L.H.G. : Monthly mean values of radiation from various part of sky at Benson, Oxfordshire,Mem.Roy.Met.Soc.,2,1927,p.11.

27. See page 92 of Ref.4.

28. Suomi V. et al : J.of Met.,11,1954,pp.276-282.

29. Whiller A. : Design factors influencing solar collector performance,Chp.III of Low Temp.Appl. of Solar Ener.,ASHRAE Tech. Cttee on Solar Ener. Utiliz.,L966, Fig.3.2.

30. Holman J.F. : Experimental methods for Engineers,McGraw-Hill Book Comp.,1971,p.38.

31. Hager N.E.,Jr. : The Rev. of Scien.Inst.,34,9,1963,p.1028.

APPENDIX 1 Programme to calculate vapour pressure e and $\sqrt{e}$ of air at dry bulb temp. t_a and relative humidity ϕ .

Step		Key	Code
0	0	CLEAR	20
	1	STOP	41
	2	1	01
	3	0	00
	4	x>y	53
	5	2	02
	6	2	02
	7	CLEARx	37
	8	2	02
	9	0	00
	a	x>y	53
	b	3	03
	c	5	05
	d	CLEARx	37
	0	.	21
	1	0	00
	2	6	06
	3	x	36
	4	↓	25
	5	e^x	74
	6	↑	27
	7	7	07
	8	.	21
	9	0	00
	a	8	10
	b	3	03
	c	x	36
	d	GOTO	44

Step		Key	Code
2	0	4	04
	1	6	06
	2	clearx	37
	3	.	21
	4	0	00
	5	7	07
	6	x	36
	7	↓	25
	8	e^x	74
	9	↑	27
	a	6	06
	b	.	21
	c	1	01
	d	3	03
3	0	4	04
	1	x	36
	2	GOTO	44
	3	4	04
	4	6	06
	5	clearx	37
	6	.	21
	7	0	00
	8	6	06
	9	5	05
	a	x	36
	b	↓	25
	c	e^x	74
	d	↑	27

Step		Key	Code
4	0	6	06
	1	.	21
	2	4	04
	3	4	04
	4	7	07
	5	x	36
	6	↓	25
	7	x	36
	8	1	01
	9	0	00
	a	0	00
	b	÷	35
	c	↓	25
	d	$\sqrt{x}$	76
5	0	END	46
	1		

TO CALCULATE:

SET RUN
PRESS GOTO(00)
CONTINUE

→INPUT
ϕ (%)
↑
t_a (°C)
↑

Display as:
z ≡ ϕ (%)
y ≡ t_a(°C)
x ≡ t_a

PRESS CONTINUE

Result :
x ≡ $\sqrt{e}$ $mb^{\frac{1}{2}}$

PRESS CONTINUE

Curve fitting for e_s:

$t \leq 10^{\circ}C$: $e_s = 6.134 \exp(.07t)$ mb

$10^{\circ}C < t < 20^{\circ}C$: $e_s = 7.083 \exp(.06t)$ "

$t \geq 20^{\circ}C$: $e_s = 6.447 \exp(.065t)$ "

APPENDIX 2 Calculations of long wave radiation from temperature measurement

From charts of temperature variation in mV scale, the temperature of the sensing plate and the air can be obtained by extrapolation from the table of emf versus temperature for copper-constantan thermocouples.

For each hour of the clear sky period observed, mean curves of air and plate temperatures are drawn on the chart to measure:

air dry bulb t_a in ^oC
air wet bulb t_w in ^oC
plate temperature t_p in ^oC

Values of t_a and t_w enable the relative humidity ϕ to be estimated from psychrometric charts. Vapour pressure e in mb is calculated by $e = \phi\, e_s$ where e_s = vapour pressure of saturated air at dry bulb temperature.

When extra heating was required, a Heathkit voltage supplier giving regulated D.C. voltage from 0 to 50 volt. The instrument also shows values of voltage and current on its scale.

Examples of calculations:

For 13 Sept 1973, from 8 pm to 9 pm, measurement gave:

$$t_p = 2^oC\ ,\quad t_a = 9^oC\ ,\quad t_w = 7^oC$$

Hence $\phi = 75\%$ and $\sqrt{e} = \underline{2.94}$

By equation (3.6)

$$R_L = \frac{5.67 \times 10^{-9} \times (275.15)^4}{0.95} = \frac{32.5}{0.95} = \underline{34.2}\ mW/cm^2$$

Black body radiation at air temperature:

$$\sigma T_a^4 = 5.67 \times 10^{-9}(282.15)^4 = 35.93\ mW/cm^2$$

Ratio $R_L/\sigma T_a^4 = 34.2/35.93 = \underline{0.952}$

These values were plotted on graphs of R_L versus t_a and $R_L/\sigma T_a^4$ versus $\sqrt{e}$ as shown in Fig. 3.23 and 3.24

For 16 Sept 1973, from 10pm to 11pm:

$t_p = 6.5^oC$ V = 2 volts
$t_a = 5.2^oC$ η = 0.85
$t_w = 4.8^oC$ R = 5.46 ohm

$$\therefore \quad \phi = 90\% \text{ and } \sqrt{e} = \underline{2.82 \text{ mb}}$$

$$T_a^4 = 34.04 \text{ mW/cm}^2$$

$$T_a^4 = 34.68 \text{ mW/cm}^2$$

$$Q = \eta V^2/RA = (0.85 \times 2^2)/(5.46 \times 50.25) = 12.4 \text{mW/cm}^2$$

$$R_L = (\epsilon_L \sigma T_p^4 - Q)/(T_L \alpha_L) = \frac{(0.95 \times 34.68 - 12.4)}{0.95 \times 0.95}$$

$$R_L = \underline{22.8 \text{ mW/cm}^2}$$

Ratio $R_L/\sigma T_a^4 = 22.8/34.04 = \underline{0.670}$

These were also plotted on same graphs as above.

Regression line for R_L and σT_a^4:

To find an equation of the form $R_L = a + b\ T_a^4$ from the sets of points obtained, the equations for linear regression $y = mx + b$ are used:

$$m = \frac{\sum_{i=1}^{n}(x_i - \bar{x})(y_i - \bar{y})}{\sum_{i=1}^{n}(x_i - \bar{x})^2}$$

$$b = \bar{y} - m\bar{x}$$

$$\bar{x} = \frac{\sum_{1}^{n} x_i}{n} \quad , \qquad \bar{y} = \frac{\sum_{1}^{n} y_i}{n}$$

These calculations were carried out with a H.P. 9100A calculator and a Hewlett Packard standard programme.

For 32 sets of R_L and σT_a^4 obtained from the measurements on 11 to 15 Sept and on 2, 9, 10 and 19 of December, the regression line was found as:

$$R_L = 1.025\, \sigma T_a^4 - 2.605$$

with $r = 0.955$ which is a good fit.

APPENDIX 3 Notes for the uses and manufacturing of the radiometer

1. Expanded polystyrene is a good insulation material but for low temperature range only. Above 100°C it melts easily, therefore heating of the element with a voltage greater than 8 volts (corresponding to about 12 watts) is not recommended.

2. Because of this low melting point, cutting of polystyrene can be done easily by an electrical wire connected to a D.C. voltage source (12 V car battery for example).

3. To glue polystyrene together or with other materials (cork, Al foils) only Bostik 401W was found suitable. Ados F_2 solution can not be used because it dissolves polystyrene.

4. To glue perspex, a special solution called Tensol No 7 or Tensol No 6 must be used. The former has two liquid components to be mixed before use, the mixture does not stick to glass and can be removed easily. The latter is an already mixed solution and more convenient to use giving same properties as the former.

5. Polyethylene cover for the radiometer is the commercial type thin film 0.002" thick, this film provides sufficient protection for the radiometer under heavy rain. Light positive pressure introduced into the space can be kept for about half a day. The cover can be replaced easily in case of accidental breakage or when clearness is reduced considerably by dirt.

APPENDIX 4 Error analysis for estimation of R_L

R_L is calculated from : $R_L = (\epsilon_L \sigma T_p^4 - Q)/T_L\alpha_L$

From Ref.(30):

$$dR_L = \left[\left(\frac{\partial R_L}{\partial \epsilon_L} d\epsilon_L\right)^2 + \left(\frac{\partial R_L}{\partial Q} dQ\right)^2 + \left(\frac{\partial R_L}{\partial T_L\alpha_L} dT_L\alpha_L\right)^2 + \left(\frac{\partial R_L}{\partial T_p} dT_p\right)^2\right]^{\frac{1}{2}}$$

Assuming: $T_L\alpha_L = 0.9$, $dT_L\alpha_L = 0.09$

$\epsilon_L = 0.95$, $d\epsilon_L = 0.047$, $dT_p = 1^oC$

$Q = 12.4$ mW/cm^2 , $dQ = 0.62$ mW/cm^2

Apply to the case where R_L is largest :

$t_p = 11^oC$, $R_L = 25.2$ mW/cm^2

$\partial R_L/\partial \epsilon_L = \sigma T_p^4 / T_L\alpha_L = 41$ mW/cm^2

$\partial R_L/\partial T_L\alpha_L = -(\epsilon_L \sigma T_p^4 - Q)/(T_L\alpha_L)^2 = -28$ mW/cm^2

$\partial R_L/\partial T_p = (4\epsilon_L \sigma T_p^3)/(T_L\alpha_L) = 0.55$

Hence

$$dR_L = \left[(41 \times 0.047)^2 + (-0.62/0.9)^2 + (-28 \times 0.09)^2 + (0.55 \times 1)^2\right]^{\frac{1}{2}}$$

$= \underline{3.3}$ mW/cm^2

Percentage error is $3.3/25.2 = \underline{13\%}$

Apply to the case where R_L is smallest:

$t_p = 2.5^oC$, $R_L = 20.7$

similar calculations give:

$dR_L = \underline{2.82}$ mW/cm^2 and percentage error is $\underline{13.6\%}$

P A R T II

STUDY OF SOLAR RADIATION AND THE PERFORMANCE OF A FLAT PLATE SOLAR WATER HEATER UNDER CHRISTCHURCH WEATHER CONDITIONS

N O M E N C L A T U R E

A	surface albedo (ratio of the short wave radiation reflected over the short wave radiation coming to a surface)
A_p	collector plate area , m^2
A_1, A_2, A_3, A_4	areas enclosed by curves on temperature chart, in^2
a	altitude of the sun, degree
α	angle of inclination from the horizontal, degree
C	convection coefficient, $Btu/hrft^{2o}F$ or $W/m^{2o}C$
C_p	specific heat of water, $Kcal/Kg^oC$
ϵ_p	emissivity of collector plate
ϵ_g	emissivity of glass
f	ratio of thermal resistance of outer glass plate to inner glass plate
F	fin efficiency
F'	collector efficiency factor
F''	flow factor
F_c	fraction of radiation absorbed by collector plate
F_e	effective transmissivity-absorptivity product of the cover system
H_i	incedent angle of sunrays on inclined surfaces, degree
H_h	incedent angle of sunrays on horizontal surfaces, degree
h_w	wind coefficient, $Btu/hrft^{2o}F$ or $W/m^{2o}C$
I	incident radiation, $Btu/hrft^2$ or cal/cm^2hr
I_c	critical radiation intensity, $Btu/hrft^2$ or cal/cm^2hr
I_{sc}	solar constant, cal/cm^2min
K	ratio of radiation on the Earth Surface over that at outside atmosphere for one day period
$\overline{K}$	ratio of radiation on the Earth surface over that at outside atmosphere for one month period
$\dot{m}$	water flowrate, Kg/hr
N	number of astrinomically hours of sunshine per day, hr
n	number of glass cover
n	solar azimuthal angle of a surface, degree
	overall efficiency
q_1, q_2, q_3	rate of heat loss in cover system, cal/cm^2hr
Q_{up}	rate of upward heat loss, cal/cm^2hr
Q_b	rate of heat loss backward, cal/cm^2hr

Q_w rate of heat collected by water, cal/cm^{2}hr

Q_T rate of total heat collected by the collector plate, cal/cm^{2}hr

R_o solar radiation intensity on a surface outside atmosphere, cal/cm^2(hr or day)

r ratio of mean to actual distance from the Earth to the Sun

R_{Dh} Direct radiation on horizontal surface , cal/cm^{2}hr

R_{Di} " " " an inclined surface, "

R_{dh} diffuse radiation on a horizontal surface, cal/cm^{2}hr

R_{di} " " " an inclined " , "

R_{Th} total radiation on a horizontal surface, cal/cm^{2}hr

R_{Ti} " " " an inclined " , "

S area coefficient, ^oChr/in^2 or cal/cm^{2}hrin^2

$t_a(T_a)$ air temperature, ^oC or ^oF (^oR)

$t_p(T_p)$ collector plate temperature, ^oC or ^oF (^oR)

t_1, t_2 glass temperature , ^oC or ^oF

t_i, t_o inlet, outlet water temperature , ^oC or ^oF

$t_s(T_s)$ effective radiant temperature of the sky, ^oC or ^oF (^oR)

T_1, T_2 transmittance of outer and inner glass plate

Δt temperature difference, ^oC

U_b backward heat loss coefficient, W/m$^2{}^oC$ or cal/cm$^2{}^o$Chr

U_{up} upward " " " , cal/cm$^2{}^o$Chr

U_o overall " " " , "

V mean wind speed , mph (miles per hour)

ω hour angle , degree

ω_s sunset hour angle , degree

z azimuth of the sun, degree

CONSTANT AND CONVERSION FACTORS

σ = Stefan-Boltzmann constant = 0.173×10^{-8} Btu/hrft$^2{}^oR^4$

or= 5.67×10^{-9} mW/cm$^2{}^oK^4$

1 Btu/hrft^2 = 3.69 cal/cm^{2}hr

1 cal/cm^2 = 0.0116 KWh/m^2

1 cal/cm^{2}hr = 11.6 W/m^2

1 W/m$^2{}^o$C = 0.086 cal/cm$^2{}^o$C

CHAPTER IV INVESTIGATION OF SOLAR RADIATION IN NEWZEALAND AND PARTICULARLY FOR CHRISTCHURCH

4.1 SOLAR ENERGY- AN INTRODUCTION:

The Sun radiates as a black body at 6000°C over a spectrum stretching from wavelength of 0.29 to 4.75 . Its radiation energy in the form of electromagnetic waves travels 93,000,000 miles (150,000,000 Km) to reach the Earth. At the boundary of the atmospheric layer, the intensity of this solar radiation is 2 cal/cm^{2}min (2.392 KW/m^2). This value is called the solar constant and was measured to the accuracy of ±1% by modern techniques.

Before reaching the Earth's surface, these rays have to travel through layers of atmosphere which contain ozone, oxygen, hydrogen, water vapour, carbon dioxide and dust particles. Some find their way straight through to the earth surface and appear as direct radiation, others, being absorbed in these substances or scattered after many reflections, form diffuse solar radiation.

The transmitted energy will thus vary according to the distance the sun rays have to travel through the atmosphere.

At noon when the sun is most nearly vertical and the distance is shortest, the amount of energy received will be greatest. In early morning or late afternoon the distance is greater hence less energy is received.

During cloudy periods, most of the radiation reaches the earth surface is diffuse radiation while on clear sky periods the ratio of diffuse to direct radiation is only 10 to 15%. The overall energy received on a cloudy day is much less than

on a clear day.

The intensity of solar radiation on any site on the earth surface can be measured by instruments called pyranometer. There are various types of pyranometers in use but the most common one used by Meteorological Offices all over the world is the Eppley pyranometer (1,2).

This instrument measures hemispherical radiation of wavelengths less than 3μ on a flat surface. The receiving surface consists of a central white disc surrounded by a concentric black surface mounted horizontally and in the centre of a clear spherical glass bulb. The inner surface is coated with highly reflective magnesium oxide and the outer ring is coated with lampblack. Ten to fifty junction thermopiles are attached to the surfaces to measure the difference in temperature between the black and white surfaces, the output is recorded by a potentiometer or galvanometer.

The diffuse component can be measured separately by another Eppley pyranometer with addition of a small disc or ring to effectively shade the measuring surface from direct sun light. Fig. 4.1 shows two versions of the Eppley pyranometers. Fig. 4.2 shows a ring device for measurement of diffuse radiation. More discriptions of other types of solarimeters and solar radiation instruments can be found in the above references.

4.2 RADIATION ON A HORIZONTAL SURFACE:

A horizontal surface on the earth receives both the direct and diffuse components of the solar radiation.

From the knowledge of solar constant and the position of

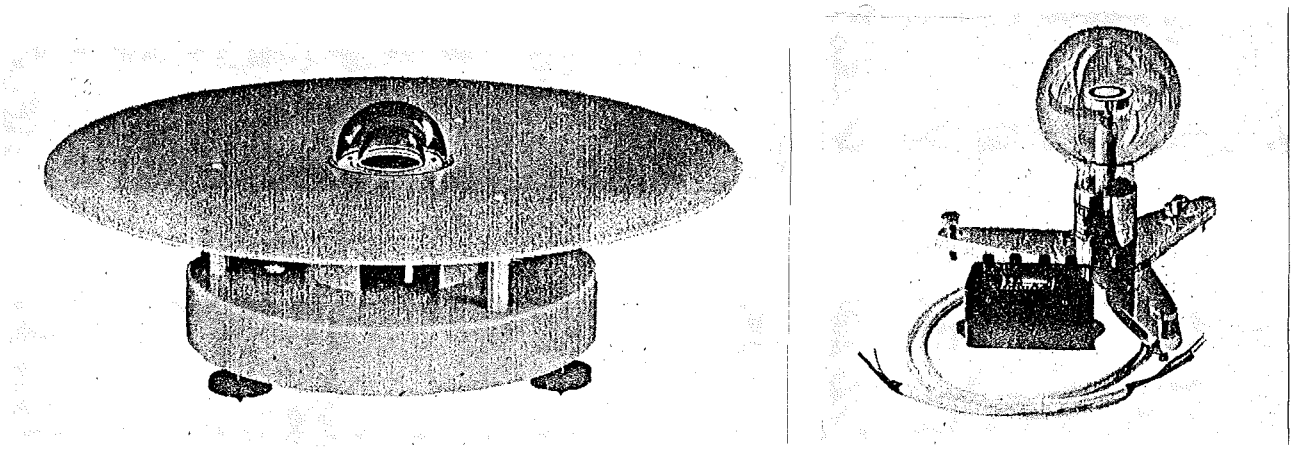

Fig. 4.1 Two versions of the Eppley pyranometer

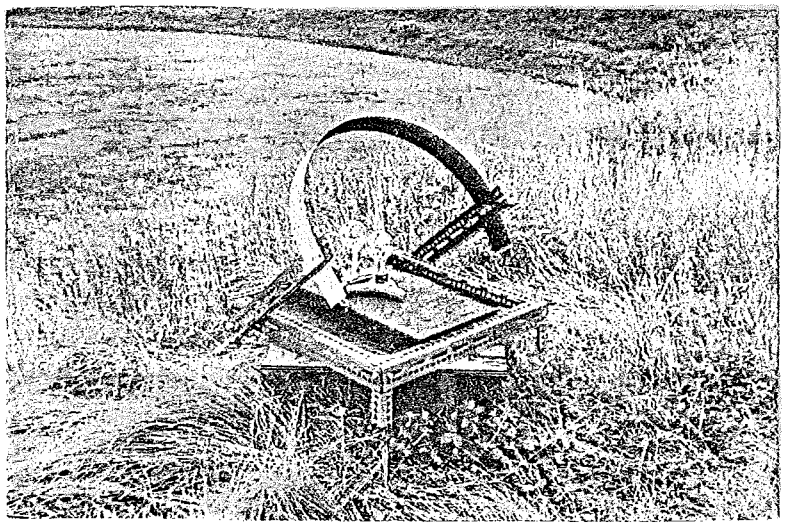

Fig. 4.2 A ring device for diffuse radiation measurement

the place in terms of its latitude, a theoretical value for the solar radiation intensity on a horizontal surface can be calculated (3).

The actual total radiation intensity on horizontal surface is usually recorded by Meteorological Offices. In New Zealand there are 5 stations to record such data: Ohakea, Auckland, Wellington, Invercargill (all from 1954) and Christchurch (from 1960). Hourly and daily totals of the solar radiation are extracted from continuous chart. Total radiation per month and average daily insolation are also given.

A convenient parameter called "K value" is usually used to describe the quantity of incident solar radiation received over any given period. It is the ratio of the amount of radiation received by a horizontal surface on the earth

over that received by a similar surface outside the earth's atmosphere during the same period.

When the period of measurement is a day, the ratio is conventionally written as K and $\bar{K}$ is used when the period is a month.

For New Zealand conditions, K for most days of the year lies between 0.1 and 0.75 corresponding to very dense cloud to clear sky conditions. $\bar{K}$ varies slowly with the seasons ranging from 0.3 to 0.7.

De Lisle (4) calculated values of daily total radiation for cloudless sky and normal atmospheric conditions from records of duration of bright sunshine. This quantity is recorded by Campbell-Stokes sunshine recorders consisting of a glass sphere which brings the sun rays to a fairly sharp focus at a certain distance from it. A paper card is placed at this

point and the duration of bright sunshine is the numbers of hours and tenths during which the focused sun rays have sufficient intensity to scorch the standard card.

The relationship for the calculation is:

$$\frac{R_{Th}}{R_o} = a + b\left(\frac{n}{N}\right)$$

Where R_{Th} is total radiation on the horizontal at the earth's surface.

R_o is the total radiation on a horzontal surface outside the atmosphere.

n is the hours of bright sunshine.

N is the astrinomically possible hours of sunshine per day.

a and b are constants, varying slightly with location and time of year. Tables showing typical values are to be found in the original paper.

These calculations gave good agreement between the calculated values and the maximum measured values recorded from 5 weather office stations.

Benseman and Cook (5) later proposed a standard year solar radiation values for 5 representative locations in New Zealand based on 11 year records for Auckland, Ohakea, Wellington and Invercargill and 5 year records for Christchurch.

The selection criteria to select typical months to make up the standard year were based on:

1. The average monthly radiation level: selected months must be within $\frac{1}{2}$ standard deviation of the long term average.

2. The monthly distribution of daily total radiation i.e. the characteristic distribution of K throughout the month as

a function of $\bar{K}$.

3. The sequence of radiation within the month. Their analysis gave these standard years for the above 5 locations.

Table 4.1 Standard Year Radiation Intensities (cal/cm^2 per day)

Months	Auck	Weltg	Ohakea	Inver	ChCh
Jan	554	571	578	518	514
Feb	464	444	495	439	469
Mar	395	355	370	302	342
Apr	299	244	271	186	241
May	195	150	182	124	153
Jun	157	121	140	88	119
Jul	186	127	151	144	130
Aug	242	207	220	181	218
Sep	342	305	324	294	283
Oct	415	416	419	389	418
Nov	485	488	541	476	539
Dec	532	549	546	538	600

For Christchurch, the mean monthly radiation data from 1969 to 1973 are presented to compare with this proposed standard year. (Table 4.2)

It can be seen that the proposed standard year frequently overestimates solar radiation intensity for the last 5 years. The overestimation is larger in percentage for low insolation months than high insolation ones, but the absolute differences are not so large. Considering the extremely variable characteristics of solar radiation, this proposed standard year is quite

useful to give an idea of how much energy available from the sun under Christchurch conditions.

Table 4.2 Comparisons of Standard Year Radiation and records for last 5 years at Christchurch (cal/cm^2 per day)

Month \ Year	Standard	69	70	71	72	73	% of difference
Jan	514	510	466	417	499	499	+ 1 to + 9
Feb	469	429	445		446	434	+ 5 to + 8
Mar	342	330	258	294	320		+ 4 to +25
Apr	241	226	237	188		218	+ 3 to +22
May	153	126	147	135	143		+ 4 to +18
Jun	119	119	97	88	115	103	+ 0 to +26
Jul	130	135	129	122	113	101	- 4 to +22
Aug	218	182		184		149	+15 to +32
Sep	283	251	254	301	289	276	- 2 to +11
Oct	418	401	387	413	384	389	+ 1 to + 8
Nov	539	482		477	440	461	+11 to +18
Dec	600	514	530	542	484	522	+10 to +19

\+ for over estimation

\- for under estimation

4.3 INFORMATION OBTAINABLE FROM THE WEATHER OFFICE:

Besides records of solar radiation on horizontal surface, other information on climatological soundings can be obtained from Christchurch Weather Bureau such as:

- wet and dry bulb temperatures for every hour rounded to the whole degree except 3-hourly measurements from 12 pm (midnight) recorded on the field book at exact readings.

- records of wind speed and direction (continuous and 3-hourly values).

- degree of cloudiness of the sky in fraction of eighths (0/8 for clear, 8/8 for overcast) at 3-hourly basis.

- rainfall records in mm.

- period of bright sunshine in hour and tenths. This information is useful where no records of solar radiation is available because estimation of solar intensity can be made from the duration of bright sunshine although the accuracy is not high. See (4,5)

From now on W.O. is used to refer to Weather Office .

4.4 RADIATION ON AN INCLINED SURFACE:

For meteorological purposes solar radiation intensity on horizontal surface is enough but for engineering applications, this data only is insufficient. Building surfaces and roofs are usually vertical or inclined, the heating and cooling load estimations for these situation require the knowledge of solar radiation on inclined surfaces. Most of the installations to utilize solar energy are also inclined to collect more energy from the sunrays. Therefore the estimation of solar radiation on inclined surfaces is important for those applications.

An inclined surface exposed to the sun receives a total radiation comprised of 3 components:

1. Direct radiation.
2. Diffuse radiation.
3. Reflected radiation from surroundings.

Radiation intensity on inclined surfaces is not normally recorded by Weather Offices. However, the total solar radiation on such surfaces can always be estimated if the direct and diffuse components of the radiation on a horizontal surface

can be separated.

Liu and Jordan (3) gave the three following relationships to enable components of radiation on inclined surfaces to be calculated from components of radiation on horizontal surface.

A. Direct radiation:

$$R_{Di} = R_{Dh} \times \frac{\cos H_i}{\cos H_h} \qquad (4.1)$$

Where R_{Di} = direct radiation on inclined surface

R_{Dh} = direct radiation on horizontal surface

H_i = angle of incidence of sunrays on inclined surface.

H_h = angle of incidence of sunrays on horizontal surface.

B. Diffuse radiation:

It is assumed that diffuse radiation is isotropically distributed over the sky. Although there is some error in this assumption because there is more radiation in the vicinity of the direction of the sun than in other directions, the error is small so that the below relation can be used:

$$R_{di} = 0.5(1 + \cos\alpha)\, R_{dh} \qquad (4.2)$$

Where R_{di} = diffuse radiation on inclined surface

R_{dh} = diffuse radiation on horizontal surface

α = inclined angle of the surface from the horizontal

C. Reflected radiation:

Because of the inclination of the surface, it receives some portion of the radiation reflected back from surroundings. This component depends on the albedo (i.e. ratio between the shortwave radiation reflected and shortwave radiation coming into a surface) of the surroundings.

$$R_f = 0.5(1 - \cos\alpha)\ A\ X\ (R_{dh} + R_{Dh}) \qquad (4.3)$$

A is albedo of surroundings ranging from 0.03 for normal field to 0.8 for snow surface.

In equation (4.1), H_h is usually well-known because it can be calculated from the la-titude of the surface and the position of the sun.

cos H_i can also be calculated for any inclined surface at any time by this equation:

$$\cos H_i = \sin a \cos\alpha + \cos a \cos n \sin\alpha \qquad (4.4)$$

Where a = altitude of the sun at the time

α = inclination from horizontal surface

n = solar surface azimuthal angle, i.e. the horizontal component of angle between the normal to the surface and the sun at the time.

Fig. 4.3 and 4.4 show the picture of all the relevant angles.

A publication of the Commonwealth Science and Industrial Research Organisation (CSIRO) at Melbourne, Australia (6) gives substantial information on solar positions and theoretical radiation intensities for 4 main centres in New Zealand : Auckland, Wellington, Christchurch and Dunedin. The following data can be found from this publication:

1. Direct, diffuse and total solar radiation on horizontal surface, vertical surfaces facing several directions and surface inclined 45° from horizontal. These are values calculated for clear sky conditions and for each hour of a typical day in every month.

2. The sun altitudes, azimuth and incident angles on a horizontal surface for each hour of a typical day in every

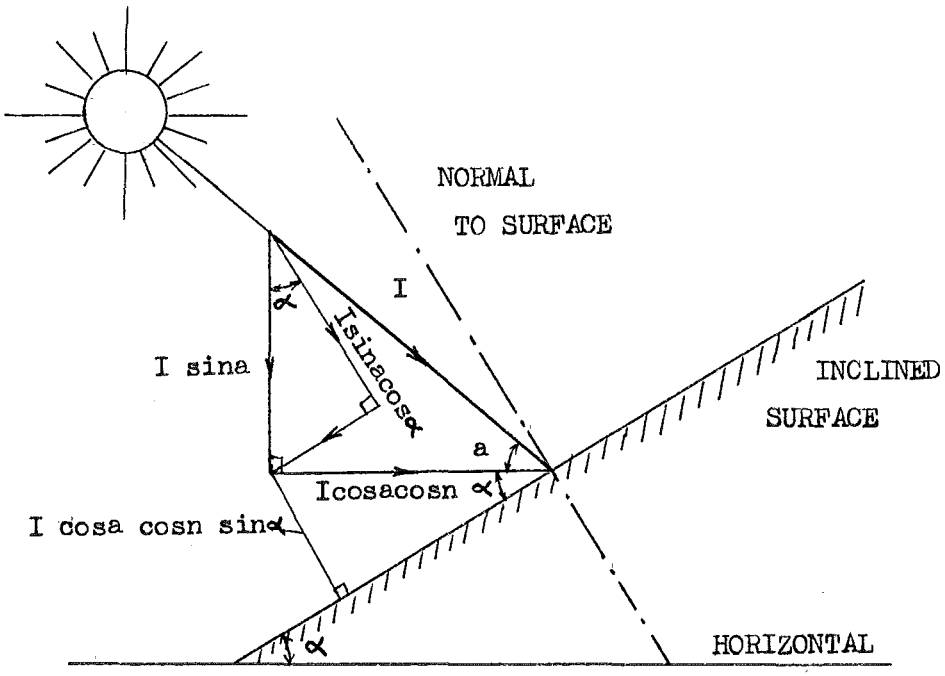

Fig. 4.3 Solar Radiation on an inclined surface

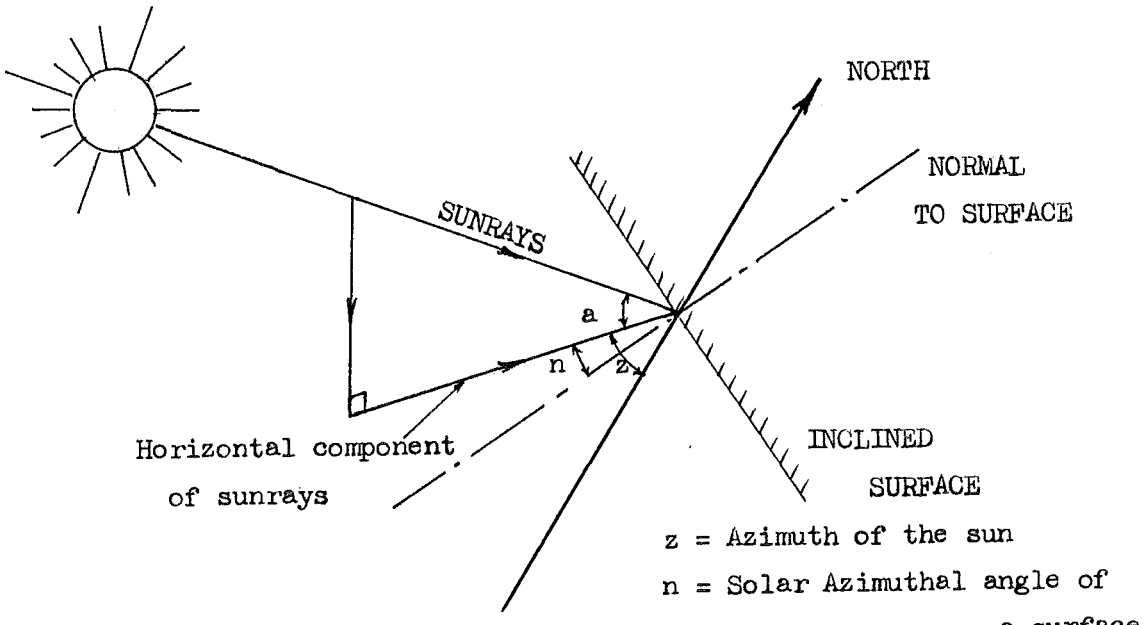

Fig. 4.4 Radiation rays with orientation of the inclined surface

Table 4.3 Incident angles of sunrays on horizontal and 40° inclined facing North surfaces.

Time	22 Oct			22 NOv			22 Dec		
	H_h	H_i	mean $\frac{\cos H_i}{\cos H_h}$	H_h	H_i	mean $\frac{\cos H_i}{\cos H_h}$	H_h	H_i	mean $\frac{\cos H_i}{\cos H_h}$
06									
07	74°	77.8°	.382	68°	78.2°	.682	68°	80.6°	.22
08	63	62.8	.883	58	64.3	.877	58	67.8	.57
09	53	48.5	1.05	47	50.5	.967	47	54	.79
10	44	34.3	1.12	30	37	1.01	36	40.4	.90
11	36	19.2	1.16	28	24.8	1.04	27	29.1	.96
12	33	7.7	1.17	24	16.6	1.04	21	21	.99
13	34	13.9	1.18	25	19.7	1.01	21	21.5	1.00
14	40	27.3	1.17	32	30.2	.996	28	30	.99
15	49	41.8	1.15	42	43.7	.926	37	41.9	.96
16	59	56.9	1.10	52	57.2	.801	48	55.2	.89
17	69	70.9	.987	63	70.8	.510	59	69.1	.77
18	80	86.2	.649	74	85.2	.138	69	82	.54
19			.142	84			80		.19

Table 4.7 Radiation on horiz.&incl. surfaces **Date:** 10-12-73

Time	Direct		Diffuse		Refl.	Total		W.O.
	R_{Dh}	R_{Di}	R_{dh}	R_{di}	R_f	R_{Th}	R_{Ti}	Rec.
05-06	0.8	0.0	3.8	3.4	0.2	4.6	3.6	4
06-07	16.6	3.6	4.8	4.2	1.0	21.4	8.8	19
07-08	31.4	18.0	5.3	4.7	1.7	36.7	24.4	35
08-09	45.5	35.7	5.6	5.0	2.4	51.1	43.1	50
09-10	57.7	51.9	5.8	5.1	3.0	63.5	60.0	62
10-11	64.4	61.8	5.7	5.0	3.3	70.1	70.1	78
11-12	71.3	70.5	6.7	5.9	3.6	78.0	80.0	79
12-13	64.0	64.0	11.4	10.0	3.5	75.4	77.5	80
13-14	70.9	70.1	6.4	5.7	3.6	77.3	79.4	80
14-15	64.4	61.5	6.1	5.4	3.3	70.5	70.2	70
15-16	54.4	48.6	5.8	5.1	2.8	60.2	56.5	58
16-17	41.8	32.3	5.4	4.8	2.2	47.2	39.3	45
17-18	27.7	14.9	4.7	4.1	1.5	32.4	20.5	29
18-19	13.4	2.6	3.6	3.1	0.8	17.0	6.5	14
19-20	2.7	0.0	1.5	1.3	0.2	4.2	1.5	3
TOTAL	627.0	535.5	82.6	72.8	33.1	709.6	641.4	701

Radiation Intensity in cal/cm^2

month. These are also calculated for a surface facing North and inclined 45° from horizontal.

3. The time of arrival and departure of the sun for typical day in every month.

Data for positions of the sun throughout the year can also be extracted from sun path diagrams prepared by Lyndon Bastings (7).

From the above references, H_i and H_h can be calculated for a typical day in every month. The ratio cos H_i/cos H_h can therefore be estimated. Table 4.3 gives values of H_i, cos H_i, H_h, cos H_h and hourly mean cos H_i/cos H_h for a surface facing North and inclined 40° from horizontal. Calculations were done for this particular inclination and on typical days (22nd) in October, November and December only to enable the performance of the solar water heater under test in the same periods to be analysed.

Necessary data for other inclinations, orientations and other months of the year can easily be extracted from the above references and calculated with the aid of a programme written to run by H.P. 9100 A calculator. (See Appendix 1 and tables 5.12, 5.13)

In order to calculate the radiation intensity on an inclined surface, the direct and diffuse components of total radiation on horizontal surface must also be known separately. R_{dh} is normally not measured. Estimation of R_{dh} from R_{Th} (total radiation on horizontal surface) can be made following the method given by Liu and Jordan (3). It was found that the ratio R_{dh}/R_{Th}, on daily basis, is a function of K only. The table below extracted from the above reference gives this

relationship.

Table 4.4

K	0.3	0.4	0.5	0.6	0.7	0.75
K_d	0.178	0.183	0.188	0.174	0.149	0.125

Where K_d = ratio of diffuse radiation over solar radiation on a surface outside atmosphere, both are measured on daily basis.

The problem is to obtain K which requires the value R_o of solar radiation intensity per day on a surface just outside the atmosphere and directly above the site. The general equation to calculate R_o is:

$$R_o = \int_{-\omega_s}^{\omega_s} r\, I_{sc} \cos H_h \, d\left(\frac{24}{2\pi}\omega\right)$$

Where I_{sc} = solar constant = 2 cal/cm^2 mim

r = ratio of mean to actual distance from earth to sun.

ω = hour angle i.e. the angle between the meridian plane passing through the sun and the meridian plane passing through the location under consideration (1 hour angle equals 15 degrees).

ω_s = sunset hour angle.

More intensive analysis can be found in the original paper by Liu and Jordan.

Incidentally during the period when tests on the solar heater were carried out, a research on solar radiation was also under experiments. Measurements of total, diffuse and net radiation on the earth surface were carried out by Mrs R. Moran from Geography Department. Three Eppley solarimeters and two

net radiometers were set up near Christchurch Weather Office measuring site, their outputs were integrated automatically by a counter and recorded on a Honeywell chart recorder at the same time. These data were kindly made available for the analysis of the performance of the test solar water heater installed at the University Campus.

Mrs. Moran is working for her Ph. D. research on the prediction of solar radiation from weather recordings. There is no doubt that her findings will give useful information for later researches on the utilization of solar energy.

The availability of these data, especially the diffuse radiation data, helped to avoid complex analysis for the estimation of R_{dh} and speed up calculations for radiation on inclined surface.

Typical charts recorded for total and diffuse solar radiation on several days of November are shown in Fig. 4.5, 4.6 and 4.7. The variation of the ratio between diffuse and total radiation with cloudiness of the sky can be seen clearly from these charts.

Tables 4.5, 4.6,and 4.7 show values of total, direct, diffuse radiation on horizontal surface obtained and the corresponding values on a 40^{o} inclined surface calculated from equations (4.1), (4.2), (4.3), and (4.4). In these calculations data of the test solar panel were used as a particular inclined surface installation.

α = 40^{o} from horizontal

A = 0.4 for concrete surface as given by Brooks and Miller (8).

$\cos H_i / \cos H_h$ from table 4.3

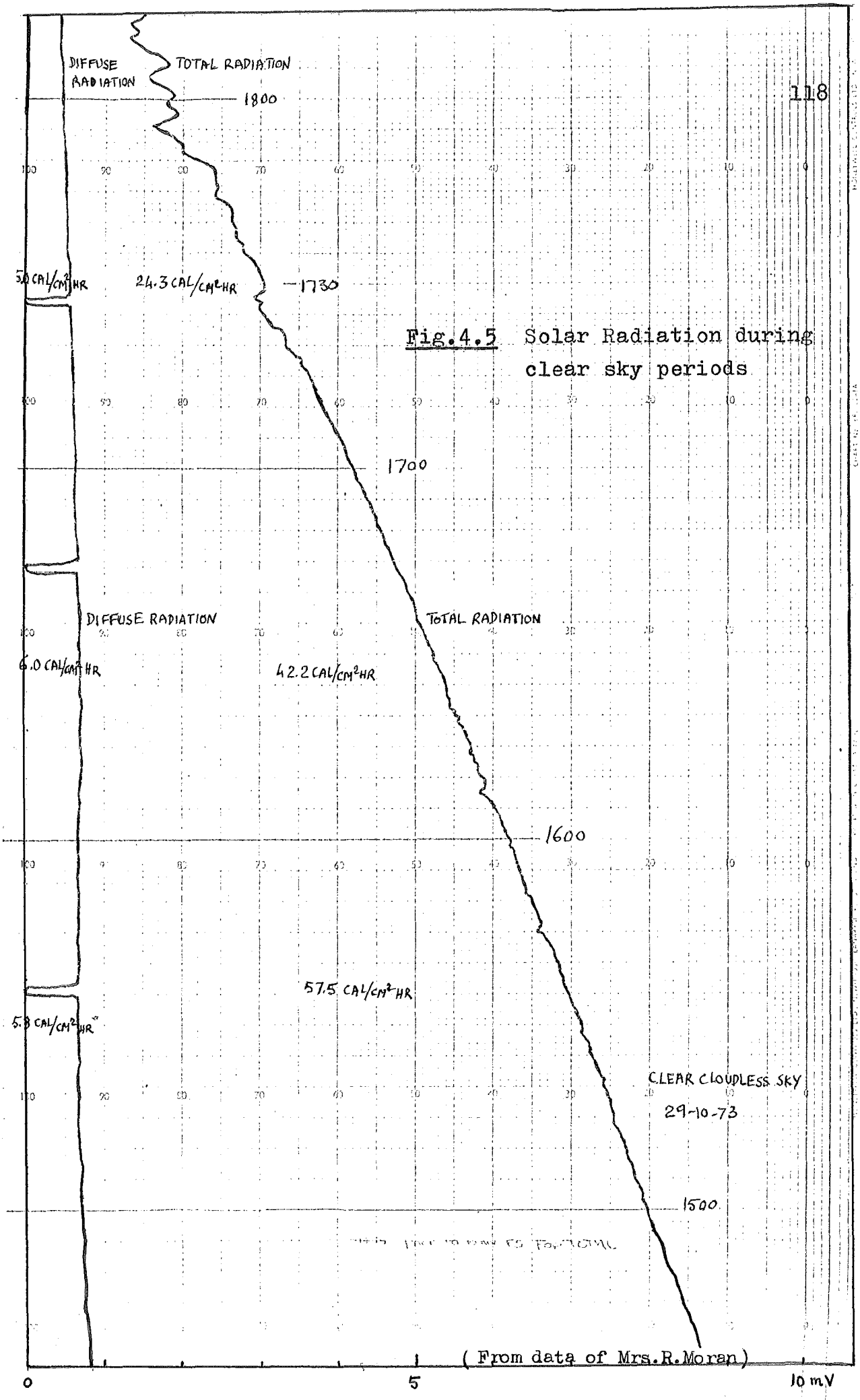

Fig.4.5 Solar Radiation during clear sky periods

(From data of Mrs.R.Moran)

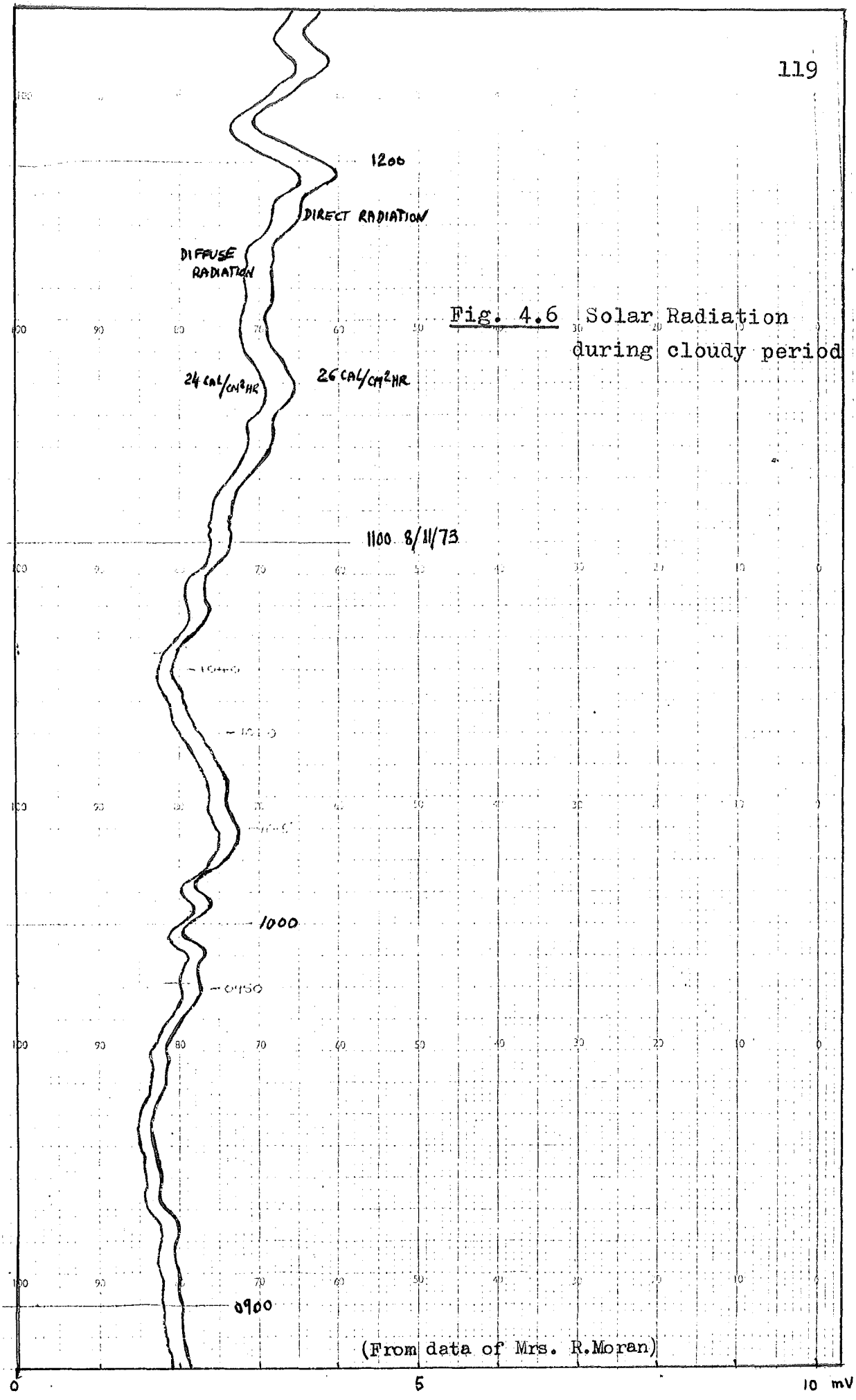

Fig. 4.6 Solar Radiation during cloudy period

(From data of Mrs. R.Moran)

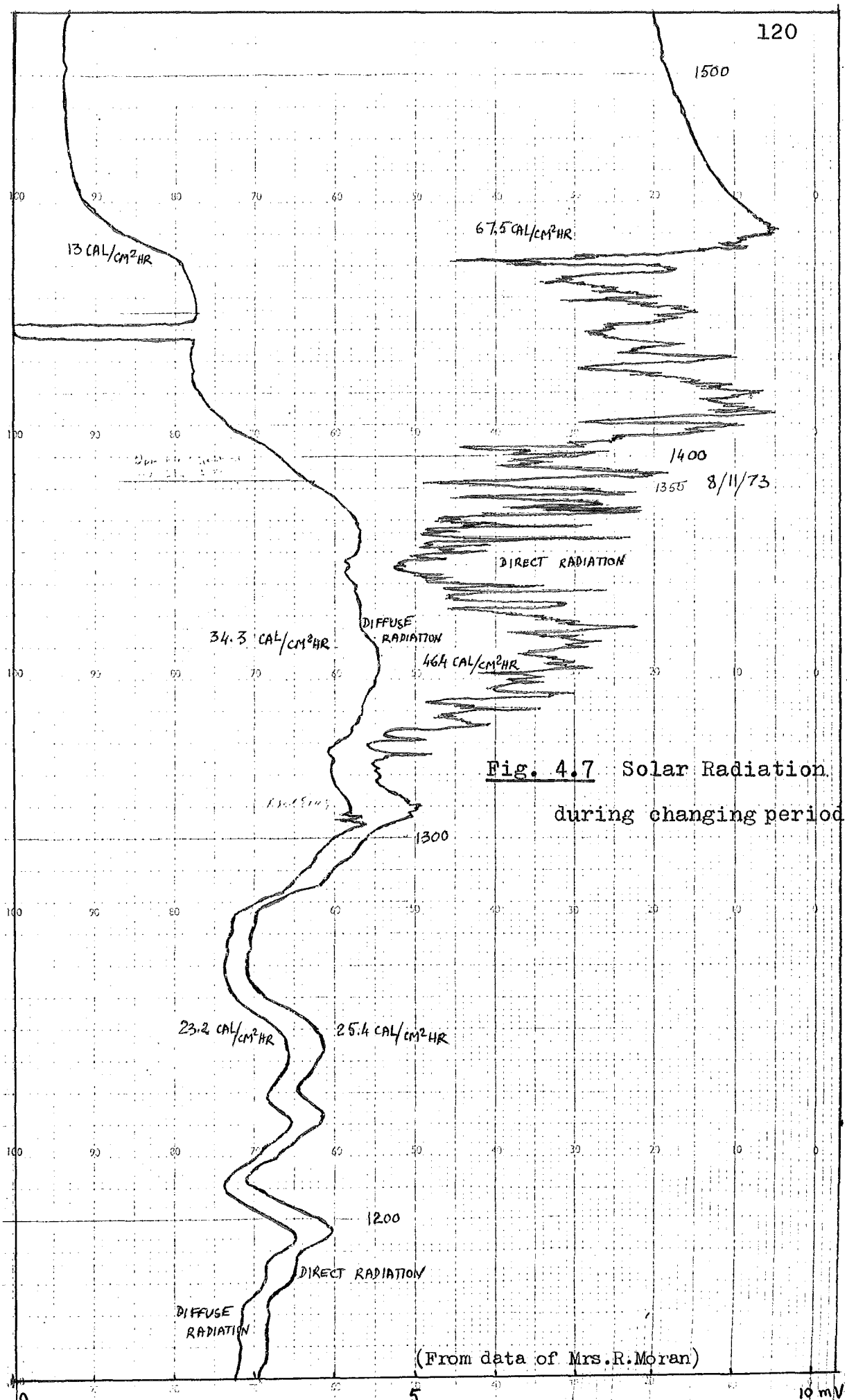

Fig. 4.7 Solar Radiation during changing period

(From data of Mrs.R.Moran)

Solar radiation on horizontal and inclined surfaces:

Table 4.5 Date: 25-10-73 Clear Intensity in cal/cm^2

Time	Direct		Diffuse		Refl.	Total		W.O.
	R_{Dh}	R_{Di}	R_{dh}	R_{di}	R_f	R_{Th}	R_{Ti}	Rec.
06-07	13.0	5.0	4.0	3.5	0.8	17.0	9.3	13
07-08	28.0	24.7	4.6	4.0	1.5	32.6	30.2	27
08-09	43.4	45.6	5.7	5.1	2.3	49.1	53.0	42
09-10	55.8	62.5	6.4	5.6	3.0	62.2	71.1	55
10-11	66.5	77.1	7.1	6.2	3.4	73.6	86.7	65
11-12	72.1	84.3	7.1	6.2	3.7	79.2	94.2	72
12-13	72.3	85.3	8.0	7.1	3.8	80.3	96.2	73
13-14	68.7	80.4	7.5	6.6	3.6	76.2	90.6	69
14-15	60.1	69.1	8.0	7.1	3.2	68.1	79.4	59
15-16	47.2	51.9	7.8	6.8	2.6	55.0	61.3	46
16-17	30.5	30.2	8.0	7.1	1.8	38.5	39.1	32
17-18	16.9	11.0	5.9	5.2	1.1	22.8	17.3	18
18-19								3
Total	574.5	627.1	80.1	70.5	30.8	654.6	728.4	574

Table 4.6 Date: 8-11-73 Intermittent cal/cm^2

Time	Direct		Diffuse		Refl.	Total		W.O.
	R_{Dh}	R_{Di}	R_{dh}	R_{di}	R_f	R_{Th}	R_{Ti}	Rec.
06-07	0.6	0.0	4.8	4.3	0.3	5.4	4.6	3
07-08	1.9	1.3	7.8	6.8	0.5	9.7	8.6	7
08-09	1.6	1.4	14.9	13.1	0.8	16.5	15.3	13
09-10	1.4	1.3	15.1	13.3	0.8	16.5	15.4	13
10-11	1.8	1.9	18.0	15.9	0.9	19.8	18.7	16
11-12	2,4	2.5	24.2	21.4	1.2	26.6	25.1	22
12-13	2.5	2.6	26.3	23.2	1.3	28.8	27.1	24
13-14	12.0	12.1	35.2	31.0	2.2	47.2	45.3	41
14-15	53.1	53.0	14.4	12.7	3.2	67.5	68.9	59
15-16	50.1	46.4	9.1	8.1	2.8	59.2	57.3	49
16-17	40.6	32.6	13.9	12.3	2.5	54.5	47.4	45
17-18	23.6	12.0	4.8	4.2	1.3	28.4	17.5	23
18-19								7
Total	191.7	167.1	188.4	166.3	17.8	380.1	351.2	322

Table 4.7 appears on page 114.

Therefore $R_{di} = 0.883\ R_{dh}$

$R_f = 0.0468\ R_{Th}$

The programme in Appendix 4 was used to speed up these calculations.

It can be seen from the above tables that during November and December an inclined surface like this panel receives less solar radiation than a horizontal surface. This is true because the ratios cos H_i/cos H_h are often less than 1 for most hours of the day and just above 1 at midday periods. Analysis for January will show the same effect but for other months of the year R_{Ti} must always be greater than R_{Th} for a 40^o inclination because this is the inclination calculated for maximun collection throughout the year. During the test periods, October was the month when this inclined surface received maximum intensity. In this month, the sunrays at midday periods are nearly normal to the surface and ratio cos H_i/cos H_h are always above 1.1 resulting in high intensities in clear days although the total radiation on a horizontal surface is not as large as in clear days of November and December. Further analyses for other months of the year in connection with solar water heating application are presented in tables 5.12, 5.13 and 5.14.

CHAPTER V THE PERFORMANCE OF A FLAT PLATE SOLAR WATER HEATER UNDER CHRISTCHURCH CONDITIONS

5.1 REVIEW:

In New Zealand, the Department of Science and Industrial Research (DSIR) had carried out researches on solar energy and possible utilization of this unlimited source several years ago.

Solar water heating applications have also been attempted by individuals throughout New Zealand for some time although not much information can be obtained on the performance of those units.

In a paper published in 1966 (9) Benseman, a research member of DSIR, concluded that only solar water heating and perhaps space heating offer any immediate promise for New Zealand climate and weather conditions.

In the same paper, he described briefly an instrument developed by his research office and called the Sun Simulator. This was used to carry out Solar Analogue Studies of water heating and other applications using Solar Energy. The advantage of this instrument is that variation in the factors such as ratio of collector area to tank capacity, amount of insulation on both collector and storage tank, materials for the collector plate etc. can be examined under identical situations so that comparisons can be made. Such experiments are certainly not practical to be carried out under actual conditions.

The typical installation of a flat plate solar water heater is shown in Fig. 5.1. A collector plate made of metal sheet on which water tubes are bonded on is exposed to the sunrays to collect energy. Copper or galvanized steel are normally used

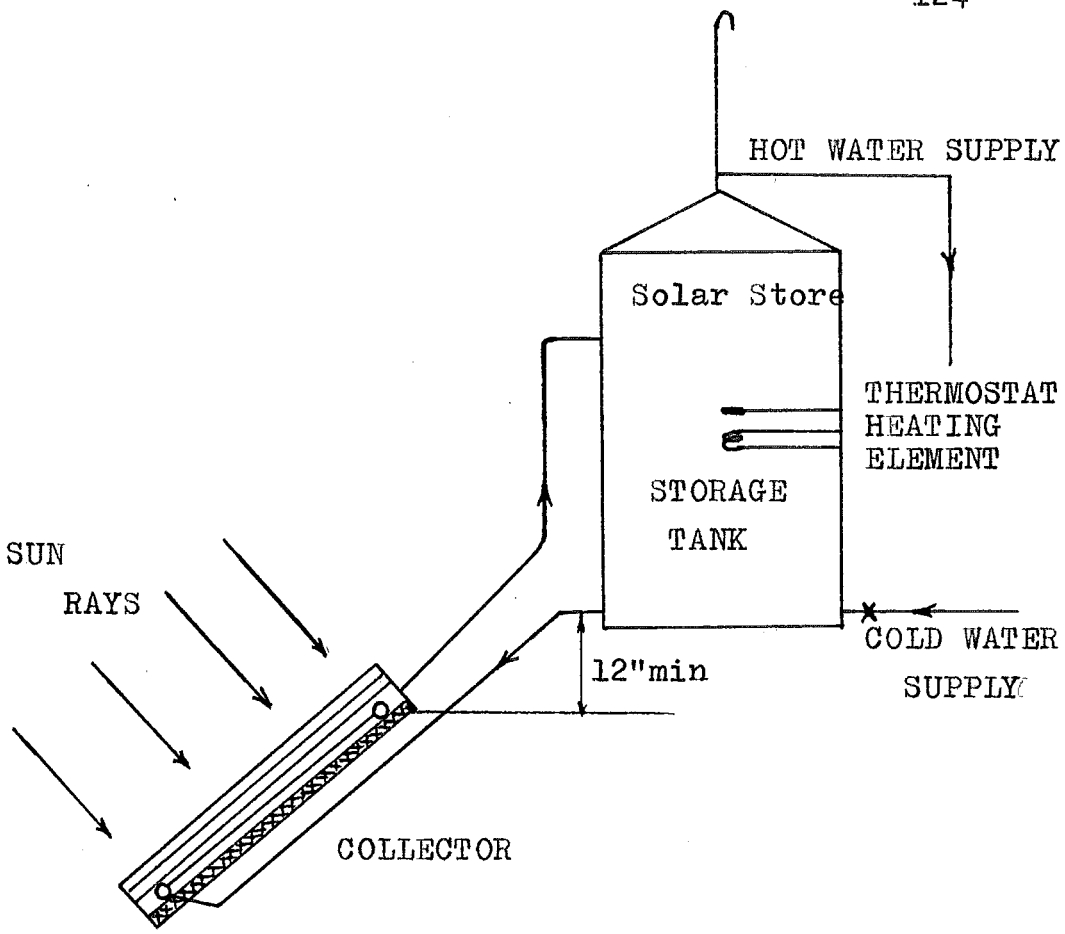

Fig. 5.1 Typical Thermosiphon System Installation

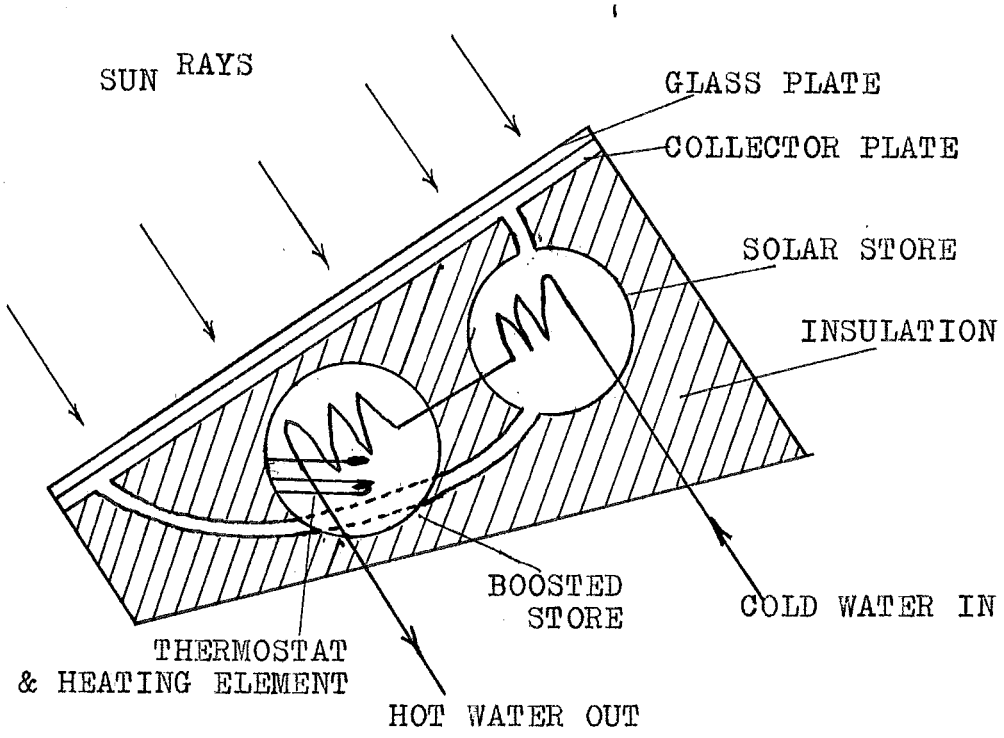

Fig. 5.2 Solar Water Heater proposed by Benseman

for both plate and water tubes. To prevent excessive heat loss, the top surface is insulated by glass plates with air spaces between and the bottom surface by some suitable materials such as fibreglass, rock or mineral wool; sand and saw dust were also used in some places but proved not very effective.

Cold water is supplied to the storage tank at the bottom through pressure reducing valve or float control valve as in ordinary hot water system. Cold water then flows down to the lower end of the collector plate and through the tubes on it. While flowing through these tubes, the water is heated by the energy collected from sunrays and flows back to the storage tank at an inlet near the top of this tank.

The flow in this system is due to the thermosiphon effect, i.e. the effect of difference in densities between hot and cold water, hot water is less dense and rises. For efficient operation and minimum amount of back siphoning at night, the upper end of the collector plate where water flows out from the panel must be at least 12" below the point where cold water leaves the storage tank. The connection pipes must also be short and insulated to minimize heat loss. Extra insulation for the storage tank is also required if this tank has to be outside as in the case when the solar panel is placed on the roof. Conventional heater and thermostat control can also be installed at the middle of the tank to boost the system during unfavourable conditions.

Several results of the Solar Analogue Studies with the help of the Sun Simulator and followed by actual experiments on some units were presented in the paper referred above. The conclusions were:

1. In general, efficiency is proportional to the quantity of incident radiation and does not differ greatly between summer and winter.

2. Performance improved with bigger collector, but doubling the area from 30 to 60 ft^2 improves the economic performance by only 45%.

3. In the thermosiphon system, the optimum store capacity, i.e. the capacity from the top of the cylinder tank to the level where hot water from the panel enters the tank is about 20 gallons. See Fig 5.1 .

Benseman also proposed a type of solar water heater where the storage tank can be placed at the same level and right behind the collector plate as shown in Fig. 5.2 . However no data on the performance of such a unit has been mentioned in the paper.

A complete different design of solar water heater has been made and installed at Wainuiomata, Wellington by S.A. Vincze. Some technical notes published in Solar Energy 1971 (10) gave the performance of that unit based on results of some tests during August and September 1969.

The so called "High-speed Cylindrical Solar Water Heater" has characteristics as shown in Fig. 5.3 . It was stated in the notes that such a unit developed a maximum of 0.980 KWh on a day having solar radiation record of 333 cal/cm^2 and a minimum of 0.724 KWh on a day receiving 289 cal/cm^2 solar radiation on a horizontal surface. The true efficiency of the unit could not be assessed because the author did not estimate the actual radiation impinging on the unit which should be more than the Weather Office records due to inclination of the set

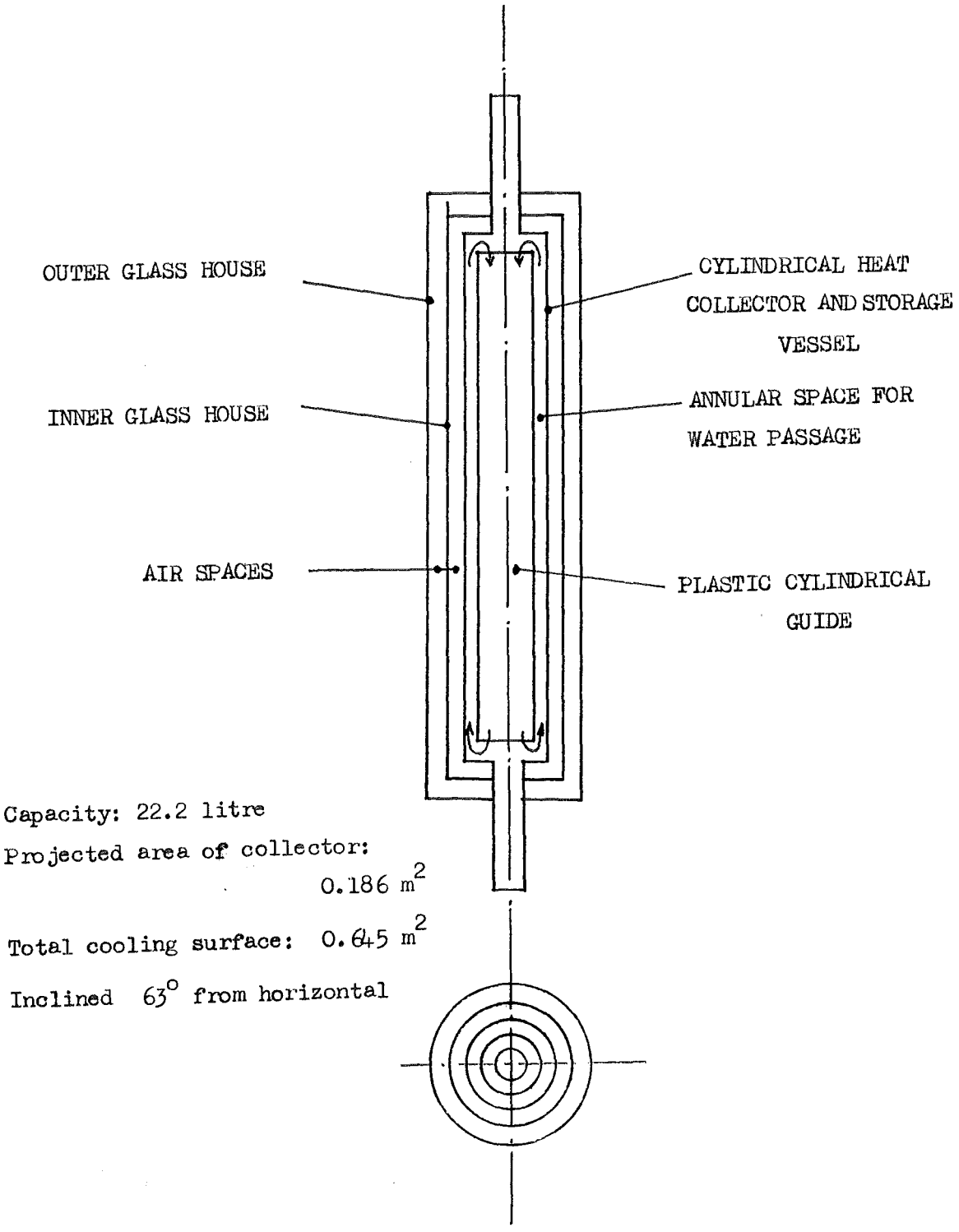

Fig. 5.3 Vincze's High-Speed Cylindrical Solar Water Heater

up and reflection from the roof.

As the threat of power shortage becomes clearer after a bad winter in 1973, when power rationing was imposed to restrict consumption and water heating was cut off during daytime, solar energy as a supplement source to electricity has regained interest.

Several solar water heating units have been installed in Christchurch over the years and some available information (11) proved that the savings were significant, up to $\frac{1}{3}$ of annual power cost.

In order to obtain detailed information on the performance of solar water heater under Christchurch conditions such as how much energy was developed, how efficient is the collection and conversion to water heating, a test unit was built by the workshop of the Mechanical Department of University of Canterbury and installed on the roof of the Chemical Engineering Building in the University Campus.

This study served as a start for further researches on the utilization of solar energy to be carried out by the Mechanical Department in coming years.

5.2 DESCRIPTIONS OF THE TEST PANEL:

(A) THE HEATER:

The design of this test panel was based mostly on the information given in the circular No. 2,1964 of the Division of Mechanical Engineering CSIRO named "Solar Water Heaters". (12)

Some modification were made to suit the wooden casing instead of pressed steel casing as described in the original paper.

Following are the general characteristics of the panel, more details of the design and manufacturing of the unit can be obtained from the above reference.

Overall dimensions: 1.12m X 1.17m (3'.8" X 3'.10")

Collector plate:

Size : 1m X 1m (after forming)

Material: gauge 26 copper sheet, semicircles formed to accomodate water tubes.

Water tubes: 7 copper tubes, 26 gauge, $\frac{1}{2}$" O.D., each 1m long.

Spacing : 145mm, datum at centre line of the plate.

Headers : 1" O.D. copper tubes, 26 gauge, each 1.3m long

Surface : painted matt black.

Tubes are brazed onto headers and soft soldered to collector plate on formed semicircle grooves.

Insulation:

Top: double glazing with 1" air space between glasses

outside glass: 32 oz. clear glass, $42\frac{7}{8}$" X $44\frac{7}{8}$"

inner glass : 26 oz. clear glass, $41\frac{7}{8}$" X $43\frac{7}{8}$"

1"space between inner glass and collector plate

Bottom: 2" fibre glass wool covered by $\frac{1}{4}$" hard board.

No edge insulation but fibre-glass insulation is extended about $\frac{3}{4}$" beyond the edges of the plate.

Casing: wooden frame made from 1" X $5\frac{1}{2}$" dressed wood, protected from weather by 26 gauge gavalnized iron flashings. One side of the frame is removable to allow alterations if necessary.

The unit was reasonably air-tight and kept water-proof by

Sealastic strips around the edges of the outer glass which was mounted on rubber U section. Fig. 5.4 and 5.7 show the collector plate and the assembly.

(B) INSTRUMENTATION:

20 thermocouples were bonded to the panel in various positions to record the temperature variations.

Fig. 5.5 shows the positions of these thermocouples.

All thermocouples are of copper-constantan type.

Thermo-couple No.	Position	Size
1 to 7	on underside of collector plate as shown in Fig. 2.4	30 gauge
8 to 11	on the outside of the back cover Fig. 2.6	30 gauge
12	water outlet	30 gauge
13	water inlet	30 gauge
14	upper air space between inner glass and collector plate	26 gauge
15	lower air space -ditto-	26 gauge
16 to 19	on the inside surface of the outer glass, directly above Nos 1, 2, 6, 7	30 gauge
20	air space between glasses (installed later, from 1-11-73)	26 gauge

These thermocouples were connected to the terminal block located at the lower corner on the back of the panel.

In order to keep a continuous record of the wet and dry bulb temperatures of the air, 2 copper-constantan thermocouples gauge 26 were placed in a white louvred box located beside the panel.

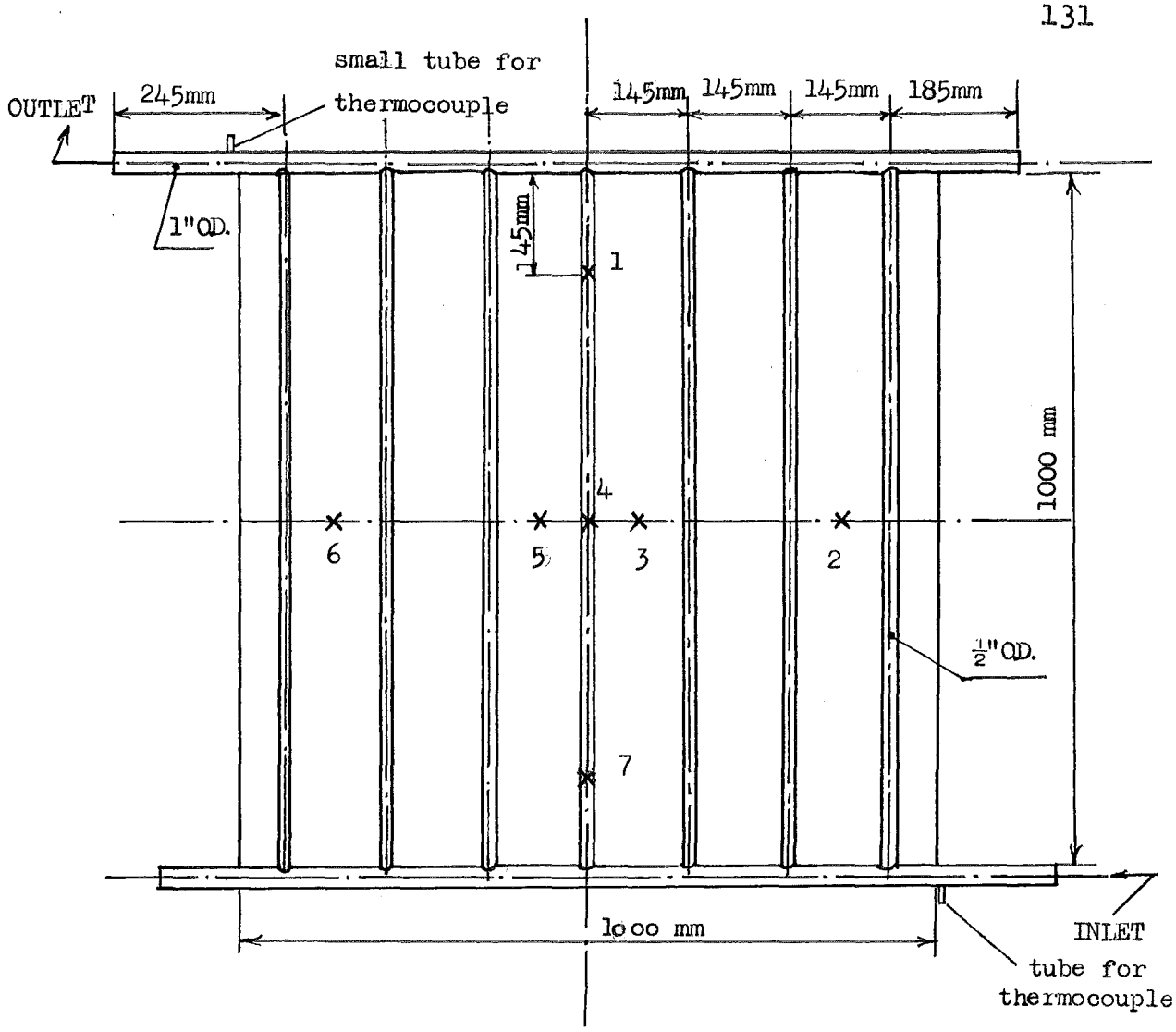

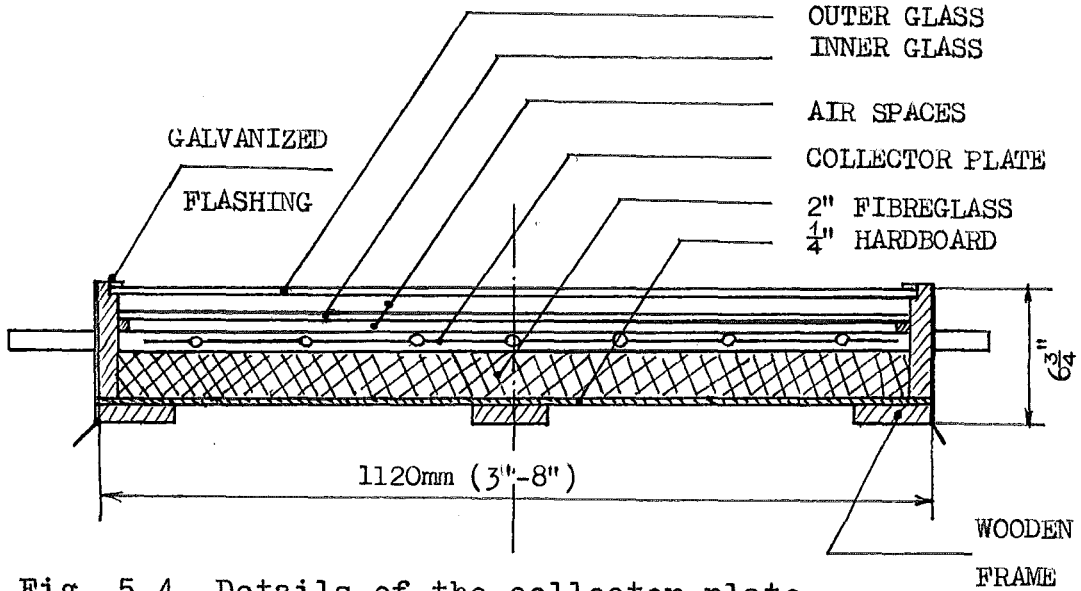

Fig. 5.4 Details of the collector plate and the assembly of the heater

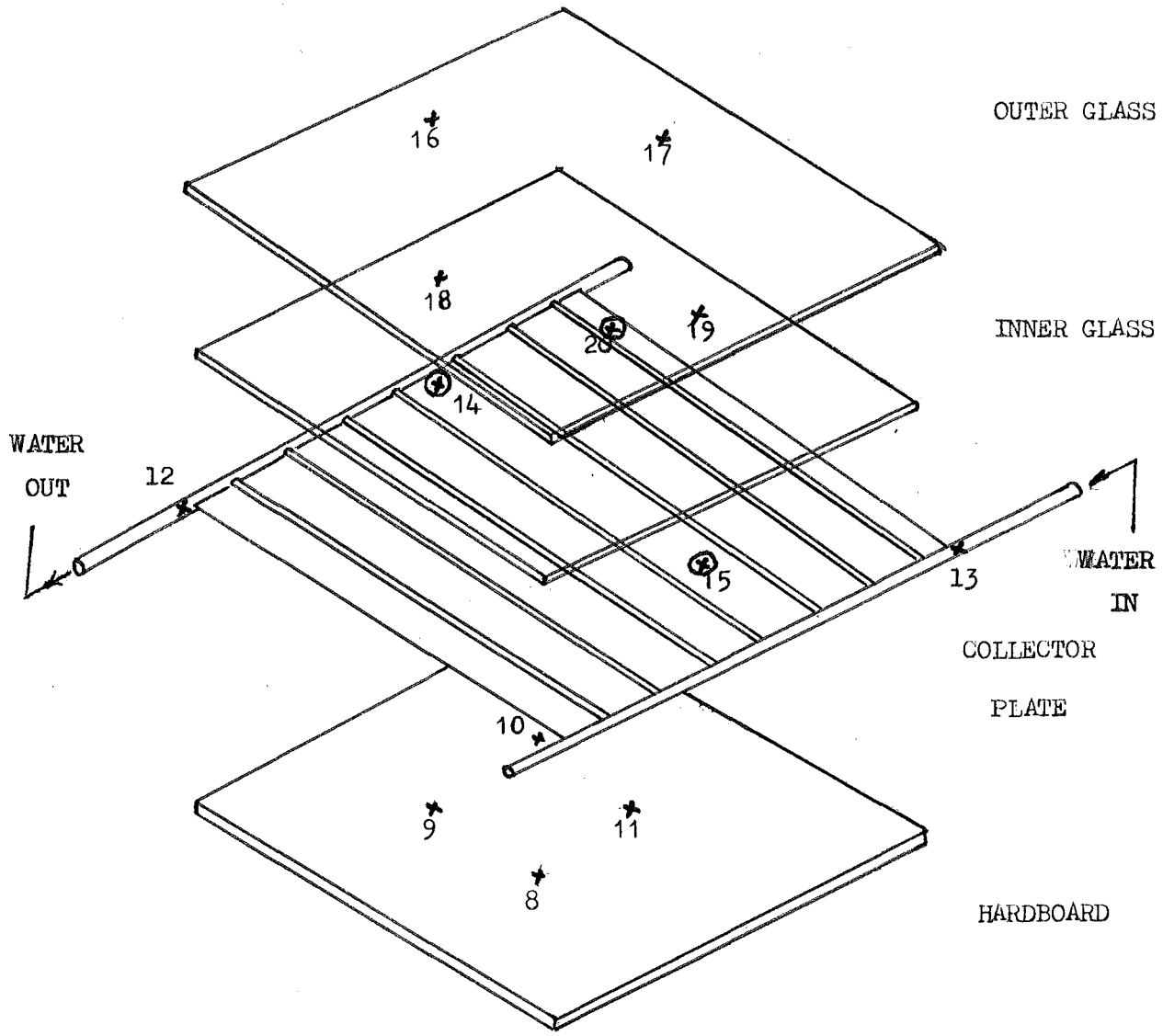

Fig. 5.5 Positions of thermocouples in the panel

Outputs of all the thermocouples were recorded by a Brown Electronik 24-channel chart recorder placed in a chamber built under the solar panel.

5.3 EXPERIMENTAL SET UP:

The solar panel was set up on the roof of the 5-storey Building of the Chemical Engineering Department.

The panel was pivoted above a stand 3 feet above the roof surface made of Dexion and wood. The stand provided a chamber to accomodate a chart recorder and a thermosflask containing ice cubes served as $0^{o}C$ reference junction for thermocouple measurements. Concrete weights were also placed on 4 corners of the stand to prevent the whole installation being flown away during strong winds.

Two pivots on the sides of the panel enabled the inclination to be set at any angle from 0^{o} to 70^{o} from the horizontal. No facility was provided to vary this angle or the facing of the panel automatically during the day.

For the initial study of this project, it was decided not to have the complete thermosiphon system installation as in Fig. 5.1 . Instead, a forced circulation system was used where water from a constant head tank 12 ft above the roof level flowed through the panel, being heated and then discharged to the drain. The installation and water circuit is shown in Fig. 5.7, 5.8, 5.9, and 5.10.

During the test period, from 10 October 1973 the panel was set facing due North and inclined 40^{o} from the horizontal. This angle was chosen because it is the optimum angle of inclination for maximum collection throughout the year at

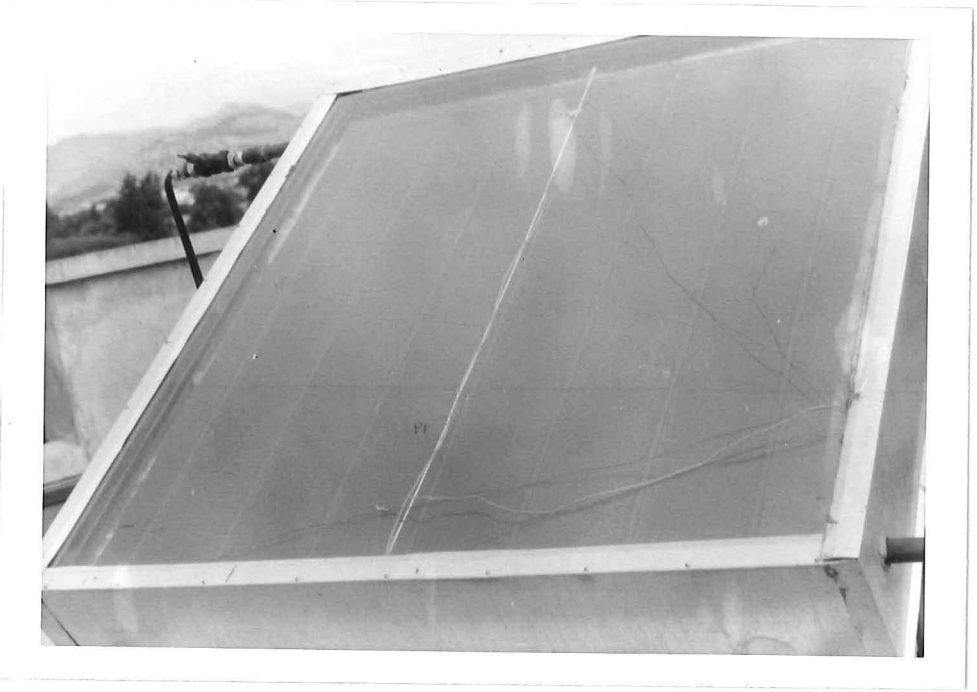

Fig. 5.6 Close up view of the solar panel

Fig. 5.7 Installation of the test (North face)

Fig. 5.8 The test panel looking from North - West

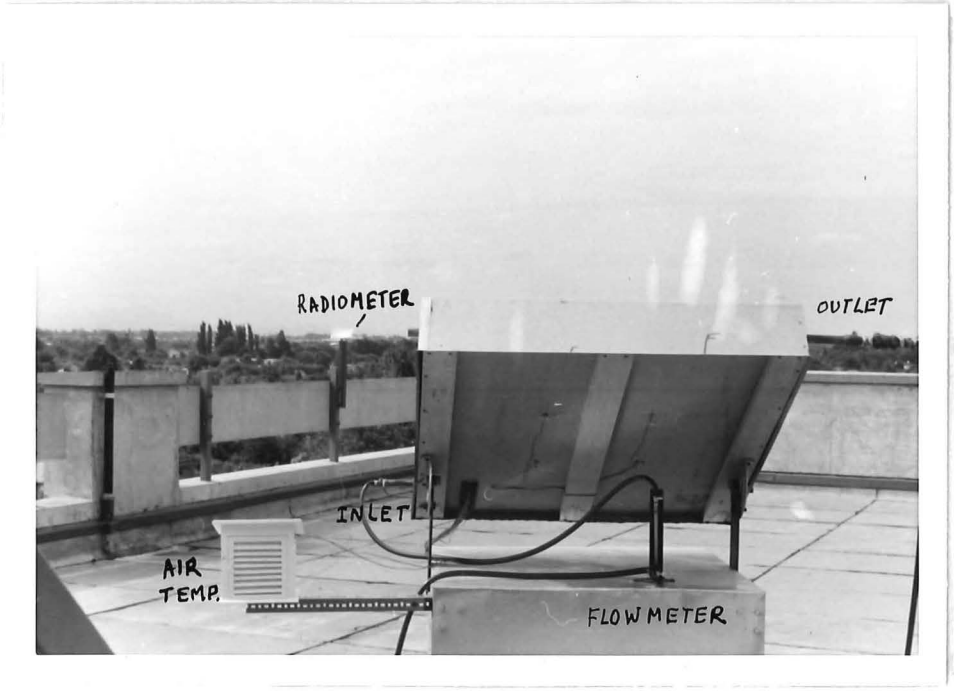

Fig. 5.9 Back side of the panel

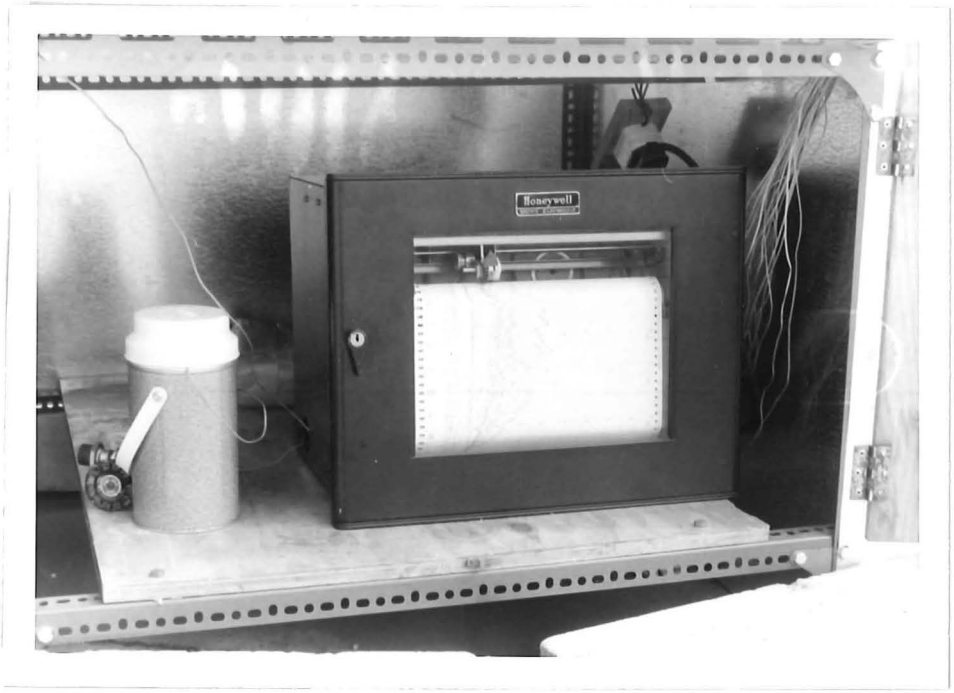

Fig. 5.10 Thermosflask for reference junction thermocouple and the recorder underneath the panel

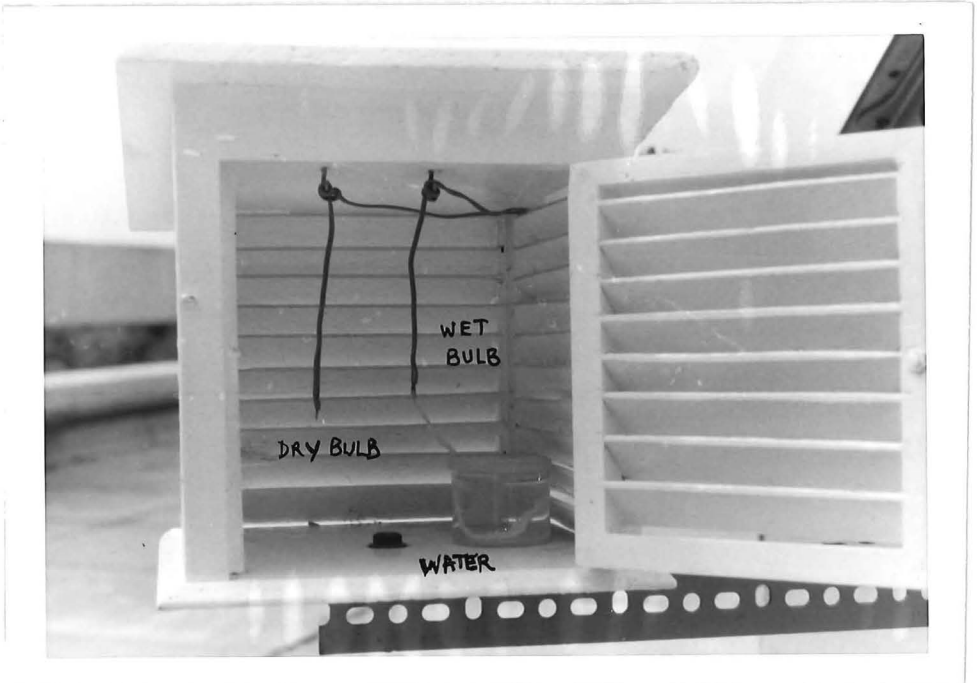

Fig. 5.11 Louvred box for air temp.measurement

Christchurch latitude (43.5°S) as suggested by Morse and Czarnecki (13).

From the terminal block, all thermocouples were connected individually to the recorder and their outputs were printed on a chart running at 2" or 1" per hour. Due to difference in the type of thermocouples used and the built-in compensation junction of the measuring circuit, the outputs were not recorded directly in degrees but in mV values on a 0 to 5 mV full scale range.

5.4 THE EXPERIMENT:

During the earlier period of the test, due to problems of too large fluctuation in water flowrates during the day and the inconsistent performance of the recorder, no quantitative analysis could be done.

As seen in Fig. 5.6, there were two ½" stop valves in the water circuit, one at the supply point and one at the outlet from the panel. The first valve was kept fully opened all the time, flowrates were varied by setting the opening of the second valve.

During the period from 10 October to 25 October 1973, at the same valve setting the flowrate could vary up to 50% from 10 a.m. to 8 p.m. See Fig. 5.12.

This fluctuation in flowrate did not follow any particular pattern as seen from this figure. Checks on the head tank and the supply point gave satisfactory performance, therefore the trouble could only result from the coarse characteristics of these stop valves. For such low flowrates, small variation in stem position could cause large fluctuations in the flow.

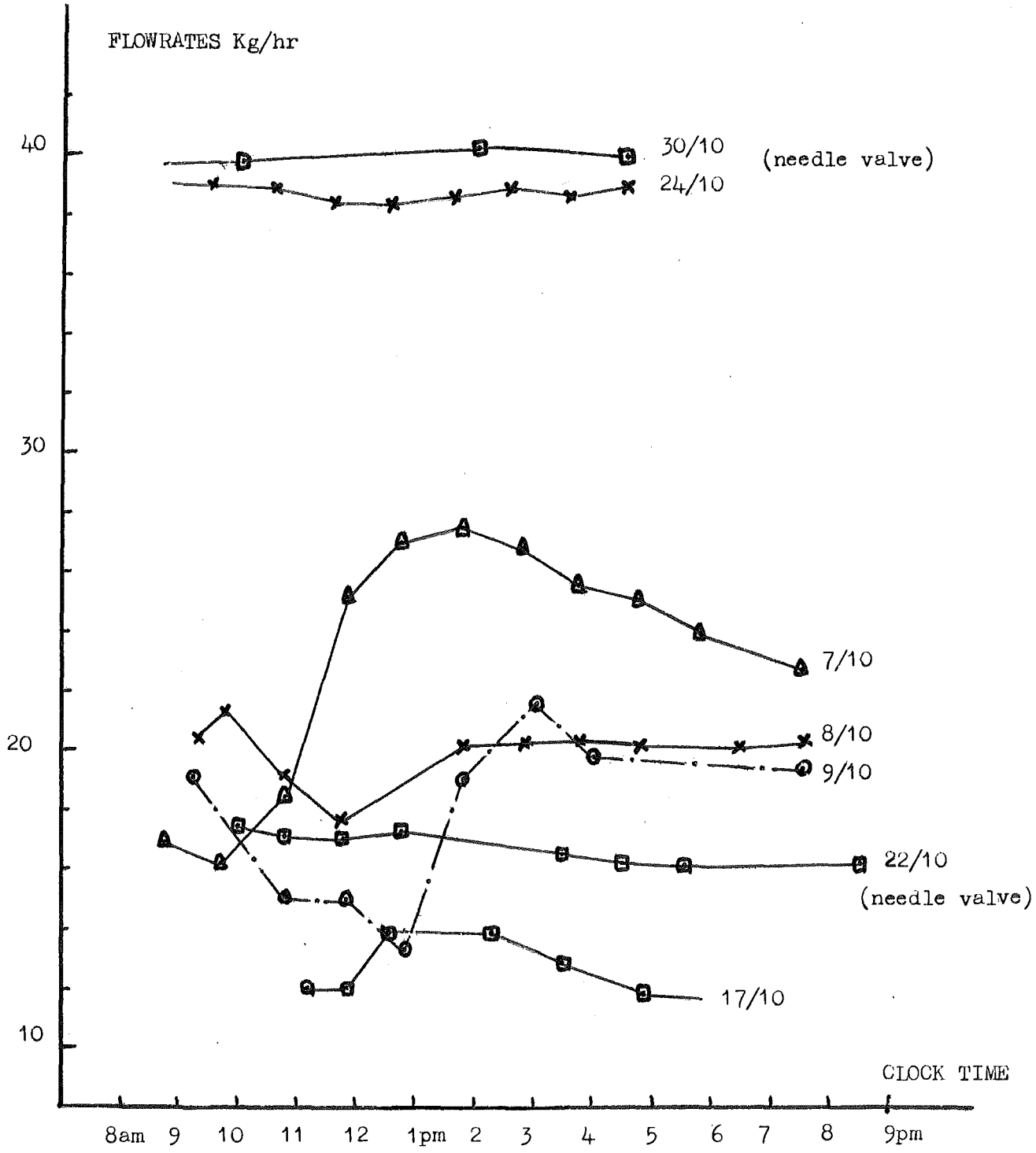

Fig. 5.12 Variation in water flowrates at the early stage of the test

A needle valve was then replaced at the outlet from the panel. Improvement was clearly noticed as shown in the same figure.

During the same period, the chart recorder also did not function properly. The slide wire and printing mechanizm developed faulty print and judder movement. These faults caused the readings of the thermocouple outputs to be too low and some times completely wrong because the potentiometer part in the recorder did not function. These faults were noticed when comparing the air temperature recorded on the chart with the records of 3-hourly temperatures measured at the Christchurch Airport by the Weather Bureau. There was a consistent 3° to 4°C difference between these two records. Experience from previous experiments in Part I and Weather Office records showed that there may be only 1° or 2°C difference between the two places.

General cleaning of the machine, its measuring mechanizm and re-calibration were done to ensure reliable results in later records.

BROKEN INNER GLASS:

On 19 October 1973, a clear and sunny day which the Weather Office recorded 542 cal/cm^2 solar radiation on a horizontal surface during 12 hours 48 minutes of bright sunshine, the outlet valve was intentionally turned to very low flowrate just after 10:10 a.m. .The temperature of the water increased and reached the point 110°C after 30 minutes, see Fig. 5.13, when a crack occurred on the inner glass of the panel. The crack, initiating from a small crack produced on the top left corner during installation ran down to the bottom end. The valve was then turned fully on to avoid built up of pressure inside the

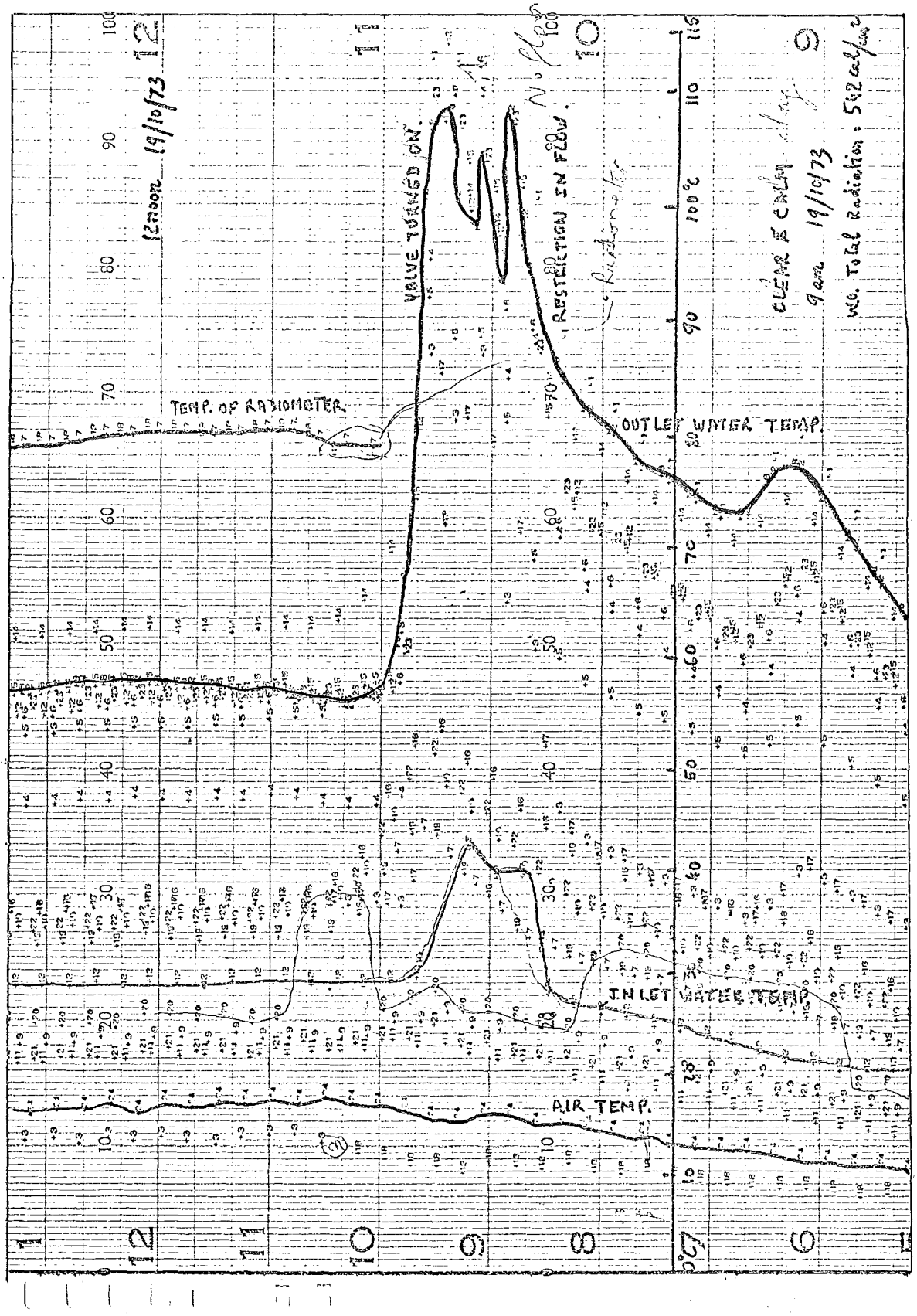

Fig. 5.13 Increase of temperatures due to restriction in water flowrate

tubes which might lead to bursting of these tubes. Boiling water and steam rushed out as the consequence of throttling process.

No further trial of this type has been made but it was clearly demonstrated that a panel of this type could be used to produce steam. The broken glass was replaced several days later.

Also from 19 October 1973 the radiometer developed for long wave radiation study in Part I was set up on the site and its output recorded on the same chart with other thermocouple readings. The output of this radiometer is, in effect, the temperature of a black plate which free-ly exchanges radiation with the sky while convective heat transfer is kept minimum by a thin polythene cover. The variation of the plate temperature of this radiometer will have a close pattern with the variation in solar radiation and this record printed on the same chart with other measurements shows the distribution of solar intensity throughout the day.

During the test period, data for hourly total radiation on a horizontal surface and weather records such as the cloudiness of the sky, wind velocity, wet and dry bulb air temperatures were obtained from Christchurch Weather Office. Valuable data on total and diffuse solar radiation for most days during the test period were also obtained from Mrs. R. Moran of Geography Department who was working on her research at a site near Weather Office measuring site.

These data, together with those recorded at the panel site are necessary for the analysis of the performance of the solar heater.

In general, the climatological situations are much the same between the installation site and the place where the obtained data were measured which are only $3\frac{1}{2}$ miles apart. However in some days when patchs of cloud were scattered at low altitude, the solar radiation intensity may differ quite considerably. One area may be obstructed from the sunbeam for half an hour or so while other places receive full sunshine. This effect can be seen on the day 6 November 1973 between 1 p.m. to 2 p.m. where the radiometer record at the site showed a drop in solar intensity while Weather Office record showed little change in the same period and Mrs. Moran's data gave the intensity of 70 cal/cm^2 from 12 noon to 1:00 p.m., 68 cal/cm^2 from 1 p.m. to 2 p.m.. See Fig. 5.14.

Typical records produced by the chart recorder are shown in Fig. 5.13 and 5.14. The continuous lines were hand-drawn from all the recorded points to allow measurements and calculations necessary for the analysis of the performance of this unit.

5.5 THEORETICAL ESTIMATIONS ON THE PERFORMANCE OF THE TEST UNIT:

Based on the method described by Whiller (15) the analysis in Appendix 2 showed that this test unit has these properties:

- Transmittance of outer glass: $T_1 = 0.850$
- Transmittance of inner glass: $T_2 = 0.864$
- Fraction of solar radiation transmitted through glasses and absorbed by the collector plate having absorptivity $\alpha = 0.95$:

$$F_c = 0.705$$

- Effective transmissivity - absorptivity product :

$$F_e = 0.748$$

This product makes allowance for the effect that the heat

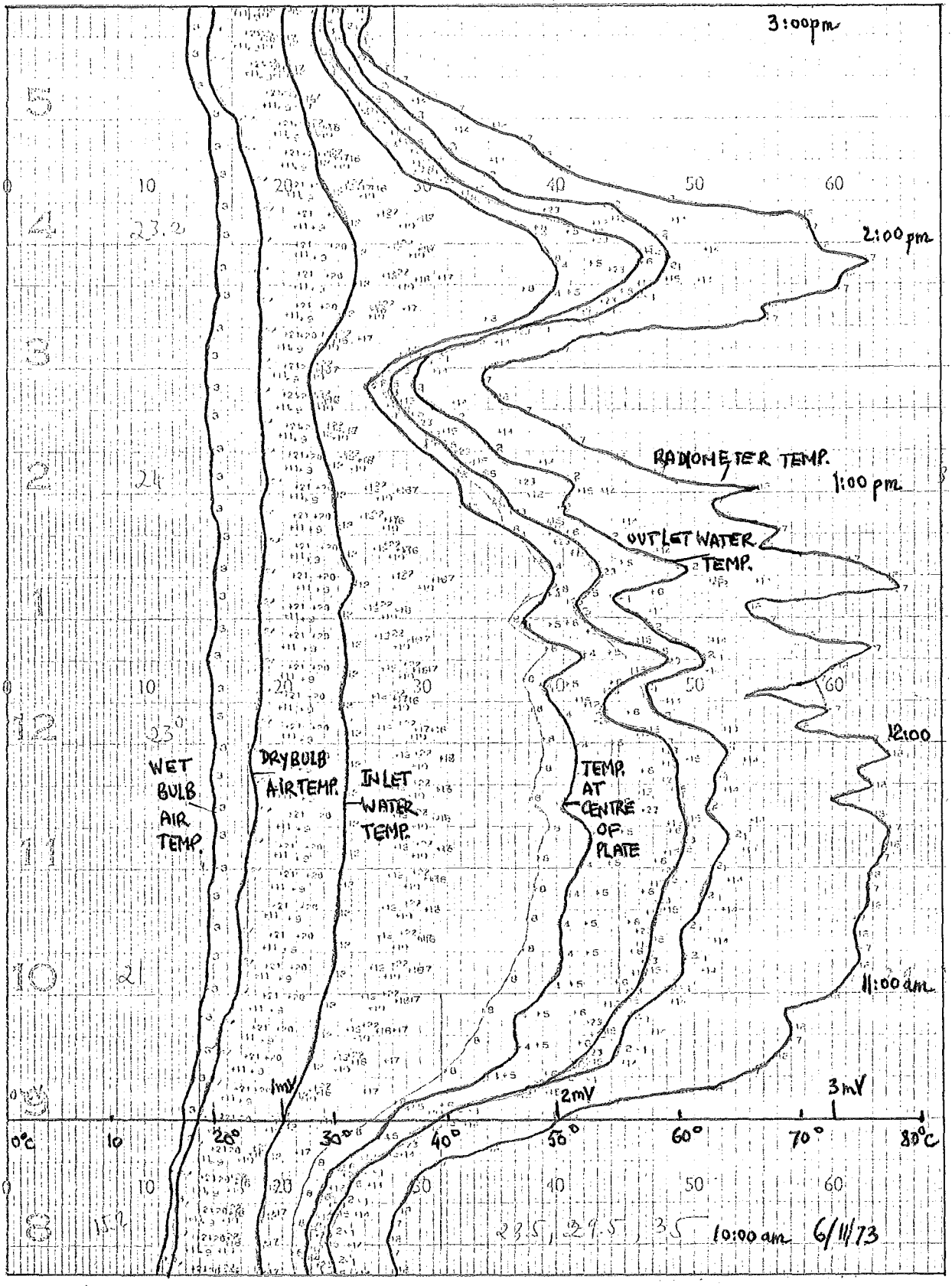

Fig. 5.14 Chart of temperature variation during daytime Operation

absorbed by glasses raises the glass temperatures and reduces the rate of outward heat loss from collector plate.

The above values are calculated for normal incident sun-rays, for other angles of incidence corrections are provided by graph in the original paper.

- Upward heat loss coefficient:

$$U_{up} = 0.298 \text{ cal/cm}^2\text{hr } ^\circ\text{C} \quad (0.61 \text{ Btu/hr ft}^2 \ ^\circ\text{F})$$

This is extrapolated from the graph in that paper assuming average plate temperature $t_p = 40^\circ\text{C}$ (104°F) and air temperature $t_a = 15^\circ\text{C}$ (68°F).

- Assuming also that the backward heat loss is 1/10 of the upward loss and other losses are negligible as proposed by Whillier, the overall heat loss coefficient for this unit was estimated as $U_o = 0.33 \text{ cal/cm}^2\text{hr } ^\circ\text{C}$.

- Fin efficiency factor for this particular tube spacing:

$$F = 0.975$$

- For a 60 lb/hr flow of water through this panel the collector efficiency factor $F' = 0.912$. This factor varies with flowrate and with different design of the collector plate.

- The flow factor between the fluid and the heat exchanger was claculated as $F'' = 0.956$ for 60 lb/hr flowrate. This factor also varies with flowrates.

- Overall efficiency of heat transfer: $F_o = F' \times F'' = 0.872$

For other flowrates, this efficiency varies as below:

Flowrate	9 Kg/hr	18 Kg/hr	27 Kg/hr	36 Kg/hr	45 Kg/hr
F_o	0.800	0.832	0.872	0.880	0.890

5.6 ACTUAL PERFORMANCE OF THE TEST UNIT:

The performance of this test panel will be examined in the following analyses:

1. Qualitative analysis:

In this part, the temperature distributions through all the measuring points in the panel are examined during heating period as well as during night-time conditions. The response of the panel to incident radiation is also studied.

2. Quantitative analysis:

This was carried out for some typical days in the 3 month period of the test. It is hoped that the results of this analysis will give relevant and useful information on some of the characteristics which most people want to know about solar water heaters. Because of the short-term limit of this initial study no economic considerations could be assessed but the following points were considered:

- The energy developed by this test unit during typical sunny, cloudy and intermittent days. This collected energy is expressed in terms of familiar energy units so that comparisons can be made.

- The efficiency of collection and overall efficiency of conversion from solar energy to useful heating power.

- The temperature which water can be heated up at some particular flowrate and insolations.

- The period of the day one can expect to heat water by solar energy.

- The distributions of all the main heat flow components occurring in the panel. This detailed analysis enables modifications on the unit to be added at right places to reduce the

loss and increase efficiency of the operation.

(A) QUALITATIVE ANALYSIS:

From the continuous records of the outputs from 19 thermocouples installed inside the panel, it is possible to examine the daily variation in temperature of inlet, outlet water, collector plate, glass and air space insulations.

1. Variation of collector plate temperatures:

Fig. 5.4 shows the positions of 7 thermocouples bonded to the collector plate.

Thermocouples No. 1, 4, 7 are bonded in the centre line of the plate where water tube is also soldered on. In general, during the heating period temperature at point 4 is 1° to 2°C lower than temperatures at point 3 and 5. There is also an increase up to 20° to 25°C from lower end to upper end (i.e. follows the flow direction of water). At night time there is little variation between these temperatures. Typical variation is shown in the table below:

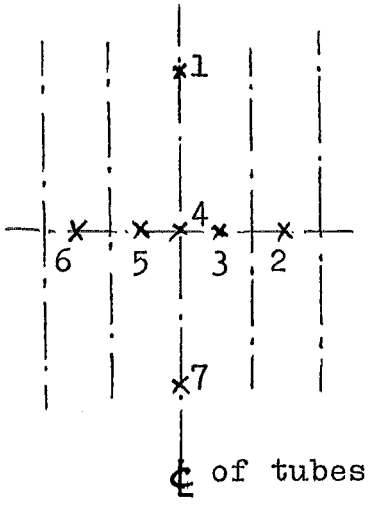

Date: 6-11-73 Temperature in $^{\circ}$C

T.C. No. \ Time	6 am	9 am	12 noon	3pm	6pm	9pm	12pm
1	18.5	27.0	63.5	32.2	27.0	23.0	23.0
3	16.0	25.0	57.5	29.0	25.0	21.2	21.0
4	17.0	24.0	57.0	28.8	25.0	22.0	22.0
5	17.1	25.8	58.6	30.2	26.0	22.5	22.2
7	16.5	22.0	38.5	25.7	23.8	21.8	21.8
Air	10.0	14.0	23.0	19.0	18.5	19.5	17.5

In the direction across the panel there is an increase in temperature toward the centre as shown in the table below. The reason is due to more concentration of insulation at the

centre of the panel and some losses cannot be avoided around the edges of the plate.

Date 6-11-73 Temperature in ^{o}C

Time / T.C.No.	6am	9am	12 noon	3pm	6pm	9pm	12pm
2	14.8	24.0	57.0	28.5	24.0	20.2	20.5
3	16.0	25.0	57.5	29.0	25.0	21.2	21.0
5	17.1	25.8	58.6	30.2	26.0	22.5	22.2
6	15.2	24.0	58.6	28.5	24.2	21.0	20.5
Air	10.0	14.0	23.0	19.0	18.5	19.5	17.5
$\bar{t}_p$	16.5	24.6	55.0	29.0	25.0	21.7	21.6

$\bar{t}_p$ is average of 7 temperatures on the plate

2. Variation of inlet and outlet water temperatures:

The temperature differences between inlet and outlet vary daily depending on the intensities of solar radiation and the flowrates of water. With constant flowrate, this variation follows the pattern of the solar radiation impinging on the surface.

The variation of inlet water temperature has close relationship with variation in air temperature. This is because the water had to flow through more than 20 ft of polythene hose laid on the concrete surface of the roof before entering the panel. Its temperature rose a little as the concrete heated up slowly under solar radiation because of the large thermal inertia of the surface. However, on flowing through the panel the water collected much more heat and the temperature difference reached a maximum of $32^{o}C$ for a flowrate of 20.4 Kg/hr on a sunny period 6-11-73 (Fig. 5.14). On 10-12-73, maximum temperature difference was only $16^{o}C$ for a flowrate of 36.9Kg/hr

as shown in Fig. 5.17. Typical variation:

Date: 6-11-73 Temperature in °C

Time / Temp.	6am	9am	12 noon	3pm	6pm	9pm	12pm
Inlet	18.5	22.0	31.0	25.2	24.5	24.0	24.5
Outlet	16.8	26.0	63.5	31.0	26.2	22.5	22.5
Mean	17.6	24.0	47.2	28.1	25.3	23.2	23.5

During the period of the test (October, November, December) the outlet water temperature starts to become higher than temperature of inlet water about 1 hour after the sun rises and begins to drop below inlet temperature 1 or 2 hours before sunset. At night time, inlet water temperature is always the highest among others and normally 1 or 2°C higher than outlet temperature. This heat loss is transferred to the collector plate to compensate for its radiation loss and keeping its temperature always at least 2 or 3 degrees above air temperature.

One may expect the temperature of outlet water to continue to be higher than the inlet temperature until the sun sets because of the thermal inertia effect of the panel. However the records showed that this is not true. The reasons are:

- The thermal capacity of this panel is not large so that the time lag between the moment of incident radiation and the steady state equilibrium is only an hour or less.

- Referring to table 4.3 of incident angles of solar rays on this inclined surface for these period, the surface of this panel did not receive any direct solar radiation until just before 7am in the morning nor after 6 pm in the afternoon.

- There is a critical intensity below which no useful heat can be produced because the heat collected must raise the whole temperature of plate to a sufficient level before heat can be transferred to the water.

According to Liu & Jordan (3), this critical intensity is estimated as:

$$I_c = U_o(t_i - t_a)F_e$$

For this panel, $I_c = 0.33(25 - 15)\ 0.748$

$= 2.5\ cal/cm^2hr$

This is well justified, because in the early hour after sunrise and an hour before sunset solar intensity is normally less than 3 cal/cm^2hr.

3. Variation of outer glass temperature:

Thermocouples No. 16, 17, 18, 19 were bonded to the under surface of the outer glass by araldite glue. It is assumed that the thermal resistance of this glass plate is small so that these temperature are very close to the temperatures on the outer surface. (The actual thermal resistance of this glass plate (0.15" thick) was calculated as 0.0036 $m^2\ ^oC/W$, compared with the resistance 0.108 $m^2\ ^oC/W$ of a layer of fibre-glass having the same thickness it is really small).

In general, these temperatures are close to each other, differences are normally less than 1^oC except during bright sunshine periods when there is a temperature gradient from the lower end to the upper end of the plate. Little variation across the panel was recorded.

At night time, these 4 temperatures are normally close to air temperature for cloudy conditions while they can be well

below air temperature during clear night sky conditions due to radiative cooling effect. Some amount of heat is transferred to the panel by convection from the air during these periods.

Typical variation is shown in the table below:

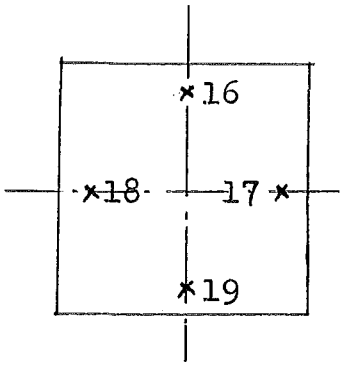

Date: 6-11-73 Temperature in ^{o}C

Time / No.	6am	9am	12 noon	3pm	6pm	9pm	12pm
16	11.0	18.2	39.0	23.2	20.8	18.2	18.0
17	10.8	17.5	37.8	22.8	20.8	18.2	18.0
18	11.0	17.5	37.8	23.0	20.4	19.0	19.0
19	12.5	18.0	35.5	23.0	22.2	20.0	19.0
Air	10.0	14.0	23.0	19.0	18.5	19.5	17.5

Later when calculations were done for the heat loss components, it was found that these glass temperature were too high, especially during sunny period, for the rate of heat loss upward calculated. Reasons for it could be due to bad contact with the glass surface so that these temperatures were not true glass temperatures but some intermediate value between air space temperature and glass temperature. (3 of these 4 thermocouples lost contact with the surface and dropped down later in the test). Some amout of solar radiation absorbed by the glass may also raise its temperature and cause more heat loss from glass to air than the actual upward heat loss from collector plate.

However, the above variation still showed the pattern of variation of the actual glass temperature to some extent.

4. Variation of air space temperatures:

a. Air space between collector plate and inner glass:

There are 2 thermocouples in this space, one near the

upper end and one near the lower end on the centre line of the panel.

The upper temperature is usually the highest temperature among those recorded. This shows the effectiveness of glass insulation whose characteristics is opaque to long wave radiation. Most of the heat is trapped above the collector plate and the convection current causes higher temperature at the upper point than the lower point.

b. Air space between glasses:

One thermocouple was placed in this air space at the time of the replacement of the broken inner glass. This air space temperature is lower than the above air space temperatures and higher than those on the glass surface as expected. Its variation compared with the inside space temperatures is shown below:

Date 6-11-73 Temperatures in ^{o}C

Time / Space temp.	6am	9am	12 noon	3pm	6pm	9pm	12pm
Upper	17.0	27.0	65.0	32.2	26.5	22.0	22.0
Lower	15.0	24.0	54.5	29.0	24.2	23.0	23.0
Between glass	14.5	23.0	49.0	28.5	24.5	20.5	20.5
Air	10.0	14.0	23.0	19.0	18.5	19.5	17.5

5. Variation of back cover temperatures:

Little difference among the 4 temperatures on the back cover was recorded although there seems to be a small increase of this difference in the flow direction during heating period.

At night time these temperature are close to air temperature and can be $1^{o}C$ lower than air temperature on some clear

nights. This and the fact that these back cover temperatures may also be lower than air temperature during cloudy and rainy periods at day time means that no heat is lost to the back under those conditions, the panel may gain some heat from the air instead.

The table below shows variation of back cover temperatures:

Date 6-11-73 Temperature in ^{o}C

Time / No.	6am	9am	12 noon	3pm	6pm	9pm	12pm
8	12.2	16.0	25.7	22.8	20.5	21.2	19.2
9	12.0	16.0	27.0	22.5	21.5	20.5	19.2
10	11.8	17.0	28.0	23.3	22.8	20.5	20.0
11	11.8	15.0	25.5	21.3	20.0	21.2	18.1
Air	10.0	14.0	23.0	19.0	18.5	19.5	17.5

Fig. 5.15 shows the overall temperature distribution at 2 sections of the panel on a sunny period.

6. Cycle of operation:

From the above temperature variations of all the main components in the panel, the operation of a solar water heater like this test unit seems to follow a cycle which can be described as below:

During the early hours of day time, usually one to two hours from sunrise, the collector plate picks up solar radiation and raises its temperature as well as temperature of other components up about $10^{o}C$ above air temperature. From then, the heat collected is transferred mostly to the water and becomes useful heating power while a smaller part is lost to surroundings through upward and backward direction. Even in a completely overcast day the amount of diffuse radiation collected

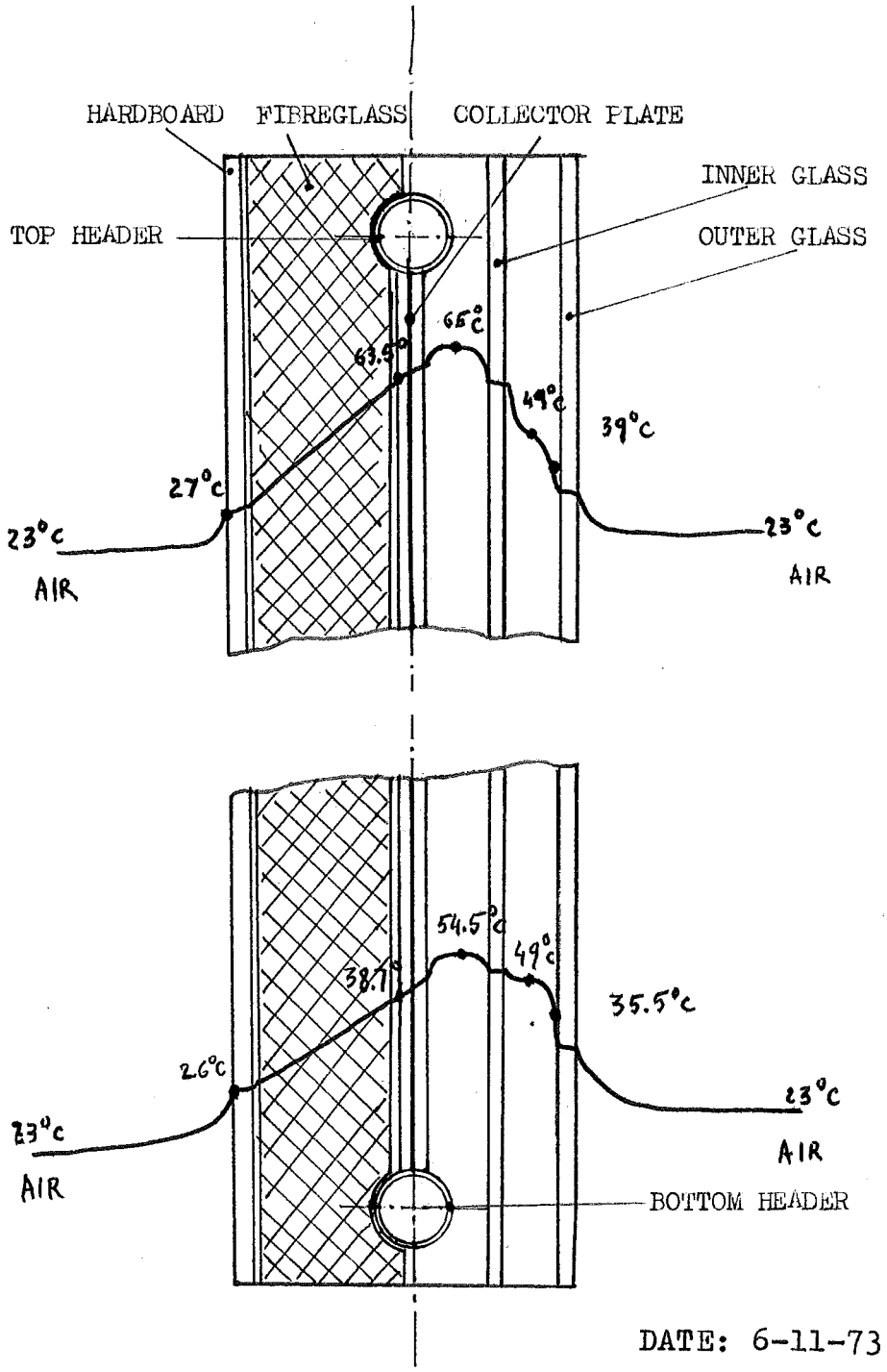

Fig. 5.15 Temperature distribution across the panel during heating period

can also be enough to keep the panel temperatures up and transfer some useful heat to water. However, no useful heating can be expected during a rainy period because radiation intensity is so low that the collector plate becomes cooler than inlet water and it absorbs heat from the water to compensate for the radiation loss. Because plate temperature never becomes lower than air temperature but it is always at least 2 to 3°C above, useful heating can still be expected when some amount of sunshine follows the rainy period.

The normal useful heating period lasts until about an hour before sunset. From then outlet water temperature begins to drop below inlet temperature as heat is removed from the flowing water. All temperatures are rather constant throughout the night and normally higher in a cloudy night than in a clear and calm night. This is the clear effect of considerable radiative cooling under clear sky condition.

Later in the test, those thermocouples on the same component were grouped together to measure the mean temperature of that component. This reduced the number of points on the chart to 12 and showed more clearly the variation of mean temperature of main components in the panel.

Fig. 5.16 to 5.19 show the cycle of operation of the solar panel and the effect of clear and cloudy sky conditions on both night and day time.

The identifications of all the points in those charts are shown in the table below:

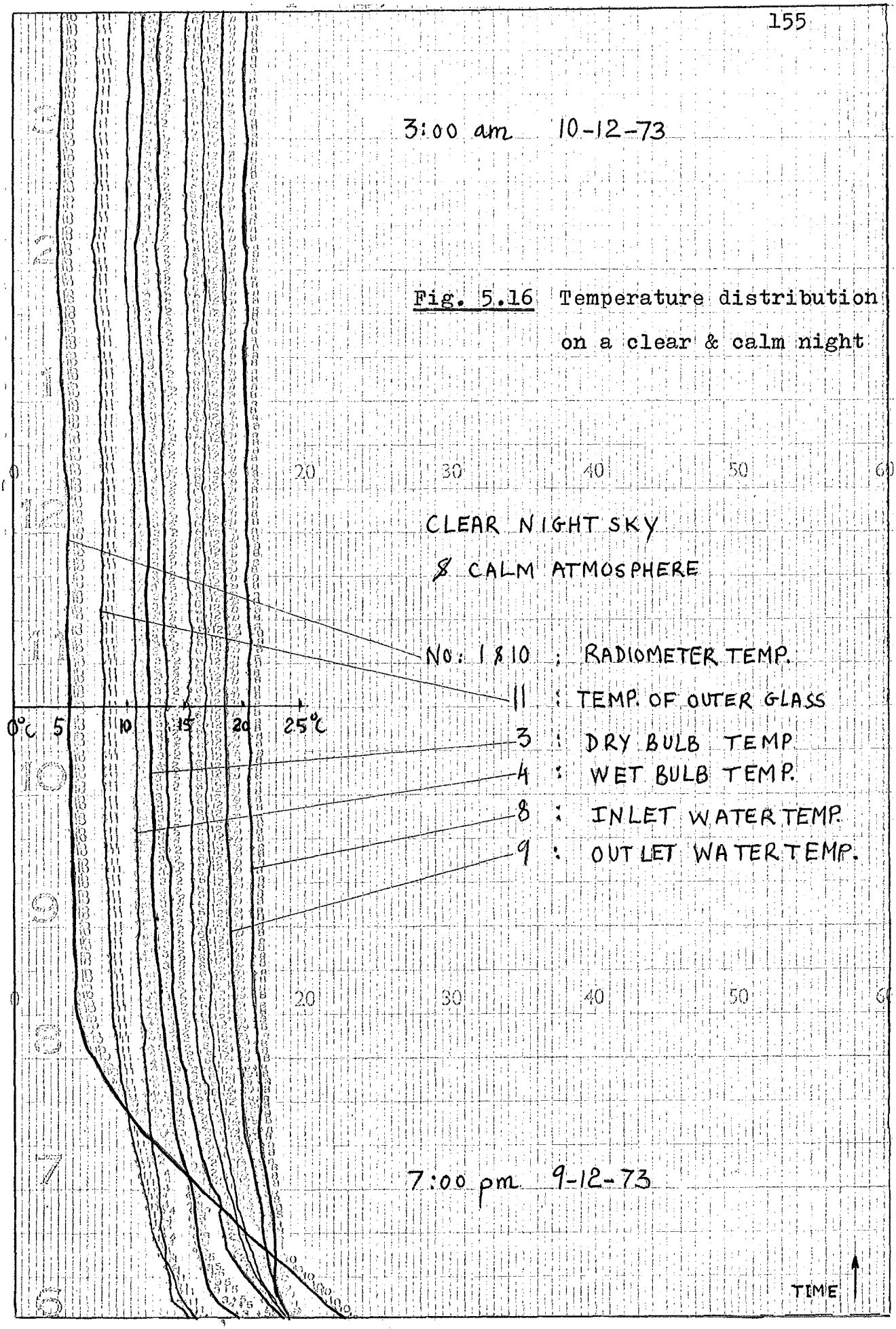

Fig. 5.16 Temperature distribution on a clear & calm night

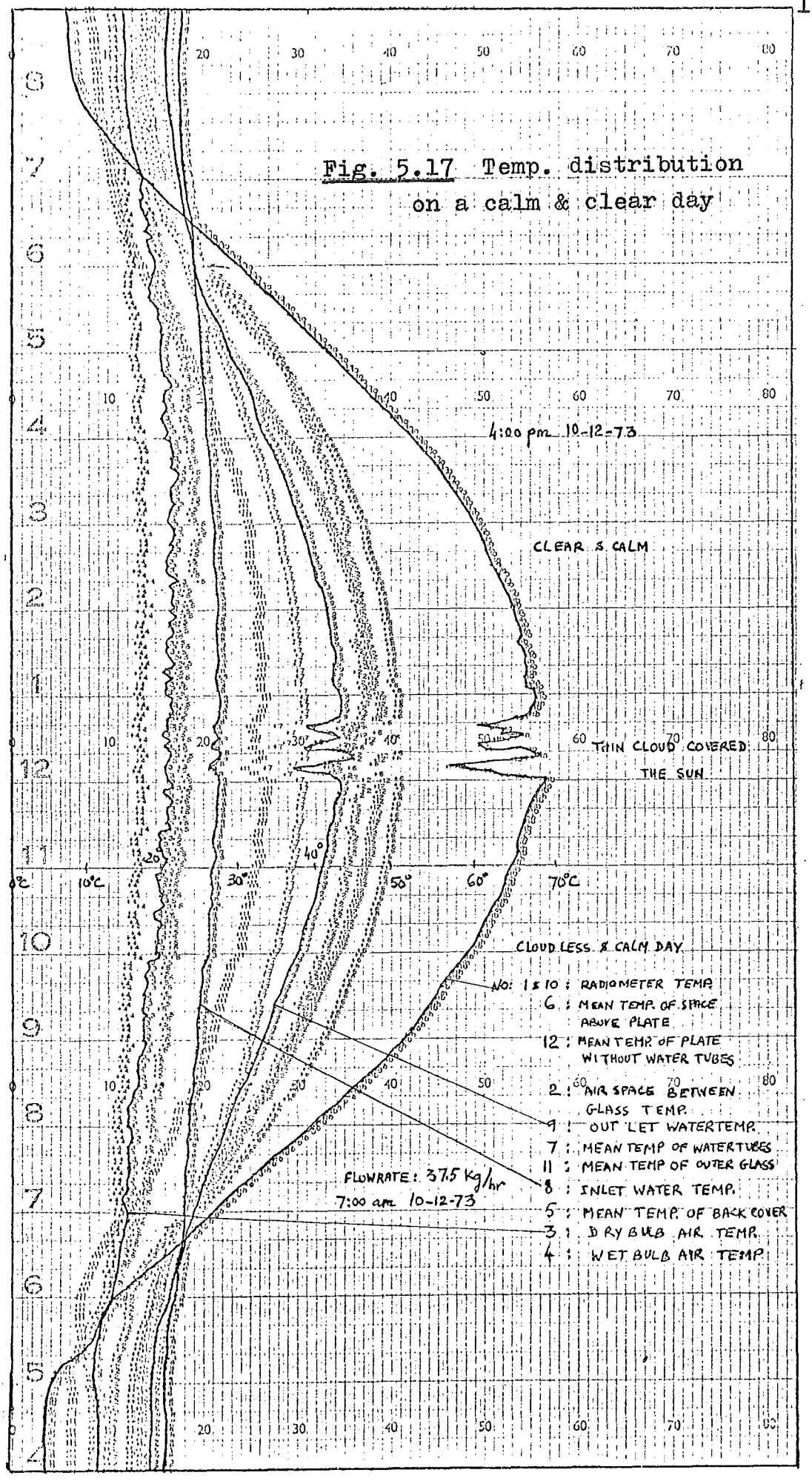

Fig. 5.17 Temp. distribution on a calm & clear day

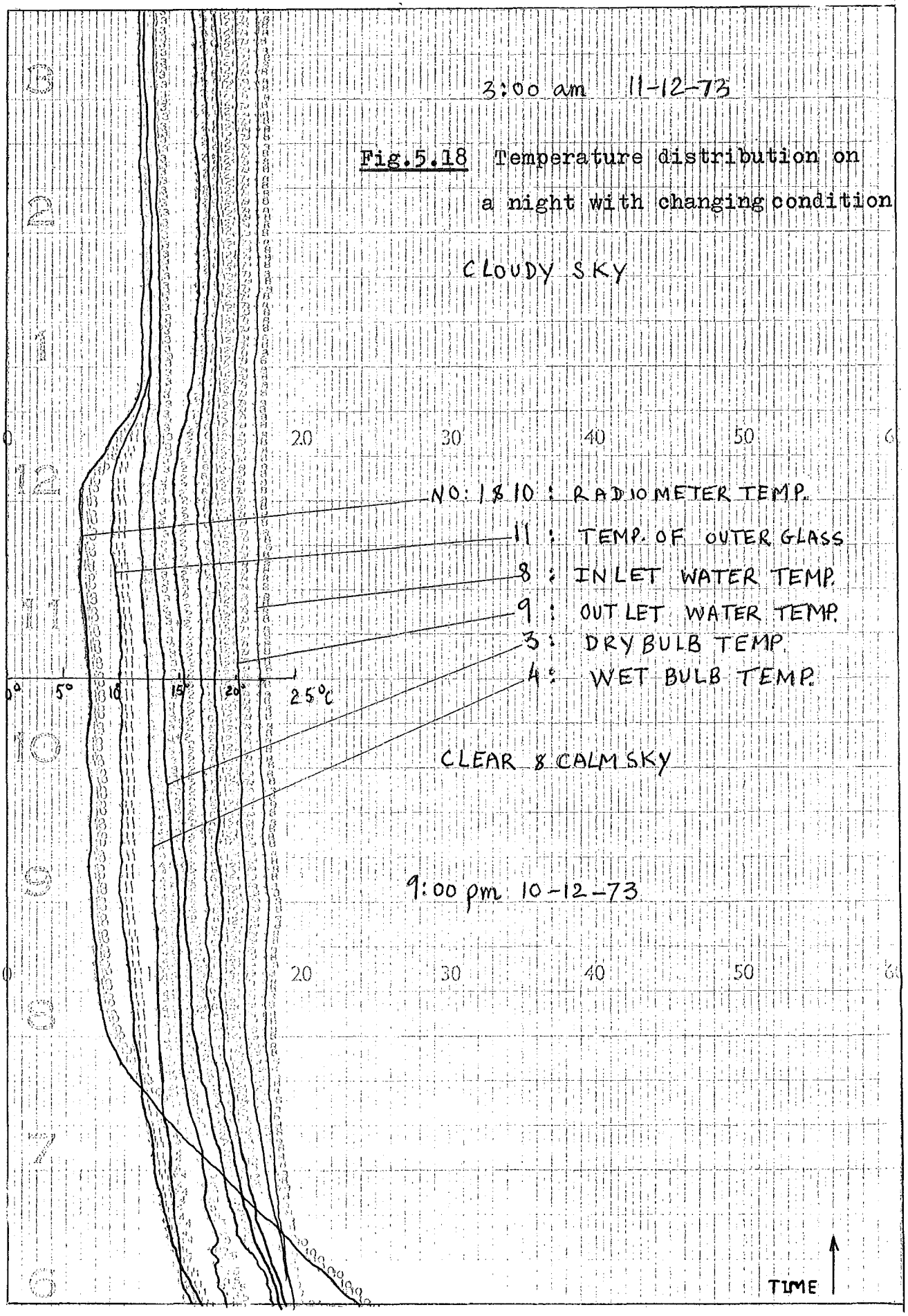

Fig.5.18 Temperature distribution on a night with changing condition

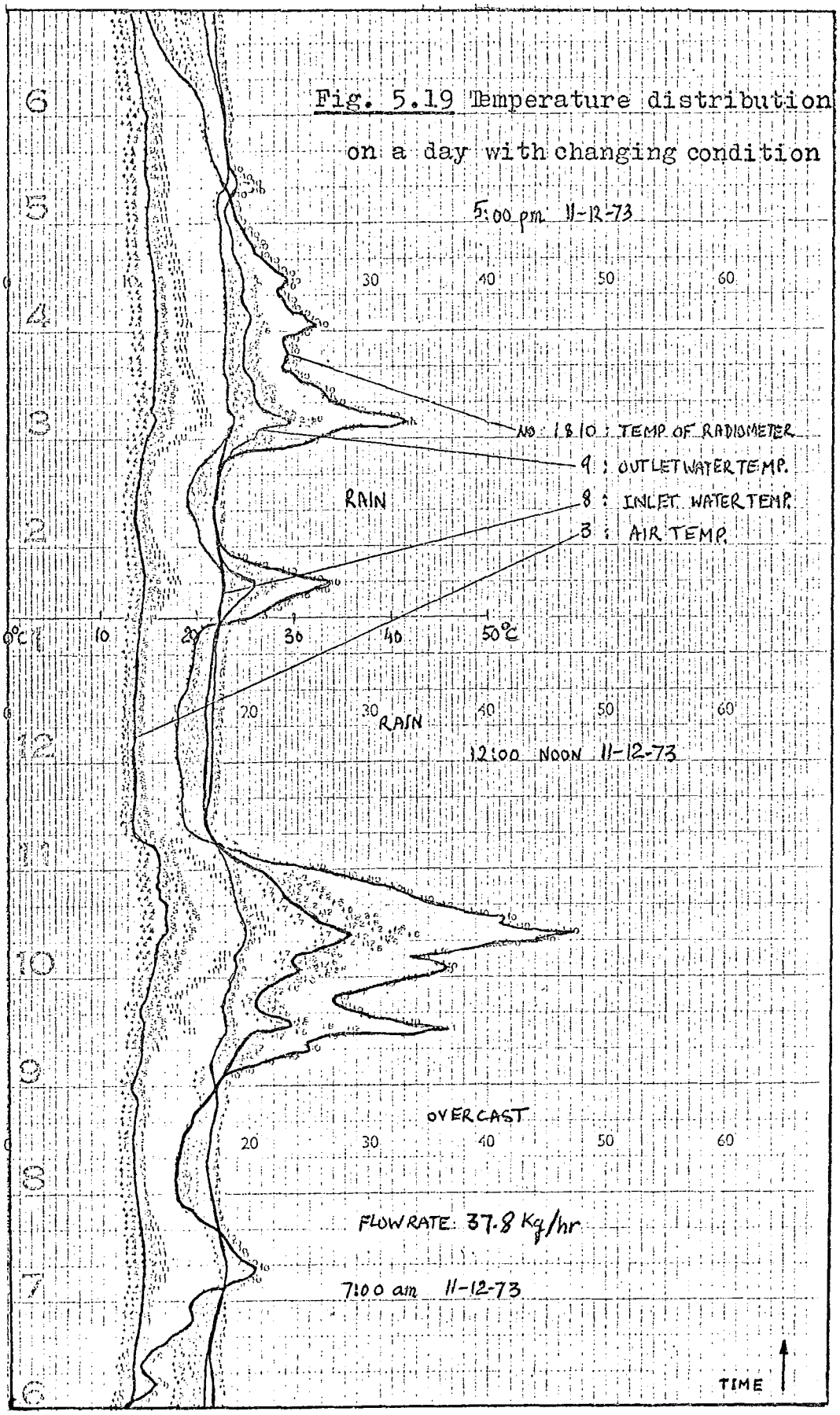

Fig. 5.19 Temperature distribution on a day with changing condition

Channel	Thermocouples Number	Measurement of
1 & 10	—	Radiometer temperature
2	20	air space between glasses
3	—	dry bulb temperature
4	—	wet bulb temperature
5	8,9,10,11 in parallel	mean back cover temp.
6	14,15 in parallel	mean temp. of air space above plate
7	1, 4, 7 in parallel	mean temp. of water tubes
8	13	Inlet water temperature
9	12	Outlet water temperature
11	16,17,18 in parallel (19 left out because it lost contact with surface)	mean glass temperature
12	2,3,5,6 in parallel	mean temp. of plate without water tubes on

(B) QUANTITATIVE ANALYSIS

In these calculations, it is assumed that the heat collected by the collector plate will be distributed in the following ways:

1. lost upward by radiation and convection.
2. lost backward through fibre glass insulation.
3. collected by water through temperature rise and becomes useful heating power.

The edge heat loss is assumed negligible compared with the above three components.

1. Heat loss upward through radiation and convection:

According to Hottel (16), this component of heat loss is governed by the following variables:

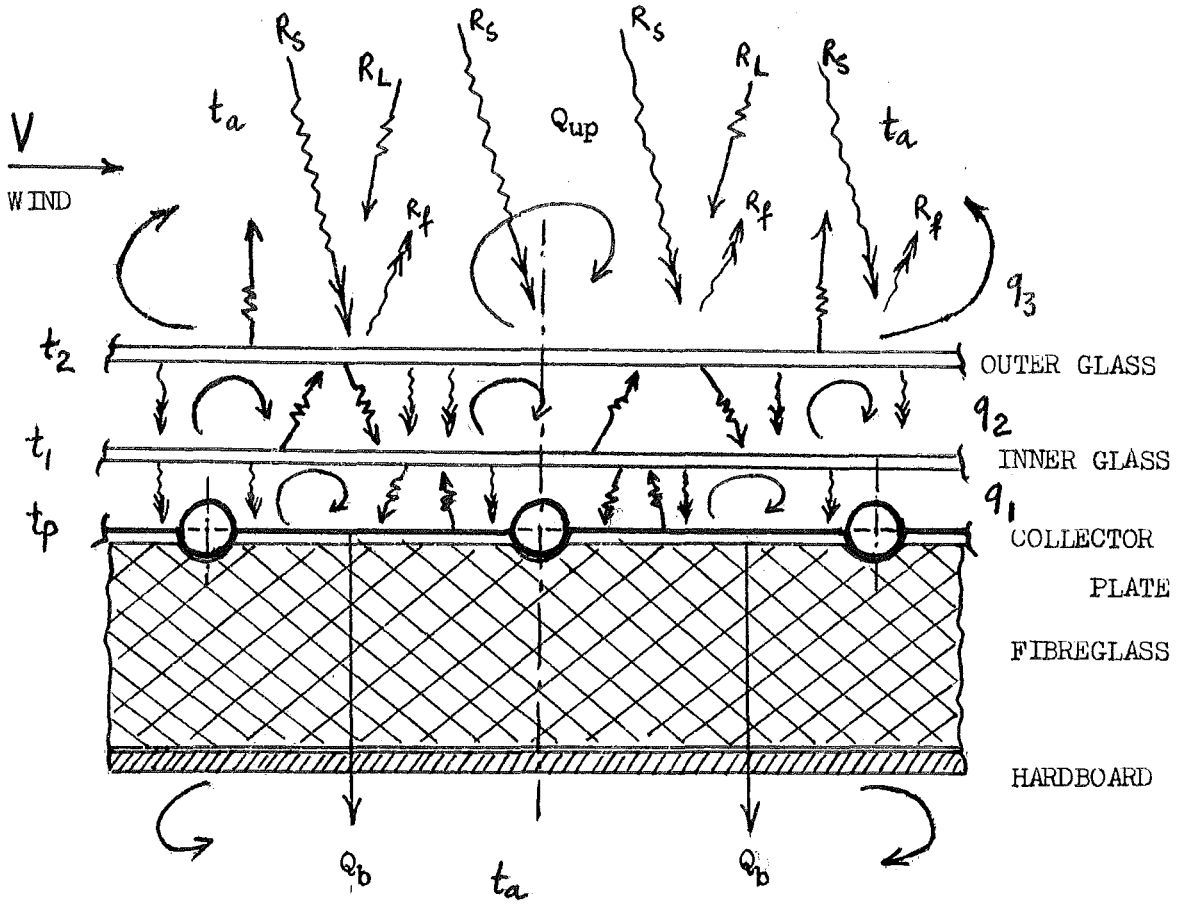

represents short wave radiation

represents long wave radiation

represents convection transfer

represents conduction transfer

Fig. 5.20 Heat transfers occurring in the solar panel

- the plate temperature
- the air and effective sky temperature
- number of glass plates and spacing
- angle of inclination of the collector surface
- wind velocity over the site

For this particular panel, referring to Fig. 5.20, the rate of heat loss from collector plate to the first glass is:

$$q_1 = C(t_p - t_1)^{5/4} + \frac{(T_p^4 - T_1^4)}{\frac{1}{\epsilon_p} + \frac{1}{\epsilon_g} - 1}$$

The first term of the equation is the convection loss due to air space between the collector plate and inner glass, C is convection coefficient. The second term is the radiation heat loss due to the difference in surface temperature between the collector plate and inner glass.

From the inner glass to the outer glass the same rate of heat loss again composed of convection loss from the top surface of inner glass to the bottom surface of outer glass and radiation loss due to difference of temperature between these two surfaces.

No radiant heat from the collector plate is transmitted through the inner glass to reach the outer glass because glass is opaque to long wave radiation.

As the thermal resistances of these glass plates are small and neglibible (see part A3), there is little difference between temperatures of top and bottom surfaces of the same glass plate and average temperature t_1, t_2 can be assumed for inner and outer glass plates.

Hence

$$q_2 = C(t_1 - t_2)^{5/4} + \frac{(T_1^4 - T_2^4)}{\frac{2}{\epsilon_g} - 1}$$

From the outer glass surface to the sky:

$$q_3 = h_w(t_2 - t_s) + \epsilon_g(T_2^4 - T_s^4)$$

In these equations:

t_p = collector plate temperature

t_1 = inner glass temperature

t_2 = outer glass temperature

C = convection coefficient

ϵ_p = emissivity of collector plate

ϵ_g = emissivity of glass

h_w = wind coefficient

t_s = effective sky radiant temperature

This t_s is the temperature at which the atmosphere above a place radiates long wave radiation to the surface as a black body. Various values are proposed for this temperature corresponding to climatological conditions. In general, it is lower than air temperature during clear sky period but very close to air temperature in cloudy days. For Christchurch conditions, this effective sky temperature is not well established although some trial measurements have been carried out in the study from part I, dry bulb temperature of air was used instead.

For steady state condition, the rate of heat loss upward is

$$Q_{up} = q_1 = q_2 = q_3$$

These equations can be solved by trial and error to give

Q_{up}, temperatures of glass are estimated each time. However, Hottel & Woertz (15) combined those relationship to obtain an equation to enable direct calculation of Q_{up} when t_p and t_a can be measured. The equation, proved valid for all the range of temperatures involved in flat plate collectors by the authors, is expressed as:

$$Q_{up} = \frac{t_p - t_a}{\frac{n}{C\left(\frac{t_p - t_a}{n+f}\right)^{\frac{1}{4}}} + \frac{1}{h_w}} + \frac{(T_p^4 - T_a^4)}{1/\epsilon_p + (2n+f-1)/\epsilon_g - n} \qquad (5.1)$$

Where n = numbers of glass plates

f = ratio of thermal resistance of the outer plate to the inner plate. The average value for 10 mph wind is 0.36 . Because of the effect of f on Q_{up} is small, this value is assumed for all following calculations.

From Whillier (14), the extrapolated value of C for an 40^o inclined surface is 0.20 Btu/hr $ft^{2o}F$ and these emissivities were used:

$$\epsilon_p = 0.95$$

$$\epsilon_g = 0.88$$

Hence, the Q_{up} expression for this case can be written as:

$$Q_{up} = \frac{t_p - t_a}{10/(0.424(t_p - t_a))^{\frac{1}{4}} + 1/h_w} + \frac{0.173 \times 10^{-8}(T_p^4 - T_a^4)}{2.871} \qquad (5.2)$$

To compute Q_{up} mean values of the plate temperature and the air temperature are estimated from the recorded data for each hour. The values for h_w are estimated from mean wind speeds taken as average of 3-hourly values recorded by the Weather Office at Christchurch Airport.

From Ref. (14), $h_w = 1 + 0.3V$ where V = wind speed in mph.

The expression for Q_{up} above requires t_p, t_a in Farenheit degrees, T_p, T_a in Rankine degrees and h_w in Btu/hrft^2°F to give Q_{up} in Btu/hrft^2. From the data recorded, t_p, t_a are estimated in Celsius degrees. To speed up calculations, a programme for H.P. 9100A calculator was written and Q_{up} in cal/cm^{2}hr is obtained directly for every input of t_p, t_a in °C and h_w in Btu/hrft^2°F. See Appendix 3.

2. Heat loss backward through fibreglass insulation:

For this calculation, the overall U-coefficient for the back insulation is estimated from data given in IHVE (Institution of Heating and Ventilating Engineers) Guide Book 1967.

Referring to Fig. 5.20, the back insulation comprises of:

Inside surface of plate	Resistance = 0.15m^2°C/W
Small air space between plate and fibreglass	Resistance = 0.11m^2°C/W
2" fibreglass, having conductivity = 0.035 W/m°C	Resistance = 1.45m^2°C/W
¼" hard board, having conductivity = 0.094W/m°C	Resistance = 0.0675m^2°C/W
Outside surface	Resistance = 0.0495m^2°C/W

(Assume: - average 5mph wind speed over back cover
- sheltered and inclined 45°
- heat flow downward)

Total resistance = 1.8270m^2°C/W

∴ Overall coefficient U_b = 0.548 W/m^2°C

Hence backward heat loss is given by:

$$Q_b = U_b A_p (t_p - t_a)$$

Where t_p, t_a are hourly average temperature.

Or Q_b can be calculated from measurement of area enclosed

by mean t_p and t_a lines on charts. See Appendix 5.

3. Useful heat collected by water:

This is the useful component of heat flows and calculated by:

$$Q_w = \dot{m} C_p \Delta t$$

where $\dot{m}$ = flowrate in Kg/hr

C_p = specific heat of water = 1 Kcal/Kg^{o}C

Δt = inlet-outlet temperature difference ^{o}C

The integrated values of Q_w for each hour are calculated from measurement of areas enclosed by inlet and outlet water temperatures.

The detailed procedures given in Appendix 5 enable the above three components of heat distribution to be estimated from records of daily variation in temperatures of water, collector plate and air.

4. Results of the analysis:

The following tables and graphs show results of the analyses carried out for some typical days in November and December.

The nett area of the collector is taken as 1 square metre. Hourly rate of heat collection and heat distributions are calculated in cal/cm^2 but the total useful energy collected by the water and mean power of the solar panel are expressed in KWh and KW to enable comparisons with ordinary heating units.

The radiation intensities on this panel were estimated from total and diffuse solar radiation records obtained from Mrs. R. Moran following the analysis in section 4.4 . On days when no such records are available (30 Nov and 4 Dec) estimations were made based on Weather Office records of total radiation.

On these two days, the sky was almost cloudy throughout the day so that it is possible to assume that all the values recorded are diffuse radiation on horizontal surface. The corresponding radiation on a 40^{o} inclined surface was then given by:

$$R_{Ti} = 0.883\ R_{dh} + 0.0468\ R_{Th}$$

$$R_{Ti} = 0.93\ R_{Th}$$

In these tables, total heat collected by the collector plate is $Q_T = Q_w + Q_b + Q_{up}$

The percentage of collection is calculated as $\frac{Q_T}{R_{Ti}} \times 100$

The efficiency of heat transfer is $\frac{Q_w}{Q_T} \times 100$

The overall efficiency is $\eta = \frac{Q_w}{R_{Ti}} \times 100$

Bright sunshine periods and radiation records appearing on every graphs are obtained from Christchurch Weather Office.

Useful heating period was taken as the time during which outlet water temperature remained higher than inlet water temperature.

Typical calculations for hourly and daily results are shown in Appendix 5.

(C) DISCUSSION:

Studying the results shown by these graphs and tables, the following points may be noticed.

1. Energy collected:

Over the period of the test on the panel, the range of performance extended from a maximum collection of 4.46 KWh on a clear day 10 December to a minimum of 0.36 KWh on 30 November, where there was no sunshine (some rainy periods) and the air temperature was low. The actual maximum energy that could be

TABLE 5.1 DATE: 6-11-73 FLOWRATE: 18 K_g/hr

Clock time-period	t_p °C	t_a °C	V mph	Q_{up} cal/cm²	%	Q_b cal/cm²	%	Q_w cal/cm²	%	Q_T cal/cm²	Radiation Intensity cal/cm² R_{Di}	R_{di}	R_f	R_{Ti}	$\frac{Q_T}{R_{Ti}}$ %	$\eta=\frac{Q_w}{R_{Ti}}$ %
06-07	17.0	10.0	5.2	1.62	83.0	0.33	17	—	—	1.95	—	2.82	0.16	2.98	—	—
07-08	20.5	11.3	5.2	2.21	35.2	0.41	6.4	3.66	58.4	6.28	0.56	7.48	0.45	8.49	74.0	43.1
08-09	24.7	13.5	5.2	2.80	27.0	0.50	4.8	7.10	68.2	10.40	1.46	14.90	0.87	17.23	66.2	41.2
09-10	28.0	14.5	11.5	3.5	22.8	0.59	3.8	11.25	73.4	15.34	2.41	21.80	1.27	25.48	60.3	44.2
10-11	39.5	17.6	11.5	6.21	17.1	0.97	2.7	29.20	80.2	36.38	20.50	26.00	2.32	48.82	74.4	59.9
11-12	55.0	22.3	11.5	10.23	15.1	1.48	2.2	56.00	82.7	67.71	52.70	20.80	3.47	76.97	88.0	72.8
12-13	50.4	23.5	17.8	8.23	14.4	1.22	2.2	46.50	83.4	55.95	39.60	28.80	3.29	71.69	78.0	64.8
13-14	42.0	23.5	17.8	5.34	15.0	0.84	2.3	29.50	82.7	35.68	33.70	31.20	3.22	68.12	Difference in sunshine	
14-15	35.3	20.8	17.8	3.98	16.4	0.65	2.7	19.6	80.9	24.23	6.54	22.20	1.48	30.22	80.0	64.6
15-16	26.8	17.0	11.5	2.49	26.3	0.44	4.6	6.54	69.1	9.47	1.55	13.90	0.81	16.26	58.4	40.3
16-17	27.0	17.6	11.5	2.39	27.9	0.42	4.9	5,76	67.2	8.57	2.62	11.70	0.77	15.09	56.8	38.2
17-18	26.0	18.5	11.5	1.88	29.2	0.33	5.1	4.23	65.7	6.44	0.87	9.68	0.59	11.14	57.8	38.0
18-19	24.0	18.0	6.9	1.46	56.8	0.25	9.7	0.86	33.5	2.57	0.14*	3.54*	0.23*	3.91*	65.6	22.0
TOTAL PER DAY				52.34	18.6	8.43	3.0	220.20	78.4	280.98				393.42	71.5	56.5

* Estimated values, not recorded.

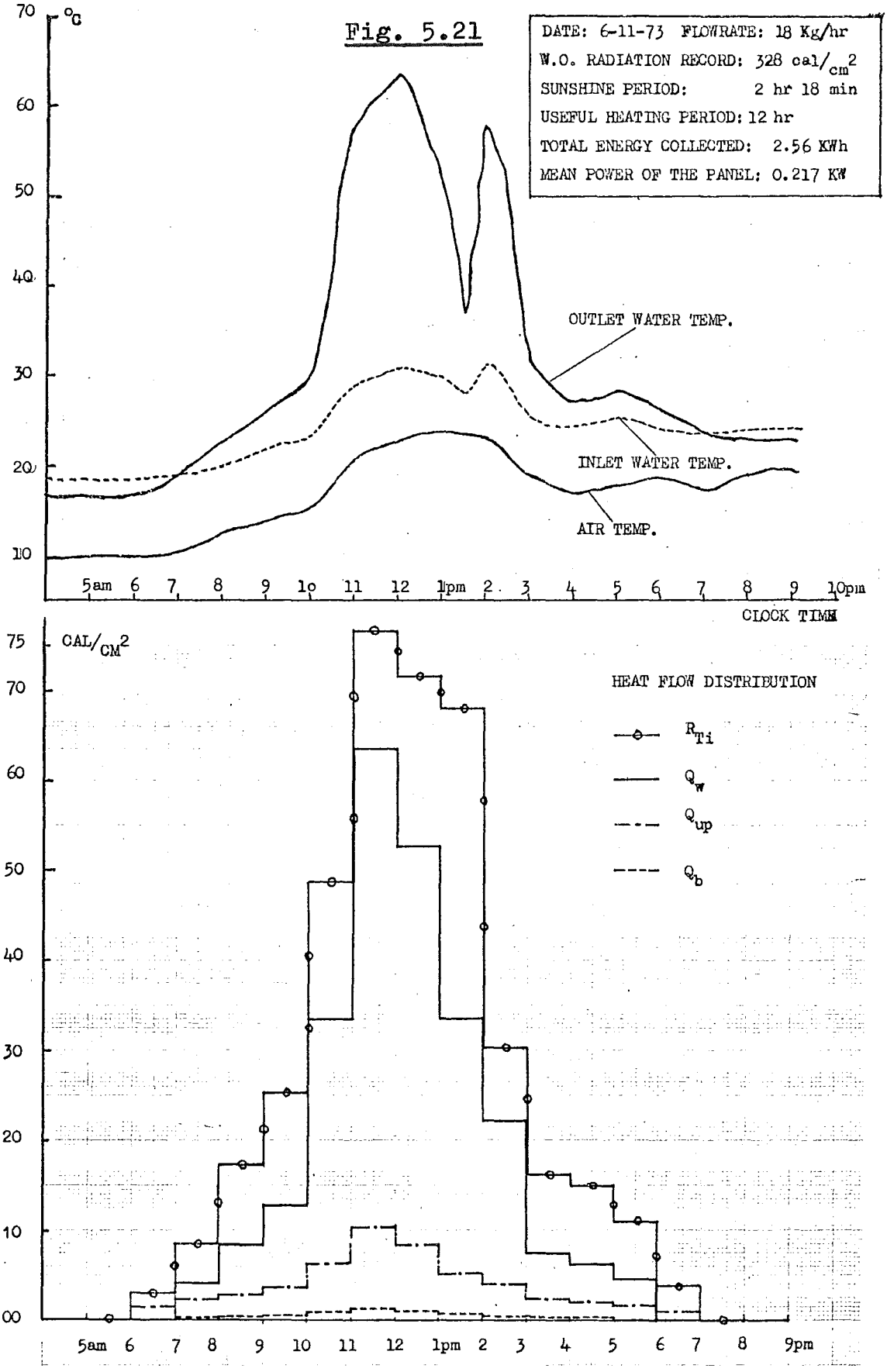
Fig. 5.21
DATE: 6-11-73 FLOWRATE: 18 Kg/hr
W.O. RADIATION RECORD: 328 cal/cm2
SUNSHINE PERIOD: 2 hr 18 min
USEFUL HEATING PERIOD: 12 hr
TOTAL ENERGY COLLECTED: 2.56 KWh
MEAN POWER OF THE PANEL: 0.217 KW
°C
OUTLET WATER TEMP.
INLET WATER TEMP.
AIR TEMP.
CLOCK TIME
CAL/CM2
HEAT FLOW DISTRIBUTION
RTi
Qw
Qup
Qb

TABLE 5.2 DATE: 7-11-73 FLOWRATE: 18 Kg/hr

Clock time-period	t_p °C	t_a °C	V mph	Q_{up} cal/cm²	Q_{up} %	Q_b cal/cm²	Q_b %	Q_w cal/cm²	Q_w %	Q_T cal/cm²	Radiation Intensity cal/cm² R_{Di}	R_{di}	R_f	R_{Ti}	$\frac{Q_T}{R_{Ti}}$ %	$\eta=\frac{Q_w}{R_{Ti}}$ %
06-07	25.2	17.0	6.9	2.04	54.4	0.36	9.6	1.35	36.0	3.75	2.14	5.94	0.85	11.93	31.4	11.3
07-08	32.6	20.0	6.9	3.35	20.2	0.55	3.3	12.70	76.5	16.60	8.70	16.30	1.46	26.46	62.7	48.0
08-09	33.7	21.0	6.9	3.40	17.5	0.58	3.0	15.40	79.5	19.38	7.75	20.40	1.49	29.64	65.4	52.0
09-10	42.5	22.5	13.2	5.78	15.3	0.90	2.4	31.10	82.3	37.78	16.78	29.80	2.40	48.98	77.1	63.5
10-11	41.8	22.7	13.2	5.49	15.5	0.87	2.5	29.00	82.0	35.36	9.97	29.60	2.02	41.59	85.0	69.8
11-12	46.7	23.5	13.2	6.91	15.7	1.05	2.4	36.00	81.9	43.96	27.90	28.40	2.76	59.06	74.4	61.0
12-13	56.6	25.2	19.0	9.98	14.9	1.44	2.1	55.60	83.0	67.02	51.60	21.60	3.48	76.68	87.4	72.5
13-14	53.2	25.5	19.0	8.63	14.8	1.25	2.2	48.40	83.0	58.28	37.20	27.00	3.15	67.35	86.5	72.0
14-15	50.0	25.2	19.0	7.57	15.2	1.11	2.2	41.20	82.6	49.88	35.30	24.00	2.94	62.24	80.1	66.3
15-16	39.8	24.3	22.4	4.40	16.3	0.69	2.6	21.85	81.1	26.94	22.40	23.40	2.37	48.17	55.9	45.4
16-17	38.5	24.3	22.4	3.99	17.3	0.64	2.8	18.40	79.9	23.03	23.41	12.10	2.02	37.53	61.4	49.0
17-18	31.1	23.0	22.4	2.12	20.8	0.38	3.7	7.70	75.5	10.20	6.50	10.30	1.14	17.94	56.9	41.8
18-19	26.1	21.3	19.5	1.18	36.6	0.21	6.6	1.83	56.8	3.22	0.55*	5.30*	0.47*	6.32*	50.9	29.0
TOTAL PER DAY				64.84	16.4	10.03	2.5	320.53	81.1	395.40				533.89	74.1	61.0

*Estimated values, not recorded

Fig. 5.22

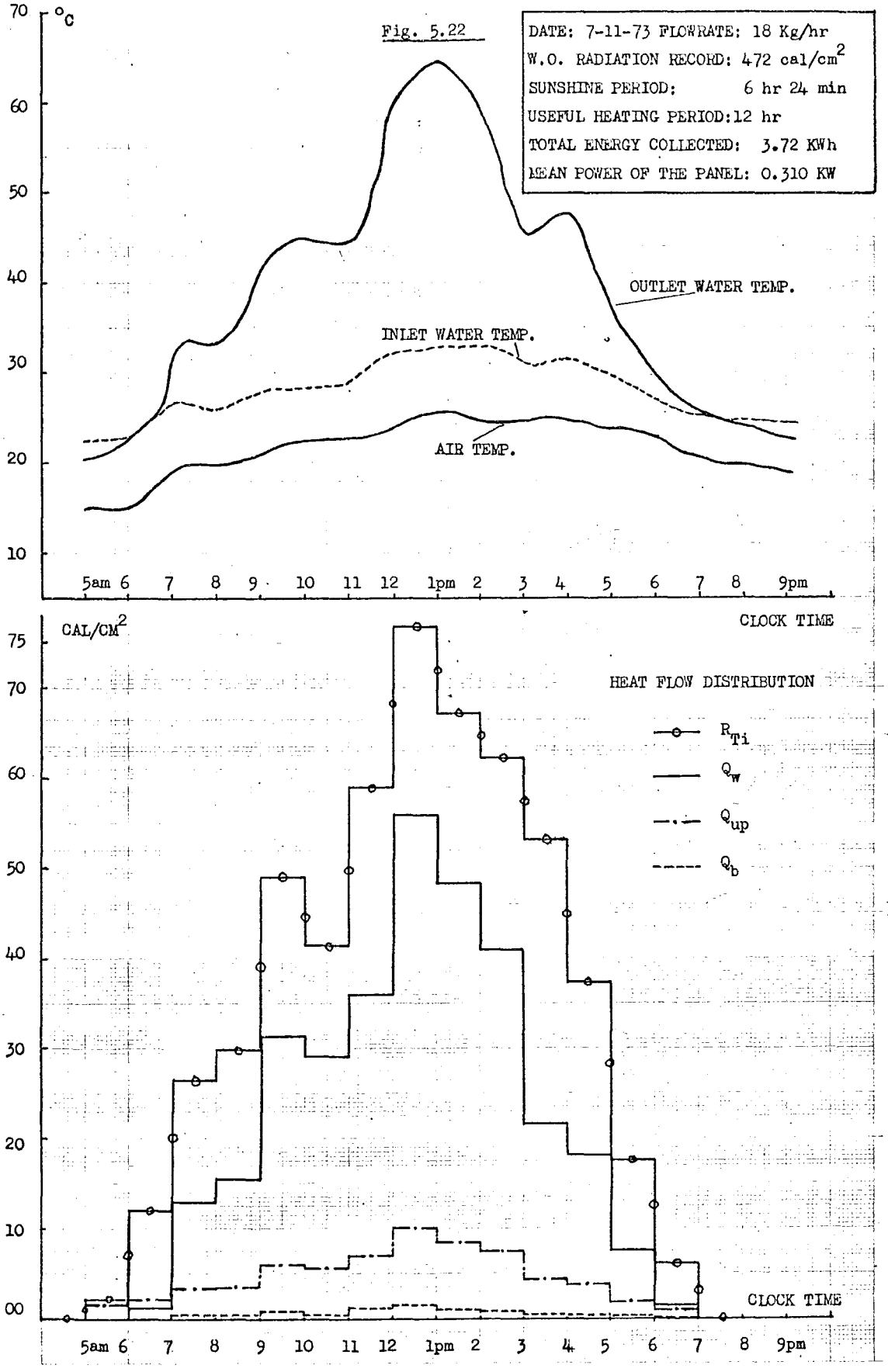
DATE: 7-11-73 FLOWRATE: 18 Kg/hr
W.O. RADIATION RECORD: 472 cal/cm2
SUNSHINE PERIOD: 6 hr 24 min
USEFUL HEATING PERIOD: 12 hr
TOTAL ENERGY COLLECTED: 3.72 KWh
MEAN POWER OF THE PANEL: 0.310 KW
°C
OUTLET WATER TEMP.
INLET WATER TEMP.
AIR TEMP.
CLOCK TIME
CAL/CM2
HEAT FLOW DISTRIBUTION
RTi
Qw
Qup
Qb
CLOCK TIME

TABLE 5.3 DATE: 8-11-73 FLOWRATE: 18.9 Kg/hr

Clock time-period	t_p °C	t_a °C	V mph	Q_{up} cal/cm²	Q_{up} %	Q_b cal/cm²	Q_b %	Q_w cal/cm²	Q_w %	Q_T cal/cm²	Radiation Intensity cal/cm² R_{Di}	R_{di}	R_f	R_{Ti}	$\frac{Q_T}{R_{Ti}}$ %	$\eta = \frac{Q_w}{R_{Ti}}$ %
06-07	22.0	14.5	4.6	1.81	84.2	0.34	15.8	—	—	2.15	—	4.30	0.25	4.55	47.3	—
07-08	23.0	14.7	4.6	2.02	65.4	0.36	11.6	0.71	23.0	3.09	1.32	6.85	0.45	8.62	35.8	8.2
08-09	25.4	16.0	4.6	2.34	31.9	0.45	6.1	4.55	62.0	7.34	1.41	13.10	0.77	15.28	48.0	29.8
09-10	28.0	18.0	8.0	2.56	30.3	0.44	5.2	5.46	64.5	8.46	1.33	13.30	0.77	15.40	54.9	35.5
10-11	30.4	19.1	8.0	2.95	28.0	0.49	4.6	7.10	67.4	10.54	1.86	15.9	0.93	18.69	56.4	38.0
11-12	33.0	20.0	8.0	3.48	23.9	0.58	4.0	10.50	72.1	14.56	2.50	21.4	1.24	25.14	57.9	41.8
12-13	34.3	20.5	10.4	3.74	23.0	0.61	3.7	11.90	73.2	16.25	2.64	23.2	1.34	27.18	59.8	43.8
13-14	41.0	22.0	10.4	5.42	17.4	0.87	2.8	24.80	79.8	31.09	12.15	31.0	2.20	45.35	68.6	54.6
14-15	49.5	22.8	10.4	8.07	16.3	1.21	2.5	40.10	81.2	49.38	53.00	12.72	3.16	68.88	71.7	58.3
15-16	45.0	23.2	10.0	6.40	16.6	0.99	2.6	31.20	80.8	38.59	46.40	8.06	2.77	57.23	67.4	54.5
16-17	35.6	22.2	10.0	3.66	20.4	0.60	3.4	13.65	76.2	17.91	32.60	12.30	2.55	47.45	37.7	28.8
17-18	30.6	21.5	10.0	2.37	28.4	0.42	5.1	5.55	66.5	8.34	12.00	4.24	1.33	17.57	47.5	31.6
18-19	25.1	19.0	10.0	1.50	66.1	0.26	11.4	0.51	22.5	2.27	0.83*	3.54*	0.47*	4.84*	46.9	10.5
TOTAL PER DAY				46.32	22.1	7.62	3.5	156.03	74.3	209.94				356.18	59.0	44.4

* Estimated values, not recorded.

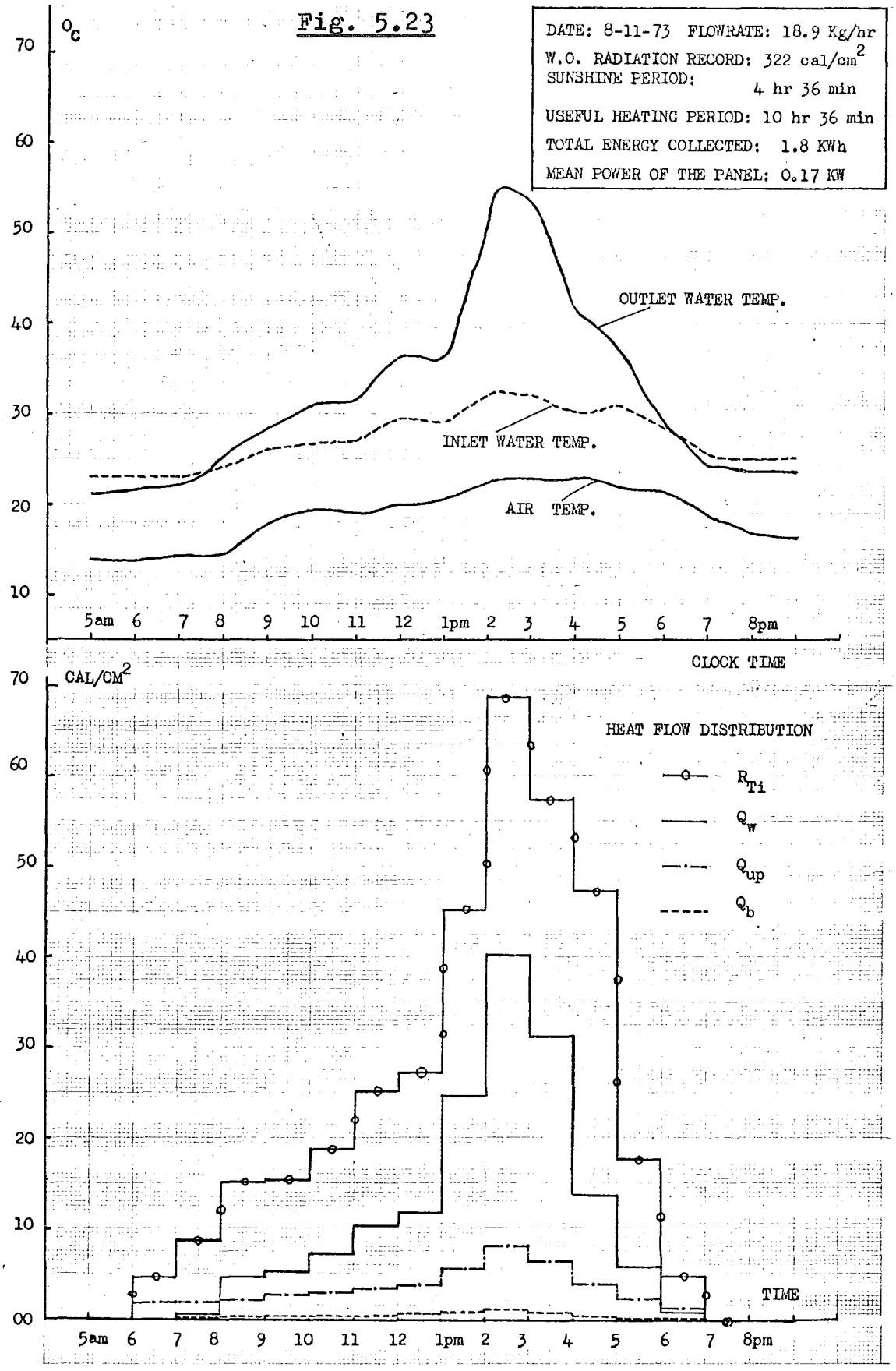
Fig. 5.23
DATE: 8-11-73 FLOWRATE: 18.9 Kg/hr
W.O. RADIATION RECORD: 322 cal/cm2
SUNSHINE PERIOD: 4 hr 36 min
USEFUL HEATING PERIOD: 10 hr 36 min
TOTAL ENERGY COLLECTED: 1.8 KWh
MEAN POWER OF THE PANEL: 0.17 KW
°C
OUTLET WATER TEMP.
INLET WATER TEMP.
AIR TEMP.
CLOCK TIME
CAL/CM2
HEAT FLOW DISTRIBUTION
R_Ti
Q_w
Q_up
Q_b
TIME
5am 6 7 8 9 10 11 12 1pm 2 3 4 5 6 7 8pm

TABLE 5.4 DATE: 30-11-73 FLOWRATE: 31.5 Kg/hr

Clock time-period	t_p °C	t_a °C	V mph	Q_{up} cal/cm^2	%	Q_b cal/cm^2	%	Q_w cal/cm^2	%	Q_T cal/cm^2	Radiation Intensity cal/cm^2 R_{Di}	R_{di}	R_f	*R_{Ti}	$\frac{Q_T}{R_{Ti}}$ %	$\eta = \frac{Q_w}{R_{Ti}}$ %
06-07														6.50	—	—
07-08	21.5	13.0	10	2.07	59.5	0.40	11.5	1.01	29.0	3.48				14.80	24.8	7.2
08-09	22.5	13.0	10	2.34	40.1	0.45	7.8	3.04	52.1	5.38				16.70	35.0	18.2
09-10	23.5	13.2	10	2.56	37.9	0.48	7.1	3.71	55.0	6.75				19.60	34.4	18.9
10-11	23.5	13.5	10	2.48	37.2	0.47	7.1	3.71	55.7	6.66				15.80	42.0	23.5
11-12	26.0	14.0	10	3.05	29.4	0.56	5.4	6.75	65.2	10.36				24.20	42.8	28.0
12-13	24.5	14.0	10	2.63	26.6	0.49	5.0	6.75	68.4	9.87				20.40	48.4	33.0
13-14	24.2	14.2	10	2.50	29.9	0.47	5.6	5.40	64.5	8.37				15.80	53.0	34.2
14-15	22.5	14.0	10	2.08	66.0	0.40	12.7	0.67	21.3	3.15				10.20	31.0	6.5
15-16														4.65	—	—
TOTAL PER DAY				19.71	36.2	3.72	6.8	31.04	57.0	54.47				138.65	39.2	22.4

* All estimated from W.O. radiation record.

Fig. 5.24

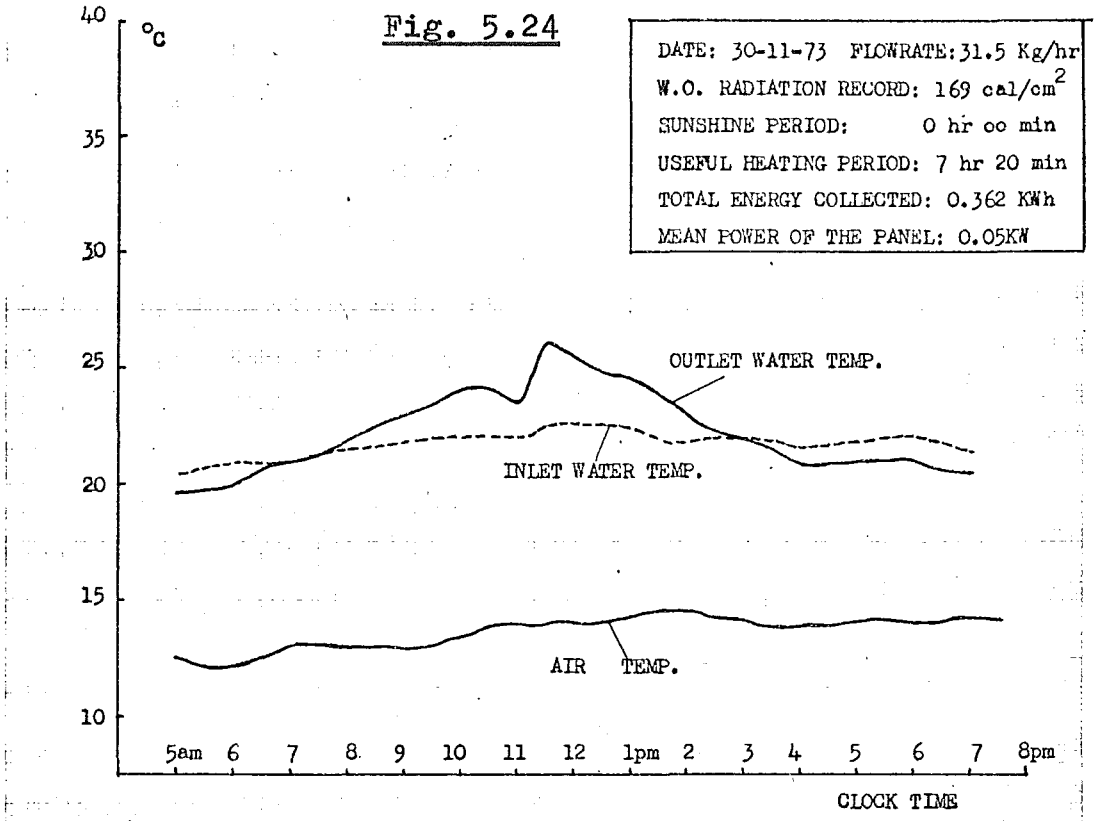
°C
40
35
30
25
20
15
10
DATE: 30-11-73 FLOWRATE: 31.5 Kg/hr
W.O. RADIATION RECORD: 169 cal/cm²
SUNSHINE PERIOD: 0 hr oo min
USEFUL HEATING PERIOD: 7 hr 20 min
TOTAL ENERGY COLLECTED: 0.362 KWh
MEAN POWER OF THE PANEL: 0.05KW
OUTLET WATER TEMP.
INLET WATER TEMP.
AIR TEMP.
5am 6 7 8 9 10 11 12 1pm 2 3 4 5 6 7 8pm
CLOCK TIME

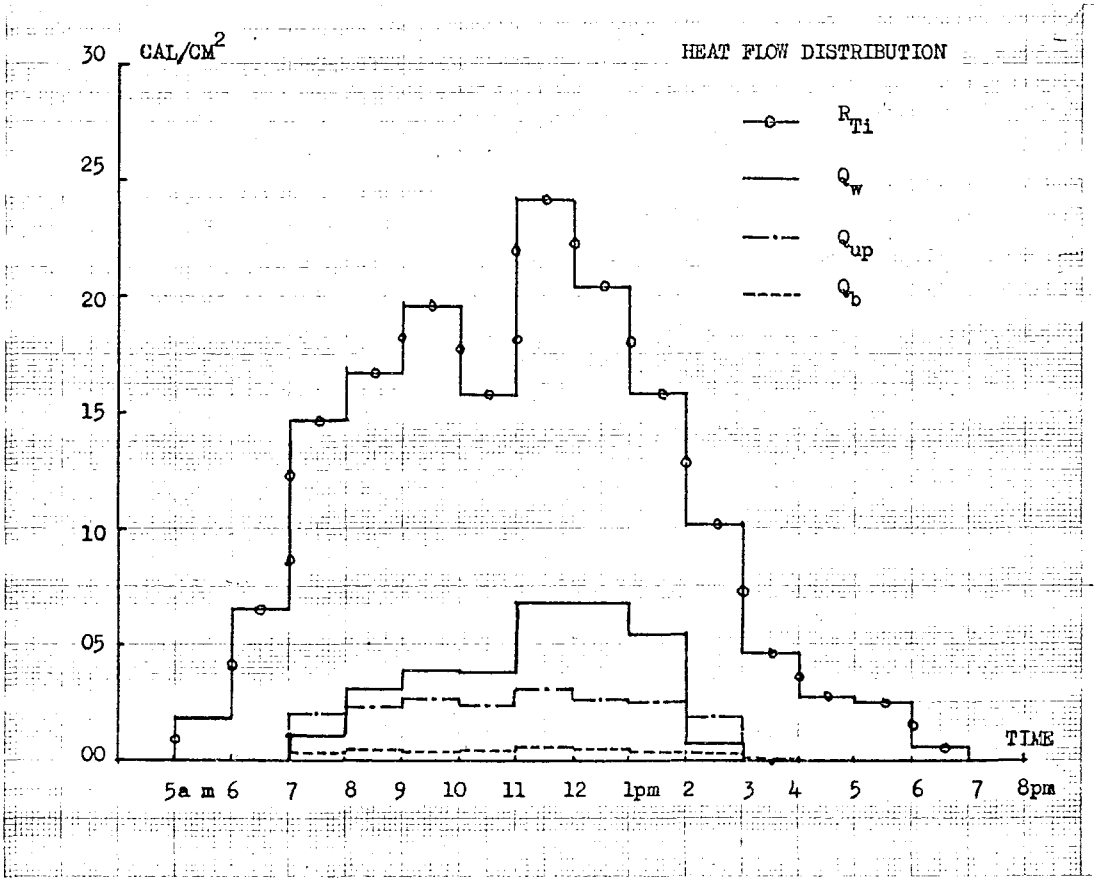
CAL/CM²
30
25
20
15
10
05
00
HEAT FLOW DISTRIBUTION
R_Ti
Q_w
Q_up
Q_b
TIME
5a m 6 7 8 9 10 11 12 1pm 2 3 4 5 6 7 8pm

TABLE 5.5 DATE: 4-12-73 FLOWRATE: 31.5 Kg/hr

Clock time-period	t_p °C	t_a °C	V mph	Q_{up} cal/cm²	%	Q_b cal/cm²	%	Q_w cal/cm²	%	Q_T cal/cm²	Radiation Intensity cal/cm² R_{Di}	R_{di}	R_f	*R_{Ti}	$\frac{Q_T}{R_{Ti}}$ %	$\eta=\frac{Q_w}{R_{Ti}}$ %
06-07	21.0	19.0	13.8	0.45	83.3	0.09	16.7	—	—	0.54				2.80	—	—
07-08	22.5	19.5	13.8	0.70	83.3	0.14	16.7	—	—	0.84				3.72	—	—
08-09	23.2	20.8	13.8	0.56	27.7	0.11	5.5	1.35	66.8	2.02				6.51	31.0	20.8
09-10	24.0	21.0	19.0	0.71	22.1	0.14	4.4	2.36	73.5	3.21				9.30	34.5	25.4
10-11	24.0	20.5	19.0	0.83	15.5	0.15	2.8	4.38	81.7	5.36				13.00	41.2	33.7
11-12	25.0	21.5	19.0	0.84	13.1	0.16	2.5	5.39	84.4	6.39				15.80	40.5	34.1
12-13	27.0	22.3	21.8	1.16	10.4	0.22	2.0	9.75	87.6	11.13				27.00	41.2	36.1
13-14	29.8	22.8	21.8	1.80	10.8	0.37	2.2	14.50	87.0	16.67				35.00	47.6	41.4
14-15	35.3	24.3	21.8	3.00	9.3	0.50	1.6	28.65	89.1	32.15				50.20	63.8	57.0
15-16	36.6	25.8	21.3	2.97	9.0	0.49	1.5	29.65	89.5	33.11				49.60	66.5	59.2
16-17	31.1	26.2	21.3	1.25	7.4	0.23	1.3	15.50	91.3	16.98				36.00	47.2	43.0
17-18	27.0	24.5	21.3	0.60	12.6	0.12	2.5	4.08	84.9	4.76				13.00	36.7	31.1
18-19	25.0	23.0	17.8	0.47	38.2	0.09	7.3	0.67	54.5	1.237				6.50	19.0	10.3
TOTAL PER DAY				15.34	11.4	2.81	2.1	116.24	86.5	134.39				268.43	50.0	43.4

* All estimated from W.O. radiation record.

Fig. 5.25

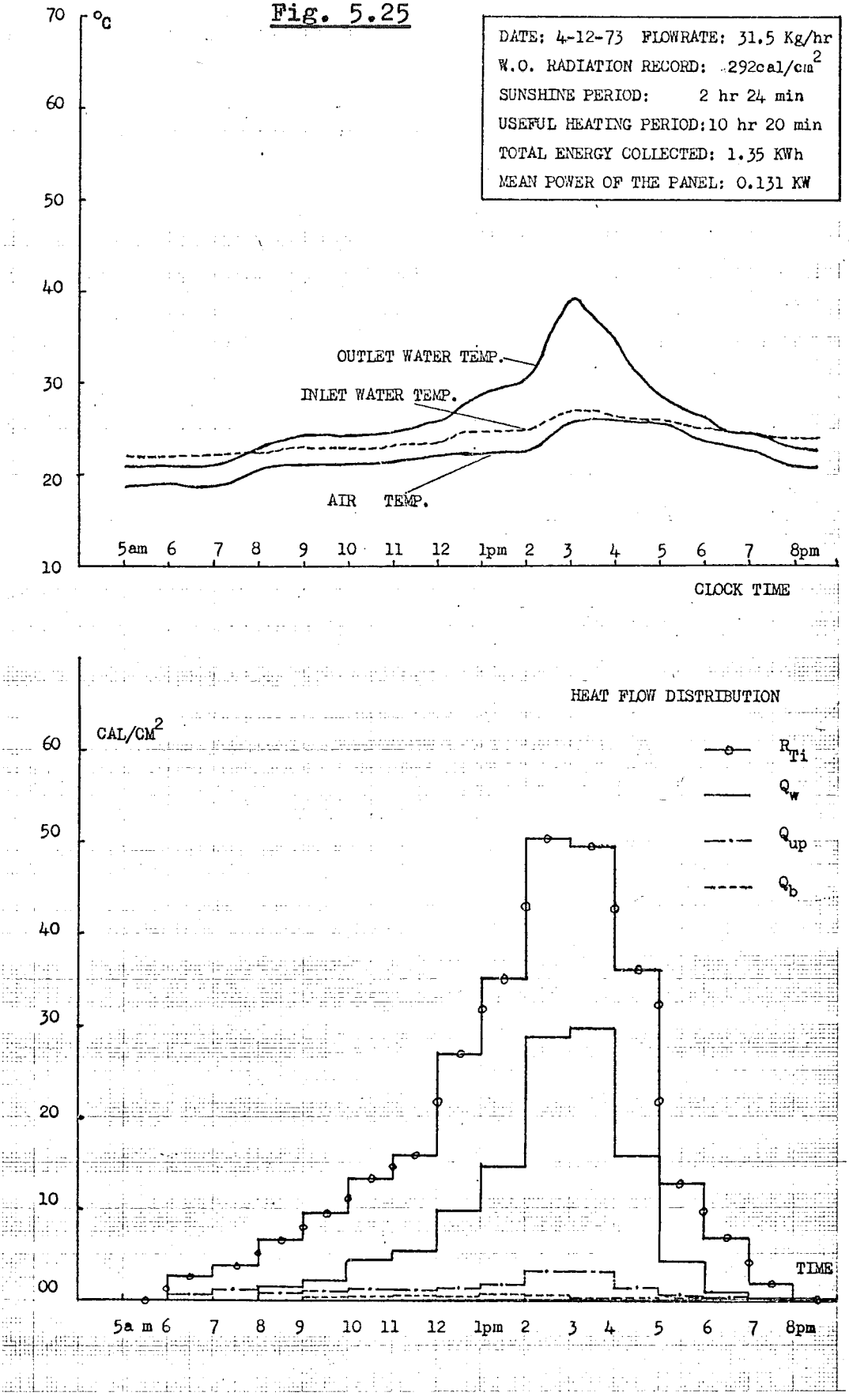
DATE: 4-12-73 FLOWRATE: 31.5 Kg/hr
W.O. RADIATION RECORD: .292cal/cm2
SUNSHINE PERIOD: 2 hr 24 min
USEFUL HEATING PERIOD: 10 hr 20 min
TOTAL ENERGY COLLECTED: 1.35 KWh
MEAN POWER OF THE PANEL: 0.131 KW
°C
70
60
50
40
30
20
10
OUTLET WATER TEMP.
INLET WATER TEMP.
AIR TEMP.
5am 6 7 8 9 10 11 12 1pm 2 3 4 5 6 7 8pm
CLOCK TIME
HEAT FLOW DISTRIBUTION
CAL/CM2
60
50
40
30
20
10
00
R Ti
Qw
Qup
Qb
TIME
5a m 6 7 8 9 10 11 12 1pm 2 3 4 5 6 7 8pm

TABLE 5.6 DATE: 6-12-73 FLOWRATE: 32.4 Kg/hr

Clock time-period	t_p °C	t_a °C	V mph	Q_{up} cal/cm^2	%	Q_b cal/cm^2	%	Q_w cal/cm^2	%	Q_T cal/cm^2	Radiation Intensity cal/cm^2 R_{Di}	R_{di}	R_f	R_{Ti}	$\frac{Q_T}{R_{Ti}}$ %	$\eta=\frac{Q_w}{R_{Ti}}$ %
06-07	20.5	12.8	2.9	1.83	83.6	0.36	16.4	—	—	2.19	0.02	3.21	0.17	3.40	—	—
07-08	22.0	13.5	2.9	2.05	83.7	0.40	16.3	—	—	2.45	0.20	8.04	0.44	8.69	—	—
08-09	23.9	14.5	2.9	2.31	30.5	0.42	5.5	4.85	64.0	7.58	0.54	16.81	0.92	18.28	41.5	26.5
09-10	25.1	15.2	6.3	2.47	22.1	0.43	3.8	8.30	74,1	11.20	5.66	30.67	1.92	38.25	29.3	21.7
10-11	26.9	16.2	6.3	2.72	19.5	0.46	3.3	10.75	77.2	13.93	1.13	28.72	1.58	31.43	44.3	34.2
11-12	32.5	17.2	6.3	4.08	14.1	0.67	2.3	24.25	83.6	29.00	1.08	25.89	1.42	28.39	Difference	
12-13	31.9	17.2	9.2	3.92	14.5	0.63	2.3	22.50	83.2	27.05	1.03	20.74	1.15	22.92	in sunshine	
13-14	32.0	17.5	9.2	3.87	14.7	0.63	2.4	21.80	82.9	26.30	4.12	36.41	2.12	42.65	61.7	51.1
14-15	30.2	17.5	9.2	3.33	15.7	0.57	2.7	17.30	81.6	21.20	4.86	34.05	2.04	40.95	51.8	42.2
15-16	26.3	16.0	11.5	2.62	18.1	0.45	3.1	11.42	78.8	14.49	1.25	23.28	1.30	25.83	56.1	44.2
16-17	23.0	15.0	11.5	1.96	41.1	0.38	8.0	2.43	50.9	4.77	0.43	11.80	0.65	12.88	37.0	18.9
17-18											0.12	6.90	0.38	7.40	—	—
18-19											0.03	3.57	0.20	3.79	—	—
TOTAL PER DAY				31.16	19.4	5.40	3.4	123.60	77.2	160.16				284.96	56.5	43.5

Fig. 5.26

DATE: 6-12-73 FLOWRATE: 32.4 Kg/hr
W.O. RADIATION RECORD: 295 cal/cm^2
SUNSHINE PERIOD: o hr oo min
USEFUL HEATING PERIOD: 8 hr 25 min
TOTAL ENERGY COLLECTED: 1.43 KWh
MEAN POWER OF THE PANEL: 0.170 KW

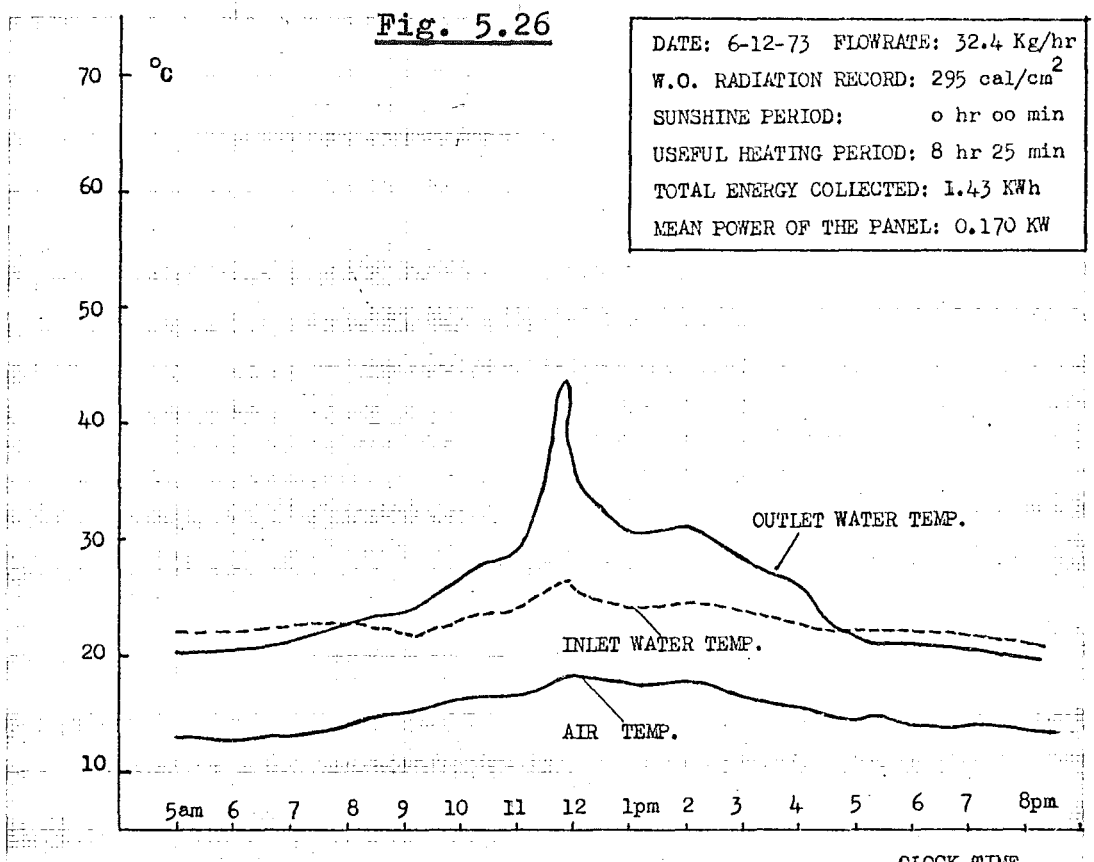

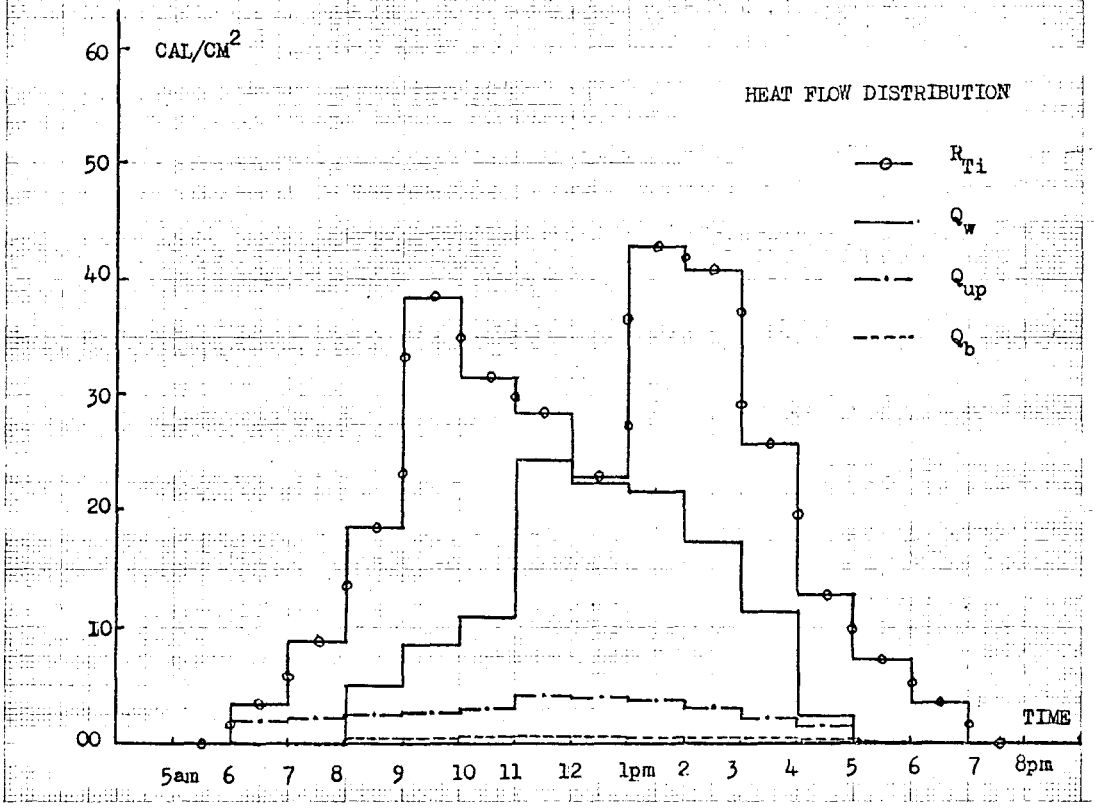

TABLE 5.7 DATE: 10-12-73 FLOWRATE: 36.9 Kg/hr

Clock time-period	t_p °C	t_a °C	V mph	Q_{up} cal/cm²	%	Q_b cal/cm²	%	Q_w cal/cm²	%	Q_T cal/cm²	Radiation Intensity cal/cm² R_{Di}	R_{di}	R_f	R_{Ti}	$\frac{Q_T}{R_{Ti}}$ %	$\eta = \frac{Q_w}{R_{Ti}}$ %
05-06												3.39	0.21	3.61	—	—
06-07	21.7	14.4	5.7	1.76	85.0	0.31	15	—	—	2.07	3.61	4.23	1.00	8.84	—	—
07-08	26.0	15.3	5.7	2.70	20.7	0.47	3.6	9.88	75.7	13.05	17.97	4.72	1.72	24.40	53.5	40.5
08-09	31.8	16.6	5.7	4.03	14.2	0.67	2.3	23.70	83.5	28.40	35.74	4.96	2.39	43.10	65.9	55.0
09-10	35.6	18.0	12.7	4.85	11.2	0.79	1.9	37.5	86.9	43.14	51.92	5.14	2.97	60.03	71.9	62.5
10-11	39.9	19.8	12.7	5.71	10.6	0.90	1.7	47.3	87.7	53.91	61.80	5.02	3.28	70.10	76.9	67.5
11-12	41.8	20.6	12.7	6.10	10.2	0.95	1.6	52.8	88.2	59.85	70.55	5.92	3.65	80.12	74.7	65.9
12-13	41.2	21.0	12.7	5.79	9.8	0.92	1.5	52.5	88.7	59.21	63.98	10.04	3.53	77.54	76.4	67.7
13-14	41.2	21.0	12.7	5.79	9.7	0.92	1.6	52.8	88.7	59.51	70.08	5.69	3.62	79.38	75.0	66.5
14-15	39.8	21.5	12.7	5.19	10.0	0.83	1.6	45.8	88.4	51.82	61.48	5.39	3.30	70.17	73.8	65.3
15-16	35.9	21.5	11.5	3.95	9.9	0.65	1.6	35.5	88.5	40.10	48.62	5.14	2.82	56.58	70.9	62.7
16-17	31.0	20.6	11.5	2.75	11.1	0.47	1.9	21.4	87.0	24.6	32.29	4.78	2.21	39.27	62.6	54.5
17-18	25.6	19.4	11.5	1.53	23.4	0.27	4.2	4.73	72,4	6.53	14.94	4.11	1.51	20.57	31.7	23.0
18-19	22.6	18.0	8.6	1.09	83.2	0.22	16.8	—	—	1.31	2.60	3,14	0.79	6.54	—	—
TOTAL PER DAY				51.22	11.6	8.33	1.8	383.91	86.6	443.46				640.25	69.2	60.0

Fig. 5.27

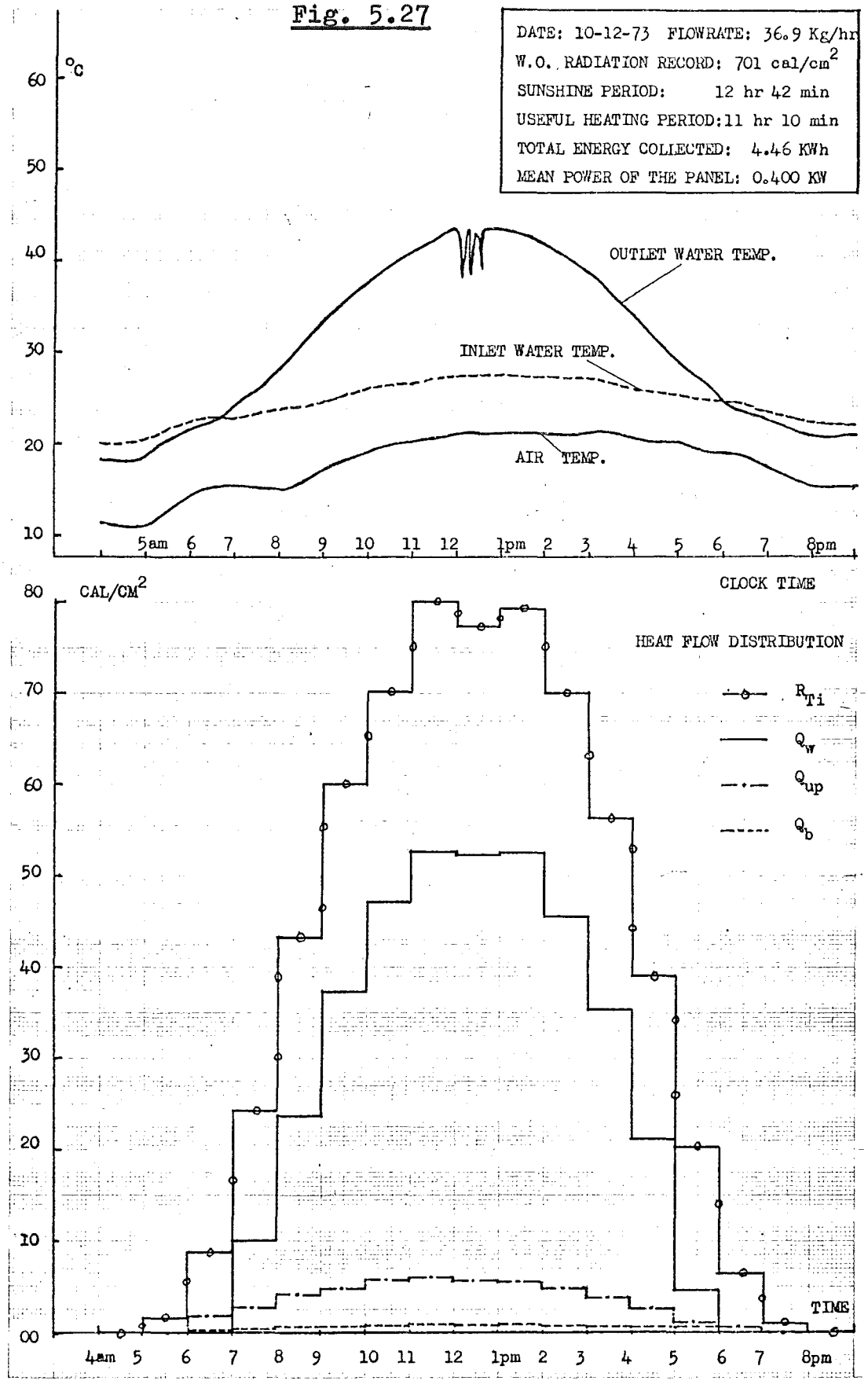
DATE: 10-12-73 FLOWRATE: 36.9 Kg/hr
W.O. RADIATION RECORD: 701 cal/cm2
SUNSHINE PERIOD: 12 hr 42 min
USEFUL HEATING PERIOD: 11 hr 10 min
TOTAL ENERGY COLLECTED: 4.46 KWh
MEAN POWER OF THE PANEL: 0.400 KW
°C
OUTLET WATER TEMP.
INLET WATER TEMP.
AIR TEMP.
5am 6 7 8 9 10 11 12 1pm 2 3 4 5 6 7 8pm
CLOCK TIME
CAL/CM2
HEAT FLOW DISTRIBUTION
R_Ti
Q_w
Q_up
Q_b
TIME
4am 5 6 7 8 9 10 11 12 1pm 2 3 4 5 6 7 8pm

TABLE 5.8 DATE: 11-12-73 FLOWRATE: 37.8 Kg/hr

Clock time-period	t_p °C	t_a °C	V mph	Q_{up} cal/cm^2	%	Q_b cal/cm^2	%	Q_w cal/cm^2	%	Q_T cal/cm^2	Radiation Intensity cal/cm^2 R_{Di}	R_{di}	R_f	R_{Ti}	$\frac{Q_T}{R_{Ti}}$ %	$\eta=\frac{Q_w}{R_{Ti}}$ %
06-07	21.0	14.0	9.2	—	—	—	—	—	—	—	0.46	7.02	0.47	7.95	—	—
07-08	22.5	14.2	9.2	—	—	—	—	—	—	—	1.08	9.74	0.60	11.42	—	—
08-09	21.2	13.5	9.2	—	—	—	—	—	—	—	0.16	8.77	0.47	9.40	—	—
09-10	25.8	14.5	9.2	2.86	19.5	0.53	3.6	11.30	76.9	14.69	2.79	22.44	1.33	26.56	55.3	42.5
10-11	30.4	16.0	9.2	3,80	13.0	0.68	2.4	24.70	84.6	29.18	5.62	32.84	2.01	40.47	72.1	61.0
11-12	22.0	14.6	9.2	1.79	47.6	0.35	10.3	1.62	43.1	3.76	0.23	7.02	0.38	7.63	49.3	21.2
12-13	21.0	13.8	5.7	—	—	—	—	—	—	—	0.19	5.20	0.28	5.68	—	—
13-14	23.2	14.2	5.7	2.15	32.5	0.42	6.4	4.04	61.1	6.61	0.41	12.88	0.70	13.99	47.2	28.9
14-15	22.0	14.0	5.7	—	—	—	—	—	—	—	0.38	9.38	0.52	10.28	—	—
15-16	26.8	15.5	4.6	2.86	18.4	0.53	3.4	12.15	78.2	15.54	0.91	21.84	1.21	23.95	64.9	50.7
16-17	25.0	15.2	4.6	2.44	27.2	0.46	5.1	6.07	67.7	8.97	0.41	13.67	0.75	14.83	60.5	40.9
17-18	23.0	14.8	4.6	2.00	83.7	0.39	16.3	—	—	2.39	0.22	9.07	0.50	9.78	—	—
18-19											0.04	4.35	0.24	4.63	—	—
TOTAL PER DAY				17.90	22.1	3.36	4.1	59.98	73.8	81.24				187.53	43.4	32.0

Fig. 5.28

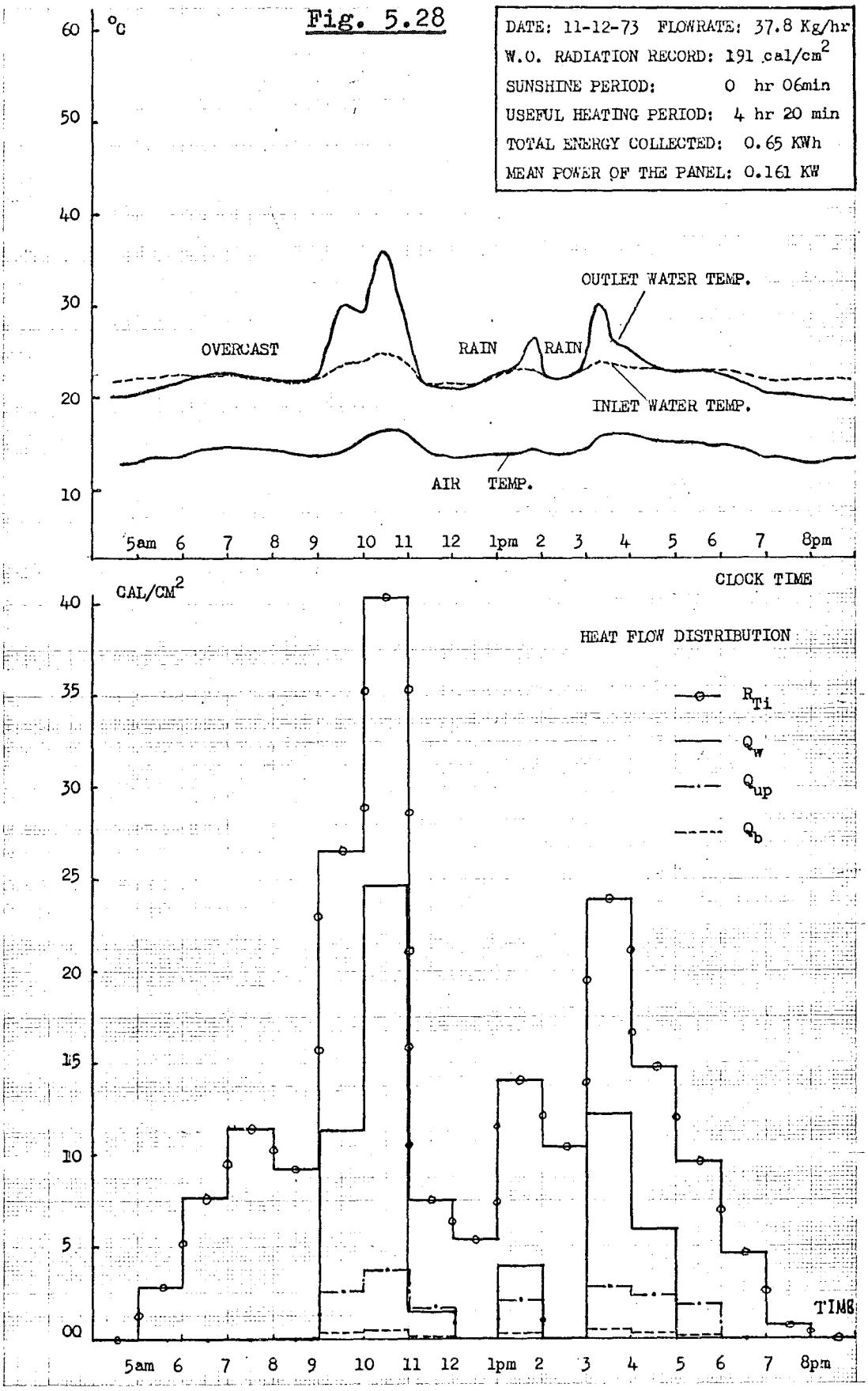
DATE: 11-12-73 FLOWRATE: 37.8 Kg/hr
W.O. RADIATION RECORD: 191 cal/cm2
SUNSHINE PERIOD: 0 hr 06min
USEFUL HEATING PERIOD: 4 hr 20 min
TOTAL ENERGY COLLECTED: 0.65 KWh
MEAN POWER OF THE PANEL: 0.161 KW
°C
60
50
40
30
20
10
OVERCAST
RAIN
RAIN
OUTLET WATER TEMP.
INLET WATER TEMP.
AIR TEMP.
5am 6 7 8 9 10 11 12 1pm 2 3 4 5 6 7 8pm
CLOCK TIME
CAL/CM2
40
35
30
25
20
15
10
5
00
HEAT FLOW DISTRIBUTION
RTi
Qw
Qup
Qb
TIME
5am 6 7 8 9 10 11 12 1pm 2 3 4 5 6 7 8pm

TABLE 5.9 DATE: 12-12-73 FLOWRATE : 37.8 Kg/hr

Clock time-period	t_p °C	t_a °C	V mph	Q_{up} cal/cm^2	%	Q_b cal/cm^2	%	Q_w cal/cm^2	%	Q_T cal/cm^2	Radiation Intensity cal/cm^2 R_{Di}	R_{di}	R_f	R_{Ti}	$\frac{Q_T}{R_{Ti}}$ %	$\eta = \frac{Q_w}{R_{Ti}}$ %
06-07											0.01	4.60	0.25	4.86	—	—
07-08	21.0	12.8	9.8	1.98	55.3	0.39	10.9	1.21	33.8	3.58	0.73	14.39	0.82	15.94	22.5	7.6
08-09	24.2	13.6	9.8	2.65	19.4	0.50	3.7	10.50	76.9	13.65	4.68	21.41	1.41	27.51	49.6	38.2
09-10	29.8	14.5	14.0	4.04	13.9	0.72	2.5	24.30	83.6	29.06	25.82	23.52	2.59	51.93	56.0	46.8
10-11	35.0	15.0	14.0	5.51	13.0	0.94	2.2	36.00	84.8	42.45	31.40	26.13	2.92	60.45	70.2	59.6
11-12	39.0	15.5	14.0	6.66	11.0	1.11	1.9	52.6	87.1	60.37	61.00	13.55	3.60	78.15	77.2	67.3
12-13	39.8	16.0	16.7	6.79	11.0	1.12	1.8	53.8	87.2	61.71	71.52	6.35	3.69	81.55	75.7	66.0
13-14	39.0	16.2	16.7	6.47	11.0	1.08	1.8	51.4	87.2	58.95	69.68	5,56	3.59	78.84	74.8	65.2
14-15	36.6	16.5	16.7	5.60	10.9	0.95	1.8	45.0	87.3	51.55	61.42	5.56	3.30	70.28	73.3	64.0
15-16	33.0	16.5	13.2	4.36	11.1	0.78	2.0	34.8	86.9	40.04	48.62	5.20	2.82	56.65	70.7	61.4
16-17	28.3	16.0	13.2	3.19	14.0	0.58	2.6	19.0	83.4	22.77	32.49	4.78	2.22	39.49	57.7	48.1
17-18	24.0	16.0	13.2	1.98	27.5	0.38	5.2	4.85	67.3	7.21	14.89	4.72	1.54	21.15	34.1	22.9
18-19	20.0	15.5	13.2	—	—	—	—	—	—	—	2.17	5.08	0.79	8.05	—	—
TOTAL PER DAY				49.33	12.6	8.55	2.2	333.46	85.4					594.85	65.7	56.2

Fig. 5.29

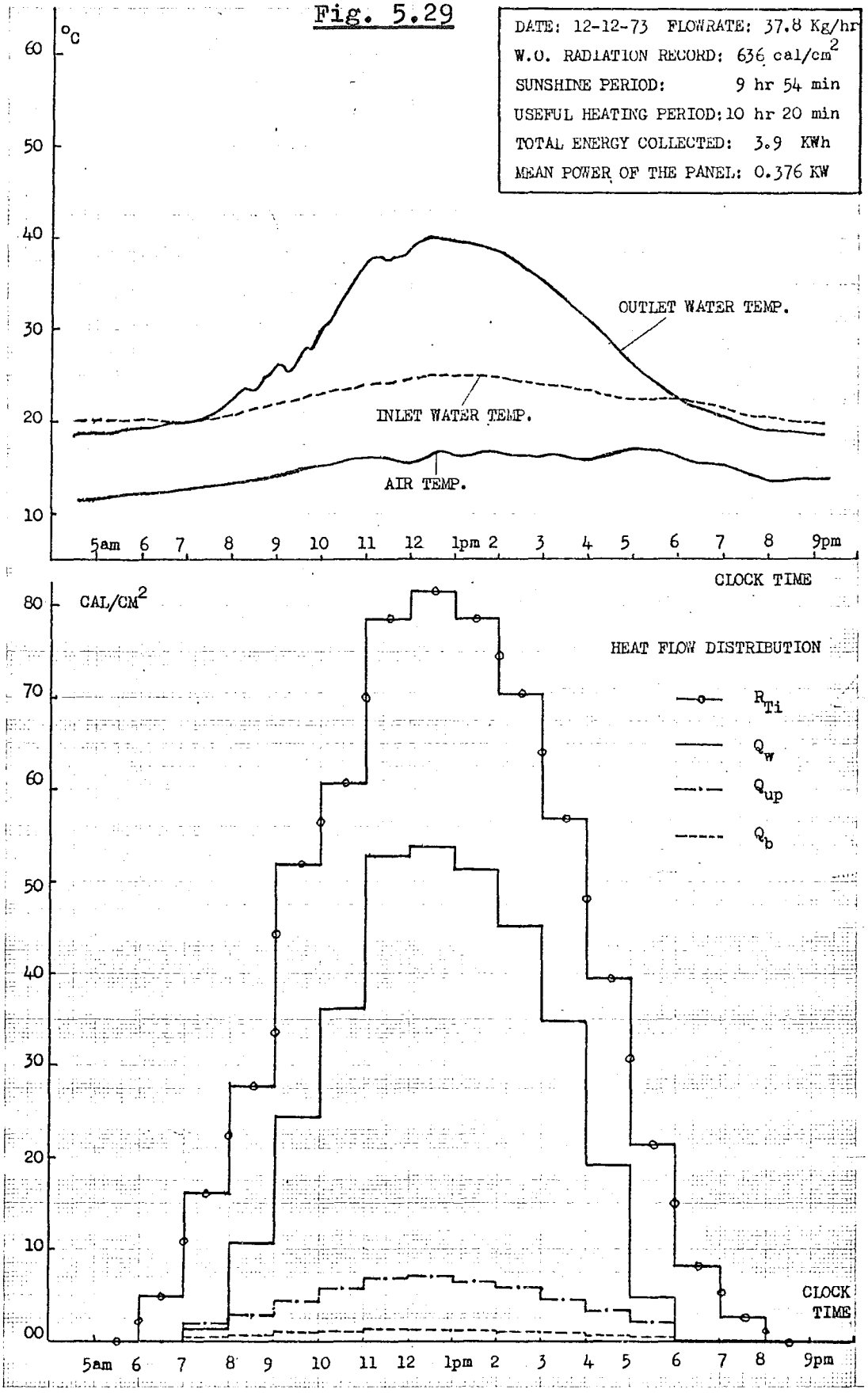
DATE: 12-12-73 FLOWRATE: 37.8 Kg/hr
W.O. RADIATION RECORD: 636 cal/cm2
SUNSHINE PERIOD: 9 hr 54 min
USEFUL HEATING PERIOD: 10 hr 20 min
TOTAL ENERGY COLLECTED: 3.9 KWh
MEAN POWER OF THE PANEL: 0.376 KW
°C
OUTLET WATER TEMP.
INLET WATER TEMP.
AIR TEMP.
CLOCK TIME
CAL/CM2
HEAT FLOW DISTRIBUTION
R Ti
Q w
Q up
Q b
CLOCK TIME
5am 6 7 8 9 10 11 12 1pm 2 3 4 5 6 7 8 9pm

utilized during December 1973 probably was more because later in the month, more days had radiation intensities above that on the 10 December.

2. Efficiencies and factors affecting performance:

Maximum overall efficiency can be as high as 72% in some periods but the maximum for daily average was 61%. Normally overall efficiency varied from 40% to 60%. The general performance increases with the amount of incident radiation as mentioned earlier (9). This is clearly shown in daily variation where the percentage of useful heat transferred to water (overall efficiency) is small in early hours and increasing with the radiation intensity. Days with high insolation showed better performance of the panel than low insolation days.

The performance is also affected by the weather condition, especially air temperature. Having the same order of insolation, the percentage of collection and overall efficiency are better when air temperature is higher. On the 6 and 7 of November, the mean air temperature at midday was high, 25 to 26°C, solar intensity was also high and these gave high percentage of collection and overall efficiency although the efficiency of heat transfer from collector plate to water was not very large because of low flow-rate.

3. Unfavourable weather conditions:

On rainy day with some periods of sunshine, some energy can also be collected, e.g. 12 December (Fig. 5.19). However when it rains throughout the day, no useful heating can be expected, e.g. 18 December, even though the Weather Office recorded a total of 113 cal/cm^2 radiation on horizontal surfaces (Fig. 5.30). At night-time, by dropping temperature while

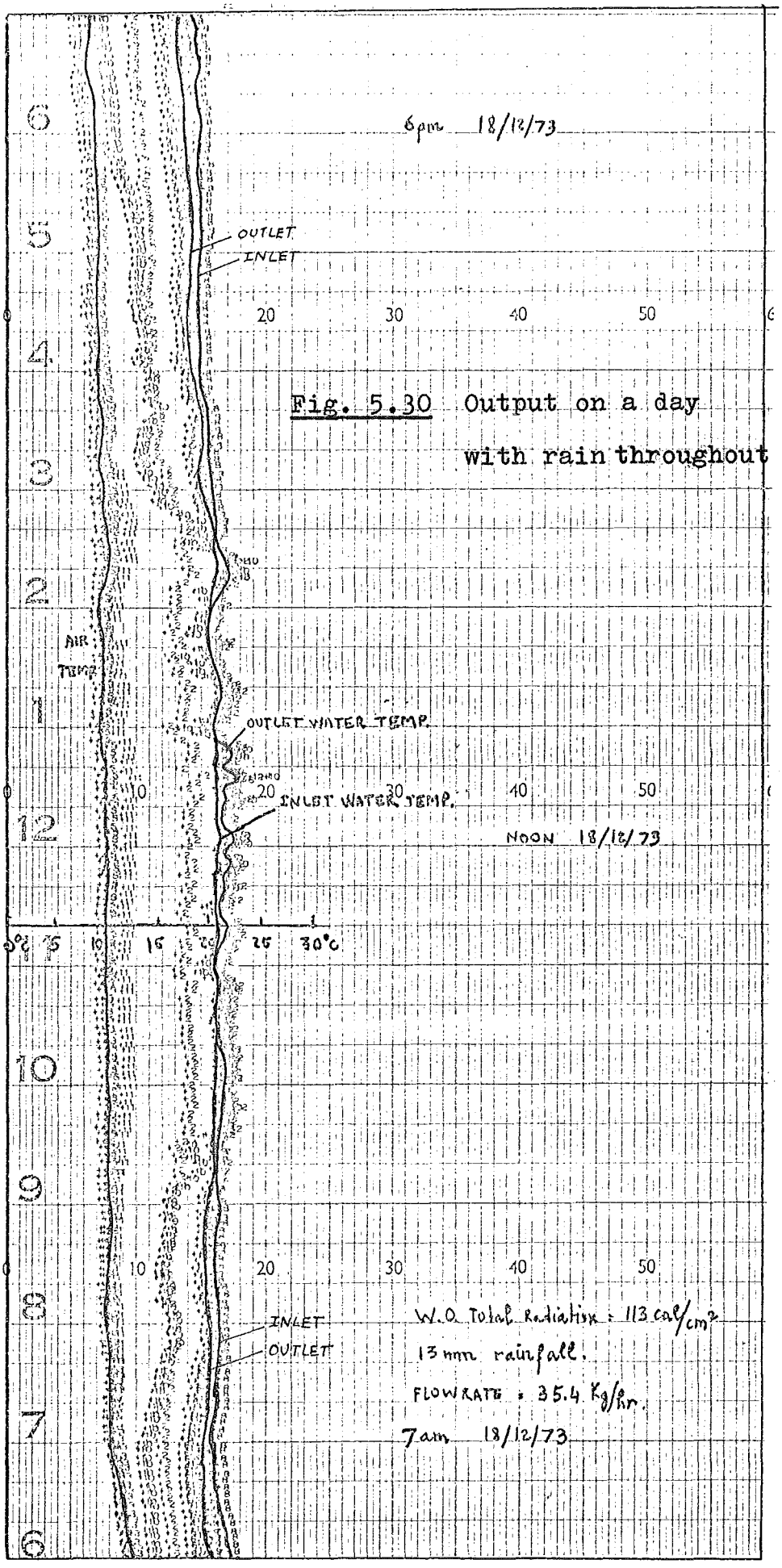

Fig. 5.30 Output on a day with rain throughout

flowing through the panel, the water normally supply 3 to 7 cal/cm^{2}hr to compensate for the radiation loss from the collector plate to the sky.

4. Temperature variations:

For thermosiphon system analysis, it is usually suggested to use the average of inlet and outlet water temperatures for the mean plate temperature. Analysis for this forced circulation system showed that the above estimation is valid only for periods of low radiation, during sunny periods the mean plate temperature may be as high as 8^{o}C above the average of inlet and outlet water temperature. This difference between the two systems lies in the difference in water flowrate and temperature rise.

In thermosiphon system, the flow is created by the virtue of difference in densities between water inside the tubes of the collector and water at the bottom of the storage tank. As the radiation intensity increases, both inlet and outlet water temperature also increase. Because at the same temperature difference of water, the difference in density is larger at high temperature range than at lower range, the flowrate increases and consequently reduces the temperature difference. However, as the flowrate increases, resistance to the flow is higher and more difference in temperature is required. Therefore for a particular insolation, there is a fixed water flowrate depending on the inlet temperature and the sizes of the connection pipes. As shown by Morse (16), the temperature difference between inlet and outlet water is nearly constant to about 2:00 pm before it begins to drop until the end of useful heating period. Fig. 5.31 shows typical variation of

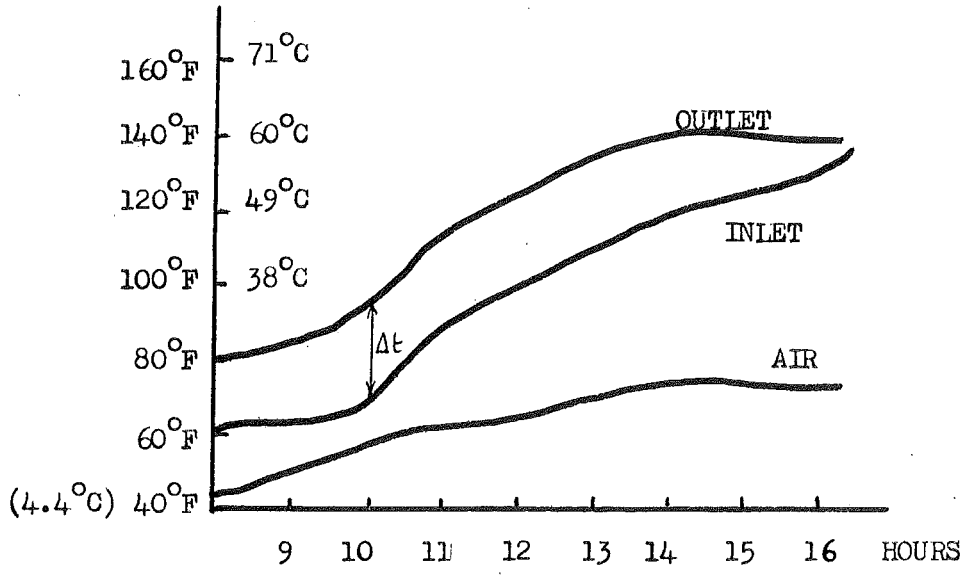

Fig. 5.31 Inlet & Outlet temperature variation for thermosiphon system. (values from Ref.16)

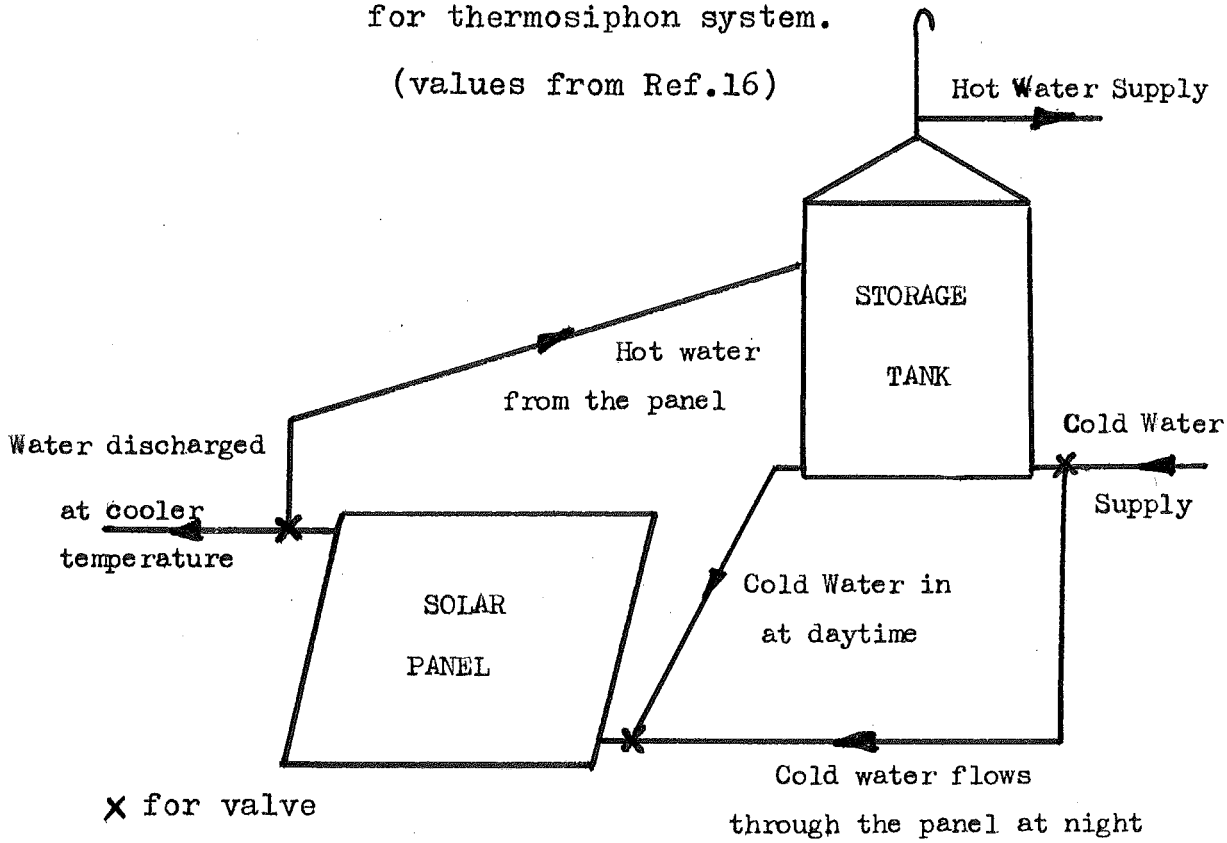

Fig. 5.32 Outline of a dual water circuit for frost prevention

water temperature in a thermosiphon system based on values measured by Morse.

The forced circulation system, on the other hand , has a constant flowrate, the temperature rise increases as radiation increases. The rise of inlet temperature throughout the day is very little compared with that of thermosiphon system. Therefore, it is more justified to assume plate temperature be the average of inlet and outlet temperatures for thermosiphon system than for forced circulation system.

5. Distribution of heat collected:

As mentioned earlier in the qualitative analysis, during early hours in the morning and late in the afternoon not much useful heat can be transferred to water. Quantitatively, usually less than 50% of the heat collection during these periods was transmitted to water. As more radiation is collected, the percentage lost backward and upward decreases. During efficient operating period (i.e. 10am to 4pm), 10%to 20% was lost upward while 1%to 2% was lost backward, the ratio of back loss to upward loss varies from 10%to 17%. This is reasonable compared with what normally suggested to allow 10%to 20% of upward loss for back loss in the total heat losses.

6. Comparisons with theoretical estimation:

For all sunny periods, the percentage of collection varied from 60%to 80%. Typical values on a clear day such as 10 Dec are very close to 74.8% which is the value for F_e estimated earlier. Low percentage of collection is expected for cloudy periods due to large portion of radiation is diffuse radiation.

The efficiency of heat transfer from collector plate to water was estimated as 80%to 89% for flowrates from 9.5 to 45.5 Kg/hr (20 to 100 lb/hr). In the test this efficiency

varied around 80%to 88% during the most efficient operating periods of the day which is in good agreement with the prediction.

The back loss coefficient was calculated as 0.548 $W/m^2{}^oC$ or 0.047 $cal/cm^2{}^oChr$. The equivalent up loss coefficient U_{up} which varied quite linearly from 0.23 cal/cm^2hr^oC for 20^oC plate temperature to 0.31 cal/cm^2hr^oC for 55^oC justified the estimated U_{up}= 0.298 cal/cm^2hr^oC for 40^oC plate temperature and 15^oC air temperature. Overall heat loss coefficient then varied from 0.277 to 0.357 cal/cm^2hr^oC, which is also well-agreed with U_o= 0.33 cal/cm^2hr^oC estimated.

7. Validity of the above results:

(a) Analyses in Appendix 6 show that in these calculations Q_w was estimated with 5% accuracy, Q_b with 4%to 5% and Q_{up} with 3%to 5%.

These were based on the error assumed as:

$\mp .5^oC$ in air temperature measurements.

$\pm\ 1^oC$ in plate temperature.

$\pm$ .5 Kg/hr in water flowrate measurements.

(b) The effect of h_w on the upward heat loss calculations is not large, for two values of h_w= 4 at 10 mph wind and h_w= 10 at 30 mph wind, maximum difference in Q_{up} is only about 1%. See Part 3 of Appendix 6.

(c) The effect of using air temperature instead of effective sky radiant temperature is an underestimation of Q_{up} by about 20%to 30% during clear sky periods, using $T_s = T_a - 10$ in Rankine degrees. For intermittent and cloudy comditions T_s is close to T_a and error is much smaller. However, the absolute value of the difference is not large as compared with the component of heat collected by water Q_w, therefore this

underestimation of Q_{up} can lead to only 3% maximum underestimation of Q_T and the percentage of collection Q_T/R_{Ti}. The percentage Q_w/Q_T is then overestimated by only 2% to 3%. Typical examples for the days of 6 Nov and 10 Dec are shown in the table below.

Table 5.10

DATE	time period	t_p °C	t_s °C	Q_{up}		Q_b		Q_w		Q_T	$\frac{Q_T}{R_{Ti}}$
				$\frac{cal}{cm^2}$	%	$\frac{cal}{cm^2}$	%	$\frac{cal}{cm^2}$	%	$\frac{cal}{cm^2}$	%
10/12	11-12	41.8	20.6	6.10	10.2	.95	1.6	52.80	88.2	59.85	74.7
	11-12	41.8	15.0	7.70	12.5	.95	1.5	52.80	86.0	61.46	76.5
	13-14	41.2	21.0	5.79	9.7	.92	1.6	52.80	88.7	59.51	75.0
	13-14	41.2	15.4	7.43	12.1	.92	1.5	52.80	86.3	61.15	77.0
6/11	11-12	55.0	22.3	10.23	15.1	1.48	2.2	56.00	82.7	67.71	88.0
	11-12	55.0	16.7	11.90	17.2	1.48	2.0	56.00	80.8	69.38	90.1
	12-13	50.4	23.5	8.23	14.4	1.22	2.2	46.50	83.4	55.95	78.0
	12-13	50.4	17.9	9.94	17.2	1.22	2.1	46.65	80.7	57.66	80.4

There is no difference in Q_w and overall efficiency η because they do not relate to t_s.

(d) In estimating the incident radiation on the panel surface, records of total and diffuse radiation from Mrs. Moran were used mainly, except on two days where Weather Office records of total radiation were used because these data were not recorded.

Weather Office records were also used as a comparison. During November there were large differences between those two records (up to 12 cal/cm^{2}hr) but later records were close enough. See table 4.5, 4.6, and 4.7 for examples. Mrs. Moran's records were used in the calculations for consistency and because separate component of total and diffuse solar radiation

were measured. The accuracy of the solarimeters which gave those records is $\pm$1%.

(D) EXTENSIONS OF RESULTS OBTAINED FROM THE TEST:

From the limited results of this test and with the knowledge of other information from previous references some estimation can be made for the performance of this type of solar water heater during the whole year.

1. Contribution potential:

Although this test panel operated on forced circulation system the results presented above may be applied to the ordinary thermosiphon system because no reference has been found to mention significant differences in efficiency between these two systems. The theoretical predictions based on the analysis following Whillier's methods have been proved close enough with actual performance. Moreover Whillier's methods have been recommended for estimation of both types of system, therefore one can expect thermosiphon system operation will give the same efficiency as found above, if not a little more owing to its variation in flowrate according to the intensity of radiation.

Based on the standard year solar radiation as proposed by Benseman and Cook, and considering the fact that these radiation intensities have overestimated the actual radiation recorded in Christchurch by about 15% on average for the last 5 years, one can use these radiation intensities as the estimated radiation on a 40° inclined surface.

Also from these test results, the overall efficiency usually varies from 40% to 60% in average weather conditions

and from the conclusion that there is little difference in efficiency between summer and winter(9) one can assume an average efficiency 50% for most months of the year except May, June and July where 40% efficiency can be assumed because of low $\bar{K}$ values.

Hence with these assumptions, the average of all year energy collected can be estimated as below.

Table 5.11 Estimated energy contribution per year

Month	$\bar{K}$	Radiation cal/cm^2 day	η %	Energy collected cal/cm^2 day	KWh/m^2 day
Jan	0.53	514	50	257	2.98
Feb	0.56	469	"	234	2.72
Mar	0.52	342	"	171	1.99
Apr	0.51	241	"	120	1.39
May	0.47	153	40	61	0.71
Jun	0.46	119	"	48	0.56
Jul	0.46	130	"	52	0.60
Aug	0.55	218	50	109	1.27
Sep	0.49	283	"	191	2.22
Oct	0.55	418	"	209	2.43
Nov	0.58	539	"	269	3.12
Dec	0.60	600	"	300	3.48
Total				2021	

Energy collected per year 2021 x 30 = 60630 cal/cm^2

or 705 KWh/m^2

Assuming also that an ordinary house requires 60 gallons (273 litres) of hot water at 60°C per day and the inlet cold

water is 20°C, the total heat required per day is 10,920 Kcal or 12.7 KWh. If the solar water heater is aimed to supply all this heat during summer months with some boosted heating by other sources during winter, the necessary area is about 4.5 m^2 based on the average collection of 2.72 KWh/m^2 per day in Feb or 3.6 m^2 based on the average of 3.48 KWh/m^2 per day in Dec . Therefore a 4 m^2 collector area unit will be adequate. Average annual contribution is 28,000 KWh giving a saving of say $28 if extra heating is provided by electricity. Based on the material cost of about $77 for this one square metre test unit, the cost for a 4 m^2 heater may be about $300. Assuming that the heater will have a life of 20 years, this saving gives the rate of return of about 7% for the expense.

2. Angle of inclination:

During this test, the unit was fixed at 40° from horizontal. This angle is based on 0.9 times the latitude of Christchurch as suggested by Morse and Czarnecki (13). From the analysis in Section 4.4, the incident angles of solar rays on an inclined surface can be calculated. With the help of the programme in Appendix 1, several angles of inclination were calculated for each month to find out the one which will receive sunrays at nearly normal incidence. Tables 5.12 and 5.13 give those angles compared with a horizontal surface for Christchurch position.

From these tables, it can be seen that the average for all year round is from 40° to 45° as suggested. However, it will be more efficient if the inclination of the panel can be made adjustable so that the angle of inclination can be changed several times a year to place the surface almost normal to

Table 5.12 Comparisons of $\cos H_i$ for different inclination

TIME	Jan		Feb		Mar		Apr		May		Jun	
	$\alpha = 0°$	$\alpha = 20°$	$\alpha = 0°$	$\alpha = 30°$	$\alpha = 0°$	$\alpha = 45°$	$\alpha = 0°$	$\alpha = 55°$	$\alpha = 0°$	$\alpha = 65°$	$\alpha = 0°$	$\alpha = 65°$
06	.116											
07	.294	.212	.178	.107	.070	.099						
08	.468	.431	.361	.359	.254	.360	.136	.423	.035	.481		
09	.625	.633	.527	.583	.421	.590	.296	.628	.187	.676	.130	.665
10	.757	.793	.666	.771	.559	.772	.425	.811	.310	.828	.253	.826
11	.852	.916	.768	.902	.658	.912	.516	.932	.396	.939	.340	.934
12	.906	.985	.826	.982	.712	.987	.562	.993	.439	.994	.386	.991
13	.914	.995	.837	.996	.718	.995	.560	.990	.435	.990	.386	.993
14	.875	.945	.798	.944	.674	.934	.511	.921	.385	.927	.341	.934
15	.793	.839	.715	.837	.584	.813	.416	.794	.293	.807	.255	.826
16	.672	.686	.591	.667	.454	.631	.284	.610	.165	.647	.132	.671
17	.522	,494	.435	.458	.293	.409	.122	.401	.010	.439		
18	.352	.292	.258	.224	.111	.159						
19	.174	.059	.072	.0								

Table 5.13 Comparisons of $\cos H_i$ for different inclination

TIME	Jul		Aug		Sep		Oct		Nov		Dec	
	$\alpha = 0°$	$\alpha = 65°$	$\alpha = 0°$	$\alpha = 60°$	$\alpha = 0°$	$\alpha = 45°$	$\alpha = 0°$	$\alpha = 30°$	$\alpha = 0°$	$\alpha = 20°$	$\alpha = 0°$	$\alpha = 20°$
06										.081		.054
07					.113	.160	.276	.239	.375	.308	.375	.286
08	.005	.439	.121	.411	.294	.416	.454	.478	.530	.513	.530	.483
09	.160	.642	.282	.615	.454	.636	.602	.677	.682	.701	.682	.676
10	.289	.807	.415	.795	.583	.813	.719	.837	.799	.850	.809	.836
11	.381	.926	.509	.925	.672	.937	.809	.953	.883	.953	.891	.939
12	.431	.990	.559	.987	.714	.995	.839	.997	.914	.996	.934	.994
13	.435	.995	.561	.991	.708	.985	.829	.979	.906	.983	.934	.992
14	.393	.939	.514	.930	.652	.911	.766	.897	.848	.911	.883	.931
15	.308	.828	.423	.813	.552	.766	.656	.754	.743	.780	.799	.821
16	.186	.676	.294	.636	.413	.581	.575	.557	.616	.616	.669	.660
17	.034	.481	.134	.432	.246	.349	.358	.340	.454	.416	.515	.464
18					.061	.099	.174	.083	.276	.191	.358	.265
19											.174	.032

sunrays most of the time. The following changes of the setting are suggested:

For Nov, Dec, Jan	= 20°	from horizontal
Feb, Mar, Apr	= 40°	" "
May, Jun, Jul, Aug	= 65°	" "
Sep, Oct	= 40°	" "

The increase in insolation due to this change is significant, for example changing from 40° inclination to 20° in Dec can increase the collection of direct component of solar radiation by 15% (compare Table 4.3 and Table 5.13).

3. Frost prevention:

As shown by some results of the night-time operation, during clear night sky periods the glass and air space temperatures may drop quite considerably. This situation often occurs during winter months, even more severe due to low air temperature. The problem of frost over the glass surface and freezing of water inside the tubes may appear in those situations.

Double glazing is therefore useful and necessary for installations under Christchurch conditions. Where the problem is not so severe as the case in city installations, some types of drapery to cover the panel surface during night-time may be sufficient. The setting of large inclination during winter months as suggested above also helps to reduce the excessive cooling loss owing to the long wave radiation from surroundings.

To avoid the problem of freezing water, one method has been proposed by Farber (18) in which a double-walled storage tank is used. The inside tank stores usable hot water, the outside tank is well-insulated and stores water with anti-freeze additive used as the heat transfer medium. This system can be

used in places where excessive radiative cooling and low air temperature occur at night-time such as in remote country-side areas.

In this test panel, the water was kept flowing all the time and the temperature drop of water during night-time was noticed while the plate temperature was always a few degrees higher than air temperature, even in clear nights where the glass temperature dropped down below air temperature. Compared with the themosiphon system where there is very little movement of water inside the tubes at night, this leads to the suggestion that a dual water circuit be connected to the panel. At day-time normal thermosiphon effect will heat up water and store in the tank, during night-time another circuit to supply flowing water through the panel at some large enough flowrate to provide compensation for the heat loss and avoid the freezing of water. A diagrammatic illustration for such a system is shown in Fig. 5.32. More study is required to design a suitable circuit and valve fittings to ensure water will flow correctly as desired.

C O N C L U S I O N S F O R P A R T II

The information on solar radiation presented in this part gave a brief review of what have been done about solar radiation in New Zealand. It helpsto locate the sources of references which may be needed in later research of solar radiation and its applications.

Compared with the Standard Year solar radiation intensity for Christchurch proposed by Benseman & Cook in 1969, recent records of radiation at Christchurch showed a significant reduction in solar radiation intensity received by a horizontal surface in the last five years. Monthly mean in these years were usually 10%to 20% lower than the corresponding values in the Standard Year which were selected from actual records in the past.

Some examples of estimation of radiation on an inclined surface from measurements on horizontal surface illustrated the method to apply for any inclined surface at any situation.

On the performance of the solar water heater, results showed that during November and December a common type solar water heater, facing North and inclined 40^{o} from horizontal, can develop from nothing on a most unfavourable day to 5 KWh per square metre of collector area on a clear sun-shine day. The efficiency of operation increased with higher insolation and varied from 40% to 60%. A normal domestic usage requires from 3 to 4 m^2 for a consumption of about 273 litres (60 gallons) hot water at $60^{o}C$ per day. Compared with heating water by electricity, a saving of at least $20 to $30 per year may be expected.

Double glazing for the solar water heater was found useful and necessary under Christchurch weather conditions. Adjustable inclination, where possible, is suggested to allow the inclination to be changed about 4 times a year for maximum collection . Otherwise, a 40^{o} inclination from horizontal is the optimum for all year round operation.

R E F E R E N C E S

1. Stringer F.T. : Techniques of Climatology, W.H. Freeman and Comp., San Francisco, p. 197.
2. Monteith J.L. : Survey of Instruments for Micrometeorology, Blackwell Scientific Publications.
3. Liu Y.H. & Jordan R.C. : Availability of Solar Energy for Flat Plate Solar Heat Collector, Chp. I of "Low Temperature Application of Solar Energy" published by ASHRAE Technical Committee on Solar Energy Utilization,1966.
4. De Lisle J.F. : Mean Daily Insolation in New Zealand,N.Z. Journal of Science 9, 1966, pp.992-1005.
5. Benseman R.F. & Cook F.W. : Solar Radiation in New Zealand The Standard Year and Radiation on Inclined Slopes, N.Z. Journal of Science 12, 1969, pp. 696-708.
6. C.S.I.R.O. : Solar Positions and Radiation Tables for Christchurch, N.Z., Building Research Bureau of N.Z. Inc., 1966.
7. Bastings L. : Sunshine and Shade - A Handbook for N.Z. Building Research Bureau of N.Z.Inc.,1967.
8. Brooks F.A. & Miller W. : Availability of Solar Energy, Chp. III of " Introduction To The Utilization of Solar Energy" edited by Zarem A.M. & Erway D.D., Mc Graw-Hill Book Company, Inc., 1963.
9. Benseman R.F. : Prospect of Solar Heating in New Zealand N.Z. Engineering 15, 1966, p. 425.
10. Vincze S.A. : A High Speed Cylindrical Solar Water Heater, Solar Energy 13, 1971, pp.339-344.
11. Williamson J. : Solar Water Heater , private reference.
12. C.S.I.R.O. : Solar Water Heaters, Circular No. 2,1964 Division of Mechanical Eng., Melbn.,Aust.
13. Morse R.N. & Czarnecki J.T. : Flat Plate Solar Absorbers. The Effect on Incident Radiation of Inclination and Orientation , C.S.I.R.O. Engineering Section (Rep. ED 6,Aug 1958).

14. Whillier A. : Design Factors Influencing Solar Collector Performance, Chp. III of "Low Temperature Application of Solar Energy" published by ASHRAE Technical Committee on Solar Energy Utilization , 1966.

15. Hottel H.C. & Woertz B.B. : The Performance of Flat Plate Solar Heat Collector, Transaction of the A.S.M.E. 64, 1942, pp. 91-104.

16. Morse R.N. : Solar Water Heaters, "Proceedings of World Symposium on Applied Solar Energy",Phoenix, Arizona, 1955, pp. 191-200.

17. Holman J.P. : Experimental Methods for Engineers, 2nd Ed. Mc Graw-Hill Book Comp., 1971, p.38.

18. Farber E.A. : Solar Energy, Its Conversion and Utilization, Solar Energy 14, 1973, pp. 243-252.

GENERAL REFERENCES

19. Francia G. : Pilot Plant of Solar Steam Generating Stations, Solar Energy 12, 1968, pp. 51-64.

20. Garg H.P. : Design and Performance of a large size Solar Water Heater, Solar Energy 14,1973, pp. 303-312.

21. Jones W.P. : Air-Conditioning Engineering, 1st Ed., Edward Arnold(Publishers), Ltd, London.

22. Khanna M.L. : The Development of a Solar Water Heater and Its Field Trials Under Indian Tropical Conditions, Solar Energy 12, 1968, p.255.

23. Mc Adams : Heat Transmission, 3rd Ed., Mc Graw-Hill Book Comp., 1954.

24. Malik M.A.S. : Review Solar Water Heating in South Africa Solar Energy 12, 1968, pp. 395-397

25. Szulmayer W. : Solar Strip Concentrator, Solar Energy 14, 1973, pp. 327-335.

Title PROGRAMME TO CALCULATE ANGLES OF INCIDENCE OF SUNRAYS ON A SURFACE INCLINED α° FROM HORIZONTAL KNOWING THE SUN ALTITUDE a AND SOLAR AZIMUTHAL ANGLE n OF THE SURFACE.

Date

Name T.V. THANH.

$$\cos H_i = \sin a.\cos\alpha + \cos a.\cos n.\sin\alpha$$

Step		Key	Code	Display x	Display y	Display z	Storage f	Storage e	Storage d	Storage c	Storage b	Storage a
0	0	CLEAR	20									
	1	STOP	41	a	n	α	← INPUT (in degrees)					
	2	x→()	23									
	3	a	13									a
	4	y→()	40									
	5	b	14								n	
	6	sinx	70	sin a	n	α						
	7	ROLL↑	22	α	sin a	n						
	8	x→()	23									
	9	C	16							α		
	a	cosx	73	cosα	sin a	n						
	b	X	36	cosα	cosα sin a	n						
	c	a	13	a								
	d	cosx	73	cos a	cosα sin a	n		TO CALCULATE:				
1	0	↑	27	cos a	cos a	cosαsin a		SET		RUN		
	1	b	14	n				PRESS		GOTO (00)		
	2	cosx	73	cos n	cos a	cosαsin a				CONTINUE		
	3	X	36		cos n cos a			→INPUT		$\alpha \rightarrow z$		
	4	C	16	α						n → y		
	5	sinx	70	sin α						a → x		
	6	X	36	sin α	Sinα cosn cosa	cosαsina		PRESS		CONTINUE		
	7	↓	25	sinαcosn cosa	Cosαsina					y display = cos Hi		
	8	+	33		cos Hi			PRESS		CONTINUE		
1	9	END	46	sinαcosn cosa	cos Hi	cosαsin a						
	a											
	b											
	c											
	d											

APPENDIX 2 Theoretical estimation of the characteristics of the test unit.

Reference: Whillier (14) (Numbers of Eqn and Fig. referred here are those in the original paper)

Symbols :

a	$a^2 = U_o/kM$
A	area
α	absorptivity of the collector plate
b	width of bond between tube and plate
B	centre line spacing of tubes
C	bond conductance
C_p	specific heat of fluid
d	inside diameter of tubes
d_o	outside diameter of tubes
F''	flow factor
F'	collector efficiency factor
F	fin efficiency
F_c	fraction of incident solar radiation that is transmitted through glass and absorbed by the plate
F_e	effective transmissivity-absorptivity product of cover system
G	fluid flowrate per unit collector area
h	heat transfer coefficient from fluid to wall
k	thermal conductivity
K	extinction coefficient
L	length of pipes in collector
L'	half spacing of tubes
M	plate thickness
Nu	Nusselt number
Pr	Prandtl number
r	reflectivity of glass
s	thickness of bond
T	transmittance for solar radiation of glass

For this unit $A = 10.9\ ft^2 (1m^2)$, $\alpha = 0.95$

outer glass 32 oz. average thickness 0.15"
inner glass 26 oz. " " 0.12"

K is assumed having average value 0.5/in

For normal incidence at outer glass:

$\exp -(0.5)(0.15) = 0.928$

$(1-r)/(1+r) = 0.917$

Transmittance for outer glass: $T_1 = 0.928 \times 0.917 = \underline{0.850}$ (Eqn 3.1)

For normal incidence at inner glass:

$\exp -(0.5)(0.12) = 0.942$

Transmittance for inner glass: $T_2 = 0.942 \times 0.917 = \underline{0.864}$

Fraction absorbed: $F_c = 1.012\ T_1 T_2$ (Eqn 3.4 b)

$= \underline{0.705}$

Effective transmissivity-absorptivity product:

$F_e = 0.705 + 0.17(1-0.928) + 0.63 \times 0.850(1-0.942)$

$\underline{F_e = 0.748}$ (Eqn 3.5 & Table 3.1)

<u>For collector plate</u>:

Assuming average $t_p = 104^\circ F$ and $t_a = 68^\circ F$

Upward heat loss coefficient:

$\underline{U_{up} = 0.61 \text{ Btu/hrft}^2{}^\circ F}$ (0.298 cal/cm^{2}hr$^\circ$C) (from Fig. 3.5)

Backward heat loss = 1/10 Upward loss

$\therefore$ Total heat loss coefficient :

$\underline{U_o = 0.67 \text{ Btu/hrft}^2{}^\circ F}$ (0.33 cal/cm^{2}hr$^\circ$C)

For copper $k = 250 \text{ Btu/hrft}^\circ F$

$a^2 = U_o/kM = \frac{0.67 \times 12}{250 \times 0.019} = 1.69$

$\therefore a = 1.3$

$\frac{1}{2}$" tubes and 5.7" spacing give $L' = \frac{5.7 - 0.5}{2} = 2.6"$

$aL' = 0.282$

$\therefore$ Fin efficiency $\underline{F = 0.975}$ (from Fig.3.10)

B = 5.7" d = 0.461" M = 0.019"

L' = 2.6" d_o = 0.5" b = 0.5"

Assume average bond conductance C = 20

For 60 lb/hr flowrate in 7 tubes, velocity of water in each tube is:

$$V = \frac{60 \times 4 \times 144}{62.4 \times \pi \times (0.461)^2 \times 7 \times 3600} = 0.033 \text{ ft/sec}$$

Reynold number $Re = \rho Vd/\mu = 0.033 \times \frac{0.461}{12} \times 134{,}700 = 171$

Prandtl number $Pr = 4.64$

$$(d/L)RePr = \frac{0.461 \times 171 \times 4.64}{12 \times 3.3} = 9.25$$

Nusselt number $Nu = 4.36 + \frac{0.067 \times 9.25}{1 + (0.04)(9.25)^{2/3}}$ (Eqn 3.18)

$$Nu = 4.89$$

Heat transfer coefficient between water and plate:

$$h = k\,Nu / d = \frac{0.36 \times 4.89 \times 12}{0.461}$$

$$h = 45.6 \text{ Btu/hrft}^{2o}\text{F}$$

From Fig. 3.7(b) in Whillier's paper :

$$BU_o/\,dh = \frac{5.7 \times 0.67}{\times\ 0.461 \times 45.6} = 0.058$$

$$d_o/B = 0.5 / 5.7 = 0.088$$

$$BU_o/C = \frac{5.7 \times 0.67}{20 \times 12} = 0.0159$$

$$B/2L'F = \frac{5.7}{2 \times 2.6 \times 0.975} = 1.125$$

$$F' = \frac{1}{0.058 + \dfrac{1}{0.088 + \dfrac{1}{0.016 + 1.125}}} = \frac{1}{0.058 + 1.04}$$

$$\underline{F' = 0.912}$$

Overall heat transfer coefficient between water and ambient:

$$U_c = F'U_o = 0.912 \times 0.67 = 0.61 \qquad \text{(Eqn 3.14)}$$

$$G = (60)/(10.9) = 5.5 \text{ lb/hrft}^2$$

$$U_c/GC_p = (0.61)/(5.5 \times 1\ ) = 0.11$$

Flow factor $F'' = \dfrac{1 - \exp(-0.11)}{0.11} = 0.956$ (Eqn 3.17)

Overall efficiency of heat transfer : $F_o = F'xF'' = 0.912 \times 0.956$

$$\underline{F_o = 0.872}$$

Similar calculations for other flowrates give:

Flowrates	40(18)	80(36)	100(45)	lb/hr(Kg/hr)
V	0.022	0.044	0.055	ft/sec
Re	114	228	284	
(d/L)PrRe	6.17	12.30	15.40	
Nu	4.72	5.04	5.19	
h	44	48	49.4	btu/hrft^{2o}F
F'	0.908	0.913	0.915	
F''	0.916	0.962	0.970	
F_o	0.832	0.880	0.890	

APPENDIX 3 Programme to calculate Q_{up} knowing t_p , t_a , h_w .

Step		Key	Code
0	0	CLEAR	20
	1	STOP	41
	2	x→( )	23
	3	a	13
	4	1	01
	5	.	21
	6	8	10
	7	×	36
	8	4	04
	9	9	11
	a	2	02
	b	+	33
	c	ROLL↓	31
	d	x→( )	23
1	0	b	14
	1	1	01
	2	.	21
	3	8	10
	4	×	36
	5	4	04
	6	9	11
	7	2	02
	8	+	33
	9	y→( )	40
	a	c	16
	b	c	16
	c	×	36
	d	×	36

Step		Key	Code
2	0	×	36
	1	b	14
	2	↑	27
	3	×	36
	4	×	36
	5	×	36
	6	↓	
	7	−	34
	8	6	06
	9	0	00
	a	.	21
	b	3	03
	c	ENTER EXP.	26
	d	1	01
3	0	0	00
	1	CHG SIGN	32
	2	×	36
	3	1	01
	4	↑	27
	5	a	13
	6	÷	35
	7	↓	25
	8	y→( )	40
	9	a	13
	a	↑	27
	b	c	16
	c	↑	27
	d	b	14

Step		Key	Code
4	0	−	34
	1	y→( )	40
	2	e	16
	3	2	02
	4	.	21
	5	3	03
	6	6	06
	7	÷	35
	8	↓	25
	9	√x	76
	a	√x	76
	b	↑	27
	c	1	01
	d	0	00
5	0	x⇄y	30
	1	÷	35
	2	↓	25
	3	+	33
	4	↓	25
	5	y→( )	24
	6	c	16
	7	÷	35
	8	a	13
	9	+	33
	a	3	03
	b	.	21
	c	6	06
	d	9	11

Step		Key	Code
6	0	÷	35
	1	END	46
	2		
	3		

TO CALCULATE:

SET RUN

PRESS GOTO(00)

CONTINUE

→INPUT t_p (°C)

↑

t_a (°C)

↑

h_w ($\frac{Btu}{hr\,°F\,ft^2}$)

Display as:

$z \equiv t_p$

$y \equiv t_a$

$x \equiv h_w$

PRESS CONTINUE

Result:

$y \equiv Q_{up}$ ($\frac{cal}{cm^2\,hr}$)

PRESS CONTINUE

APPENDIX 4

Title: PROGRAMME TO CALCULATE R_{Di}, R_{di}, R_f AND R_{Ti} FROM R_{Dh}, R_{dh} AND R_{Th} WITH THE RATIO $\cos Hi/\cos H_h$ Date page 1/1

Name T. V. THANH

$$\begin{cases} R_{Di} = R_{Dh} \cos Hi/\cos H_h \\ R_{di} = 0.883\ R_{dh} \text{ (for } \alpha = 40^\circ \text{ facing North)} \\ R_f = 0.0468\ R_{Th} \text{ (for } \alpha = 40^\circ \text{ and } A = 0.4) \end{cases}$$

Step	Key	Code	Display x	Display y	Display z	Storage f	e	d	c	b	a
0 0	CLEAR	20									
1	STOP	41	R_{Dh}	R_{dh}	$\cos Hi/\cos H_h$	← INPUT DATA					
2	y→()	40									
3	a	13									R_{Dh}
4	+	33	R_{Dh}	R_{Th}	$\cos Hi/\cos H_h$						
5	ROLL↑	22	$\cos Hi/\cos H_h$	R_{Dh}	R_{Th}						
6	×	36		R_{Di}							
7	y→()	40									
8	b	14								R_{Di}	
9	↓	25	R_{Di}	R_{Th}	R_{Th}	TO CALCULATE:					
a	•	21				SET RUN					
b	0	00				PRESS GOTO (00)					
c	4	04				CONTINUE					
d	6	06				→INPUT $\cos Hi/\cos H_h$, R_{dh}, R_{Dh}					
1 0	8	10	0.0468	R_{Th}		PRESS CONTINUE					
1	×	36		R_f	R_{Th}	OUTPUT: R_{Di} at x					
2	•	21				R_{di} at y					
3	8	10				R_f at z					
4	8	10				PRESS CONTINUE					
5	3	03	0.883	R_f		OUTPUT: R_{Ti} at y					
6	↑	27	0.883	0.883	R_f	PRESS CONTINUE					
7	a	13	R_{dh}	0.883.							
8	×	36		R_{di}	R_f						
9	b	14	R_{Di}								
a	STOP	41	R_{Di}	R_{di}	R_f	DISPLAY 3 COMPONENTS OF RADIATION					
b	+	33									
c	↓	25									
d	+	33									
2 0	END	46	$R_{Di} + R_{di}$	R_{Ti}	R_f	TOTAL RADIATION					

NOTE: Steps 0a → 10 and 12 → 15 can be changed with appropriate values for different inclination and surroundings

APPENDIX 5 Procedures for heat loss calculations.

From the records of daily variation in temperature of water, collector plate, and air temperature, the three components Q_{up} , Q_b , Q_w can be estimated for every hour during the useful heating period.

STEPS IN CALCULATIONS:

1. Use planimeter to measure area A_1 enclosed by inlet and outlet water temperature curves. (in square inches)

2. Use planimeter to measure area A_2 enclosed by the air temperature curve and the curve of mean temperature of the plate where no water tube is bonded on (i.e. mean given by thermocouples number 2,3,5,6).

3. Measure area A_3 enclosed by the air temperature curve and the curve of mean temperature of water tubes (i.e. mean given by thermocouples number 1,4,7)

4. Take the average of areas A_2 and A_3 to obtain area A_4

The mean temperature of the collector plate t_p is taken as the mean of those thermocouples above . This temperature is well above the average of inlet and outlet water temperature as suggested by some references.

5. To estimate the heat collected by water:

During the range of temperatures from $20^{\circ}C$ to $65^{\circ}C$ as encountered in this test, the average output for copper-constantan thermocouples is $0.042\ mV/^{\circ}C$. For a 5 mV fullscale range of the chart, 1" on the chart represents 0.45 mV or $10.7\ ^{\circ}C$ temperature difference. If chart speed is 1" per hour, 1 in^2 of area on the chart is equivalent to $10.7^{\circ}C$-hr .

For one hour period, the total heat collected by water is

$$Q_w = \int_{t_1}^{t_2} \dot{m}C_p\,\Delta t\,dt = \dot{m}C_p \int_0^1 \Delta t\,dt \quad \text{for constant flowrate.}$$

The integration is the area enclosed by inlet and outlet temperature curves in one hour period (area A_1).

Hence

$$Q_w = \dot{m}(Kg/hr) \times C_p(Kcal/Kg^{\circ}C) \times A_1(in^2) \times 10.7\left(\frac{^{\circ}Chr}{in^2}\right)$$

or $Q_w = \dot{m} \times 10.7 \times A_1$ Kcal/hr

Because the area of this unit is 1 m^2, the rate of heat collected by water in one hour expressed in cal/cm^2per hour is :

$$\underline{Q_w} = \frac{10.7\ \dot{m}\ A_1 \times 10^3}{10^4} = \underline{1.07\ \dot{m}\ A_1} \quad cal/cm^2hr$$

6. To estimate the heat loss backward :

For one hour period the heat lost through the back is:

$$Q_b = \int_{t_1}^{t_2} U_b\ A_p\ \Delta t\ dt = U_b\ A_p \int_0^1 \Delta t\ dt$$

This integration is represented by the average area A_4

$$\therefore\ Q_b = U_b(W/m^{2o}C) \times A_p(m^2) \times A_4(in^2) \times 10.7(^oChr/in^2)$$

$$Q_b = 10.7\ U_bA_4 \quad Wh \quad \text{because} \quad A_p = 1\ m^2$$

or this can be expressed in cal/cm^2hr as :

$$Q_b = \frac{10.7\ U_bA_4 \times 3600}{4.18 \times 10^4}$$, as U_b was calculated in section B.2 of Chapter 5 to be 0.548 W/m^{2o}C, the final formula for Q_b is :

$$\underline{Q_b = 0.505\ A_4} \quad cal/cm^2hr \quad \text{for 1"/hr chart speed}$$

and $$\underline{Q_b = 0.252\ A_4} \quad cal/cm^2hr \quad \text{for 2"/hr chart speed}$$

7. To estimate the upward heat loss:

Based on the average area A_4, the mean air temperature and plate temperature are drawn which enclose the same area as A_4. With mean wind speed V calculated from W.O. records, h_w is estimated and these three items t_p, t_a, h_w are substituted in equation (5.2) to calculate Q_{up} . The programme in Appendix 3 is used to obtain Q_{up} in cal/cm^2hr with three inputs t_p, t_a, (in ^oC) and h_w (in Btu/hrft^{2o}F) .

8. Total heat collected :

Other losses are assumed negligible so that the total heat collected is:

$$Q_T = Q_w + Q_b + Q_{up}$$

Examples of calculations:

Date: 7-11-73 Time period: 1pm to 2pm

Chart speed 2"/hr $\dot{m}$ = 18 Kg/hr

Measurements by planimeter give:

$A_1 = 5.02$ in^2 $A_2 = 5.56$ in^2

$A_3 = 4.50$ in^2 $A_4 = 5.03$ in^2

$Q_w = 0.535 \times 18 \times 5.02 = 48.4$ cal/cm^2

$Q_b = 0.252 \times 5.03 = 1.26$ cal/cm^2

$t_p = 53.2^oC$, $t_a = 25.5^oC$, V = 19 mph , $h_w = 6.7$

$\therefore Q_{up} = 8.63$ cal/cm^2

$Q_T = 48.4 + 1.26 + 8.63 = 58.29$ cal/cm^2

Percentage of heat lost upward : 8.63/58.29 = 14.8%

Percentage of heat lost backward: 1.26/58.29 = 2.2%

Percentage of heat collected by water : 48.4/58.29= 83.0%

For radiation intensity on the surface :

$R_{Th} = 67.42$ cal/cm^2)
$R_{dh} = 30.59$ ") obtained for horizontal surface
$R_{Dh} = 36.83$ ")

$\therefore R_{Di} = 36.83 \times 1.01 = 37.20$ cal/cm^2

$R_{di} = 30.59 \times 0.883 = 27.00$ "

$R_f = 67.42 \times 0.0468 = 3.15$ "

$R_{Ti} = 67.35$ "

Percentage of collection : $Q_T/R_{Ti} = 58.29/67.35 = 86.5\%$

Overall efficiency : $Q_w/R_{Ti} = 48.4/67.35 = 72.0\%$

Similar calculations give rates of heat loss and heat collected for other hours of the day . Total for 7-11-73 was:

$Q_T = 395.40$ cal/cm^2 , $Q_w = 320.53$ cal/cm^2 (81.1%)

$Q_b = 10.03$ " (2.5%)

$R_{Ti} = 533.89$ " $Q_{up} = 64.84$ " (16.4%)

Percentage of collection for whole day : 395.4/533.89 =74.1%

Overall efficiency for whole day : 320.53/533.89 = 61%

In terms of KWh units, Q_w is expressed as :

$$Q_w = \frac{320.53 \times 4.18 \times 10^4}{3600 \times 10^3} = 3.72 \text{ KWh/m}^2$$

Period during which outlet temperature remained higher than inlet temperature was 12 hours, the mean power of the panel then equals:

$3.72/12 = 0.310$ KW/m^2

APPENDIX 6 Error Analysis

1. Error in Q_w :

Q_w is calculated from the equation $Q_w = S \times \dot{m} \times A_1$

where S is area coefficient having values:

$S = 1.07^{\circ}C\text{-hr/in}^2$ for 1"/hr chart speed

and $S = 0.535$ " for 2"/hr " "

Assuming the error in the recorded temperature is $\pm 0.5^{\circ}C$, error in S is :

$\pm 0.05^{\circ}C\text{-hr/in}^2$ for 1"/hr chart speed

and ± 0.025 " for 2"/hr " "

Assume also that error in flowrate $\dot{m}$ is ± 0.5 Kg/hr

and error in area A_1 is ± 0.01 in^2

From Ref. 17,

$$dQ_w = \left[\left(\frac{\partial Q_w}{\partial S} dS\right)^2 + \left(\frac{\partial Q_w}{\partial \dot{m}} d\dot{m}\right)^2 + \left(\frac{\partial Q_w}{\partial A_1} dA_1\right)^2 \right]^{\frac{1}{2}}$$

For the equation above :

$$\frac{\partial Q_w}{\partial S} = \dot{m}A_1 \quad , \quad \frac{\partial Q_w}{\partial \dot{m}} = A_1 S \quad , \quad \frac{\partial Q_w}{\partial A_1} = \dot{m}S$$

Typical values for 10 Dec, from 1pm to 2pm :

$\dot{m} = 36.9$ Kg/hr , $A_1 = 1.34$ in^2 , $S = 1.07$, $Q_w = 52.8$

$$dQ_w = \left[(36.9 \times 1.34 \times 0.05)^2 + (1.34 \times 1.07 \times 0.5)^2 + (36.9 \times 1.07 \times 0.01)^2 \right]^{\frac{1}{2}}$$

$$dQ_w = (2.47^2 + 0.71^2 + 0.39^2)^{\frac{1}{2}} = 2.58$$

Hence percentage error in Q_w is $2.58/52.8 = \underline{4.9\%}$

For 7 Nov , from 10am to 11am :

$\dot{m} = 18$ Kg/hr , $A_1 = 3$ in^2 , $S = 0.535$, $Q_w = 29$

$$dQ_w = (18 \times 3 \times 0.025)^2 + (3 \times 0.535 \times 0.5) + (18 \times 0.535 \times 0.01)^2 \quad ^{\frac{1}{2}}$$

$$dQ_w = (1.35^2 + 0.8^2 + 0.096^2)^{\frac{1}{2}} = 1.6$$

Percentage error in Q_w is $1.6/29 = \underline{5.5\%}$

From these two examples, one can conclude that the error for Q_w is about 5% for large flowrates and high radiation intensity, and about 6% for small flowrates and low insolation.

2. Error in Q_b :

Q_b is calculated from the equation $Q_b = S \times A_4$

where S is area coefficient having values:

$S = 0.505$ cal/cm^{2}hr-in^2 for 1"/hr chart speed

$S = 0.252$ " " for 2"/hr " "

Error in S is :

$$\frac{(\pm\ 0.5)x\ 0.548\ x\ 3600}{4.18\ x\ 10^4} = \pm\ 0.023\ \text{cal/cm}^2\text{hrin}^2$$

Error in A_4 is $\pm$ 0.01 in^2

Similar to the above analysis,

$$dQ_b = \left[\left(\frac{\partial Q_b}{\partial S}dS\right)^2 + \left(\frac{\partial Q_b}{\partial A}dA\right)^2\right]^{\frac{1}{2}}$$

For 10 Dec, from 1pm to 2pm :

$$S = 0.505\ ,\quad A_4 = 1.82\ \text{in}^2\ ,\quad Q_b = 0.92$$

$$dQ_b = (1.82\ x\ 0.023)^2 + (0.505\ x\ 0.01)^2\ ^{\frac{1}{2}}$$

$$dQ_b = \left[(0.042)^2 + (0.005)^2\right]^{\frac{1}{2}} = 0.042$$

hence percentage error for Q_b is: $0.042/0.92 = \underline{4.6\%}$

3. Error in Q_{up} :

Q_{up} is calculated by this equation :

$$Q_{up} = \frac{(t_p - t_a)}{36.9\left(\frac{t_p - t_a}{2.36}\right)^{\frac{1}{4}} + \frac{3.69}{h_w}} + 1.63\ x\ 10^{-10}(T_p - T_a)$$

(a) Effect of uncertaity in estimating h_w :

h_w is estimated from average wind speed over 3-hourly period, to find the change in Q_{up} due to h_w , values of $h_w = 4$ for 10 mph wind and $h_w = 10$ for 30 mph wind are substituted in the above equation. Typical results are presented below showing that the effect of using different h_w is small.

Date	Time	h_w=4	h_w=10	dQ_{up}	% diff.
10/12	11-12	6.09	6.15	0.06	0.98
6/11	11-12	10.21	10.32	0.11	1.08

(b) Error due to estimation of temperature t_p, t_a :

From the expression of Q_{up} above one can write:

$$\frac{\partial Q_{up}}{\partial t_p} = \frac{29.8(t_p-t_a)^{\frac{1}{4}} + 3.69/h_w - (t_p-t_a)(29.8/4)(t_p-t_a)^{-\frac{3}{4}}}{\left[(29.8(t_p-t_a)^{\frac{1}{4}} + 3.69/h_w)\right]^2} + 4x1.63x10^{-10}T_p^3$$

$$\frac{\partial Q_{up}}{\partial t_p} = \frac{22.35(t_p-t_a)^{\frac{1}{4}} + 3.69/h_w}{(29.8(t_p-t_a)^{\frac{1}{4}} + 3.69/h_w)^2} + 6.52 \times 10^{-10}T_p^3$$

Similarly, the expression for $Q_{up}/\ t_a$ is:

$$\frac{\partial Q_{up}}{\partial t_a} = \frac{-(22.35(t_p-t_a)^{\frac{1}{4}} + 3.69/h_w)}{(29.8(t_p-t_a)^{\frac{1}{4}} + 3.69/h_w)^2} - 6.52 \times 10^{-10}T_a^3$$

Error due to t_a is assumed as $\pm$ 0.5°C or $\pm$ 0.9°F or°R
Error due to t_p is assumed as $\pm$ 1.0°C or $\pm$ 1.8°F or°R
In those equations t_p , t_a are in °F and T_p , T_a are in °R

For 10 Dec , from 11am to 12noon typical values were

$t_p = 41.8°C = 107.2°F$ $\quad T_p = 567.2°R$
$t_a = 20.6°C = 69\ °F$ $\quad T_p = 529\ °R$
$h_w = 4.8$ Btu/hrft^2°F $\quad Q_{up} = 6.10$ cal/cm^2

$$\therefore \frac{\partial Q_{up}}{\partial t_p} = \frac{22.35(38.2)^{\frac{1}{4}} + 3.69/4.8}{(29.8(38.2)^{\frac{1}{4}} + 3.69/4.8)^2} + 6.52 \times 10^{-10}(567.2)^3$$
$$= 56.17/(74.77)^2 + 0.12 = 0.130$$

$$\frac{\partial Q_{up}}{\partial t_a} = -\left(\frac{56.17}{74.77^2}\right) - 6.52 \times 10^{-10}(529)^3 = -0.106$$

$$dQ_{up} = \left((0.13 \times 1.8)^2 + (-0.106 \times 0.9)^2 \right)^{\frac{1}{2}} = \underline{0.252}$$

Hence percentage error for Q_{up} is $0.252/6.10 = \underline{4.2\%}$

For 6 Nov , from 11am to 12 noon :

$t_p = 55°C = 131°F$ $\quad T_p = 591°R$
$t_a = 23.3°C = 72.2°F$ $\quad T_a = 532.2°R$
$h_w = 4.45$ $\quad Q_{up} = 10.23$

$\therefore\ Q_{up}/\ t_p = 0.144 \qquad Q_{up}/\ t_a = -0.107$

$dQ_{up} = \underline{0.276}$

Percentage error in this case is $0.276/10.23 = \underline{2.7\%}$

Therefore , the percentage error of Q_{up} is said from 3% to 5%.

APPENDIX 7 — Estimation of Costs for the Solar Project

1. Material cost of the Solar Panel:

- Copper tubes and Copper sheet (26 gauge)	$ 45-00
- 2 sheet of clear glass	15-80
- Pine timber	7-07
- Rubber U section	2-40
- 2 sheets of 26 gauge galvanized iron	6-64
Sub Total	$ 76-91

2. Additional cost for instrumentation :

- Glass replacement	$ 6-42
- 1 sheet of galvanized iron for the stand	2-49
- Dexion framing for the stand	7-20
- Thermocouples	50-00
Sub Total	65-90

3. Labour cost of manufacturing, installing and repairing:

50 hours @ $3-50 per hour	$175-00
TOTAL	$317-81

G E N E R A L C O N C L U S I O N S

In this study, both long wave and short wave components of the thermal radiation from the Sun and Sky to the Earth were considered.

In Chapter I, the analytical study of the long wave radiation from the Sky gave knowledge of the nature of this radiation component. Its main dependence on water vapour in the atmosphere was clearly shown in the analysis. If the distribution of water vapour in the atmosphere can be measured, the long wave radiation from Sky can be estimated by one of several radiation charts.

Chapter II introduced the methods of measuring long wave radiation, the difficulty of isolating this component from other heat transfer modes and the instruments used. The empirical formulae presented in this chapter represent all the suggestions up to date, to estimate the amount of long wave radiation from the Sky, and hence the radiative loss to the Sky, from meteorological observations at the site. These formulae are useful for engineering and architectural purposes because they do not require measurement of vertical distribution of water vapour in the air. Within the range of temperature encountered the difference due to these formulae is small, less than 8%, and may be insignificant in many cases.

A simple radiometer was designed and used to carry out some trial measurement under Christchurch weather condition. Descriptions of this radiometer and the experimental work are

presented in Chapter 3. The results were that this radiometer can measure the long wave radiation from Sky with about 13% accuracy. This accuracy is low due to several estimations in the response of the radiometer. Measurements by this radiometer during September and December 1973 showed a close relationship with Swinbank's formula

$$R_L = 1.195\,\sigma T_a^4 - 17.09 \quad (mW/cm^2)$$

More measurements of finer accuracy are required to verify this finding.

Calibration of the radiometer can increase the accuracy of the measurement by eliminating all the uncertainty in the response of the radiometer.

Solar radiation was investigated briefly in Chapter IV which introduced the methods of measuring and estimating solar radiation on horizontal and inclined surface . Several particular radiation data for Christchurch were presented. Sources for more information were also located for further work in this direction.

The application of solar energy to water heating was considered in Chapter V which concentrated particularly on Christchurch conditions.

From tests carried out on a test panel during October, November and December 1973, conclusions on the performance of such a panel under Christchurch conditions were:

- The daily energy contribution varied from 0 to 5 KWh per m^2 of collector plate area during the test period.

- Efficiency of operation (percentage of heat collected by water over the heat of solar radiation impinging on the heater surface) were from 40 to 60%.

- Estimations based on the test results and others' findings suggest that a house in Christchurch requires about 4 m^2 of collector area to supply 60 gallons of hot water at 60^{o}C per day during summer period. Extra heating by other sources is required in winter time.

- Variation in angle of inclination throughout the year is suggested where possible to give maximum collection and more saving.

With the increasing interest in solar water heating due to energy shortage this information may be useful for some applications. As far as the University is concerned, this study is only a beginning for further research on the utilization of solar energy in the coming years.

In connection with this water heating application, the whole year performance can be experimented to compare with the above estimations. Modifications of the flat plate collector to produce steam at low pressure can be considered and methods for frost prevention are worth investigation.